# University of Alberta

Gain Analysis and Stability of Nonlinear Control Systems

by

Vahid Zahedzadeh

A thesis submitted to the Faculty of Graduate Studies and Research
in partial fulfillment of the requirements for the degree of

Doctor of Philosophy
in
Controls

Department of Electrical and Computer Engineering


Fall 2009
Edmonton, Alberta

## Examining Committee

Dr. Horacio J. Marquez, Electrical and Computer Engineering

Dr. Tongwen Chen, Electrical and Computer Engineering

Dr. Alan Francis Lynch, Electrical and Computer Engineering

Dr. Mahdi Tavakoli, Electrical and Computer Engineering

Dr. Amos Ben-Zvi, Chemical and Materials Engineering

Dr. Khashayar Khorasani, Electrical and Computer Engineering, Concordia University

*To My Mom and Dad*
*To All South Azerbaijanis Who Are Struggling To Preserve Their Identity...*

# Abstract

The complexity of large industrial engineering systems such as chemical plants has continued to increase over the years. As a result, flexible control systems are required to handle variation in the operating conditions. Some of the challenging elements in the design of control systems are nonlinearity, disturbances and uncertainty in the process model. In the classical approach, first the plant model should be linearized at the nominal operating point and then, a robust controller should be designed for the resulting linear system. However, the performance of a controller designed by this method deteriorates when operation deviates from the nominal point. When the distance between the operating region and the nominal operating point increases, this performance degradation may lead to instability.

In the context of traditional linear control, one method to solve this problem is to consider the impact of nonlinearity as "uncertainty" around the nominal model and design a controller such that the desired performance is satisfied for all possible systems in the uncertainty set. As the size of uncertainty increases, conservatism occurs and at some point, it becomes impossible to design a controller that can provide satisfactory performance.

One of the methods proposed to overcome the aforementioned shortcomings is the so-called Multiple Model approach. Using Multi Models, local designs are performed for various operating regions and membership functions or a supervisory switching scheme is used to interpolate or switch among the controllers as the operating point moves among local regions. Since the Multiple Model method is a natural extension of the linear control method, it inherits some benefits of linear control such as simplicity of analysis and implementation. However, all these benefits are valid locally. For example, the multiple model method may be vulnerable when global stability is taken into account.

The core objective of this thesis is to develop new tools to study stability of closed-loop

nonlinear systems controlled by local controllers in order to improve design of multiple model control systems. For example, one of the aims of this work is to investigate how to determine the region where closed loop system is stable. A secondary objective is to study the effects of the exogenous signals on stability of such systems.

To achieve these goals, first, new representations for nonlinear systems, called $\zeta_A$ and $\zeta_{AB}$ representations, are proposed. In $\zeta_A$ and $\zeta_{AB}$ representations, initial state contributes to the feedback interconnection as an exogenous input. These representations can be used to develop new tools for non-zero state nonlinear systems based on the input-output theory. The $\zeta_A$ and $\zeta_{AB}$ representations convert a nonlinear system with non-zero initial state into a combination of a memoryless nonlinearity and a linear system with some input signals. The way initial state is handled by these representations provides a novel viewpoint on all aspects of investigating nonlinear systems.

Using these representations, stability of nonlinear systems with non-zero initial states can be investigated by the input-output stability methods. Based on this usage, a new framework is developed for the analysis of stability of systems by the $\zeta_A$ and $\zeta_{AB}$ representations. For local stability, a method developed to find a pair of local areas, namely $\Delta$ and $\Upsilon$, where belonging the initial state to $\Delta$ implies staying the state inside $\Upsilon$. The methods are also extended to forced systems.

To compute an upper bound on the $\mathcal{L}_1$, $\mathcal{L}_2$ and $\mathcal{L}_\infty$ norms of a class of nonlinear systems, a new method is proposed based on the $\zeta_A$ and $\zeta_{AB}$ representations. Another Method, which provides tighter bounds, is proposed to find an upper bound on the induced $\mathcal{L}_2$ norm. Both methods are only applicable to globally Lipschitz systems. To overcome this restriction, another tool is developed for local conditions, namely, an upper bound on system output is derived for bounded input and initial state. This method is restricted to the $\mathcal{L}_\infty$ induced norm.

To measure the distance between local systems in multiple model method, some researchers have suggested to use the gap metric. However, since there are no straight-forward method to compute the nonlinear gap metric and using linear gap metric can not guarantee global stability of the system, the mentioned problem is still unsolved. In this thesis based on $\zeta_A$ and $\zeta_{AB}$ representations, a method is proposed to compute an upper bounds on the

gap metric and the corresponding stability margin for a class of nonlinear systems.

The minimum gain of an operator is defined, some of its properties are derived and some computational methods are developed to calculate the minimum gain. Based on the minimum gain of operators, the large gain theorem is stated. The large gain theorem asserts that the feedback loop will be stable if the minimum loop gain is greater than one.

To study disturbance attenuation of a closed loop multitank system, the proposed methods are utilized. It is assumed that a proportional controller is used to control the level of the liquid in one of the tanks. The mathematical model of the open loop system is derived using physics of the plant. The gray box identification method is used to identify the model parameters and the disturbance attenuation of the system is investigated by the proposed method.

# Acknowledgements

The present work has been assisted by many people who had directly or indirectly helped and supported me over the years of my research study. First of all, I would like to express my deepest gratitude towards my supervisors Dr. Horacio J. Marquez and Dr. Tongwen Chen for their guidance, enormous patience, cautiously reviewing manuscripts, discussions and consistent encouragements during the period of research. Without their insight, suggestions, and excitement, this work would have never taken place.

It has been a great honor to work with Dr. Marquez because of his invaluable experience, novel ideas and immense knowledge in nonlinear systems. I appreciate his friendly supervision, generous encouragement and patient guidance. I am thankful to Dr. Chen for his immense knowledge and ability in mathematics and control systems as well as his useful comments on my work.

I am privileged to be part of the friendly environment of the Advanced Control Laboratory. I would like to thank all the members of the group, both past and present, for making it a great place to work. Many thanks to Adarsha Swarnakar, Betty (Batool) Labibi, Reza Banaei, Iman Izadi. I also would like to thank Amr, Masood, Danlei and Jingbo.

I would like to thank the administrative support staff of the department for their efforts especially Pinder Bains and Kathleen Forbes.

Finally, I want to thank my family, especially my parents, for their love, encouragement, and help, which kept me going during the more difficult times.

# Table of Contents

# List of Tables

# List of Figures

# Nomenclature

| | |
|---|---|
| $\mathbf{B}^p(c, \xi)$ | The open ball with center $c$ and radius $\xi$ with norm $p$ |
| $\gamma(\cdot)$ | $\gamma_p(\cdot)$ for all $0 < p \leq \infty$ |
| $\gamma_p(\cdot)$ | The induced norm (gain) of the operator |
| $\mathbf{T}_T$ | The Truncation operator |
| $\mathcal{L}_p$ | $\mathcal{L}_p^r$ where $r$ is a finite integer which can be understood from the text |
| $\mathcal{L}_p^r$ | The Lebesgue $p$-space of $r$-vector valued functions |
| $\mathbb{C}$ | The field of complex numbers |
| $\mathbb{R}$ | The field of real numbers |
| $\mathbb{R}^n$ | The space of $n \times 1$ real vectors |
| $\nu(\cdot)$ | The minimum gain |
| Im$(\cdot)$ | Imaginary part |
| Re$(\cdot)$ | Real part |
| sat$(\cdot)$ | The saturation function |
| $f_T(t)$ | The truncation of $f(t)$ |
| $I_{n\times n}$ | The $n \times n$ identity matrix |
| LHP | The left half plan of the complex plane |
| LTI | Linear time invariant |
| MATLAB | Matrix Laboratory |
| RBS | Random binary sequence |

| | |
|---|---|
| RHP | The right half plan of the complex plane |

# Chapter 1

# Introduction

## 1.1 Overview of Multi-Model Control Systems

The development of large industrial engineering systems such as chemical plants has lead to gradual increase in their complexity. In turn, this complexity demands suitable control systems that should have enough flexibility to be able to handle variations in the operating conditions. Nonlinearity, disturbances and uncertainty in the process or its model are three challenging elements in the design of control systems. The classical approach consists of linearizing the plant model at the nominal operating point and designing a robust controller for the resulting linear system. Although excellent results have been reported in literature, it is well known that the performance of a controller designed by this method deteriorates when operation deviates from the nominal point. This performance degradation may lead to instability when the distance between the operation region and the nominal operating point increases.

To solve this problem in the context of the traditional linear control, the impact of nonlinearity has been considered as "uncertainty" around the nominal model and based on the size of nonlinearity, the controller is designed such that the desired performance is satisfied for all possible systems in the uncertainty set. It is clear that the size of the uncertainty increases as the operating point of the system prowls in a large area. In turn, conservatism occurs as the size of uncertainty increases. At some point, it becomes impossible to design a controller that can provide satisfactory performance.

Thanks to the fact that the model derived by linearization describes the process quite accurately in a small region about the linearization point, some methods are introduced in the literature to overcome the aforementioned shortcomings. In the so-called gain scheduling method, local designs are performed for various operation regions and a gain-scheduling scheme is built to interpolate among the controllers as the operating point moves among

local regions [43] [44] [45] [46]. Although satisfactory results have been reported for some applications and gain scheduling is well-accepted among practitioners today, this method suffers from the lack of a theoretical support for global behavior.

Another linearization-based method, conceptually similar to the gain scheduling method, is the so-called Multiple Model or Multi Model method [17] [7] [28]. The only difference with the gain scheduling approach is that the interpolation is substituted by either membership functions or supervisory switching. In both forms, the switching is done based on the current states. While in the form of membership functions the current states of the system determine the weighting among the local controllers; in the supervisory form, a supervisor selects the suitable local controller from a bank of local controllers, based on the current state of the process.

The main advantage of the Multiple Model method is that it is a natural extension of the linear control method and inherits some benefits of linear control such as simplicity of analysis and implementation. However, it should be taken into account that all these benefits are valid locally. When the global behavior of the system is being investigated, most of the advantages are yet to be established. When it comes to global stability, which is one of the most important features of a control system, multiple model method may be vulnerable. Some researchers have suggested to use the gap metric to measure the distance between local systems [9] [38]. However, since there are no straight-forward methods to compute the nonlinear gap metric and using linear gap metric can not guarantee global stability of the system, the mentioned problem is still unsolved.

The core objective of this thesis is to develop new tools to study stability of closed-loop nonlinear systems controlled by local controllers. This is to say that the aim of our work is to investigate how to determine the region where a closed loop system is stable and to study the effect of the exogenous signals on stability of such systems.

## 1.2 Structure and Outline of the Thesis

### 1.2.1 Thesis Overview

In Chapter 2, after introducing the notation and presenting some preliminary results, a new representation for unforced nonlinear systems, called the $\zeta_A$ representation is proposed. Having only an input-output structure, the $\zeta_A$ representation is an equivalent structure of an unforced nonlinear system, where the initial state is also represented by an input. Then, the $\zeta_A$ representation is extended to forced systems.

In the $\zeta_A$ representation and its extended version for forced systems, which is called $\zeta_{AB}$ representation, a nonlinear system is arranged as a feedback interconnection of a memoryless nonlinearity and a linear system with the initial state as an input signal. The main difference between this decomposition and traditional ones is in the way the initial state is dealt with. Here, the initial state contributes to the feedback interconnection as an exogenous input while in traditional methods, any change in the initial state is handled by defining a new operator.

Chapter 3, starts by investigating stability of unforced nonlinear systems by the $\zeta_A$ representation. Based on operator-theoretic methods, a new framework is developed for the analysis of stability of nonlinear systems. In the proposed approach, since the initial state is considered as an input, stability of an unforced nonlinear system can be investigated by the input-output stability methods and stability of the nonlinear system is interpreted as the input-output stability of the resulting feedback system. Using classical tools, sufficient conditions for global and local stability of the system are obtained. For local stability, the notion of *stability regions* is introduced and is shown to be useful in applications. Then, local stability of unforced nonlinear systems is studied with a new definition of region of attraction, which extends into two regions. Sufficient conditions for local stability in term of those regions are derived. Some examples are given to show the effectiveness of the results. It is important to note that our method does not require finding a Lyapunov-type function.

Chapter 3 continues by investigating stability of forced nonlinear systems. Both global stability and local stability of forced nonlinear systems are considered. Using the $\zeta_A$ and $\zeta_{AB}$ representations of nonlinear systems, some sufficient conditions for global and local stability of forced nonlinear systems are derived.

In Chapter 4, the problem of computing the $\mathcal{L}_p$ operator norm of a nonlinear system is considered. Since it is important to quantify the influence of various inputs on various signals inside the system, this measure has several applications. One of them is in control systems, where the attenuation of disturbance signals is required. The proposed method can be optimized based on some selected parameters. The proposed theorems are applicable to a class of nonlinear systems. However, a method is also provided for computing an upper bound on the induced $\mathcal{L}_\infty$ norm for systems which are not in this class. To illustrate the methods, some examples are also given. The weighting method is introduced in the last section of this chapter. The weighting technique can be used to reduce the intrinsic conservativism in the aforementioned method. An example is also provided to show the

usage of the weighting technique.

Chapter 5 deals with the computation of the gap metric and stability margin for nonlinear systems. The gap metric, which was introduced to systems and control theory by Zames and El-Sakkary [55], can be used to measure system uncertainty. For linear time-invariant (LTI) systems, much work has been done to compute the gap metric. The extension of the gap metric to larger classes of systems was initiated in [10], where the metric is extended to time-varying linear plants. Later, the parallel projection operator for nonlinear systems [5] and its relationship to the differential stabilizability of nonlinear feedback systems [11] paved the road to the extension of the gap metric to a pseudo-metric on nonlinear operators [13].

Unfortunately, there is no generally applicable method of computing the gap metric for nonlinear systems. In fact, there are only a few examples in literature for the computation of the gap metric. Moreover, methods used in those examples are highly dependent upon the case of interest. This is also the case for the corresponding stability margin which can be used to determine the ball of uncertainty in the sense of the gap metric.

In Chapter 5, some upper bounds on the gap metric and the stability margin are derived and based on the methods proposed in Chapter 4, these bounds are computed.

In Chapter 6, stability of nonlinear systems is studied by a proposed method. The method fits in the context of input-output approach to study nonlinear systems. This approach, which was initiated by Popov, Zames, and Sandberg, in the 1960s [42] [56] [32], is one of the well-accepted and widely-used methods to study stability of systems. In fact, many of the recent developments in control theory, such as robust control and small-gain based nonlinear stabilization techniques are the results of this approach. Here, systems are considered as mappings from an input space of functions into an output space and the well-behaved input and output signals are considered as members of input and output spaces. Therefore, if the “well-behaved” inputs produce well-behaved outputs, the system is called stable.

The well-known small-gain theorem is the main contribution of the input-output approach in control theory. According to the small gain theorem, the feedback loop will be stable if the loop gain is less than one. According to our proposed theorem in Chapter 6, the large gain theorem, the feedback loop will be stable if the minimum loop gain is greater than one. In Chapter 6, first we introduce the minimum gain of operators. Then, a new stability condition is derived for feedback systems based on the minimum gains of the open-loop systems. An example is also provided to illustrate the usage of the large gain theorem.

The last chapter, Chapter 7, is the usage of the methods introduced in Chapter 4 in investigating disturbance attenuation of closed-loop systems. There is no doubt that disturbance attenuation is one of the most important objectives in any closed-loop system. Therefore, it is important to quantify the influence of various inputs on various signals inside the system and develop a tool to calculate such quantities.

The system of interest is a multitank system, consisting of three tanks placed one above another. Due to gravity, the liquid flows through the tanks. The objective of the control system is to control the level of the liquid in the middle tank by the flow rate of the liquid entering to the top tank. We study the effect of a disturbance signal, which enters through the output of the plant, on the state of the closed-loop system. The chapter starts with the identification of the plant by the gray box method and continues by investigating the disturbance attenuation of the system.

### 1.2.2 The $\zeta_A$ and $\zeta_{AB}$ Representations

The $\zeta_A$ and $\zeta_{AB}$ representations are equivalent structures of nonlinear systems, which involve only an input-output structure. In this setting, the initial states representing initial conditions is represented as an input. In these representations, a nonlinear system is arranged as a feedback interconnection of a memoryless nonlinearity and a linear system with the initial state as an input signal. Although interconnection of a memoryless nonlinearity with a linear system has been widely used in literature, the way the initial state is dealt with is the main difference between our decomposition and traditional ones. In $\zeta_A$ and $\zeta_{AB}$ representations, the initial state contributes to the feedback interconnection as an exogenous input while in traditional methods, any change in the initial state is handled by defining a new operator.

Consider the following systems:

$$N_1 : \dot{x}(t) = f_1(t, x(t)) \tag{1.1}$$

$$N_2 : \ \dot{x}(t) = f_2(t, x(t), u(t)) \tag{1.2}$$

where $f_1$ and $f_2$ are locally Lipschitz. $N_1$ is an unforced system and $N_2$ is a forced one. In Chapter 2, it is shown that $N_1$ is equivalent to the structure depicted in Fig. 1.1(a) and $N_2$ is equivalent to the ones shown in Fig. 1.1(b) and Fig. 1.1(c). Structures in Fig. 1.1(a) and Fig 1.1(b) are called $\zeta_A$ representation and the one in Fig. 1.1(c) is called $\zeta_{AB}$ representation. The operators $\Phi$, $\Gamma$, $\Omega$ and $\Theta$ are introduced in Chapter 2. These representations are widely used in all other chapters of this thesis.

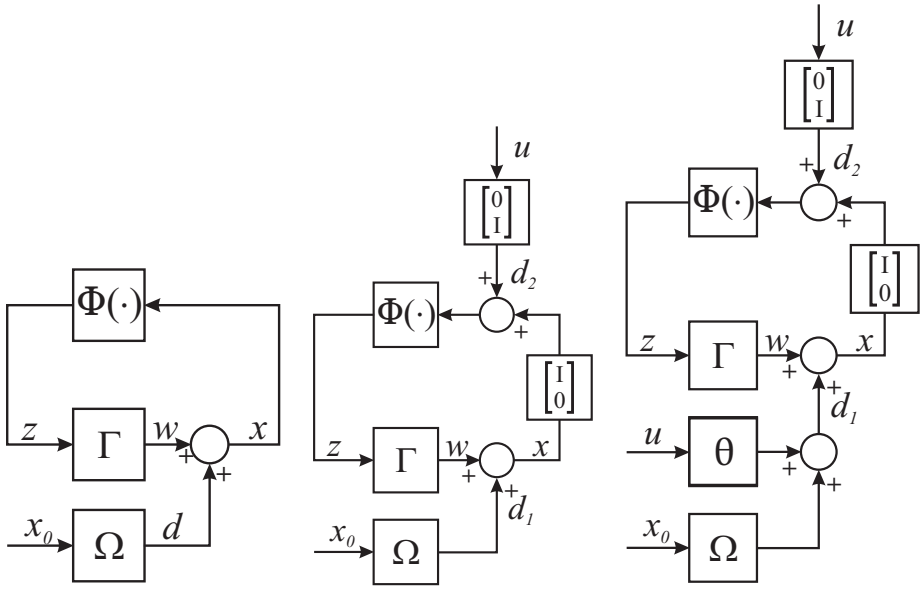


(a) $\zeta_A$ for unforced systems (b) $\zeta_A$ for forced systems (c) $\zeta_{AB}$ for forced systems

Figure 1.1: $\zeta_A$ and $\zeta_{AB}$ representations.

### 1.2.3 Stability of Nonlinear Systems

The fact that the $\zeta_A$ and $\zeta_{AB}$ representations convert a nonlinear system with non-zero initial state to a combination of a memoryless nonlinearity and a linear system with some input signals and the way the initial state is handled by these representations provide a novel viewpoint on all aspects in investigating nonlinear systems. Stability as one of the challenging issues in design and analysis of nonlinear systems can also be studied by these new tools. In Chapter 3, a new framework is developed for the analysis of stability of systems by the $\zeta_A$ and $\zeta_{AB}$ representations. The effectiveness of this usage is originated in the fact that using these representations, stability of nonlinear systems with non-zero initial states can be investigated by the input-output stability methods and stability is interpreted as input-output stability of the resulting feedback systems.

The main contributions of Chapter 3 are Theorems 3.2.1, 3.2.2, 3.2.3, 3.2.4, 3.3.1, 3.3.2 and 3.3.3. Theorems 3.2.1 and 3.2.2 provide new methods to check stability in the sense of Lyapunov for an unforced nonlinear system by norm of some relevant operators; without finding any Lyapunov-like function. For local stability, Theorem 3.2.3 can be used to find some local areas, $\Delta$ and $\Upsilon$, if the initial state $x_0$ is in $\Delta$, then the state will stay in $\Upsilon$. Theorem 3.2.4 is asymptotic version of Theorem 3.2.3. Roughly speaking, Theorem 3.3.1 is an extension of Theorem 3.2.1 to forced systems. Similarly, Theorem 3.3.2 is the extension of Theorem 3.2.3 to forced nonlinear systems. For asymptotic stability of forced nonlinear

systems in a local sense, Theorem 3.3.3 provides the aforementioned $\Delta$ and $\Upsilon$ regions.

### 1.2.4 The Induced Norm of Nonlinear Systems

Most of the computational techniques developed for nonlinear systems are restricted to a narrow class of nonlinear systems for which a particular function, e.g. Lyapunov function or storage function, can be found. Unfortunately, there is not a straight-forward method to find such functions and they can usually be obtained by trial and error [27] [24]. Computing the $\mathcal{L}_p$ operator norm of a nonlinear system is not an exception. In this work, we propose a method to compute an upper bound on the $\mathcal{L}_1$, $\mathcal{L}_2$ and $\mathcal{L}_\infty$ norms of a class of nonlinear systems. The method is based on the $\zeta_A$ and $\zeta_{AB}$ representations of nonlinear systems. The first proposed theorem in this context is Theorem 4.1.1 which provides an upper bound on induced $\mathcal{L}_p$ norms. The next theorem, Theorem 4.1.2 gives tighter bound for the case $p = 2$. Both theorems suffer from a restrictive condition, namely 4.4. Theorem 3.3.2 can be used to overcome the restriction with the cost of providing only local conditions, i.e. an upper bound on the system output is derived for bounded input and initial state. This method is restricted to $\mathcal{L}_\infty$ induced norm.

### 1.2.5 The Gap Metric

Stability and performance of feedback control systems are considerably impacted by model uncertainty. Unlike the linear time-invariant (LTI) systems, where much work has been done to study this effect, the topic for nonlinear systems is quite immature. The gap metric is one of the useful tools to investigate the effect of model uncertainty on control systems. For LTI systems, it has been shown that a perturbed system can be stabilized by any controller which is designed for the nominal system if and only if the distance between the perturbed system and the nominal system is small in the gap metric. The gap metric is also extended to a pseudo-metric on nonlinear operators [13].

The computation of the gap metric for LTI system was developed by Georgiou [12]. Unlike the LTI system case, there is no generally applicable method of computing the gap metric for nonlinear systems. In fact, there are only a few examples in literature for the computation of the gap metric. Moreover, those methods are highly dependent upon the case of interest. This is also the case for the corresponding stability margin which can be used to determine the ball of uncertainty in the sense of the gap metric.

In Chapter 5, we propose a method to compute the gap metric and the corresponding stability margin for a class of nonlinear systems. The method is based on $\zeta_A$ and $\zeta_{AB}$

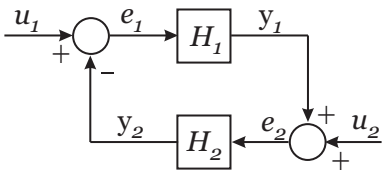


Figure 1.2: The feedback system.

representations. The key results are Theorems 5.3.1 and 5.3.2 which provide upper bounds on the gap metric and the stability margin, respectively. We use the methods proposed in Chapter 4 to calculate the bounds. An example is also provided to illustrate the effectiveness of the results and comparison between the direct computation and the suggested methods.

### 1.2.6 Large Gain Theorem

One of the key results in the input-output stability theory is the small gain theorem, which provides a sufficient condition for stability of interconnected systems. Roughly speaking, the theorem states that the feedback loop will be stable if the loop gain is less than one. For the feedback system depicted in Fig. 1.2, the small gain theorem states that the closed loop system is stable if $\gamma(H_1) \cdot \gamma(H_2) < 1$ where $\gamma(\cdot)$ denotes the gain of operators. This simple rule has been a basis for numerous stabilization techniques such as nonlinear $\mathcal{H}_\infty$ control [15].

In our approach, we first define the minimum gain of an operator $\nu(\cdot)$ as

$$\nu(H) = \inf_{0 \neq u \in \mathcal{U}} \frac{\|(Hu)_T\|}{\|u_T\|} \tag{1.3}$$

where $H : \mathcal{U} \to \mathcal{Y}$ is an operator, $(\cdot)_T$ denotes the Truncation operator, the infimum is taken over all $u \in \mathcal{U}$ and all $T$ in $\mathbb{R}^+$ for which $u_T \neq 0$. Then, some of the properties of the minimum gain are derived and its computation for some cases is discussed. Particularly, it has been showed that the minimum gain satisfies the *positivity* and the *positive homogeneity* properties but fails to satisfy the triangle inequality. Finally, the large gain theorem, Theorem 6.3.1, is stated. Roughly speaking, the large gain theorem asserts that the feedback loop will be stable if the minimum loop gain is greater than one. For the feedback system depicted in Fig. 1.2, the large gain theorem states that the closed loop system is stable if $\nu(H_1) \cdot \nu(H_2) > 1$.

### 1.2.7 The Multitank System

To show applicability and effectiveness of the proposed methods in Chapter 4, we apply Theorem 3.3.2 to study disturbance attenuation of a closed loop system. The system of

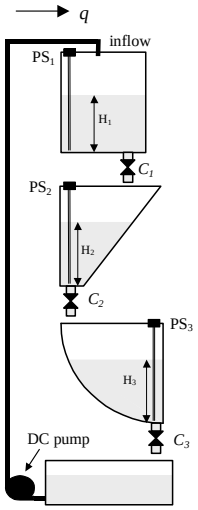


Figure 1.3: Configuration of the multi-tank system.

interest, which is called Multitank system, consists of three tanks placed one above another and due to gravity, the liquid flows through the tanks. The top tank has a constant cross section while the other two have variable cross sections as shown in Fig. 1.3. A pump is used to circulate liquid from the supply tank into the upper tank. We assume that a proportional controller is used to control the level of the liquid in the middle tank by the flow rate of the liquid entering to the top tank.

In chapter 7, which devotes to investigating disturbance attenuation of the controlled Multitank system, first we derive the mathematical model of the open loop system using physics of the plant. The model, which is nonlinear, consists of four parameters that are depend on the configuration of the system. After running some experiments on the plant and collecting data, we use the gray box identification method to identify the parameters. Finally, the disturbance attenuation of the system is investigated by the proposed method in Theorem 3.3.2. A summary of results is presented in Table 7.2.

## 1.3 Contributions

The content of this thesis has been published and presented in the following international journals and conferences:

- Chapter 3: A significant part of this chapter was published in IET Control Theory & Applications [50] and IEEE Conference on Decision and Control, San Diego, 2006 [49].

- Chapter 4: The contents of this chapter were published in American Control Conference, New York, 2007 [54] and accepted for publication in IEEE Transaction on Automatic Control [51].
- Chapter 5: The contents of this chapter were published in American Control Conference, Seattle, 2008 [52].
- Chapter 6: The contents of this chapter were published in American Control Conference, Seattle, 2008 [53].

# Chapter 2

# $\zeta_A$ and $\zeta_{AB}$ Representations

## 2.1 Introduction

Almost all dynamical systems encountered in nature are ruled by nonlinear characteristics and linear models are usually used in order to simplify analysis. Although, for most applications linear models are accurate enough to be used to represent systems in a small region, they fail to provide accurate results when larger operating region is needed to be considered.

In this section, first, we introduce the notation and present some preliminaries results. Next, a new representation for unforced nonlinear systems, called $\zeta_A$ representation, is introduced. The $\zeta_A$ representation is an equivalent structure of an unforced nonlinear system, which involves only an input-output structure. The initial state is also represented by an input in the $\zeta_A$ representation. Finally, an elegant extension of the $\zeta_A$ representation to forced systems, called the $\zeta_{AB}$ representation, is presented.

## 2.2 Background

In general, nonlinear representations can be classified into three types [4]:

- system input-output representation,
- state-space representation, and
- model-free representation.

In the input-output representation, the input-output behavior of a system without any state is considered. In this representation, systems are assumed as mappings from an input space of functions into an output space. Using this approach, one of the well-accepted and widely-used methods to study stability of systems is developed [27] [42] [56] [32]. The state-space representation, on the other hand, highlights states of systems. In this representation,

the dynamic of the system is represented by some states affected by the inputs and the output depends on both the states and inputs [24] [27]. Nonlinear systems, which cannot be modeled by the mentioned methods, might be represented by model-free representations [4].

In the proposed method, a nonlinear system is arranged as a feedback interconnection of a memoryless nonlinearity and a linear system with initial state as an input signal. The main difference between our decomposition and traditional ones is in the way initial state is dealt with. In our method, initial state contributes to the feedback interconnection as an exogenous input while in traditional methods, any change in initial state is handled by defining a new operator. In our approach, since initial state is considered as an input, stability of unforced nonlinear system can be investigated by the input-output stability methods and stability of the nonlinear system is interpreted as the input-output stability of the resulting feedback system.

## 2.3 Notation, Preliminaries, and Computation

### 2.3.1 Notation

Let $\mathbb{R}$ and $\mathbb{C}$ denote the fields of real and complex numbers, respectively. $\mathbb{R}^n$ denotes the space of $n \times 1$ real vectors. The Euclidean norm in $\mathbb{R}^n$ is denoted by $\|\cdot\|$. $I_{n\times n}$ denotes the $n \times n$ identity matrix. LHP and RHP stand for left and right half plan of the complex plane, respectively. Let $\mathbf{B}^p(c, \xi)$ denote the open ball with center $c$ and radius $\xi$ with norm $p$, i.e. $\mathbf{B}^p(c, \xi) := \{x |\ \|x - c\|_p < \xi\}$. $\mathcal{L}_p^r$ denotes Lebesgue $p$-space of $r$-vector valued functions on $[0, \infty]$, with norm $\|\cdot\|$ defined as $\|f\|_p := \left(\int_0^\infty \|f(t)\|^p\, dt\right)^{1/p}$ for $1 \le p \le \infty$ and $\|f\|_\infty := \operatorname{ess\,sup}_{t\in\mathbb{R}} \|f(t)\|$. Usually $r$ is a finite integer; we drop $r$ and write $\mathcal{L}_p$ instead of $\mathcal{L}_p^r$. To distinguish among various norm notations, we indicate the space as a subscript for the norm, such as $\|\cdot\|_{\mathbb{R}^n}$ or $\|\cdot\|_{\mathcal{L}_p}$. Whenever the space is not mentioned, norms with $t$ argument denote Euclidean norm at $t$ and without $t$ denote the $\mathcal{L}_p$ norm where $p$ is as a general number or can clearly be understood from the text. Let $\mathbf{T}_T$ denotes the Truncation operator: for $f(t)\,,\ 0 \le t < \infty,\ \mathbf{T}_T\, f(t) = f(t)$ on $[0, T]$, and zero otherwise. We also denote the truncation of $f(t)$ by $f_T(t) := \mathbf{T}_T\, f(t)$. For an operator $\lambda : \mathcal{L}_p \to \mathcal{L}_p$, let $\gamma_p(\lambda)$ stand for the induced norm (gain) of the operator defined as

$$\gamma_p(\lambda) := \sup_{0 \ne u \in \mathcal{L}_p} \frac{\|(\lambda u)_T\|}{\|u_T\|} \tag{2.1}$$

where the supremum is taken over all $u \in \mathcal{L}_p$ and all $T$ in $\mathbb{R}^+$ for which $u_T \ne 0$. Let $\gamma(\lambda)$ denote $\gamma_p(\lambda)$ for all $0 < p \le \infty$.

**Definition 2.3.1.** *Maximum overshoot* of a signal $x(t)$ is

$$M_P := \frac{\|x\|_{\mathcal{L}_\infty}}{\|x(0)\|_\infty} \tag{2.2}$$

In this thesis, we will frequently use operator gains. In this section, we take a brief look at some of the computational methods for norms.

### 2.3.2 Continuous-time, LTI operators

Let $g(t)$ be the impulse response of a stable linear time invariant (LTI) system. We will denote by $\Gamma$ the convolution operator defined by $\Gamma(z(t)) = \int_0^t g(t-\tau)z(\tau)d\tau$. To compute the gain of $\Gamma$, we use the following lemma that is taken from [2], page 234 (Table 1):

**Lemma 2.3.1.** *Suppose that $\Gamma$ is a linear time-invariant stable operator with impulse response $g(t) : \mathbb{R}^+ \to \mathbb{R}^{n\times n}$. Let $G(s)$ denotes the Laplace transform of $g(t)$. Define*

$$\tilde{g}_{n\times n} := \begin{bmatrix} \|g_{11}\|_{\mathcal{L}_1} & \|g_{12}\|_{\mathcal{L}_1} & \cdots & \|g_{1n}\|_{\mathcal{L}_1} \\ \|g_{21}\|_{\mathcal{L}_1} & \|g_{22}\|_{\mathcal{L}_1} & \cdots & \|g_{2n}\|_{\mathcal{L}_1} \\ \vdots & \vdots & \ddots & \vdots \\ \|g_{n1}\|_{\mathcal{L}_1} & \|g_{n2}\|_{\mathcal{L}_1} & \cdots & \|g_{nn}\|_{\mathcal{L}_1} \end{bmatrix} \tag{2.3}$$

*Then*

$$\gamma_1(\Gamma) = \|\tilde{g}\|_1 \tag{2.4a}$$

$$\gamma_\infty(\Gamma) = \|\tilde{g}\|_\infty \tag{2.4b}$$

$$\gamma_2(\Gamma) = \|G(s)\|_{\mathcal{H}_\infty} \tag{2.4c}$$

where $\|\cdot\|_{\mathcal{H}_\infty}$ denotes $\mathcal{H}_\infty$ norm. Some standard algorithms to compute the $H_\infty$-norm can be found in several references. See for example [57]. To compute $\|g_{ij}\|_{\mathcal{L}_1} = \int_0^\infty |g_{ij}(t)|dt$ for strictly proper systems, any numerical integral approximation method, e.g. rectangular and trapezoidal, can be used.

### 2.3.3 Autonomous and non-autonomous memoryless nonlinearities

In this section, the operator of interest is in the form of $\Phi(t, x(t))$, where $\Phi(\cdot,\cdot) : \mathbb{R}^+ \times \mathbb{R}^n \to \mathbb{R}^n$. It is also assumed that $\Phi(t, 0) = 0$.

**Lemma 2.3.2.** *Suppose that there exists a constant $\mu_p$ such that*

$$\|\Phi(t, x)\|_p \le \mu_p\|x\|_p, \ \forall x \in \mathbb{R}^n, \ \forall t \ge 0 \tag{2.5}$$

*then $\gamma_p(\Phi) \le \mu_p$.*

*Proof.* See reference [41] pp. 40. □

With direct computation, the $\infty$-norm, 2-norm and 1-norm of a memoryless autonomous nonlinear operator can be found approximately with arbitrary accuracy. MATLAB can also be used to find the aforementioned norms.

**Example 2.3.1.** Consider the following memoryless nonlinearity.

$$\Phi(x) = \begin{bmatrix} \Phi_1(x) \\ \Phi_2(x) \\ \Phi_3(x) \end{bmatrix} = \begin{bmatrix} -0.2\,x_2 + \sin(0.5\,x_2) - \sin(0.5\,x_3) \\ -0.2\,x_1 + \sin(0.5\,x_1) - \sin(0.5\,x_3) \\ 1 - \cos(0.5\,x_1) + \sin(0.5\,x_2) \end{bmatrix}$$

where $x = \begin{bmatrix} x_1 & x_2 & x_3 \end{bmatrix}^{\mathrm{T}}$. Let

$$g(x_1, x_2, x_3) := \frac{\|x\|_2}{\|\Phi(x)\|_2} = \frac{\sqrt{x_1^2 + x_2^2 + x_3^2}}{\sqrt{\Phi_1^2(x_1, x_2, x_3) + \Phi_2^2(x_1, x_2, x_3) + \Phi_3^2(x_1, x_2, x_3)}}.$$

Using the "fminsearch" command of MATLAB, the minimum of $g(x_1, x_2, x_3)$ is $1.2678$ and consequently $\gamma_2(\Phi) \approx \frac{1}{1.2678} = 0.7888$.

### 2.3.4 $\Omega$-operator

**Definition 2.3.2.** For continuous-time, we define operator $\Omega$ as

$$\Omega(x(t)) := e^{At} x_0 \tag{2.6}$$

where $A \in \mathbb{R}^{n \times n}$ with all eigenvalues in LHP and $x(0) = x_0$. Similarly, for discrete-time

$$\Omega(x(t)) := A^t x_0 \tag{2.7}$$

where $A \in \mathbb{R}^{n \times n}$ with all eigenvalues in $\mathbb{D}$ and $x(0) = x_0$.

**Lemma 2.3.3.** *If* $x_i(0) < \infty\,, \forall i = 1 \cdots n$ *then* $\Omega(x) \in \mathcal{X}_p$.

*Proof.* The proofs for continuous-time and discrete-time are the same and only the first one comes here. Since $x_i(0) < \infty$, $\|x(0)\|_p < \infty$. On the other hand, because all eigenvalues of $A$ are in LHP, $\|e^{At}\|_p < \infty$, $\forall t \geq 0$. Since $\Omega(x) = e^{At} x_0$, $\|\Omega(x)(t)\|_p < \|e^{At}\|_p \|x_0\|_p < \infty$. This completes the proof for $p = \infty$. For $p = [1, \infty)$, in addition, $e^{At}$ is a continuous time signal and vanishes as $t \to \infty$. Therefore $\|e^{At}\|_{\mathcal{L}_p}^p = \int_0^\infty \|e^{At}\|_p^p dt < \infty$. We have $\|\Omega(x)\|_{\mathcal{L}_p} = \int_0^\infty \|e^{At} x_0\|_p^p dt \leq \int_0^\infty \|e^{At}\|_p^p \|x_0\|_p^p dt = \|x_0\|_p^p \cdot \int_0^\infty \|e^{At}\|_p^p dt = \|x_0\|_p^p \cdot \|e^{At}\|_{\mathcal{L}_p}^p < \infty$, and consequently, $\Omega(x) \in \mathcal{L}_p$. □

We have the following lemma about the gain of $\Omega$.

**Lemma 2.3.4.** *For continuous-time, the $\mathcal{L}_\infty$-gain of $\Omega$, which is defined by (2.6), is*

$$\gamma_\infty(\Omega) = \|e^{At}\|_{\mathcal{L}_\infty} \tag{2.8}$$

*And for discrete-time, where $\Omega$ defined by (2.7),*

$$\gamma_\infty(\Omega) = \|A^t\|_{\ell_\infty} \tag{2.9}$$

*Proof.* The proofs for continuous-time and discrete-time are the same and only the first one comes here. First we show that $\|e^{At}\|_{\mathcal{L}_\infty}$ is an upper bound for $\gamma_\infty(\Omega)$.

$$\|e^{At}x_0\|_{\mathcal{L}_\infty} \leq \|e^{At}\|_{\mathcal{L}_\infty}\|x_0\|_\infty \leq \|e^{At}\|_{\mathcal{L}_\infty}\|x(t)\|_{\mathcal{L}_\infty} \tag{2.10}$$

Next, we show that this upper bound is achievable for an input signal. Let $x(t) = I_{n\times n}\ \forall t \geq 0$, then $\|x(t)\|_{\mathcal{L}_\infty} = 1$ and $\|e^{At}x_0\|_{\mathcal{L}_\infty} = \|e^{At}\|_{\mathcal{L}_\infty}$. This completes the proof. □

**Lemma 2.3.5.** *The following equations are true for $\Omega$:*

*(i)* $\|\Omega(x)\|_{\mathcal{L}_2} = \|e^{At}\|_{\mathcal{L}_2} \cdot \|x_0\|_2$ *for continuous-time*

*(ii)* $\|\Omega(x)\|_{\ell_2} = \|A^t\|_{\ell_2} \cdot \|x_0\|_2$ *for discrete-time*

*(iii)* $\|\Omega(x)\|_{\mathcal{L}_1} \leq \|e^{At}\|_{\mathcal{L}_1} \cdot \|x_0\|_1$ *for continuous-time*

*(iv)* $\|\Omega(x)\|_{\ell_1} \leq \|A^t\|_{\ell_1} \cdot \|x_0\|_1$ *for discrete-time*

*Proof.* Since proofs are similar for continuous-time and discrete-time, we only prove (i) and (iii) here.
(i).

$$\begin{aligned}
\|\Omega(x_0)\|_{\mathcal{L}_2}^2 &= \int_0^\infty (e^{At}x_0)^*\ (e^{At}x_0)\, dt \\
&= \int_0^\infty x_0^*\,(e^{At})^*\ (e^{At})\, x_0\, dt \\
&= x_0^* \int_0^\infty (e^{At})^*\ (e^{At})\, dt\, x_0 \\
&= x_0^*\, \|e^{At}\|_{\mathcal{L}_2}^2\, x_0 \\
&= \|x_0\|_2^2\, \|e^{At}\|_{\mathcal{L}_2}^2
\end{aligned}$$

(iii).

$$\begin{aligned} \|\Omega(x_0)\|_{\mathcal{L}_1} &= \int_0^\infty \|e^{At}x_0\|_1\, dt \\ &\leq \int_0^\infty \|e^{At}\|_1\|x_0\|_1\, dt \\ &= \|x_0\|_1 \int_0^\infty \|e^{At}\|_1\, dt \\ &= \|x_0\|_1\|e^{At}\|_{\mathcal{L}_1} \end{aligned} \tag{2.11}$$

□

Lemma 2.3.5 gives the 2-norm gain of $\Omega$-operators and an upper bound for the 1-norm gain. Denoting the upper bound of $\gamma_1$ by $\hat{\gamma_1}$, we have

$$\gamma_2(\Omega) = \|e^{At}\|_{\mathcal{L}_2} \tag{2.12a}$$

$$\hat{\gamma_1}(\Omega) := \|e^{At}\|_{\mathcal{L}_1} \tag{2.12b}$$

for continuous-time and

$$\gamma_2(\Omega) = \|A^t\|_{\ell_2} \tag{2.12c}$$

$$\hat{\gamma_1}(\Omega) := \|A^t\|_{\ell_1} \tag{2.12d}$$

for discrete-time.

**Example 2.3.2.** Let

$$A = \begin{bmatrix} -0.225 & -0.175 & 0.075 & 0.525 \\ 0.200 & -0.400 & -0.150 & 0.200 \\ 0.200 & -0.400 & -0.400 & 0.200 \\ 0.125 & -0.125 & -0.125 & -0.625 \end{bmatrix}$$

Fig. 2.1 shows $\|e^{At}\|_\infty$ and $\|A^t\|_\infty$ versus $t$. Computation shows that $\gamma_\infty(\Omega) \approx 1.4351$ for continuous-time and $\gamma_\infty(\Omega) = 1.2$ for discrete-time.

**Lemma 2.3.6.** *For any $\Omega$-operator, $\gamma_\infty(\Omega) \geq 1$.*

*Proof.* Since for $t = 0$, $e^{At} = I$ and $A^t = I$. It turns out that $\|e^{At}\|_{\mathcal{L}_\infty} \geq 1$ and $\|A^t\|_{\ell_\infty} \geq 1$. Consequently, $\gamma_\infty(\Omega) \geq 1$. □

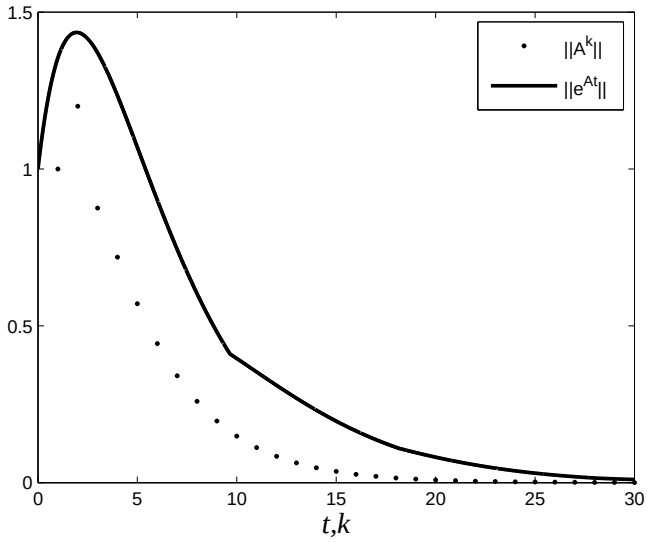


Figure 2.1: $\|e^{At}\|_\infty$ and $\|A^t\|_\infty$ versus $t$ in Example 2.3.2.

## 2.4 $\zeta_A$ Representation

### 2.4.1 Continuous-time systems

Assume that the nonlinear system of interest is

$$\dot{x}(t) = f(t, x(t)) \tag{2.13}$$

where $f : \mathbb{R}^+ \times \mathbb{R}^n \to \mathbb{R}^n$ is locally Lipschitz. It is well-known, [27], that stability for other points or any desired trajectory can be transformed to the study of the stability of the origin. Let $A \in \mathbb{R}^{n\times n}$ whose all eigenvalues are in LHP. Define

$$\begin{aligned} &\Phi(t, x) : \mathbb{R}^+ \times \mathbb{R}^n \to \mathbb{R}^n \\ &\Phi(t, x) := f(t, x) - Ax \end{aligned} \tag{2.14}$$

and consequently

$$\dot{x} = Ax + \Phi(t, x) \tag{2.15}$$

The block diagram of (2.15) is depicted in Fig. 2.2. $\Phi(t, x)$ is a non-autonomous static nonlinearity and $\Lambda$ is a linear system with the following state equation.

$$\Lambda : \dot{x} = Ax + z \tag{2.16}$$

It is well-known, e.g. [3], that the response of $\Lambda$ is

$$x(t) = e^{At}x_0 + \int_0^t e^{A(t-\tau)}z(\tau)\, d\tau \tag{2.17}$$

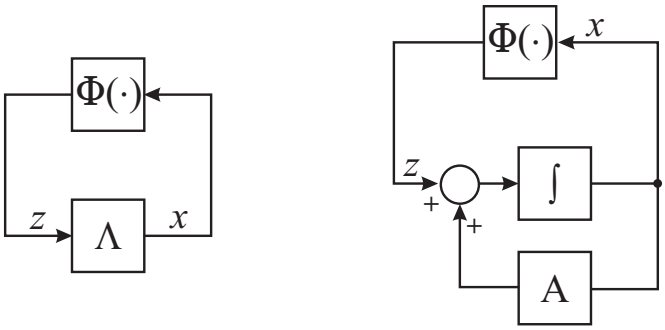


Figure 2.2: Block diagram for (2.15) and (2.24).

which reveals that $\Lambda$ is not a linear operator for $x_0 \neq 0$. Let

$$\Gamma : \mathcal{L}_p \to \mathcal{L}_p, \quad \Gamma(z(t)) := \int_0^t e^{A(t-\tau)} z(\tau)\, d\tau, \tag{2.18a}$$

and

$$\Omega : \mathcal{L}_p \to \mathcal{L}_p, \quad \Omega(x(t)) := e^{At} x(0) \tag{2.18b}$$

Since $A$ is a stable matrix, it is easy to prove that $\Gamma : \mathcal{L}_p \to \mathcal{L}_p$, $\Omega : \mathcal{L}_p \to \mathcal{L}_p$ and also $\Gamma$ are linear autonomous operators and $\Omega$ is a $\Omega$-operator which is defined in Section 2.3.4. The state space representations for $\Gamma$ is

$$\Gamma : \left[\begin{array}{c|c} A & I \\ \hline I & 0 \end{array}\right] \tag{2.19}$$

Let $\Lambda_{x_0}$ denote $\Lambda$ with the initial condition $x_0$. Therefore,

$$\Lambda_{x_0}(z(t)) := e^{At} x_0 + \int_0^t e^{A(t-\tau)} z(\tau)\, d\tau \tag{2.20}$$

substituting (2.18) and (2.20),

$$\Lambda_{x_0}(z(t)) = \Omega(x_0(t)) + \Gamma(z(t)) \tag{2.21}$$

Since $\Phi$ is static, the structure shown in Fig. 2.2 can be represented by its equivalent, which is depicted in Fig. 2.3. This representation of the nonlinear system will be referenced to as the $\zeta_A$ representation with operator ordered set $[\Phi, \Gamma, \Omega]$.

### 2.4.2 Discrete-time systems

In this case, we assume that the nonlinear system of interest is

$$x(t+1) = f(t, x(t+1)) \tag{2.22}$$

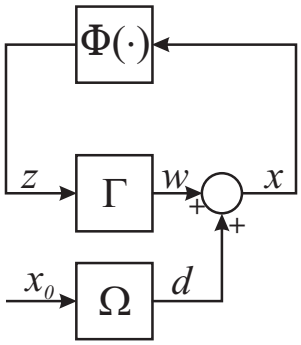


Figure 2.3: Equivalent block diagram using new operators.

where $f : \mathbb{Z}^+ \times \mathbb{R}^n \to \mathbb{R}^n$ is locally Lipschitz. Let $A \in \mathbb{R}^{n\times n}$ have all of its eigenvalues inside the unit circle. Define

$$\begin{aligned} &\Phi(t,x) : \mathbb{Z}^+ \times \mathbb{R}^n \to \mathbb{R}^n \\ &\Phi(t,x) := f(t,x) - Ax \end{aligned} \tag{2.23}$$

and consequently

$$x(t+1) = Ax(t) + \Phi(t, x(t)) \tag{2.24}$$

The block diagram of (2.24) is depicted in Fig. 2.2. $\Phi(t,x)$ is a static nonlinearity and $\Lambda$ is a linear system with the following state equation.

$$\Lambda : x(t+1) = Ax(t) + z(t) \tag{2.25}$$

It is well-known, e.g. [8], that the response of $\Lambda$ is

$$x(t) = A^t\, x_0 + \sum_{l=0}^{t} A^{t-l-1} z(l) \tag{2.26}$$

which reveals that $\Lambda$ is not a linear operator for $x_0 \neq 0$. Let

$$\Gamma : \ell_p \to \ell_p, \quad \Gamma(z(t)) := \sum_{l=0}^{t} A^{t-l-1} z(l), \tag{2.27a}$$

and

$$\Omega : \ell_p \to \ell_p, \quad \Omega(x(t)) := A^t x(0) \tag{2.27b}$$

Since $A$ is a stable matrix, it is not hard to prove that $\Gamma : \ell_p \to \ell_p$, $\Omega : \ell_p \to \ell_p$ and also $\Gamma$ is a linear autonomous operator and $\Omega$ is a $\Omega$-operator defined in Section 2.3.4. The state space representations for $\Gamma$ is $\left[\begin{array}{c|c} A & I \\ \hline I & 0 \end{array}\right]$. Let $\Lambda_{x_0}$ denote $\Lambda$ with the initial condition equals $x_0$. Therefore,

$$\Lambda_{x_0}(z(t)) := A^t\, x_0 + \sum_{l=0}^{t} A^{t-l-1} z(l) \tag{2.28}$$

substituting (2.27) in (2.28),

$$\Lambda_{x_0}(z(t)) = \Omega(x(t)) + \Gamma(z(t)) \tag{2.29}$$

Similar to the continuous-time case, since $\Phi$ is static, the structure shown in Fig. 2.2 can be represented by its equivalent, which is depicted in Fig. 2.3. This representation of the discrete nonlinear system will be referenced to as the $\zeta_A$ representation with operator ordered set of $[\Phi, \Gamma, \Omega]$.

## 2.5 $\zeta_{AB}$ Representation

### 2.5.1 Continuous-time systems

For forced nonlinear systems, suppose that the system of interest is

$$N: \ \dot{x}(t) = f(t, x(t), u(t)) \tag{2.30}$$

where $f : \mathbb{R} \times \mathbb{R}^n \times \mathbb{R}^m \to \mathbb{R}^n$ is locally Lipschitz. Let $A \in \mathbb{R}^{n\times n}$ and $B \in \mathbb{R}^{n\times m}$. Define

$$\Phi(x, u, t) := f(t, x, u) - Ax - Bu. \tag{2.31}$$

Let

$$\Theta : \mathcal{L}_p \to \mathcal{L}_p, \quad \Theta(u(t)) := \int_0^t e^{A(t-\tau)} Bu(\tau)\, d\tau, \tag{2.32}$$

and $\Gamma$ and $\Omega$ be defined in the same formulas as in (2.18). The nonlinear system is equivalent to the structure represented in Fig. 2.4(a). This representation of the nonlinear system is called the $\zeta_{AB}$ representation with ordered operator set $[\Phi, \Gamma, \Theta, \Omega]$.

It is important to note that $\left[\begin{array}{c|c} A & I \\ \hline I & 0 \end{array}\right]$ and $\left[\begin{array}{c|c} A & B \\ \hline I & 0 \end{array}\right]$ are state-space realizations for $\Gamma$ and $\Theta$, respectively. Since $A$ and $B$ are chosen arbitrary, $\zeta_A$ and $\zeta_{AB}$ representations are not unique. A useful choice for the $\zeta_{AB}$ representation is $B = 0$, which implies $\theta = 0$ and simplifies the $\zeta_{AB}$ structure as the structure shown in Fig. 2.4(b). For forced systems, this representation is also called $\zeta_A$ representation.

### 2.5.2 Discrete-time systems

Similarly, for a forced nonlinear system with the following state equation

$$N: \ x(t+1) = f(t, x(t), u(t)) \tag{2.33}$$

where $f : \mathbb{Z}^+ \times \mathbb{R}^n \times \mathbb{R}^m \to \mathbb{R}^n$ is locally Lipschitz, let $A \in \mathbb{R}^{n\times n}$ have all of its eigenvalues inside the unit circle and $B \in \mathbb{R}^{n\times m}$. Define

$$\Phi(x, u, t) := f(t, x, u) - Ax - Bu. \tag{2.34}$$

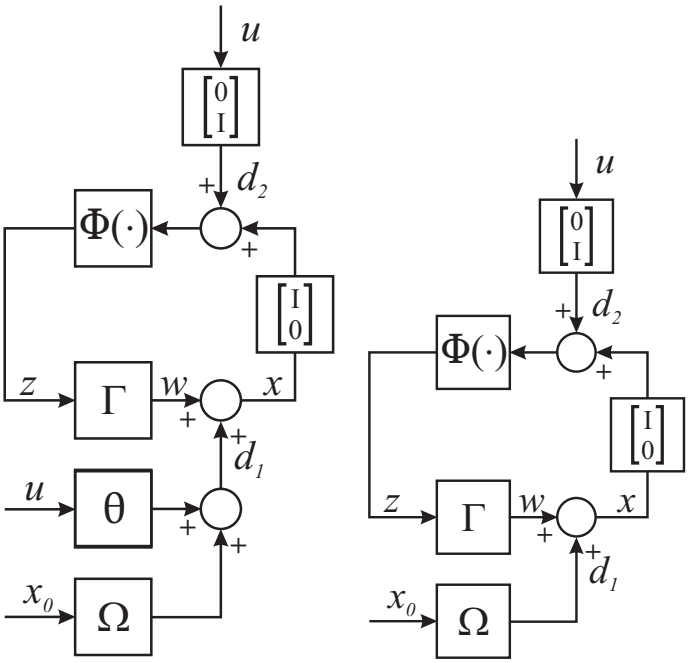


(a) $\zeta_{AB}$ (b) $\zeta_A$

Figure 2.4: $\zeta_A$ and $\zeta_{AB}$ representations for forced systems.

Let

$$\Theta : \ell_p \to \ell_p, \quad \Theta(u(t)) := \sum_{l=0}^{t} A^{t-l-1} B u(l) \tag{2.35}$$

and $\Gamma$ and $\Omega$ be defined in the same formulas as in (2.27). The nonlinear system is equivalent to the structure represented in Fig. 2.4(a). This representation of the nonlinear system is called the $\zeta_{AB}$ representation with ordered operator set $[\Phi, \Gamma, \Theta, \Omega]$.

It is important to note that $\left[\begin{array}{c|c} A & I \\ \hline I & 0 \end{array}\right]$ and $\left[\begin{array}{c|c} A & B \\ \hline I & 0 \end{array}\right]$ are state-space realizations for $\Gamma$ and $\Theta$, respectively. Since $A$ and $B$ are chosen arbitrary, $\zeta_A$ and $\zeta_{AB}$ representations are not unique. A useful choice for the $\zeta_{AB}$ representation is $B = 0$, which implies $\theta = 0$ and simplifies the $\zeta_{AB}$ structure as the structure shown in Fig. 2.4(b). For forced systems, this representation is also called $\zeta_A$ representation.

# Chapter 3

# Stability

## 3.1 Introduction

The traditional approach to study stability involves Lyapunov methods [27] [40] [24]. In these methods, the notion of stability is restricted to unforced systems and stability of *equilibrium points*. The analysis requires finding a so-called Lyapunov function, whose derivatives along the system trajectories must be negative definite, or semi-definite. Finding this function is usually challenging, thus limiting the application of this method.

An alternative way to study the stability of nonlinear systems is the so-called *input-output* stability approach. The input-output theory of systems was initiated in the 1960s by G. Zames and I. Sandberg [56] [32]. Unlike the Lyapunov method, the input-output stability theory considers systems as mappings from an input space of functions into an output space. This method suffers from a problem similar to the Lyapunov method. Indeed, the study of stability in this method involves finding a storage function, which is as difficult to find as a Lyapunov function.

In [35], bridging in some sense the two classical notions of stability, the concept of *input to state stability (ISS)* was introduced. Roughly speaking, in an ISS system, if the inputs are small, then system trajectories converge to a ball in state space, whose radius depends upon the input size, see [33], [34] and the references therein for more details. This notion differs from the input-output theory mainly in that it takes into account the initial states, which are ignored in the input-output stability. It is also different from stability in the sense of Lyapunov because it considers forced systems. Checking for ISS is usually very difficult as it requires finding a so-called ISS Lyapunov function with very stringent conditions.

Along with the aforementioned three major approaches, stability of systems, in its various forms, continues to inspire researchers. Motivated by the classical small gain theorem,“nonlinear” small gain theorems are discussed in [21], [39], and [18]. The notion of

non-uniform in time robust global asymptotic output stability is introduced in [22] for a wide class of systems. An extension of the second method of Lyapunov to study the stability of infinite-dimensional discrete-time systems is presented in [29].

In this chapter, we study stability of nonlinear systems. Using the $\zeta_A$ representation for nonlinear systems, we develop a new framework for the analysis of stability of systems based on operator-theoretic methods. In our approach, since initial state is considered as an input, stability of unforced nonlinear system can be investigated by the input-output stability methods and stability of the nonlinear system is interpreted as the input-output stability of the resulting feedback system. After decomposing the system, sufficient conditions for global and local stability of the system are derived using classical tools. For local stability, the notion of *stability regions* is introduced and is shown to be useful in applications. A method to compute the stability region is also developed. It is important to note that our method does not require finding a Lyapunov-type function.

This chapter has two sections. The first section is devoted to stability of unforced systems. In the first part, the $\zeta_A$ representation is used to provide sufficient conditions for global stability and global asymptotic stability of unforced nonlinear systems in terms of conditions on the gain of certain operators. In the second part of the section, local stability of unforced nonlinear systems is studied with a new definition of region of attraction, which extends into two regions. Sufficient conditions for local stability in term of those regions are derived. Some examples are given to show the effectiveness of the results.

In the second section of this chapter, stability of forced nonlinear system is studied. This section also consists of two parts. In the first part, global stability and in the second part local stability of forced nonlinear systems are considered. Using the $\zeta_A$ and $\zeta_{AB}$ representations of nonlinear systems, some sufficient conditions for global and local stability of forced nonlinear systems are derived.

## 3.2 Unforced Systems

### 3.2.1 Global Stability

The following theorem provides a sufficient condition for stability of unforced nonlinear systems.

**Theorem 3.2.1.** *Given a continuous time system of the form (2.13) with $\zeta_A$ representation of $[\Phi, \Gamma, \Omega]$,*

*(i) if $\gamma_\infty(\Phi) \cdot \gamma_\infty(\Gamma) < 1$ then the system is globally stable in sense of Lyapunov.*

*(ii) if, in addition to (i),* $\gamma_2(\Phi) \cdot \gamma_2(\Gamma) < 1$ *then the system is globally asymptotically stable in sense of Lyapunov.*

The following lemma (e.g [25] pp. 491), which is a corollary of the Barbalat's lemma, will be used in the proof.

**Lemma 3.2.1.** *Consider the function* $\phi : \mathbb{R}^+ \to \mathbb{R}$. *If* $\phi, \dot{\phi} \in \mathcal{L}_\infty$, *and* $\phi \in \mathcal{L}_p$ *for some* $p \in [1, \infty)$, *then* $\lim_{t\to\infty} \phi(t) = 0$.

*Proof.*

(i) In this section of the proof all of the norms are either $\infty$-norm or $\mathcal{L}_\infty$-norm, depending on the case. Because both $\Omega$ and $\Gamma$ map zero into zero, their biases are zero. According to Lemma 2.3.3, $\|x_0\| < \infty$ implies that $d \in \mathcal{L}_\infty$. According to the small gain theorem, e.g. [27], $\gamma_\infty(\Phi).\gamma_\infty(\Gamma) < 1$ implies that all internal signals of the system are in $\mathcal{L}_\infty$. To show that the system is stable in the sense of Lyapunov, it is enough to show that for any given $\epsilon$ there exists $\delta$ such that $\|x_0\|_{\mathbb{R}^n} < \delta \Longrightarrow \|x(t)\|_{\mathbb{R}^n} < \epsilon$ for all $t \geq 0$. Without loss of generality, it can be assumed that the norm in $\mathbb{R}^n$ is $\|.\|_\infty$, e.g. [40]. We claim that for any given $\epsilon$, $\delta$ can be chosen as $\delta < \frac{1-\gamma_\infty(\Phi)\gamma_\infty(\Gamma)}{\gamma_\infty(\Omega)}\epsilon$. To prove this, since $\|x_0\| < \delta < \frac{1-\gamma_\infty(\Phi)\gamma_\infty(\Gamma)}{\gamma_\infty(\Omega)}\,\epsilon$ then $\|d(t)\| \leq \gamma_\infty(\Omega)\|x_0\| < (1 - \gamma_\infty(\Phi)\gamma_\infty(\Gamma))\,\epsilon$. Besides, $\|x\| \leq \|d\| + \|w\|$ and $\|w\| \leq \gamma_\infty(\Phi)\gamma_\infty(\Gamma)\|x\|$. Therefore $\|x\| \leq \frac{1}{(1-\gamma_\infty(\Phi)\gamma_\infty(\Gamma))}\|d\| < \epsilon$. Since for any given $\epsilon$ there exists some $\delta < \frac{1-\gamma_\infty(\Phi)\gamma_\infty(\Gamma)}{\gamma_\infty(\Omega)}\,\epsilon$, stability is global. It is important to note that since $\gamma_\infty(\Omega) \geq 1$, $\gamma_\infty(\Phi) \geq 0$ and $\gamma_\infty(\Gamma) \geq 0$ then $\frac{1-\gamma_\infty(\Phi)\gamma_\infty(\Gamma)}{\gamma_\infty(\Omega)} \leq 1$ and $\delta \leq \epsilon$.

(ii) In this section of proof, all of the norms are either 2-norm or $\mathcal{L}_2$-norm unless it is clarified. According to lemma 2.3.5(i), $\|x_0\| < \infty$ implies that $\|d\| = \gamma_2(\Omega).\|x_0\| < \infty$ and consequently $d \in \mathcal{L}_2$. According to small gain theorem, e.g. [27], $\gamma_2(\Phi).\gamma_2(\Gamma) < 1$ implies that all internal signals of the system are in $\mathcal{L}_2$. Therefore, $x \in \mathcal{L}_\infty \cap \mathcal{L}_2$ and consequently there exists closed set $\mathcal{D}$ such that $x(t) \in \mathcal{D}$ for all $t$. Assuming that $f(x,t)$ is locally Lipschitz in $\mathcal{D}$, there exists $\mu$ such that

$$\forall\, x_1, x_2 \in \mathcal{D} \qquad \|f(x_2,t) - f(x_1,t)\|_\infty \leq \mu\|x_2 - x_1\|_\infty \tag{3.1}$$

Taking $x_1 = 0$ and $x_2 = x(t)$

$$\forall\, x(t) \in \mathcal{D} \qquad \|f(x(t),t)\|_\infty \leq \mu\|x(t)\|_\infty \tag{3.2}$$

Since $x \in \mathcal{L}_\infty$, $\|x(t)\|_\infty \leq \|x\|_{\mathcal{L}_\infty}$ for all $t$. Substituting in (3.2), $\|\dot{x}(t)\|_\infty = \|f(x(t),t)\|_\infty \leq \mu\|x\|_{\mathcal{L}_\infty}$ for all $t$. In turn, this means that $\dot{x} \in \mathcal{L}_\infty$. Now, we use the corollary of the Barbalat's lemma, i.e. 3.2.1. Assuming $\phi(t) := \|x(t)\|_2^2 = x^T(t)x(t)$, it is trivial that $\phi \in \mathcal{L}_\infty$.

Since $\dot{x} \in \mathcal{L}_\infty$, we have

$$\dot{\phi}(t) = \dot{x}^T(t)x(t) + x^T(t)\dot{x}(t) < \infty, \quad \forall\, t \tag{3.3}$$

which means $\dot{\phi} \in \mathcal{L}_\infty$. On the other hand,

$$\int_0^\infty |\phi(t)|dt = \int_0^\infty \|x(t)\|_2^2 dt = \|x\|_{\mathcal{L}_2}^2 < \infty \tag{3.4}$$

that reveals that $\phi \in \mathcal{L}_1$. Corollary 3.2.1 implies that $\lim_{t\to\infty} \phi(t) = 0$ and consequently $\lim_{t\to\infty} x(t) = 0$. □

**Theorem 3.2.2.** *Given a discrete time system of the form (2.22) with $\zeta_A$ representation of $[\Phi, \Gamma, \Omega]$,*

*(i) if $\gamma_\infty(\Phi) \cdot \gamma_\infty(\Gamma) < 1$ then the system is globally stable in sense of Lyapunov.*

*(ii) if, in addition to (i), $\gamma_2(\Phi) \cdot \gamma_2(\Gamma) < 1$ then the system is globally asymptotically stable in sense of Lyapunov.*

*Proof.* The proof follows the same lines as the proof of Theorem 3.2.2 and is omitted. It is important to note that in the discrete-time domain, $x \in \ell_2 \cap \ell_\infty$ implies that $x(t) \to 0$ as $t \to \infty$ and there is no need for the second part of the proof where the corollary of Barbalat's lemma is used. □

Theorems 3.2.1 and 3.2.2 can be used to check the stability of nonlinear systems with the help of the mentioned computation methods. Moreover, $A$ plays the role of a free parameter. It is important to note that both theorems state sufficient conditions for stability. This implies that it is sufficient to find just one $A$ which satisfies the conditions of the theorems. If such a matrix $A$ is found the system is stable even if there exists other $A$ matrices which fail the conditions. If such a matrix $A$ cannot be found or does not exist, the stability or instability of the system can not be proven using these theorems.

To compare the results with LTI systems, consider the following perturbed LTI system

$$\dot{x} = (M + \Delta M)x \tag{3.5}$$

Let $\Phi(x) = (M + \Delta M + \alpha I)x$ where $\alpha > 0$. Consequently, $A = -\alpha I$ and $\Gamma$ defined as (2.18a) or equivalently (2.19). To compute $\gamma_\infty(\Gamma)$, Lemma 2.3.1 can be used. The impulse response of $\Gamma$ is $G(s) = \frac{1}{s-\alpha} I$ and $g_{ii}(t) = e^{-\alpha t}$ and $g_{ij}(t) = 0$ for $i \neq j$. Equation (2.3) implies $\|\tilde{g}_{ii}(t)\| = 1$ and $\|\tilde{g}_{ij}(t)\| = 0$ for $i \neq j$. Consequently, $\gamma_2(\Gamma) = \frac{1}{\alpha}$ and $\gamma_\infty(\Gamma) = 1$.

On the other hand, $\gamma_\infty(\Phi) = \|M+\Delta M+\alpha I\|_\infty$. According to Theorem 3.2.1, the stability condition is $\|M + \Delta M + \alpha I\|_\infty < 1$ or equivalently $\lambda_{\max}(M + \Delta M) < -\alpha < 0$, where $\lambda_{\max}$ denotes the maximum eigenvalue. This is to say that the perturbation $\Delta M$ should not move the eigenvalues of the system to RHP or $j\omega$ axis.

**Example 3.2.1.** Consider the following nonlinear system

$$\dot{x} = f(x) = \begin{cases} 0.25\,x_1 - x_2 - \text{sat}\,(x_1) - \text{sat}\,(x_2) \\ 4\,x_1 - 3\,x_2 - \text{sat}\,(x_1) - \sin(x_2) \end{cases} \tag{3.6}$$

where $\text{sat}\,(x) = \text{sgn}\,(x)\ \min(1, |x|)$ and $\text{sgn}\,(\cdot)$ is the signum function. Let

$$A = \begin{bmatrix} -0.25 & -1.5 \\ 3.5 & -3.5 \end{bmatrix}. \tag{3.7}$$

Therefore,

$$\Phi(x) = f(x) - A\,x = \begin{cases} 0.5\,x_1 + 0.5\,x_2 - \text{sat}\,(x_1) - \text{sat}\,(x_2) \\ 0.5\,x_1 + 0.5\,x_2 - \text{sat}\,(x_1) - \sin(x_2) \end{cases}.$$

Figure 3.1 shows the plot of $\frac{\|\Phi(x)\|}{\|x\|}$ versus $\|x\|$ established at $10^6$ randomly chosen points. Using methods described in Sections 2.3.2 to 2.3.4, we have $\gamma_\infty(\Phi) = 1$, $\gamma_\infty(\Gamma) = 0.9531$, $\gamma_2(\Phi) = 1$, and $\gamma_2(\Gamma) = 0.8217$. Since $\gamma_\infty(\Phi)\,\gamma_\infty(\Gamma) = 0.9531 < 1$, the system is globally stable. More interestingly, $\gamma_2(\Phi)\,\gamma_2(\Gamma) = 0.8217 < 1$ implies that the system is asymptotically globally stable. To illustrate the system response, the phase portrait as well as the vector field diagram are depicted in Fig. 3.2.

*Remark* 3.2.1. It is important to notice that the converse Lyapunov theorem [24] [27] guarantees that there exists a Lyapunov function for any stable system. However, there is not a general method to find it. Indeed, the process of finding or constructing a Lyapunov function can be challenging. For instance, the trivial candidate of Lyapunov function, i.e. $V(x) = \frac{1}{2}(\alpha\,x_1^2 + \beta\,x_2^2)$ where $\alpha, \beta > 0$, cannot pass the conditions of Lyapunov functions in the previous example. To see this,

$$\begin{aligned} \dot{V}(x) &= [\alpha x_1 \quad \beta x_2] \cdot f(x) \\ &= 0.25\,\alpha\,x_1^2 + (4\,\beta - \alpha)\,x_1\,x_2 - 3\,\beta x_2^2 \\ &\quad - \alpha\,x_1(\text{sat}\,(x_1) + \text{sat}\,(x_2)) - \beta\,x_2(\text{sat}\,(x_1) + \sin(x_2)) \end{aligned} \tag{3.8}$$

Apparently, $\dot{V}(x_1, 0) = \alpha\,x_1(0.25\,x_1 - \text{sat}\,(x_1))$. For any $x_1 > \max(1, 4\,\alpha)$, we have $\dot{V} > 0$; thus, $V(x)$ fails the Lyapunov conditions and cannot be used to prove stability of the system.

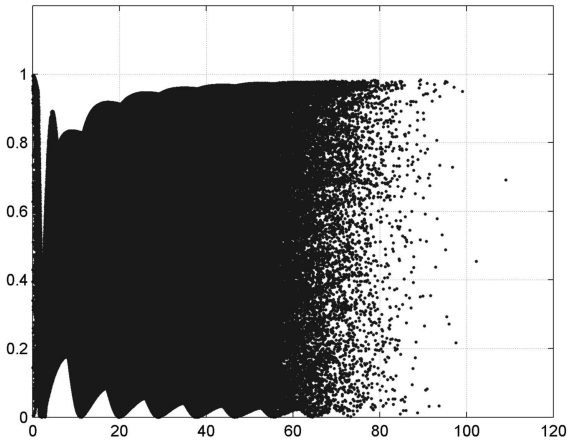


(a) $\frac{\|\Phi(x)\|_2}{\|x\|_2}$ versus $\|x\|_2$

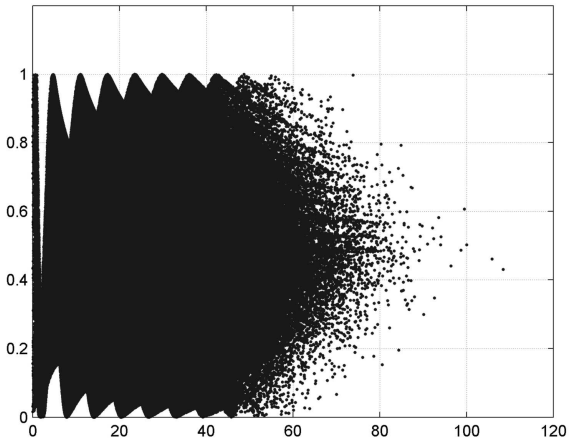


(b) $\frac{\|\Phi(x)\|_\infty}{\|x\|_\infty}$ versus $\|x\|_\infty$

Figure 3.1: $\gamma_2(\Phi)$ and $\gamma_\infty(\Phi)$ in Example 3.2.1.

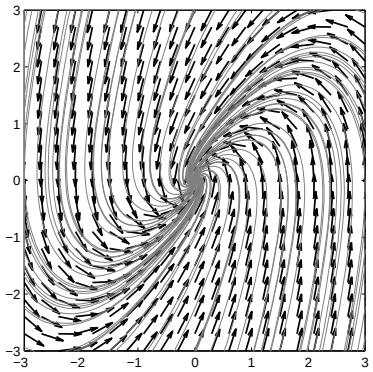


Figure 3.2: Phase portrait for Example 3.2.1.

**Example 3.2.2.** Consider the following nonlinear system

$$\begin{cases} \dot{x_1} &= -2\,x_1 + x_2 + \sin(0.5\,x_2) - \sin(0.5\,x_3) \\ \dot{x_2} &= -x_1 - x_2 + \sin(0.5\,x_1) - \sin(0.5\,x_3) \\ \dot{x_3} &= 1 - x_3 - \cos(0.5\,x_1) + \sin(0.5\,x_2) \end{cases} \tag{3.9}$$

Let $A = \begin{bmatrix} -2.0 & 1.2 & 0 \\ -0.8 & -1.0 & 0 \\ 0 & 0 & -1.0 \end{bmatrix}$ and

$$\Phi(x_1, x_2, x_3) = \begin{bmatrix} -0.2\,x_2 + \sin(0.5\,x_2) - \sin(0.5\,x_3) \\ -0.2\,x_1 + \sin(0.5\,x_1) - \sin(0.5\,x_3) \\ 1 - \cos(0.5\,x_1) + \sin(0.5\,x_2) \end{bmatrix} \tag{3.10}$$

Similar to the previous examples, we use the computational methods introduced in Section 2.3.1. We plot $\frac{\|\Phi(x)\|}{\|x\|}$ versus $\|x\|$ instead of plotting versus $x_1$, $x_2$ and $x_3$. plots are established at $2 \times 10^6$ randomly chosen points. As shown in Fig. 3.3, $\gamma_2(\Phi) \approx 0.8$ and $\gamma_\infty(\Phi) \approx 0.8$. Computation also shows that $\gamma_2(\Gamma) \approx 1.000$ and $\gamma_\infty(\Gamma) \approx 1.0005$. Since $\gamma_\infty(\Phi)\,\gamma_\infty(\Gamma) = 0.7938 < 1$ and $\gamma_2(\Phi)\,\gamma_2(\Gamma) = 0.7846 < 1$, the system is globally asymptotically stable.

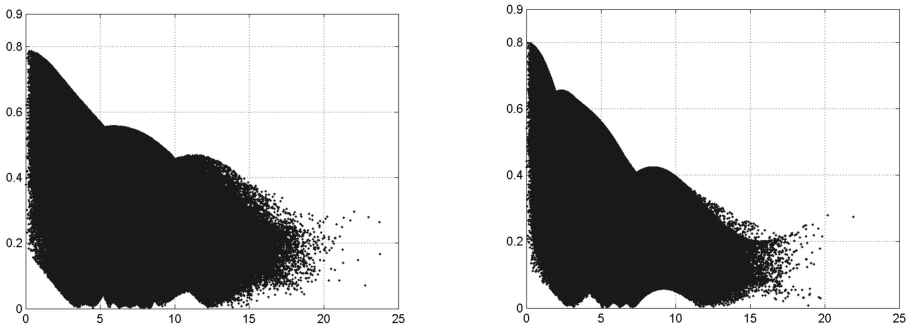


(a) $\frac{\|\Phi(x)\|_2}{\|x\|_2}$ versus $\|x\|_2$ (b) $\frac{\|\Phi(x)\|_\infty}{\|x\|_\infty}$ versus $\|x\|_\infty$

Figure 3.3: Local gains in Example 3.2.2.

### 3.2.2 Local Stability

**Definition 3.2.1.** Given a nonlinear system of the form either (2.13) or (2.22), we define the ordered pair $[\Delta, \Upsilon]$ as follows:

$$[\Delta, \Upsilon] := \{\Delta, \Upsilon \subset \mathbb{R}^n;\ x(0) \in \Delta \Rightarrow x(t) \in \Upsilon, \forall t \geq 0\} \tag{3.11}$$

We will refer to $\Delta$ and $\Upsilon$ as the $\Delta$ and $\Upsilon$ regions and collect all $[\Delta, \Upsilon]$ pairs of a system in a set denoted by $\mathcal{S}_{\Delta\Upsilon}$.

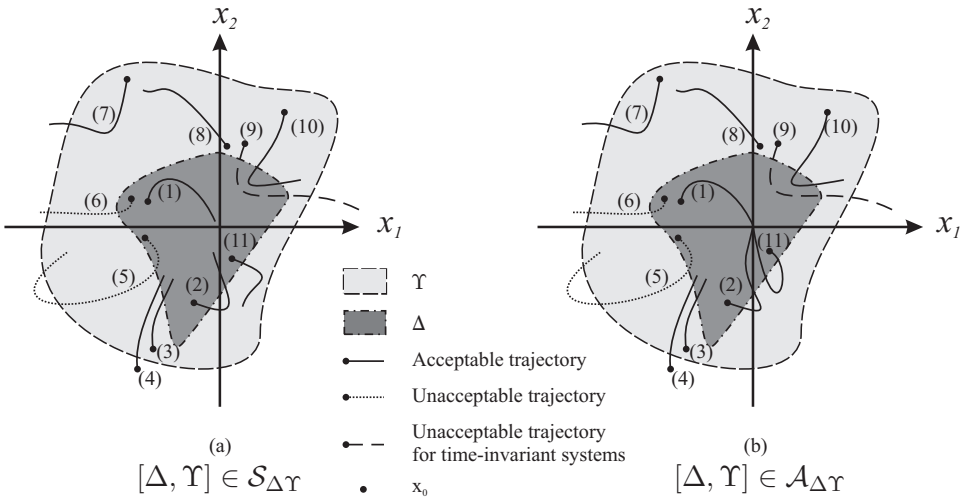


Figure 3.4: Acceptable and unacceptable trajectories.

**Definition 3.2.2.** For a given system, if $[\Delta, \Upsilon] \in \mathcal{S}_{\Delta\Upsilon}$ and for any $x(0) \in \Delta$ we have $x(t) \to 0$ as $t \to \infty$ then $\Delta$ and $\Upsilon$ are called asymptotic regions and we collect all such pairs in $\mathcal{A}_{\Delta\Upsilon}$.

Fig. 3.4 shows acceptable and unacceptable trajectories for both $[\Delta, \Upsilon] \in \mathcal{S}_{\Delta\Upsilon}$ and $[\Delta, \Upsilon] \in \mathcal{A}_{\Delta\Upsilon}$. As shown in this figure, $[\Delta, \Upsilon] \in \mathcal{S}_{\Delta\Upsilon}$ guarantees that the trajectories starting from inside of $\Delta$, such as (1),(2), and (11), will stay inside $\Upsilon$. Therefore, trajectories (5) and (6) can never occur because both trajectories cross the boundary of the $\Upsilon$ region. Notice that there is no guarantee that trajectories starting inside of $\Upsilon$, such as (7), stay inside $\Upsilon$. The definition of $\mathcal{S}_{\Delta\Upsilon}$ assures that trajectories such as (5) and (6) which start from $\Delta$ and go outside of $\Upsilon$ are not possible. An interesting case is (9). This case is possible for non-autonomous systems but impossible for autonomous systems. The reason is that for autonomous systems we can transfer $t = 0$ to any $t = t_0$. Since this trajectory passed through $\Delta$, we can transfer the starting point to any point on the trajectory which is also inside $\Delta$. With the new starting point, $[\Delta, \Upsilon] \in \mathcal{S}_{\Delta\Upsilon}$ guarantees that the trajectory will stay inside $\Upsilon$ which is not observed by (9). Therefore, for autonomous systems, any trajectory, which has intersection with $\Delta$, stays inside $\Upsilon$. Fig. 3.4(b) is very similar to Fig. 3.4(a). The only difference is that all trajectories starting from $\delta$, such as (1) and (2), terminate at the origin. For autonomous systems, any trajectory which has a point inside $\delta$ also end at the origin for the same reason explained earlier. Therefore, for autonomous systems, (3), (4) and (10) (and also (5), (6) and (9)) should also terminate at the origin.

**Corollary 3.2.1.** *If* $[\Delta, \Upsilon] \in \mathcal{S}_{\Delta\Upsilon}$

- $\Delta \subset \Upsilon$,
- $\Delta = \Upsilon$ *implies that* $\Upsilon$ *is an invariant set for the nonlinear system.*

**Proposition 3.2.1.** *Consider a system with* $\zeta_A$ *representation of* $[\Phi, \Gamma, \Omega]$. *Assume that* $\Upsilon$ *is a given bounded subset of* $\mathbb{R}^n$, *i. e.* $\|x\|_p < \epsilon$ *for all* $x \in \Upsilon$ *and* $p \in \{2, \infty\}$. *Let* $0 < \delta \leq \frac{1-\gamma_p(\Phi)\gamma_p(\Gamma)}{\gamma_p(\Omega)}\epsilon$ *and*

$$\Delta := \{x \in \mathbb{R}^n \,,\ \|x\|_p < \delta\} \tag{3.12}$$

*Then* $[\Delta, \Upsilon] \in \mathcal{S}_{\Delta\Upsilon}$.

*Proof.* The proof follows a routine similar to the proof of Theorem 3.2.1 and is omitted. □

Proposition 3.2.1 shows a method to compute $[\Delta, \Upsilon]$ regions.

**Definition 3.2.3.** Local gain $\gamma_p^{\mathcal{D}}(\Phi)$ of a static operator $\Phi$, where $p \in \{2, \infty\}$, is the maximum $p$-norm gain of the operator for all of the members inside the region $\mathcal{D}$, respectively. i.e.

$$\gamma_p^{\mathcal{D}}(\Phi) = \sup_{\substack{x \in \mathcal{D} - \{0\} \\ \forall t \geq 0}} \frac{\|\Phi(t,x)\|_p}{\|x\|_p} \tag{3.13}$$

**Theorem 3.2.3.** *Consider a nonlinear system with state space representation of either (2.13) or (2.22), and let* $[\Phi, \Gamma, \Omega]$ *be a* $\zeta_A$ *representation. Let* $M_p > \gamma_\infty(\Omega)$ *be a fixed number and*

$$\hat{\mathcal{D}} := \left\{ x \in \mathbb{R}^n \mid \gamma_\infty^{\hat{\mathcal{D}}}(\Phi) < \frac{1}{\gamma_\infty(\Gamma)}\left(1 - \frac{\gamma_\infty(\Omega)}{M_P}\right) \quad \forall t \geq 0 \right\} \tag{3.14a}$$

*Assume that* $\mathcal{D}$ *is a simply connected subset of* $\hat{\mathcal{D}}$ *that includes the origin. Let* $\xi = \inf_{x \in \partial\mathcal{D}} \|x\|_\infty$ *where* $\partial\mathcal{D}$ *is the boundary of* $\mathcal{D}$. *Let* $\Upsilon$ *be a ball inside* $\mathcal{D}$ *centered at the origin with radius* $\epsilon < \xi$. *i.e.*

$$\Upsilon = \{x \in \mathcal{D} \mid \|x\|_\infty < \epsilon\} \tag{3.14b}$$

*and let*

$$\Delta := \left\{ x \in \mathbb{R}^n \mid \|x\| < \delta,\ \delta := \frac{1 - \gamma_\infty^{\hat{\mathcal{D}}}(\Phi)\gamma_\infty(\Gamma)}{\gamma_\infty(\Omega)}\,\epsilon \right\} \tag{3.14c}$$

*Then,*

1. $[\Delta, \Upsilon] \in \mathcal{S}_{\Delta\Upsilon}$

2. *if $x_0 \in \Delta$ then $M_P$ is the maximum overshoot of $x(t)$.*

*Proof.* Since $M_p > \gamma_\infty(\Omega)$, (3.14a) reveals that $\gamma_\infty^{\hat{\mathcal{D}}}(\Phi)\gamma_\infty(\Gamma) < 1$. To prove the theorem we reason by contradiction. Since we assumed that systems of our interest are locally Lipschitz, trajectories of the system are continuous. As a consequence, if $x$ were to leave $\Upsilon$, it should cross the boundary of $\Upsilon$. Suppose that $x$ crosses the boundary of $\Upsilon$ at $t = T$; then $\|\mathbf{T}_T x\| = \|x_T\| = \epsilon$. Since the boundary of $\Upsilon$ is in $\mathcal{D}$, $\|x_T\| \leq \|d_T\| + \|w_T\| \leq \gamma_\infty(\Omega)\|x_0\| + \gamma_\infty^{\hat{\mathcal{D}}}(\Phi)\gamma_\infty(\Gamma)\|x_T\|$. Then $\|x_T\| \leq \frac{\gamma_\infty(\Omega)}{1-\gamma_\infty^{\hat{\mathcal{D}}}(\Phi)\gamma_\infty(\Gamma)}\|x_0\| < \frac{\gamma_\infty(\Omega)}{1-\gamma_\infty^{\hat{\mathcal{D}}}(\Phi)\gamma_\infty(\Gamma)}\delta < \epsilon$. Which contradicts the fact that $\|x_T\| = \epsilon$. Therefore, $x(t) \in \Upsilon;\ \forall t \geq 0$. That is $[\Delta, \Upsilon] \in \mathcal{S}_{\Delta\Upsilon}$. To show the second part, from (3.14a), we have $\frac{\gamma_\infty(\Omega)}{1-\gamma_\infty^{\hat{\mathcal{D}}}(\Phi)\gamma_\infty(\Gamma)} < M_p$. On the other hand, $\|x\| \leq \frac{\gamma_\infty(\Omega)}{1-\gamma_\infty^{\hat{\mathcal{D}}}(\Phi)\gamma_\infty(\Gamma)}\|x_0\| < M_p\|x_0\|$ □

**Theorem 3.2.4.** *Let $[\Phi, \Gamma, \Omega]$ be a $\zeta_A$ representation for a nonlinear system in the form of either (2.13) or (2.22). Let $\Upsilon := \{x \in \mathbb{R}^n \mid \|x\| < \epsilon\}$ and $\Delta := \{x \in \mathbb{R}^n \mid \|x\| < \delta, \}$. If $[\Delta, \Upsilon] \in \mathcal{S}_{[\Delta,\Upsilon]}$ and $\gamma_2^\Upsilon(\Phi).\gamma_2(\Gamma) < 1$ then $[\Delta, \Upsilon] \in \mathcal{A}_{[\Delta,\Upsilon]}$.*

*Proof.* Since $[\Delta, \Upsilon] \in \mathcal{S}_{[\Delta,\Upsilon]}$, any trajectory starting from $\Delta$ will stay inside $\Upsilon$. According to the $\zeta_A$ representation, $\|x\|_{\mathcal{L}_2} < \frac{1-\gamma_2^\Upsilon(\Phi)\,\gamma_2(\Gamma)}{\gamma_2(\Omega)}\|x_0\|_2 < \infty$ and consequently $x \in \mathcal{L}_2$.

For discrete-time systems, since $\gamma_2^\Upsilon(\Phi).\gamma_2(\Gamma) < 1$, $\|x\|_{\ell_2} < \infty$ and as a result $x(t) \in \ell_2$. Consequently $x(t) \to 0$ as $t \to \infty$. It turns out that $[\Delta, \Upsilon] \in \mathcal{A}_{[\Delta,\Upsilon]}$.

For continuous-time systems, Corollary 3.2.1 should be used. Since $x(t) \in \Upsilon$ for all $t$, $x \in \mathcal{L}_\infty$ and consequently $x \in \mathcal{L}_2 \cap \mathcal{L}_\infty$. The proof, which is omitted here, follows the same outline as the proof of Theorem 3.2.1(ii) with $\mathcal{D} \equiv \Upsilon$.

□

**Corollary 3.2.2.** *Let $[\Phi, \Gamma, \Omega]$ be a $\zeta_A$ representation for a nonlinear system in the form of either (2.13) or (2.22). If there exists a region around the origin $\hat{\mathcal{D}}$ where $\gamma_\infty^{\hat{\mathcal{D}}}(\Phi)\gamma_\infty(\Gamma) < 1$, then the system is locally stable. If in addition $\gamma_2^{\hat{\mathcal{D}}}(\Phi)\gamma_2(\Gamma) < 1$, then the system is locally asymptotically stable.*

*Proof.* Since $\gamma_\infty^{\hat{\mathcal{D}}}(\Phi)\gamma_\infty(\Gamma) < 1$, there exists $M_p > \gamma_\infty(\Omega)$ such that $\gamma_\infty^{\hat{\mathcal{D}}}(\Phi) < \frac{1}{\gamma_\infty(\Gamma)}\left(1 - \frac{\gamma_\infty(\Omega)}{M_P}\right)$. Let $\mathcal{D}$ be a simply connected subset of $\hat{\mathcal{D}}$ that includes the origin. Let $\xi = \inf_{x\in\partial\mathcal{D}} \|x\|_\infty$ where $\partial\mathcal{D}$ is the boundary of $\mathcal{D}$. For any $\epsilon$ that satisfies $0 < \epsilon < \xi$, $\Delta$ and $\Upsilon$ can be constructed as (3.14) and $\delta > 0$ in (3.14c) can be found. Theorem 3.2.3 guarantees that $[\Delta, \Upsilon] \in \mathcal{S}_{\Delta\Upsilon}$ or equivalently

$$\|x(0)\| < \delta \Longrightarrow \|x(t)\| < \epsilon,\ \forall t \geq 0 \tag{3.15}$$

The second part is trivial consequence of Theorem 3.2.4. □

**Corollary 3.2.3.** Sufficient condition of stability in Lyapunov Linearization Method

*If the linearized system of a nonlinear system is stable, the nonlinear system is locally asymptotically stable.*

*Proof.* Let $A$ be the linearized part, i.e. $A = \frac{\partial f(x)}{\partial x}\Big|_{x=0}$. Since $A$ is stable, $\gamma_\infty(\Gamma) < \infty$ and $\gamma_2(\Gamma) < \infty$. Since $\Phi(x)$ only includes the higher order terms in $x$, the exists a region around the origin $\hat{\mathcal{D}}$ where $\gamma_\infty^{\hat{\mathcal{D}}}(\Phi)$ and $\gamma_2^{\hat{\mathcal{D}}}(\Phi)$ can be made arbitrarily small. Thus, Corollary 3.2.2 implies local asymptotic stability of the nonlinear system. □

**Example 3.2.3.** Consider the following nonlinear system.

$$\begin{cases} \dot{x}_1 = -2x_1 + x_2 - \sqrt{x_1^3}/3 + x_2^2/4 \\ \dot{x}_2 = -2x_1 + 2x_2 + x_1^2/10 - 5\sin(x_2)/2 \end{cases} \tag{3.16}$$

Let choose $A = \begin{bmatrix} -2 & 1 \\ -2 & -3 \end{bmatrix}$ then $\Phi(x) = \begin{cases} -\sqrt{x_1^3}/3 + x_2^2/4 \\ +5x_2 + x_1^2/10 - 5\sin(x_2)/2 \end{cases}$. Using (2.4b) and (2.8) respectively, $\gamma_\infty(\Gamma) = 0.5378$ and $\gamma_\infty(\Omega) = 1$. Direct computation, as discussed in Section 2.3.3, gives $\gamma_\infty(\Phi) = \infty$, which implies that Theorem (3.2.1) can not be applied. Assume that $M_P = 1.5$, then $\gamma_\infty^{\mathcal{D}}(\Phi) < \frac{1}{\gamma_\infty(\Gamma)}\left(1 - \frac{\gamma_\infty(\Omega)}{M_p}\right) = 0.6197$. $\gamma_\infty(\Phi)$ is plotted versus $x$ in Fig. 3.5(a) and its junction with the plan $\gamma_\infty^{\mathcal{D}}(\Phi)$ is marked. The junction determines the boundary of $\mathcal{D}$, as shown in Fig. 3.5(c). $\gamma_2(\Phi)$ and its junction with $\frac{1}{\gamma_2(\Gamma)}$ are shown in Fig. 3.5(b). Since $\mathcal{L}_\infty$-norm is used, the largest ball inside $\mathcal{D}$, i.e. $\Upsilon$, is the square shown in Fig. 3.5(c). Since $M_P = 1.5$, the largest $\Delta$ area is another square inside $\Upsilon$ and smaller than it with factor $M_P$, as shown in Fig. 3.5(c). Theorem 3.2.3 guarantees that any trajectory starting from inside $\Delta$ will stay inside $\Upsilon$. Moreover, since $\Upsilon$ and $\Delta$ are placed inside the region where $\gamma_2(\Phi)\gamma_2(\Gamma) < 1$, Theorem 3.2.4 guarantees that all trajectories starting from $\Delta$ end at the origin. Since the system is autonomous, this is also the case for all trajectories which has intersection with $\Delta$. System trajectories as well as some of its responses to various initial conditions are depicted in Fig. 3.6. In the first graph, since the initial states (or one of them) are not in $\Delta$, stability is not guaranteed and the system is unstable. For the rest, initial states are in $\Delta$ and consequently, the system is stable and states terminate at the origin.

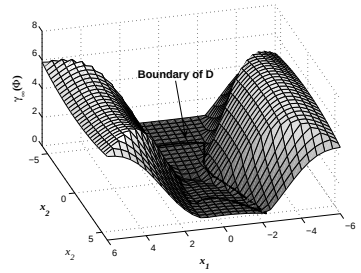


(a) $\gamma_\infty(\Phi)$ crossed by $\frac{1}{\gamma_2(\Gamma)}\left(1-\frac{\gamma_\infty(\Omega)}{M_p}\right)$

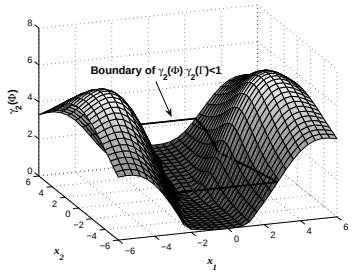


(b) $\gamma_2(\Phi)$ crossed by $\frac{1}{\gamma_2(\Gamma)}$

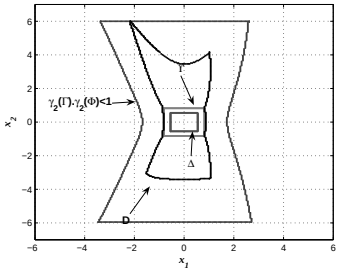


(c) Regions

Figure 3.5: Various regions in Example 3.2.3

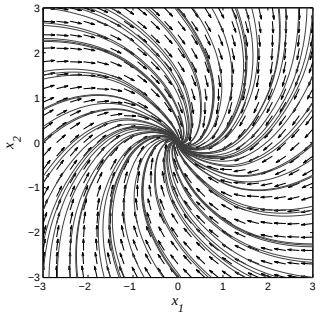

(a) System trajectories for Example 3.2.3

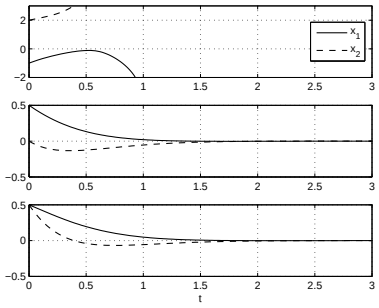


(b) Some responses for the system in Example 3.2.3

Figure 3.6: Simulation results for Example 3.2.3.

## 3.3 Forced Systems

### 3.3.1 Global Stability

**Proposition 3.3.1.** *For a forced nonlinear system with $\zeta_{AB}$ representation of $[\Phi, \Theta, \Gamma, \Omega]$, if $u \in \mathcal{X}_p$ and $\gamma_p(\Phi)\gamma_p(\Gamma) < 1$ then $x \in \mathcal{X}_p$ for any initial state $x_0$.*

*Proof.* The proof for discrete-time systems is very similar to the continuous-time case and is omitted.

Since $A$ is stable, $\|e^{At}\|_{\mathcal{L}_p} < \infty$ and $u \in \mathcal{L}_p$ implies that $\|d_1\| \leq \|e^{At}\|_{\mathcal{L}_p} \cdot \|x_0\|_p + \gamma_\infty(\theta)\|u(t)\|_p < \infty$ and $d_1 \in \mathcal{L}_p$. On the other hand, since $\left\| \begin{bmatrix} 0 \\ I_{m\times m} \end{bmatrix} \right\|_p = 1$, and $u \in \mathcal{L}_p$ then $d_2 \in \mathcal{L}_p$. According to small gain theorem, e.g. [27], since input signals to the loop, i.e. $d_1$,$d_2$, are in $\mathcal{L}_p$ and $\left\| \begin{bmatrix} I_{n\times n} \\ 0 \end{bmatrix} \right\|_p = 1$, $\gamma_p(\Phi) \cdot \gamma_p(\Gamma) < 1$ implies that all internal signals of the system are in $\mathcal{L}_p$. Therefore, $x \in \mathcal{L}_p$ □

**Definition 3.3.1.** A nonlinear system in the form of either (2.30) or (2.33) is called *stable in general* or *generally stable* if

$$\forall \epsilon > 0, t \geq 0 \; \exists \delta, \eta > 0; \quad \left.\begin{matrix} \|x_0\| < \delta \\ \|u(t)\| < \eta\delta \end{matrix}\right\} \Rightarrow \|x(t)\| < \epsilon \tag{3.17}$$

In addition, if for any $x_0$ and input that satisfies $u(t) \to 0$ as $t \to \infty$, the state also satisfies $x(t) \to 0$ as $t \to \infty$, then the system is called *asymptotically generally stable*.

Any Euclidean norm can be used in the definition but once a norm is chosen, it should be used for all norms. Besides, it is trivial to show that if a system is general (asymptotic) stable using an arbitrary Euclidean norm, the property holds for all Euclidean norms.

**Definition 3.3.2.** A system is called $\mathcal{X}_p$*−(asymptotically) generally stable* or $\mathcal{X}_p$*− (asymptotically) stable in general* if it is (asymptotically) generally stable for input $u \in \mathcal{X}_p$.

**Lemma 3.3.1.** *For a generally (asymptotically) stable system, if $u = 0$ then the system is (asymptotically) stable in sense of Lyapunov.*

*Proof.* The proof follows directly from the definition by taking $u = 0$. □

**Lemma 3.3.2.** *ISS systems are generally stable.*

*Proof.* Considering that $\|u\|_{\mathcal{X}_\infty} < \epsilon_1$ implies that there exists $\epsilon_2$ such that $\|u(t)\|_p < \epsilon_2$ for all $t > 0$ and $p \in [1, \infty)$, this lemma is very similar to Lemma 2.7 in [36] and the proof follows same outline as its proof. □

**Lemma 3.3.3.** *A generally stable system is ISS stable if and only if there exists a class $\mathcal{K}$ function $\sigma_1$ and $T > 0$ such that $x(t) \leq \sigma_1(\|u\|_{\mathcal{L}_\infty})$ for all $t > T$.*

*Proof.* This lemma is also similar to Lemma 2.7 in [36] and the proof is the same. □

Lemmas 3.3.2 and 3.3.3 show that the set of ISS systems is a subset of the set of generally stable systems but the inverse is not true in general. Generally speaking, for a generally stable system the condition in Lemma 3.3.3 should be satisfied to guarantee ISS stability.

The following theorem provides a sufficient condition for stability of systems in general.

**Theorem 3.3.1.** *For a forced nonlinear system with $\zeta_{AB}$ representation of $[\Phi, \Theta, \Gamma, \Omega]$,*

*(i) If $\gamma_\infty(\Phi) \cdot \gamma_\infty(\Gamma) < 1$ then the system is $\mathcal{X}_\infty-$ globally generally stable.*

*(ii) In addition to (i), if $\gamma_2(\Phi).\gamma_2(\Gamma) < 1$ then the system is $\mathcal{X}_2 \cap \mathcal{X}_\infty-$ globally asymptotically generally stable.*

*Proof.* The proof for discrete-time systems is very similar and is omitted.
(i) In this section of the proof, all norms are either $\infty$-norm or $\mathcal{L}_\infty$-norm depend on the case. According to Proposition 3.3.1, since $u \in \mathcal{L}_\infty$ then $x \in \mathcal{L}_\infty$. To show that the system is generally stable, it is enough to show that for any given $\epsilon$ there exist $\delta$ and $\eta$ such that $\left.\begin{matrix}\|x_0\|_\infty < \delta \\ \|u(t)\|_\infty < \eta\delta\end{matrix}\right\} \Rightarrow \|x(t)\|_\infty < \epsilon$ for all $t \geq 0$. Choose $\eta > 0$ arbitrary. We claim that for any given $\epsilon$, $\delta$ can be chosen as $\delta < \frac{1-\gamma_\infty(\Phi)\gamma_\infty(\Gamma)}{\eta(\gamma_\infty(\Theta)+\gamma_\infty(\Phi)\gamma_\infty(\Gamma))+\gamma_\infty(\Omega)}\epsilon$. To prove,

$$\begin{aligned}
\|x\| &\leq \|d_1\| + \|w\| \\
&\leq \|d_1\| + \gamma_\infty(\Phi)\gamma_\infty(\Gamma)(\|d_2\| + \|x\|) \\
&\leq \gamma_\infty(\Omega)\|x_0\| + [\gamma_\infty(\Theta) + \gamma_\infty(\Phi)\gamma_\infty(\Gamma)]\|u\| + \gamma_\infty(\Phi)\gamma_\infty(\Gamma)\|x\| \\
&< \gamma_\infty(\Omega)\delta + [\gamma_\infty(\Theta) + \gamma_\infty(\Phi)\gamma_\infty(\Gamma)]\,\eta\delta + \gamma_\infty(\Phi)\gamma_\infty(\Gamma)\|x\| \\
&< (\gamma_\infty(\Omega) + \eta\,[\gamma_\infty(\Theta) + \gamma_\infty(\Phi)\gamma_\infty(\Gamma)])\,\delta + \gamma_\infty(\Phi)\gamma_\infty(\Gamma)\|x\|
\end{aligned}$$

then $\|x\| < \frac{\gamma_\infty(\Omega)+\eta(\gamma_\infty(\Theta)+\gamma_\infty(\Phi)\gamma_\infty(\Gamma))}{1-\gamma_\infty(\Phi)\gamma_\infty(\Gamma)}\delta < \epsilon$. Since for any given $\epsilon$ there exists some $\delta$, stability is global.

(ii) According to Proposition (3.3.1), since $u \in \mathcal{L}_2 \cap \mathcal{L}_\infty$ then $x \in \mathcal{L}_2 \cap \mathcal{L}_\infty$ and consequently there exist closed sets $\mathcal{D}_u$ and $\mathcal{D}_x$ such that $u(t) \in \mathcal{D}_u$ and $x(t) \in \mathcal{D}_x$ for all $t$. Assuming that $f(x, u, t)$ is locally Lipschitz in both $u \in \mathcal{D}_u$ and $x \in \mathcal{D}_x$, there exists $\mu$ such that

$$\forall\, x_1, x_2 \in \mathcal{D}_x,\ \forall\, u \in \mathcal{D}_u, \quad \|f(x_2, u, t) - f(x_1, u, t)\|_\infty \leq \mu\|x_2 - x_1\|_\infty \tag{3.18}$$

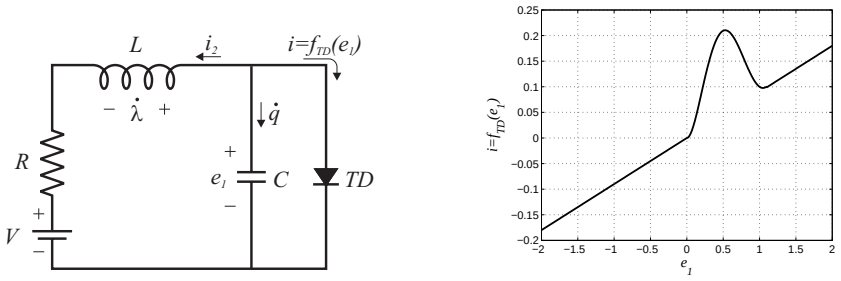


(a) The circuit (b) Tunnel diode characterization

Figure 3.7: Tunnel diode oscillator in Example 3.3.1.

Taking $x_1 = 0$ and $x_2 = x(t)$

$$\forall\, x(t) \in \mathcal{D}_x,\ \forall\, u(t) \in \mathcal{D}_u, \quad \|f(x(t), u(t), t)\|_\infty \leq \mu \|x(t)\|_\infty \tag{3.19}$$

Since $x \in \mathcal{L}_\infty$, $\|x(t)\|_\infty \leq \|x\|_{\mathcal{L}_\infty}$ for all $t$. Substituting in (3.19),

$$\|\dot{x}(t)\|_\infty = \|f(x(t), u(t), t)\|_\infty \leq \mu \|x\|_{\mathcal{L}_\infty} \tag{3.20}$$

for all $t$. In turn, this means that $\dot{x} \in \mathcal{L}_\infty$. Considering $x \in \mathcal{L}_2 \cap \mathcal{L}_\infty$ and $\dot{x} \in \mathcal{L}_\infty$, the rest of the proof follows same lines of the proof of Theorem 3.2.1(ii) and omitted here. □

Similar to Section 3.2.1, $A$ and $B$ play the role of free parameters in Proposition 3.3.1 and Theorem 3.3.1. Likewise, it is sufficient to find just one pair of $A$ and $B$ which satisfies the conditions of the proposition or the theorem. If such a pair is found, the proposition or the theorem can be used even if there exists other pairs of $A$ and $B$ matrices which fail the conditions. If such a pair of $A$ and $B$ cannot be found or does not exist, the proposition or the theorem cannot be used.

**Example 3.3.1.** (*"Hard" tunnel diode oscillator*) ( [37] pp. 446) The network of Fig. 3.7(a) represents a tunnel diode with some associated capacitance and inductance, biased by a combination of voltage source and resistance. The state equations for this network may be written as

$$\begin{aligned} \dot{q} &= -i_2 - f_{TD}(e_1), & e_1 &= \tfrac{q}{C}, \\ \dot{\lambda} &= e_1 - R i_2 - V, & i_2 &= \tfrac{\lambda}{L}, \end{aligned} \tag{3.21}$$

where the function $f_{TD}(e_1)$ represents the tunnel diode branch relation. Let $x_1 := q = e_1$, $x_2 := -\lambda = -i_2$, $R = 1$, $L = 1$, $u = V$ and $f_{TD}(\cdot)$ be

$$i = f_{TD}(e_1) = \begin{cases} -1.7e_1^5 + 6.6e_1^4 - 8.4e_1^3 + 3.6e_1^2 & 0 < e_1 \leq 1.1 \\ 0.09e_1 & \text{otherwise} \end{cases}$$

which is depicted in Fig. 3.7(b). Substituting defined states,

$$\dot{x} = f(x) = \begin{cases} x_2 - f_{TD}(x_1) \\ -x_1 - x_2 + u \end{cases}$$

Choosing $A = \begin{bmatrix} -0.3 & 1 \\ -1 & -1 \end{bmatrix}$, we have $\Phi(x) = \begin{pmatrix} 0.3x_1 - f_{TD}(x_1) \\ 0 \end{pmatrix}$. Computation shows that $\gamma_\infty(\Phi) = \gamma_2(\Phi) < 0.3$, $\gamma_\infty(\Gamma) < 2.17$ and $\gamma_2(\Gamma) = 1.641$. Since $\gamma_2(\Phi).\gamma_2(\Gamma) < 1$ and $\gamma_\infty(\Phi).\gamma_\infty(\Gamma) < 1$, according to Theorem 3.3.1, the system is $\mathcal{L}_2 \cap \mathcal{L}_\infty-$ globally asymptotically generally stable. This means that for any initial state and input $\{u \in \mathcal{L}_2 \cap \mathcal{L}_\infty : \lim_{t\to\infty} u \to 0\}$, state is bounded and approaches 0 as $t \to \infty$.

### 3.3.2 Local Stability

**Theorem 3.3.2.** *Let $[\Phi, \Theta, \Gamma, \Omega]$ be a $\zeta_{AB}$ representation for a nonlinear system. Let $\eta > 0$ and $M_p > \gamma_\infty(\Omega) + \eta\gamma_\infty(\theta)$ and*

$$\hat{\mathcal{D}} := \left\{ \begin{bmatrix} x \\ u \end{bmatrix} \in \mathbb{R}^{n+m} \;\middle|\; \gamma_\infty^{\hat{\mathcal{D}}}(\Phi) < \frac{M_p - \gamma_\infty(\Omega) - \eta\gamma_\infty(\theta)}{(M_p + \eta)\gamma_\infty(\Gamma)} \right\} \tag{3.22}$$

*Let $\mathcal{D} := \mathbf{B}^\infty(o, \xi_D)$ be an open ball inside $\hat{\mathcal{D}}$. Let $\mathcal{D}_x$ and $\mathcal{D}_u$ be the images of $\mathcal{D}$ under $\begin{bmatrix} I_{n\times n} & 0_{n\times m} \\ 0_{m\times n} & 0_{m\times m} \end{bmatrix}$ and $\begin{bmatrix} 0_{n\times n} & 0_{n\times m} \\ 0_{m\times n} & I_{m\times m} \end{bmatrix}$, respectively. Consequently, $\mathcal{D}_x$ and $\mathcal{D}_u$ are also open balls in $\mathbb{R}^n$ and $\mathbb{R}^m$ respectively. Let $\xi_x$ and $\xi_u$ denote respectively their radius, i.e. $\mathcal{D}_x = \mathbf{B}^\infty(0, \xi_x)$ and $\mathcal{D}_u = \mathbf{B}^\infty(0, \xi_u)$. Choose $\epsilon$ and $\delta$ such that $0 < \epsilon < \xi_x$ and*

$$0 < \delta \leq \frac{1 - \gamma_\infty^{\mathcal{D}}(\Phi)\gamma_\infty(\Gamma)}{\gamma_\infty(\Omega) + \eta(\gamma_\infty(\Theta) + \gamma_\infty^{\mathcal{D}}(\Phi)\gamma_\infty(\Gamma))}\,\epsilon$$

*If $\|u\|_{\mathcal{X}_\infty} < \min(\eta\,\delta, \xi_u)$ and $\|x_0\|_\infty \leq \delta$, then*

$$\|x\|_{\mathcal{X}_\infty} < \epsilon \tag{3.23}$$

*Proof.* The proof for discrete-time systems is very similar and is omitted. In this proof, vector norms are Euclidean $\infty$-norm for constant vectors and $\mathcal{X}_\infty$-norm for time-varying ones.

It is trivial that $M_p - \gamma_\infty(\Omega) - \eta\gamma_\infty(\theta) < M_p + \eta$; therefore $\gamma_\infty^{\mathcal{D}}(\Phi)\gamma_\infty(\Gamma) < 1$. We use contradiction to prove the theorem. Since we assumed that systems of interest are locally Lipschitz, system trajectories are continuous. Consequently, if $x$ were to leave the ball with radius $\epsilon$, it should cross the boundary of the ball. Suppose that $x$ crosses the boundary at $t = T$. As a result, $\|\mathbf{T}_T x\| = \|x_T\| = \epsilon$. Since $\epsilon < \xi_x$ and $\|u\| < \min(\eta\,\delta, \xi_u)$ guarantees

that $u \in \mathcal{D}_u$, we have $\begin{bmatrix} x_T \\ u_T \end{bmatrix} \in \mathcal{D}$ and consequently

$$\begin{aligned}
\|x_T\| &\leq \|d_{1T}\| + \|w_T\| \\
&\leq \|d_{1T}\| + \gamma_\infty^{\mathcal{D}}(\Phi)\gamma_\infty(\Gamma)(\|d_{2T}\| + \|x_T\|) \\
&\leq \gamma_\infty(\Theta)\|u_T\| + \gamma_\infty(\Omega)\|x_0\| + \gamma_\infty^{\mathcal{D}}(\Phi)\gamma_\infty(\Gamma)\|x_T\| + \gamma_\infty^{\mathcal{D}}(\Phi)\gamma_\infty(\Gamma)\|u_T\| \\
&\leq \gamma_\infty(\Omega)\|x_0\| + [\gamma_\infty(\Theta) + \gamma_\infty^{\mathcal{D}}(\Phi)\gamma_\infty(\Gamma)]\|u_T\| + \gamma_\infty^{\mathcal{D}}(\Phi)\gamma_\infty(\Gamma)\|x_T\| \\
&< \gamma_\infty(\Omega)\delta + \left[\gamma_\infty(\Theta) + \gamma_\infty^{\mathcal{D}}(\Phi)\gamma_\infty(\Gamma)\right]\eta\delta + \gamma_\infty(\Phi)^{\mathcal{D}}\gamma_\infty(\Gamma)\|x_T\| \\
&= \left(\gamma_\infty(\Omega) + \eta\left[\gamma_\infty(\Theta) + \gamma_\infty^{\mathcal{D}}(\Phi)\gamma_\infty(\Gamma)\right]\right)\delta + \gamma_\infty^{\mathcal{D}}(\Phi)\gamma_\infty(\Gamma)\|x_T\| \qquad (3.24)
\end{aligned}$$

Then

$$\begin{aligned}
\epsilon &= \|x_T\| < \frac{\gamma_\infty(\Omega) + \eta\left[\gamma_\infty(\Theta) + \gamma_\infty^{\mathcal{D}}(\Phi)\gamma_\infty(\Gamma)\right]}{1 - \gamma_\infty^{\mathcal{D}}(\Phi)\gamma_\infty(\Gamma)}\|x_0\| \\
&\leq \frac{\gamma_\infty(\Omega) + \eta\left[\gamma_\infty(\Theta) + \gamma_\infty^{\mathcal{D}}(\Phi)\gamma_\infty(\Gamma)\right]}{1 - \gamma_\infty^{\mathcal{D}}(\Phi)\gamma_\infty(\Gamma)}\,\delta \\
&\leq \epsilon \qquad (3.25)
\end{aligned}$$

Which is a contradiction. Therefore, $x(t) \in \Upsilon;\ \forall t \geq 0$. That is $[\Delta, \Upsilon] \in \mathcal{S}_{\Delta\Upsilon}$. To show the second part, from (3.22), with some mathematical manipulation, we have $\frac{\gamma_\infty(\Omega)+\eta\left[\gamma_\infty(\Theta)+\gamma_\infty^{\mathcal{D}}(\Phi)\gamma_\infty(\Gamma)\right]}{1-\gamma_\infty^{\mathcal{D}}(\Phi)\gamma_\infty(\Gamma)} \leq M_p$. On the other hand, with a very similar procedure to (3.25),

$$\|x\| < \frac{\gamma_\infty(\Omega) + \eta\left[\gamma_\infty(\Theta) + \gamma_\infty^{\mathcal{D}}(\Phi)\gamma_\infty(\Gamma)\right]}{1 - \gamma_\infty^{\mathcal{D}}(\Phi)\gamma_\infty(\Gamma)}\|x_0\| \leq M_p\|x_0\|.$$

□

**Theorem 3.3.3.** *In Theorem 3.3.2, if in addition $\mathcal{D}$ satisfies $\gamma_2(\Gamma)\gamma_2^{\mathcal{D}}(\Phi) < 1$ Then $[\Delta, \Upsilon] \in \mathcal{A}_{[\Delta,\Upsilon]}$ for $\{u \in \mathcal{X}_2 \cap \mathcal{X}_\infty : \|u\|_{\mathcal{X}_\infty} < \min(\eta\,\delta, \xi_u)\}$.*

*Proof.* The proof for discrete-time systems is very similar and is omitted.

Theorem 3.3.2 guarantees that $[\Delta, \Upsilon] \in \mathcal{S}_{[\Delta,\Upsilon]}$ for all $u$ that satisfies

$$\{u \in \mathcal{L}_2 \cap \mathcal{L}_\infty : \|u\|_{\mathcal{L}_\infty} < \min(\eta\,\delta, \xi_u)\}$$

which means that $x$ stays in $\Upsilon \subset \mathcal{D}_x$. Since $\|u\|_{\mathcal{L}_\infty} < \xi_u$, $u \in \mathcal{D}_u$ then $\begin{bmatrix} x \\ u \end{bmatrix} \in \mathcal{D}$. According to Small Gain Theorem, $\gamma_2(\Gamma).\gamma_2^{\mathcal{D}}(\Phi) < 1$ guarantees that the loop is $\mathcal{L}_2$ internally stable and $x \in \mathcal{L}_2$ if $d_1$ and $d_2$ are in $\mathcal{L}_2$. Since $x_0 < \infty$ and $u \in \mathcal{L}_2$, $d_1$ and $d_2$ are in $\mathcal{L}_2$. Consequently, $x \in \mathcal{L}_2$. By the argument used in the proof of Theorem 3.3.1, it is easy to show that $\dot{x} \in \mathcal{L}_\infty$. Having $x \in \mathcal{L}_2 \cap \mathcal{L}_\infty$ and $\dot{x} \in \mathcal{L}_\infty$, Corollary 3.2.1 can be used as the proof of 3.2.1(ii) to show that $x \to 0$ as $t \to \infty$. This shows that $[\Delta, \Upsilon] \in \mathcal{A}_{[\Delta,\Upsilon]}$.

□

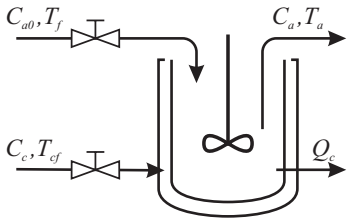


Figure 3.8: A simplified schematic of CSTR system.

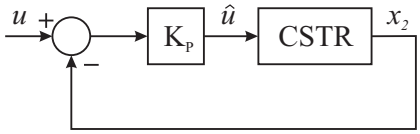


Figure 3.9: The CSTR system controlled by a proportional controller.

**Example 3.3.2.** Consider an example of continuous-stirred tank reactor (CSTR) system shown in Fig. 3.8, where an irreversible, first-order reaction takes place. CSTR is used to convert reactants to products. The reactant is fed constantly into a vessel where a chemical reaction takes place and yields the desired product. The heat generated by the chemical reaction is removed by the coolant medium that is circulated through a jacket. The following mathematical model is taken from [47],

$$\begin{cases} \dot{\hat{x}}_1 = -\hat{x}_1 + D_a(1-\hat{x}_1)e^{\frac{\hat{x}_2}{1+\frac{\hat{x}_2}{\varphi}}} \\ \dot{\hat{x}}_2 = -\hat{x}_2 + B_h D_a(1-\hat{x}_1)e^{\frac{\hat{x}_2}{1+\frac{\hat{x}_2}{\varphi}}} + \beta_h(\hat{u}-\hat{x}_2) \end{cases} \tag{3.26}$$

where $\hat{x}_1$, $\hat{x}_2$, and $\hat{u}_1$ are the dimensionless reagent conversion, the temperature (output), and the coolant temperature (input), respectively. The numerical values for the coefficients are $D_a = 0.072$, $\varphi = 20$, $B_h = 8$, and $\beta_h = 0.3$

Three operating points are considered in [9]. One of them is an unstable point, $\hat{u}_{10} = 0, \hat{x}_{10} = 0.4472$, and $\hat{x}_{20} = 2.7517$. Let transfer the origin of the state plane into this unstable point, which is investigated here. Therefore, we define $x_1 := \hat{x}_1 - \hat{x}_{10}$ and $x_2 = \hat{x}_2 - \hat{x}_{20}$. We study the closed-loop system which is depicted in Fig. 3.9 where $K_P = 100$ is a proportional controller and $u$ is an exogenous input which can be interpreted as sensor noise or disturbance. This controller can stabilize the closed-loop system locally. In this example, we want to determine the corresponding local region.

The state equations for closed-loop system are

$$\begin{cases} \dot{x_1} = -x_1 - 0.4472 + 0.072(0.5528 - x_1)e^{\frac{20x_2+55.034}{22.7517+x_2}} \\ \dot{x_2} = -31.3x_2 - 3.5772 + 0.576(0.5528 - x_1)e^{\frac{20x_2+55.034}{22.7517+x_2}} + 30u \end{cases} \tag{3.27}$$

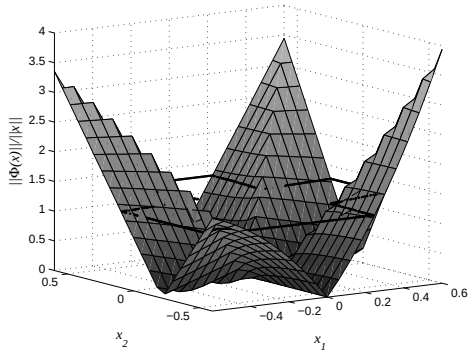


Figure 3.10: $\frac{\|\Phi(x)\|_\infty}{\|x\|_\infty}$ and the boundary of $\mathcal{D}$.

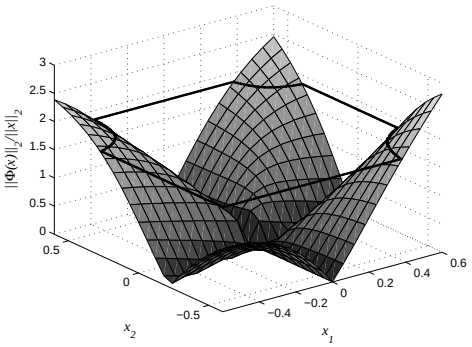


Figure 3.11: $\frac{\|\Phi(x)\|_2}{\|x\|_2}$ and the boundary of $\gamma_2(\Gamma)\gamma_2(\Phi) < 1$.

Let $A = \begin{bmatrix} -1.81 & 0.357 \\ -6.474 & -28.143 \end{bmatrix}$ and $B = \begin{bmatrix} 0 \\ 30 \end{bmatrix}$ then $\Phi(x) = \begin{bmatrix} \Phi_1(x) \\ \Phi_2(x) \end{bmatrix}$ where $\Phi_1(x) = -0.81x_1 - 0.357x_2 - 0.4472 + 0.072(0.5528 - x_1)e^{\frac{20x_2+55.034}{22.7517+x_2}}$ and $\Phi_2(x) = -3.157x_2 + 6.474x_1 - 3.5772 + 0.576(0.5528 - x_1)e^{\frac{20x_2+55.034}{22.7517+x_2}}$. Computation shows that upper bound can not be found for $\gamma_\infty(\Phi)$ and $\gamma_2(\Phi)$. Therefore, global stability can not be proved. For the linear systems, computation with the given methods gives $\gamma_\infty(\Gamma) < 0.5354, \gamma_2(\Gamma) = 0.5423, \gamma_\infty(\Theta) < 1.221$, and $\gamma_\infty(\Omega) = 1$. Let $\eta = 0.1$ and $M_P = 3 > \gamma_\infty(\Omega) + \eta\gamma_\infty(\Theta)$. Since $\Phi$ is independent from $u$, $\hat{\mathcal{D}} \subset \mathbb{R}^2$. For this example, since $\hat{\mathcal{D}}$ is simply connected set, $\hat{\mathcal{D}} = \mathcal{D}$. The surface of $\frac{\|\Phi(x)\|_\infty}{\|x\|_\infty}$ as well as the boundary of $\mathcal{D}$ is depicted in Fig. 3.10. Fig. 3.11 shows $\frac{\|\Phi(x)\|_2}{\|x\|_2}$ and the boundary of $\gamma_2(\Gamma)\gamma_2(\Phi) < 1$. The various subsets of $\mathbb{R}^2$ are depicted in Fig. 3.12. The maximum value for $\epsilon$ is $0.1519$ and consequently the maximum value for $\Delta$ is $0.0402$. According to Theorem 3.3.2, for any input $u$ which satisfies $\|u\|_{\mathcal{L}_\infty} < \eta\delta = 0.004$ and any initial state satisfying $\|x_0\|_\infty < \delta = 0.0402$, $x$ is bounded as $\|x\|_{\mathcal{L}_\infty} < \epsilon = 0.1519$. Besides, in addition to the mentioned condition, if $u \in \mathcal{L}_2$ and $u \to 0$ as $t \to \infty$ then $x \to 0$ as $t \to \infty$, according to Theorem 3.3.3.

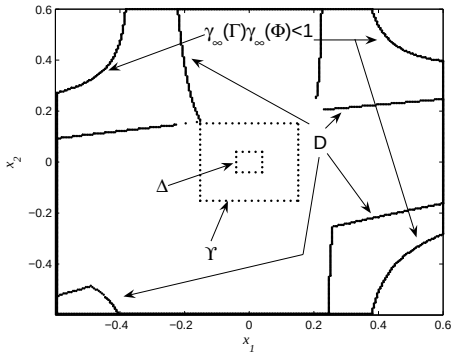


Figure 3.12: Various sets in Example 3.3.2.

## 3.4 Chapter Summary

In this chapter, we have considered stability of nonlinear systems. Our results are applicable to a variety of nonlinear systems. The suggested method of checking stability of nonlinear systems has significant computational advantage compared to previous work, in the sense that there is no need to find any Lyapunov-like function. Initial insight for our formulation was provided by a new representation for nonlinear systems, which transforms a nonlinear system, with non-zero initial state, into a feedback interconnection of two operators. Then, some well-known concepts from input-output theory were used to derive sufficient conditions for stability of the original nonlinear system. Finally, local stability of nonlinear systems was studied with a new definition of region of attraction. Since the new representation is not unique for a nonlinear system, all suggested methods can be optimized based on the selected parameters in the representation. This optimization will be the subject of future work.

# Chapter 4

# Upper bounds

## 4.1 Introduction

The complex structure of nonlinear systems is the major obstacle in the development of simple and efficient computational methods to test stability, compute system norms, etc. As a consequence, a majority of the computational techniques available in the literature are restricted to a narrow class of nonlinear systems for which a particular function, e.g. Lyapunov function or storage function, can be found by trial and error [27], [24].

In this chapter, we consider the problem of computing the $\mathcal{L}_p$ operator norm of a nonlinear system, a problem which has remained a challenge in the systems literature. The importance of this problem originates from the fact that the influence of various inputs on various signals inside the system can be quantified by such a measure. One of the applications of this measure is in control systems, where the attenuation of disturbance signals is required. The subject has attracted considerable attention for both linear and nonlinear systems. For linear systems, computing the $\mathcal{L}_p$ norm(s) has a well established solution; see, for example, reference [2]. For nonlinear systems, however, computation of the $\mathcal{L}_p$ operator norm continues to be a challenge. In [6], the $\mathcal{L}_\infty$-gain of nonlinear systems is characterized by means of the value function of an associated variational problem. The $\mathcal{L}_2$ gain, also referred to as the $\mathcal{H}_\infty$ gain of a nonlinear system, can be approximated using storage functions and the theory of dissipative systems [48]. This approach is, however, conservative and finding storage functions is difficult; see also [20] for a numerical approximation of the $\mathcal{H}_\infty$ norm. In [31], a computational method is proposed to compute the $\mathcal{L}_2$ induced norm for single-input linear systems with saturation.

In this chapter, we propose a method to compute an upper bound on the $\mathcal{L}_1$, $\mathcal{L}_2$ and $\mathcal{L}_\infty$ norms of a class of continuous-time nonlinear systems. Our method can be optimized based on some selected parameters. For systems not included in this class, a method is also

provided for computing an upper bound of the $\mathcal{L}_\infty$ norm.

This chapter is organized as follows: In section 4.1.1, we propose a method to compute upper bounds on the induced norm of nonlinear systems and provide two illustrative examples. In section 4.2, we introduce the weighting method, which can be used to reduce the intrinsic conservativism in the aforementioned method. An example is provided to illustrate the usage of the weighting technique.

### 4.1.1 The proposed method

In this section, we obtain a computable upper bound for induced operator norms. We will use the structure shown in Fig. 2.4(b); namely, the $\zeta_A$ representation for forced system. In this structure, it is trivial to show that

$$\begin{aligned}\|x\|_{\mathcal{L}_p} &\leq \|w\|_{\mathcal{L}_p} + \|d\|_{\mathcal{L}_p} \\ &\leq \gamma_p(\Gamma)\gamma_p(\Phi)\left\|\begin{bmatrix} x \\ u \end{bmatrix}\right\|_{\mathcal{L}_p} + \|d\|_{\mathcal{L}_p} \\ &\leq \gamma_p(\Gamma)\gamma_p(\Phi)\left\|\begin{bmatrix} x \\ u \end{bmatrix}\right\|_{\mathcal{L}_p} + \gamma_p(\Omega)\|x_0\|_p\end{aligned} \tag{4.1}$$

The computation of $\gamma_p(\Gamma)$, $\gamma_p(\Omega)$ and $\gamma_p(\Phi)$ was discussed in Reference [49].

**Lemma 4.1.1.** *The following equation is true for $x, u \in \mathcal{L}_p$:*

$$\left\|\begin{bmatrix} x \\ u \end{bmatrix}\right\|_{\mathcal{L}_p} \leq \|x\|_{\mathcal{L}_p} + \|u\|_{\mathcal{L}_p} \tag{4.2}$$

*Moreover, if $x, u \in \mathcal{L}_2$*

$$\left\|\begin{bmatrix} x \\ u \end{bmatrix}\right\|^2_{\mathcal{L}_2} = \|x\|^2_{\mathcal{L}_2} + \|u\|^2_{\mathcal{L}_2} \quad . \tag{4.3}$$

*Proof.* The proof is trivial and is omitted. □

The first part of this lemma, (4.2), is true for all Banach spaces; however, the second part is true when the temporal norm is $\mathcal{L}_2$ with the Euclidean 2-norm chosen as the corresponding spatial norm.

**Theorem 4.1.1.** *Let $[\Phi, \Gamma, \Omega]$ be a $\zeta_A$ representation for a forced system, $N$. If*

$$\gamma_p(\Gamma)\gamma_p(\Phi) < 1 \tag{4.4}$$

*then*

$$\gamma_p(N) \leq \frac{\gamma_p(\Gamma)\gamma_p(\Phi)}{1 - \gamma_p(\Gamma)\gamma_p(\Phi)}. \tag{4.5}$$

*Proof.* Substituting (4.2) in (4.1) implies that

$$\|x\| \leq \gamma_p(\Gamma)\gamma_p(\Phi)\left(\|x\| + \|u\|\right) + \gamma_p(\Omega)\|x_0\|. \tag{4.6}$$

Thus

$$(1 - \gamma_p(\Gamma)\gamma_p(\Phi))\|x\| \leq \gamma_p(\Gamma)\gamma_p(\Phi)\|u\| + \gamma_p(\Omega)\|x_0\|. \tag{4.7}$$

Since $\gamma_p(\Gamma)\gamma_p(\Phi) < 1$,

$$\|x\| \leq \frac{\gamma_p(\Gamma)\gamma_p(\Phi)}{1 - \gamma_p(\Gamma)\gamma_p(\Phi)}\|u\| + \frac{\gamma_p(\Omega)}{1 - \gamma_p(\Gamma)\gamma_p(\Phi)}\|x_0\| \tag{4.8}$$

which implies (4.5). □

Inequality (4.5) can be used as an upper bound for the $\mathcal{L}_p$ induced norm. It is important to note that since the $\zeta_A$ representation is not unique, the solution of the following minimization problem is the lowest upper bound that can be obtained by our method:

$$\gamma_p(N) \leq \min_A \frac{\gamma_p(\Gamma)\gamma_p(\Phi)}{1 - \gamma_p(\Gamma)\gamma_p(\Phi)} \tag{4.9}$$

where $\Gamma(s) = \left[\begin{array}{c|c} A & I \\ \hline I & 0 \end{array}\right]$ and $\Phi(x,u) = f(x,u) - Ax$. Unfortunately, there is no existing method to find $A$ which provides the lowest upper bound. A good strategy is to define a function in MATLAB with input $A$ and output $\frac{\gamma_p(\Gamma)\gamma_p(\Phi)}{1-\gamma_p(\Gamma)\gamma_p(\Phi)}$ and use *fminsearch* to minimize it.

The method provided by Theorem 4.1.1 is general in the sense of the induced norm, $\gamma_p$. An interesting case occurs when the temporal norm is $\mathcal{L}_2$ with the Euclidean 2-norm chosen as the corresponding spatial norm. The reason is that a quite mature theory, namely; $\mathcal{H}_\infty$ optimization, has been developed for linear systems in this case. Suppose $\Gamma$ is a continuous-time linear time-invariant stable operator with impulse response $g(t) : \mathbb{R}^+ \to \mathbb{R}^{n\times n}$ $(g(t) : \mathbb{Z}^+ \to \mathbb{R}^{n\times n})$. Let $G(s)$ denote the Laplace transform of $g(t)$. We have

$$\gamma_2(\Gamma) := \|G(s)\|_{\mathcal{H}_\infty} \tag{4.10}$$

In this case, the following theorem provides lower upper bounds for the induced norm $\gamma_2$ than Theorem 4.1.1.

**Theorem 4.1.2.** *Let $[\Phi, \Gamma, \Omega]$ be a $\zeta_A$ representation for a forced system, $N$. If $\gamma_2(\Gamma)\gamma_2(\Phi) < 1$ then*

$$\gamma_2(N) \leq \frac{\gamma_2(\Gamma)\gamma_2(\Phi)}{\sqrt{1 - \gamma_2(\Gamma)^2\gamma_2(\Phi)^2}}. \tag{4.11}$$

*Proof.* Inequality (4.1) implies that

$$(\|x\| - \gamma_2(\Omega)\|x_0\|)^2 \leq \left(\gamma_2(\Gamma)\gamma_2(\Phi)\left\|\begin{bmatrix} x \\ u \end{bmatrix}\right\|\right)^2 \tag{4.12a}$$

Using (4.3),

$$\|x\|^2 - 2\gamma_2(\Omega)\|x_0\|\|x\| + \gamma_2(\Omega)^2\|x_0\|^2 \leq \gamma_2(\Gamma)^2\gamma_2(\Phi)^2\left(\|x\|^2 + \|u\|^2\right) \tag{4.12b}$$

For simplicity, let $\alpha := \gamma_2(\Gamma)\gamma_2(\Phi)$

$$\|x\|^2 - \frac{2\gamma_2(\Omega)}{1-\alpha^2}\|x_0\|\|x\| + \frac{\gamma_2(\Omega)^2}{1-\alpha^2}\|x_0\|^2 \leq \frac{\alpha^2}{1-\alpha^2}\|u\|^2. \tag{4.12c}$$

Hence

$$\left(\|x\| - \frac{\gamma_2(\Omega)}{1-\alpha^2}\|x_0\|\right)^2 \leq \frac{\alpha^2\gamma_2(\Omega)^2}{(1-\alpha^2)^2}\|x_0\|^2 + \frac{\alpha^2}{1-\alpha^2}\|u\|^2. \tag{4.12d}$$

Since $a^2 + b^2 \leq (a+b)^2$ for all $a, b \geq 0$, we have

$$\|x\| - \frac{\gamma_2(\Omega)}{1-\alpha^2}\|x_0\| \leq \frac{\alpha\gamma_2(\Omega)}{(1-\alpha^2)}\|x_0\| + \frac{\alpha}{\sqrt{1-\alpha^2}}\|u\| \tag{4.12e}$$

Consequently

$$\|x\| \leq \frac{\gamma_2(\Gamma)\gamma_2(\Phi)}{\sqrt{1-\gamma_2(\Gamma)^2\gamma_2(\Phi)^2}}\|u\| + \frac{\gamma_2(\Omega)}{1-\gamma_2(\Gamma)\gamma_2(\Phi)}\|x_0\| \tag{4.12f}$$

which implies (4.11). □

Similarly, the solution of the following minimization problem is the lowest upper bound that can be obtained by our method:

$$\gamma_2(N) \leq \min_A \frac{\gamma_2(\Gamma)\gamma_2(\Phi)}{\sqrt{1-\gamma_2(\Gamma)^2\gamma_2(\Phi)^2}} \tag{4.13}$$

where $\Gamma(s) = \left[\begin{array}{c|c} A & I \\ \hline I & 0 \end{array}\right]$ and $\Phi(x,u) = f(x,u) - Ax$. Equivalently,

$$\gamma_2(N) \leq \min_A \frac{1}{\sqrt{\left\|(sI-A)^{-1}\right\|_{\mathcal{H}_\infty}^{-2} \gamma_2^{-2}(f(x,u)-Ax) - 1}}. \tag{4.14}$$

**Example 4.1.1.** (*RLC circuit with non-ideal inductor*) The network of Fig. 4.1 represents a RLC circuit with a non-ideal inductor. The inductor has nonzero resistance and saturation characteristic as shown in Fig. 4.2(a), where $\lambda$ is the flux linkage. The relationship of the magnetic flux linkage to terminal voltage of an inductor is given by Faraday's law; namely $v_L(t) = d\lambda(t)/dt$. The state equations for this network may be written as

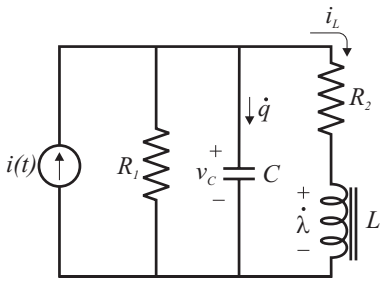


Figure 4.1: RLC circuit in Example 4.1.1.

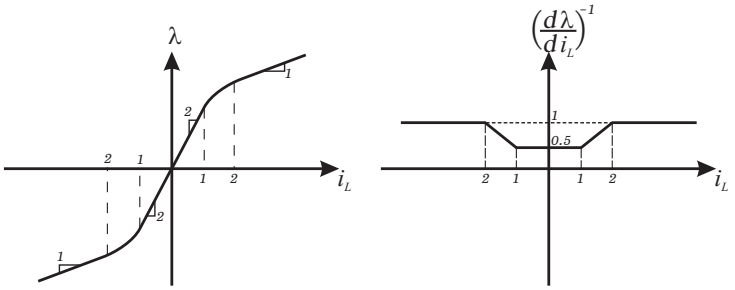


Figure 4.2: The characteristic of the inductance in Example 4.1.1.

$$v_L = \dot{\lambda} = \frac{d\lambda}{di_L}\frac{di_L}{dt} \tag{4.15a}$$

$$\frac{di_L}{dt} = \left(\frac{d\lambda}{di_L}\right)^{-1}(v_C - R_2 i_L) \tag{4.15b}$$

where $\left(\frac{d\lambda}{di_L}\right)^{-1}$ is depicted in Fig. 4.2(b) versus $i_L$, and

$$C\frac{dV_C}{dt} = i - \frac{V_C}{R_1} - i_L. \tag{4.15c}$$

Defining $x_1 := i_L$, $x_2 := v_C$ and $u := i$,

$$\begin{cases} \dot{x}_1 &= (x_2 - R_2 x_1)\left(\frac{d\lambda}{dx_1}\right)^{-1} \\ \dot{x}_2 &= \frac{u}{C} - \frac{x_2}{R_1 C} - \frac{x_1}{C} \end{cases}. \tag{4.15d}$$

Let $R_1 = \frac{1}{2}$, $R_2 = 1$ and $C = 2$. Assuming $A = \begin{bmatrix} -1 & 0.5 \\ -0.5 & -1 \end{bmatrix}$, we have

$$\Phi(x_1, x_2, u) = \begin{bmatrix} x_1 - 0.5\, x_2 + (x_2 - x_1)\left(\frac{d\lambda}{dx_1}\right)^{-1} \\ \frac{u}{C} \end{bmatrix}. \tag{4.15e}$$

We use the computational methods that has been introduced in [49]. Since there are three independent variables in $\gamma_p(\Phi)$, i.e. $x_1$, $x_2$ and $u$, we plot $\frac{\|\Phi(x,u)\|}{\left\|\begin{bmatrix} x \\ u \end{bmatrix}\right\|}$ versus $\left\|\begin{bmatrix} x \\ u \end{bmatrix}\right\|$ instead of

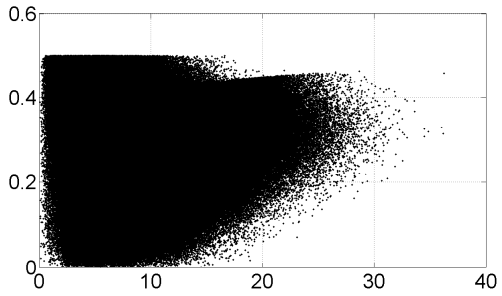


(a) $p = 1$

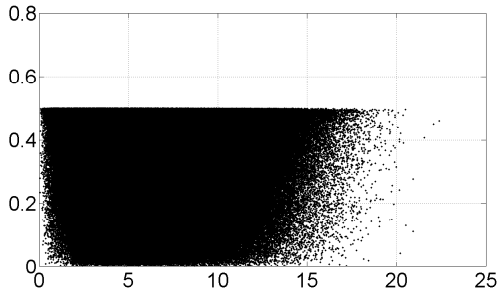


(b) $p = 2$

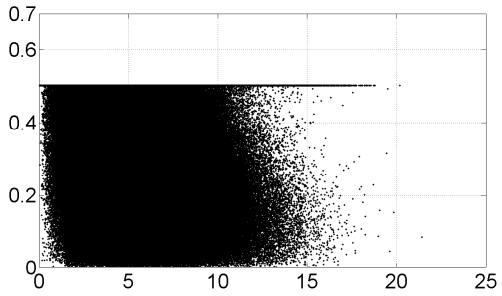


(c) $p = \infty$

Figure 4.3: Gain of $\|\Phi(x,u)\|_p$ versus $\left\|\begin{bmatrix} x \\ u \end{bmatrix}\right\|_p$ in Example 4.1.1.

plotting versus $x_1$, $x_2$ and $u$, as shown in Fig. 4.3. Therefore, $\gamma_1(\Phi) \approx 0.50$, $\gamma_2(\Phi) \approx 0.50$ and $\gamma_\infty(\Phi) \approx 0.50$. Computation also shows that $\gamma_1(\Gamma) \approx 1.237$, $\gamma_2(\Gamma) \approx 1.00$ and $\gamma_\infty(\Gamma) \approx 1.237$. Theorems 4.1.1 and 4.1.2 imply that $\gamma_1(N) \leq 1.62$, $\gamma_2(N) \leq 0.577$ and $\gamma_\infty(N) \leq 1.62$, respectively.

There is no doubt that the condition $\gamma_p(\Gamma)\gamma_p(\Phi) < 1$ in Theorems 4.1.1 and 4.1.2 is restrictive. For example, polynomial systems are excluded by the aforementioned condition. The following theorem might be used to overcome this shortcoming. The result provides an upper bound on system output for bounded input and initial state.

**Theorem 4.1.3.** *Let $[\Phi, \Theta, \Gamma, \Omega]$ be a $\zeta_{AB}$ representation for a nonlinear system. Let $\eta > 0$ and $M_p > \gamma_\infty(\Omega) + \eta\gamma_\infty(\theta)$ and*

$$\hat{\mathcal{D}} := \left\{ \begin{bmatrix} x \\ u \end{bmatrix} \in \mathbb{R}^{n+m} \;\middle|\; \gamma_\infty^{\hat{\mathcal{D}}}(\Phi) < \frac{M_p - \gamma_\infty(\Omega) - \eta\gamma_\infty(\theta)}{(M_p + \eta)\gamma_\infty(\Gamma)} \right\}. \tag{4.16}$$

*Let $\mathcal{D} := \mathbf{B}^\infty(0, r_D)$ be an open ball inside $\hat{\mathcal{D}}$. Assume that $\mathcal{D}_x$ and $\mathcal{D}_u$ are the images of $\mathcal{D}$ under $\left[\begin{array}{c|c} I_{n\times n} & 0_{n\times m} \\ \hline 0_{m\times n} & 0_{m\times m} \end{array}\right]$ and $\left[\begin{array}{c|c} 0_{n\times n} & 0_{n\times m} \\ \hline 0_{m\times n} & I_{m\times m} \end{array}\right]$, respectively. Therefore, $\mathcal{D}_x$ and $\mathcal{D}_u$ are also open balls in $\mathbb{R}^n$ and $\mathbb{R}^m$ respectively. Let $r_x$ and $r_u$ denote respectively their radius, i.e. $\mathcal{D}_x = \mathbf{B}^\infty(0, r_x)$ and $\mathcal{D}_u = \mathbf{B}^\infty(0, r_u)$. Choose $\epsilon$ and $\delta$ such that $0 < \epsilon < r_x$ and*

$$0 < \delta \leq \frac{1 - \gamma_\infty^{\mathcal{D}}(\Phi)\gamma_\infty(\Gamma)}{\gamma_\infty(\Omega) + \eta(\gamma_\infty(\Theta) + \gamma_\infty^{\mathcal{D}}(\Phi)\gamma_\infty(\Gamma))}\,\epsilon$$

*If $\|u\|_{\mathcal{L}_\infty} < \min(\eta\,\delta, r_u)$ and $\|x_0\|_\infty \leq \delta$, then*

$$\|x\|_{\mathcal{L}_\infty} < \epsilon. \tag{4.17}$$

*Proof.* It is trivial that $M_p - \gamma_\infty(\Omega) - \eta\gamma_\infty(\theta) < M_p + \eta$; therefore $\gamma_\infty^{\mathcal{D}}(\Phi)\gamma_\infty(\Gamma) < 1$. We use contradiction to prove the theorem. Since we have assumed that systems of interest are locally Lipschitz, system trajectories are continuous. Consequently, if $x$ were to leave the ball with radius $\epsilon$, it should cross the boundary of the ball. Suppose that $x$ crosses the boundary at $t = \tau$. As a result, $\|\mathbf{T}_\tau x\| = \|x\|_\tau = \epsilon$. Since $\epsilon < r_x$ and $\|u\| < \min(\eta\,\delta, r_u)$ guarantees that $u \in \mathcal{D}_u$, we have $\begin{bmatrix} x_\tau \\ u_\tau \end{bmatrix} \in \mathcal{D}$ and consequently

$$\begin{aligned}
\|x_\tau\| &\leq \|d_{1\tau}\| + \|w_\tau\| \\
&\leq \|d_{1\tau}\| + \gamma_\infty^{\mathcal{D}}(\Phi)\gamma_\infty(\Gamma)(\|d_{2\tau}\| + \|x_\tau\|) \\
&\leq \gamma_\infty(\Theta)\|u_\tau\| + \gamma_\infty(\Omega)\|x_0\| \\
&\quad + \gamma_\infty^{\mathcal{D}}(\Phi)\gamma_\infty(\Gamma)\|x_\tau\| + \gamma_\infty^{\mathcal{D}}(\Phi)\gamma_\infty(\Gamma)\|u_\tau\| \\
&\leq \gamma_\infty(\Omega)\|x_0\| + [\gamma_\infty(\Theta) + \gamma_\infty^{\mathcal{D}}(\Phi)\gamma_\infty(\Gamma)]\|u_\tau\| \\
&\quad + \gamma_\infty^{\mathcal{D}}(\Phi)\gamma_\infty(\Gamma)\|x_\tau\| \\
&< \gamma_\infty(\Omega)\delta + \left[\gamma_\infty(\Theta) + \gamma_\infty^{\mathcal{D}}(\Phi)\gamma_\infty(\Gamma)\right]\eta\delta \\
&\quad + \gamma_\infty^{\mathcal{D}}(\Phi)\gamma_\infty(\Gamma)\|x_\tau\| \\
&= \left(\gamma_\infty(\Omega) + \eta\left[\gamma_\infty(\Theta) + \gamma_\infty^{\mathcal{D}}(\Phi)\gamma_\infty(\Gamma)\right]\right)\delta \\
&\quad + \gamma_\infty^{\mathcal{D}}(\Phi)\gamma_\infty(\Gamma)\|x_\tau\|
\end{aligned} \tag{4.18}$$

Then

$$\begin{aligned}\epsilon &= \|x_\tau\| \\ &< \frac{\gamma_\infty(\Omega)+\eta\left[\gamma_\infty(\Theta)+\gamma_\infty^{\mathcal{D}}(\Phi)\gamma_\infty(\Gamma)\right]}{1-\gamma_\infty^{\mathcal{D}}(\Phi)\gamma_\infty(\Gamma)}\|x_0\| \\ &\leq \frac{\gamma_\infty(\Omega)+\eta\left[\gamma_\infty(\Theta)+\gamma_\infty^{\mathcal{D}}(\Phi)\gamma_\infty(\Gamma)\right]}{1-\gamma_\infty^{\mathcal{D}}(\Phi)\gamma_\infty(\Gamma)}\,\delta \\ &\leq \epsilon \end{aligned} \tag{4.19}$$

Which is a contradiction. Therefore, $x(t) < \epsilon;\ \forall t \geq 0$, i.e. $\|x\| < r_x$. □

**Example 4.1.2.** Consider a multi-tank system depicted in Fig. 4.4. Suppose that a proportional controller is utilized to adjust the fluid level in the second tank $H_2$ by input flow $q$. The problem of interest is to find an upper bound on the gain of the closed loop system shown in Fig. 4.5. The following mathematical model is taken from [19]:

$$\begin{cases} \frac{dH_1}{dt} = \frac{1}{aw}\left(q - C_1 H_1^{\alpha_1}\right) \\ \frac{dH_2}{dt} = \frac{1}{cw+\frac{H_2}{H_{2max}}bw}\left(C_1 H_1^{\alpha_1} - C_2 H_2^{\alpha_2}\right) \end{cases} \tag{4.20}$$

The transfer function of the controller is $K(s) = K_P$. Let $x_1 := H_1 - H_{10}$, $x_2 := H_2 - H_{20}$ and $q = q_0 - K_P(x_2 + u)$ where $H_{10}$ and $H_{20}$ are operating points and $q_0$ is the corresponding input. It is trivial that $q_0 = C_1 H_{10}^{\alpha_1} = C_2 H_{20}^{\alpha_2}$. The numerical values for the coefficients are $a = 0.25$, $w = 0.035$, $H_{2max} = 0.35$, $b = 0.345$, $c = 0.1$, $C_1 = 5.66 \times 10^{-5}$, $C_2 = 5.58 \times 10^{-5}$, $\alpha_1 = 0.29$ and $\alpha_2 = 0.226$ [19]. Suppose $K_P = 10^{-5}$. The state equations for the closed-loop system are

$$\begin{cases} \dot{x}_1 = \frac{1}{aw}\left(q_0 - K_P(x_2+u) - C_1(x_1+H_{10})^{\alpha_1}\right) \\ \dot{x}_2 = \frac{1}{cw+\frac{x_2+H_{20}}{H_{2max}}bw}\left(C_1(x_1+H_{10})^{\alpha_1} - C_2(x_2+H_{20})^{\alpha_2}\right) \end{cases} \tag{4.21}$$

and $\dot{x} = \begin{pmatrix} \dot{x}_1 \\ \dot{x}_2 \end{pmatrix} = f(x,u)$. Let

$$A = \begin{pmatrix} -0.0072 & -0.0114 \\ 0.0094 & -0.0118 \end{pmatrix}, \quad B = \begin{pmatrix} -0.0114 \\ 0 \end{pmatrix}, \tag{4.22}$$

which are linearized parts of $f(x,u)$ at $x = 0$ and $u = 0$, i.e. $A = \left.\frac{\partial f(x,u)}{\partial x}\right|_{x,u=0}$ and $B = \left.\frac{\partial f(x,u)}{\partial u}\right|_{x,u=0}$. Therefore,

$$\Phi(x,u) = \begin{bmatrix} 0.00373 + 0.0072x_1 - 0.00647(x_1+0.15)^{0.29} \\ \frac{5.66\times10^{-5}(x_1+0.15)^{0.29} - 5.58\times10^{-5}(x_2+0.0934)^{0.226}}{0.0067+0.0345x_2} - 0.0094x_1 + 0.01176x_2 \end{bmatrix}. \tag{4.23}$$

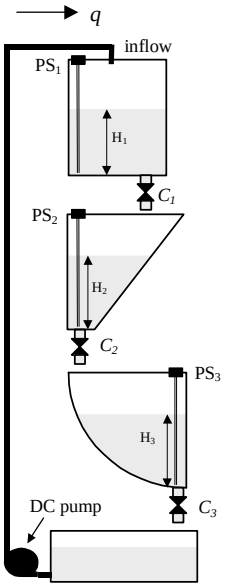


Figure 4.4: Configuration of the multitank system [19].

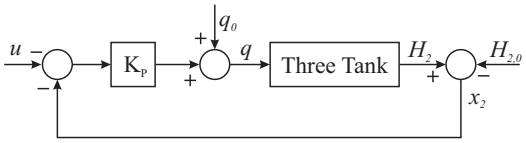


Figure 4.5: Closed loop multitank system.

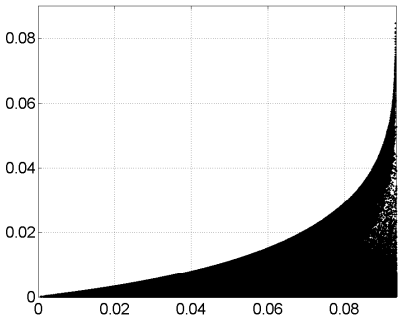


Figure 4.6: $\frac{\|\Phi(x)\|_\infty}{\|x\|_\infty}$ versus $\|x\|_\infty$.

Computation with the methods proposed in [50] provides $\gamma_\infty(\Gamma) < 151.3$, $\gamma_\infty(\Theta) < 0.9756$, and $\gamma_\infty(\Omega) = 1.036$. Let $\eta = 3.0382$ which gives $M_P = 4 > \gamma_\infty(\Omega) + \eta\gamma_\infty(\Theta)$. Since $\Phi$ is independent from $u$, $\hat{\mathcal{D}} \subset \mathbb{R}^2$. $\frac{\|\Phi(x)\|_\infty}{\|x\|_\infty}$ versus $\|x\|_\infty$ is depicted in Fig. 4.6. Since $\hat{\mathcal{D}}$ is independent of $u$, $r_u = \infty$. Let us take $\hat{\mathcal{D}}$ as the region where $\frac{\|\Phi(x)\|_\infty}{\|x\|_\infty} < 0.0023$, i.e. $\gamma_\infty^{\mathcal{D}}(\Phi) = 0.0023$. Consequently $r_x = 0.0155$. Let $\epsilon = 0.015$ and $\delta = 0.0019 \leq \frac{1-\gamma_\infty^{\mathcal{D}}(\Phi)\gamma_\infty(\Gamma)}{\gamma_\infty(\Omega)+\eta(\gamma_\infty(\Theta)+\gamma_\infty^{\mathcal{D}}(\Phi)\gamma_\infty(\Gamma))}\epsilon$. According to Theorem 4.1.3, for any input $u$ which satisfies $\|u\|_{\mathcal{L}_\infty} < \min(\eta\delta, r_u) = 0.00587$ and any initial state satisfying $\|x_0\|_\infty < \delta = 0.0019$, $x$ is bounded as $\|x\|_{\mathcal{L}_\infty} < \epsilon = 0.015$.

## 4.2 Weighting Technique

As shown in the previous section, the proposed methods are based on the $\zeta_A$ representation. Adding some weighting on state or input vectors may tighten the calculated bounds. However, there is no general rule which provides useful weighting matrices; therefore, they should be chosen by trial and error. In this section, we study the effect of the weighting and we show the effectiveness by an example.

In the $\zeta_A$ representation for continuous-time systems shown in Fig. 2.3, let $\hat{x} := W_x x$ where $W_x$ is nonsingular. Consequently,

$$\dot{\hat{x}} = W_x A W_x^{-1}\hat{x} + W_x\Phi(W_x^{-1}\hat{x}) \tag{4.24}$$

Denoting $\hat{A} := W_x A W_x^{-1}$, $\hat{\Phi}(x) := W_x\Phi(W_x^{-1}x)$, $\hat{\Gamma} := \left[\begin{array}{c|c} \hat{A} & I \\ \hline I & 0 \end{array}\right]$ and $\Omega(x(t)) := e^{\hat{A}t}x_0$, it is easy to show that ordered operator set $[\hat{\Phi}, \hat{\Gamma}, \hat{\Omega}]$ is a $\zeta_A$ representation for the weighted system, i.e. the system with initial state $\hat{x}_0 := W_x x_0$ and state $\hat{x}$.

Similarly, in the $\zeta_{AB}$ representation shown in Fig. 2.4(a) for continuous-time systems,

let $\hat{x} := W_x x$ and $\hat{u} := W_u u$ where $W_x$ and $W_u$ are nonsingular. Consequently,

$$\dot{\hat{x}} = W_x A W_x^{-1}\hat{x} + W_x B W_u^{-1}\hat{u} + W_x \Phi(W_x^{-1}\hat{x}, W_u^{-1}\hat{u}) \tag{4.25}$$

Denoting $\hat{A} := W_x A W_x^{-1}$, $\hat{B} := W_x B W_u^{-1}$, $\hat{\Phi}(x,u) := W_x \Phi(W_x^{-1}x, W_u^{-1}u)$, $\hat{\Gamma} := \left[\begin{array}{c|c} \hat{A} & I \\ \hline I & 0 \end{array}\right]$, $\hat{\Theta} := \left[\begin{array}{c|c} \hat{A} & \hat{B} \\ \hline I & 0 \end{array}\right]$ and $\Omega(x(t)) := e^{\hat{A}t}x_0$, it is trivial to show that ordered operator set $[\hat{\Phi}, \hat{\Gamma}, \hat{\Theta}, \hat{\Omega}]$ is a $\zeta_{AB}$ representation for the weighted system, i.e. the system with input $\hat{u}$, state $\hat{x}$ and initial state $\hat{x}_0$. A very similar argument can be made for forced system with $\zeta_A$ representation.

It is important to note that the mapping $\hat{u} \to \hat{x}$ is different than $u \to x$. However, Theorems 4.1.1, 4.1.2 and 4.1.3 can be used to find corresponding upper bounds for the weighted system. Then, using the definitions of $\hat{x}$, $\hat{u}$ and $\hat{x}_0$, the corresponding bounds can be found for the main system. Suppose that the inequality found for the weighted system is $\|\hat{x}\|_p \leq \gamma_{p,u} \|\hat{u}\|_p + \gamma_{p,x_0} \|\hat{x}_0\|_p$ where $\gamma_{p,u}$ and $\gamma_{p,x_0}$ are derived by either (4.8) or (4.12f). Therefore,

$$\begin{aligned} \|x\| &\leq \left\|W_x^{-1}\right\| \|\hat{x}\| \\ &\leq \left\|W_x^{-1}\right\| \gamma_u \|\hat{u}\| + \left\|W_x^{-1}\right\| \gamma_{x_0} \|\hat{x}_0\| \\ &\leq \left\|W_x^{-1}\right\| \gamma_u \|W_u\| \|u\| + \left\|W_x^{-1}\right\| \gamma_{x_0} \|W_x\| \|x_0\| . \end{aligned} \tag{4.26}$$

It is important to note that norms used for $\left\|W_x^{-1}\right\|$ and $\|W_u\|$ are the corresponding induced norms. Similarly, if an upper bound obtained for the weighted system is $\gamma(\hat{N})$ then

$$\gamma(N) \leq \left\|W_x^{-1}\right\| \gamma(\hat{N}) \|W_u\| . \tag{4.27}$$

There is no method to compute $\left\|W_x^{-1}\right\|$ and $\|W_u\|$ in general. However, in some special cases, such as the case where 2-norm is used for the spatial norm or the case where weighting matrices are multiplication of a scalar by the identity matrix, $\left\|W_x^{-1}\right\|$ and $\|W_u\|$ can be calculated. The following example illustrates the usage and effectiveness of the weighting technique.

**Example 4.2.1.** Consider the following nonlinear system

$$N : \begin{cases} \dot{x}_1 = -x_1 + x_2 + 0.5\text{sat}\,(x_2) - 0.25\sin(x_1) + 0.25\text{sat}\,(u) \\ \dot{x}_2 = -x_1 - x_2 + 0.5\text{sat}\,(x_1) - 0.25\sin(x_2) - 0.25u \end{cases} \tag{4.28}$$

where sat $(\cdot)$ is depicted in Fig. 4.7. Let $A = \begin{bmatrix} -0.9 & 0.9 \\ -0.9 & -1.1 \end{bmatrix}$. Hence,

$$\Phi(x_1, x_2, u) = \begin{bmatrix} -0.1x_1 + 0.1x_2 + 0.5\,\text{sat}\,(x_2) - 0.25\,\sin(x_1) + 0.25\,\text{sat}\,(u) \\ -0.1x_1 + 0.1x_2 + 0.5\text{sat}\,(x_1) - 0.25\sin(x_2) - 0.25u \end{bmatrix}. \tag{4.29}$$

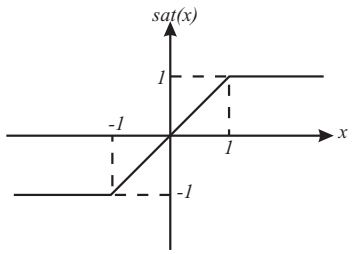


Figure 4.7: The saturation function sat $(\cdot)$.

Table 4.1: Derived bounds with various $W_u$ (Example 4.2.1).

| $W_u$ | $\gamma_1(\hat{N})$ | $\gamma_2(\hat{N})$ | $\gamma_\infty(\hat{N})$ | $\gamma_1(N)$ | $\gamma_2(N)$ | $\gamma_\infty(N)$ |
|---|---|---|---|---|---|---|
| 1.75 | 1.361 | 0.580 | 3.029 | 2.382 | 1.015 | 5.301 |
| 1 | 1.66 | 0.71 | 5.95 | 1.66 | 0.71 | 5.95 |
| 2 | 1.290 | 0.575 | 2.30 | 2.58 | 1.15 | 4.6 |
| minimum | | | | 1.66 | 0.71 | 4.6 |

Let $W_u = 1.75$ and $W_x = I_{2\times 2}$. Therefore, $\left\|W_x^{-1}\right\| = 1$ and $\|W_u\| = 1.75$. As shown in Fig. 4.8, we plot $\frac{\left\|\hat{\Phi}(\hat{x},\hat{u})\right\|}{\left\|\begin{bmatrix}\hat{x}\\ \hat{u}\end{bmatrix}\right\|}$ versus $\left\|\begin{bmatrix}\hat{x}\\ \hat{u}\end{bmatrix}\right\|$ instead of plotting versus $\hat{x}_1$, $\hat{x}_2$ and $\hat{u}$. Therefore, $\gamma_1(\hat{\Phi}) \approx 0.46$, $\gamma_2(\hat{\Phi}) \approx 0.5$ and $\gamma_\infty(\hat{\Phi}) \approx 0.6$. Computation also shows that $\gamma_1(\hat{\Gamma}) \approx 1.253$, $\gamma_2(\hat{\Gamma}) \approx 1.003$ and $\gamma_\infty(\hat{\Gamma}) \approx 1.253$. Therefore, $\gamma_1(\hat{N}) \leq 1.361$, $\gamma_2(\hat{N}) \leq 0.58$ and $\gamma_\infty(\hat{N}) \leq 3.029$. Using (4.27), $\gamma_1(N) \leq 2.382$, $\gamma_2(N) \leq 1.015$ and $\gamma_\infty(N) \leq 5.301$. The results obtained for various values of $W_u$ are summarized in Table 4.1. As can be seen, tighter bounds can be found by trying different values for the weighting matrices.

## 4.3 Chapter Summary

This chapter offers a contribution to the calculation of upper bounds on the $\mathcal{L}_1$, $\mathcal{L}_2$ and $\mathcal{L}_\infty$ induced operator norms of continuous-time nonlinear systems. Based on the $\zeta_A$ representation of nonlinear systems, methods are presented to compute the aforementioned bounds.

The main limitation of the proposed methods is inequality (4.4) that restricts the usage of the method for a class of the nonlinear systems and the freedom on choosing the parameter $A$. To lessen the restrictions encountered in the computation of the $\mathcal{L}_\infty$ norm of a system, a method is given to compute an upper bound on the $\mathcal{L}_\infty$ norm of the system output with respect to $\mathcal{L}_\infty$ norm of the input. This method does not suffer from the previous limitations. In the last section, our methods are improved by the use of a weighting technique on the $\zeta_A$ representation. An example is provided to show the effectiveness of the weighting technique.

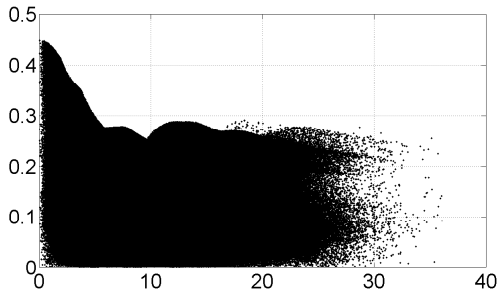


(a) $p = 1$

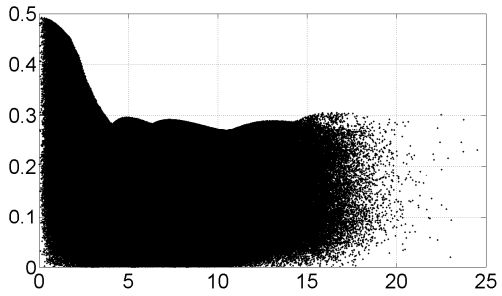


(b) $p = 2$

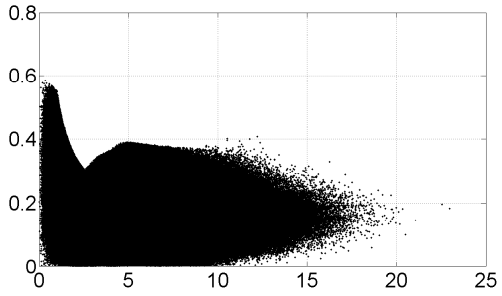


(c) $p = \infty$

Figure 4.8: Gain of $\left\|\hat{\Phi}(\hat{x},\hat{u})\right\|_p$ versus $\left\|\begin{bmatrix}\hat{x}\\ \hat{u}\end{bmatrix}\right\|_p$ in Example 4.2.1 for $W_u = 1.75$.

# Chapter 5

# The Gap Metric

## 5.1 Introduction

Model uncertainty often has a significant effect on stability and performance of feedback control systems. For linear time-invariant (LTI) systems, much work has been done to study this effect. One important concept used to measure system uncertainty is the gap metric which was introduced to systems and control theory by Zames and El-Sakkary [55]. For LTI systems, it has been shown that a perturbed system can be stabilized by any controller which is designed for the nominal system if and only if the distance between the perturbed system and the nominal system is small in the gap metric. The computation of the gap metric for LTI systems was developed by Georgiou [12].

The extension of the gap metric to larger classes of systems was initiated in [10], where the metric was extended to time-varying linear plants. Later, the parallel projection operator for nonlinear systems [5] and its relationship to the differential stabilizability of nonlinear feedback systems [11] paved the road to the extension of the gap metric to a pseudo-metric on nonlinear operators [13].

Unlike the LTI system case, there is no generally applicable method of computing the gap metric for nonlinear systems. In fact, there are only a few examples in literature for the computation of the gap metric. Moreover, those methods are highly dependent upon the case of interest. This is also the case for the corresponding stability margin which can be used to determine the ball of uncertainty in the sense of the gap metric.

This chapter deals with the computation of the gap metric and stability margin for nonlinear systems. We will consider the extension of the gap metric to nonlinear systems given in [13]. We derive upper bounds on the gap metric and the stability margin with respect to the operator norm (gain) of the plant, perturbed system and controller and based on the results of Chapter 4 on the upper bound of the gain of nonlinear systems. The suggested

methods are only applicable to a class of nonlinear systems which satisfy an inequality.

The chapter is organized as follows: In Section 5.2, first, we introduce the notation. Then, the gap metric for the nonlinear systems is introduced. The main contribution of this paper is contained in Section 5.3 where Theorems 5.3.1 and 5.3.2 are stated and proved. These theorems provide upper bounds on the gap metric and the stability margin, respectively. In Section 5.3, an example is also solved to illustrate the effectiveness of the results and comparison between the direct computation and the suggested methods. Since the literature suffers from the lack of widely-applicable computation methods and there are just a few examples which are highly dependent to the studied systems, it is indeed hard to construct example which both satisfies our required condition and is compatible by the previously suggested methods such as the method used in [13].

## 5.2 Background

### 5.2.1 Notation

Let $\mathcal{U} := \mathcal{L}$ and $\mathcal{Y} := \mathcal{L}$ denote input and output signal spaces, respectively. A nonlinear time-varying system can be thought of as a possibly unbounded operator $H : \mathcal{D}_h \rightarrow \mathcal{Y}$ where $\mathcal{D}_h \subseteq \mathcal{U}$. The action of $H$ on any $u \in \mathcal{D}_h$ is denoted by $Hu$. A system $H$ is called *stable* if $\mathcal{D}_h = \mathcal{U}$. For an operator $H : \mathcal{U} \rightarrow \mathcal{Y}$ , let $\gamma(H)$ stand for the induced norm (gain) of the operator defined as

$$\gamma(H) := \sup_{\substack{u \in \mathcal{U} \\ u \neq 0}} \frac{\|Hu\|_T}{\|u\|_T} \tag{5.1}$$

where the supremum is taken over all $u \in \mathcal{U}$ and all $T$ in $\mathbb{R}^+$ for which $u_T \neq 0$. Let $\gamma_p(H)$ stand for $\gamma(H)$ in $\mathcal{L}_p$. A system $H$ is called *finite gain stable (fg-stable)* if $H0 = 0$ and $\gamma(H) < \infty$.

### 5.2.2 The Gap Metric

Let $[P, C]$ denote the feedback configuration shown in Figure 5.1. This configuration is standard in literature, e.g. [13] and can be described by the following equations.

$$\begin{aligned} y_1 &= Pu_1 \\ u_2 &= Cy_2 \\ u_0 &= u_1 + u_2 \\ y_0 &= y_1 + y_2 \end{aligned} \tag{5.2}$$

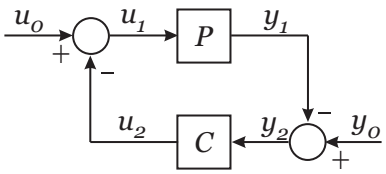


Figure 5.1: The standard feedback configuration, $[P, C]$.

where $P$ and $C$ denote the nominal plant and the controller and $u_0$ and $y_0$ are the input and measurement disturbances, respectively. Let $u_i \in \mathcal{U}$, $y_i \in \mathcal{Y}$ and $w_i := \begin{bmatrix} u_i \\ y_i \end{bmatrix}$ for $i \in \{0, 1, 2\}$ and $\mathcal{W} := \mathcal{U} \times \mathcal{Y}$. We assume that the product of the instantaneous gains of $P$ and $C$ is less than one. This assumption guarantees the well-posedness of the feedback configuration, e.g. [13] [1]. Similar to [13], we assume that the feedback configuration is always well-posed. The closed-loop operator is defined as

$$H_{P,C} : \mathcal{W} \to \mathcal{W} \times \mathcal{W}\,,\ H_{P,C} : w_0 \mapsto (w_1, w_2). \tag{5.3}$$

The graph of the plant is

$$\mathcal{G}_P = \left\{ \begin{pmatrix} u \\ Pu \end{pmatrix} \,:\, u \in \mathcal{U},\, Pu \in \mathcal{Y} \right\} \subset \mathcal{W}. \tag{5.4}$$

If the domain of $P$ is $U$, the condition $Pu \in \mathcal{Y}$ is unnecessary. To have compatible notation with [13], we define the graph of $C$ as follows

$$\mathcal{G}_C = \left\{ \begin{pmatrix} Cy \\ y \end{pmatrix} \,:\, Cy \in \mathcal{U},\, y \in \mathcal{Y} \right\} \subset \mathcal{W}. \tag{5.5}$$

In some literature, e.g [5], this graph is also called inverse graph. Let

$$\mathcal{M} := \mathcal{G}_P\,,\ \mathcal{N} := \mathcal{G}_C. \tag{5.6}$$

The following operators are useful in the study of the closed-loop system stability.

$$\Pi_{\mathcal{M}||\mathcal{N}} := \Pi_1 H_{P,C}\,,\ \Pi_{\mathcal{N}||\mathcal{M}} := \Pi_2 H_{P,C} \tag{5.7}$$

where $\Pi_i : \mathcal{W} \times \mathcal{W} \to \mathcal{W}$ denote the natural projection onto the $i$th component $(i \in \{1, 2\})$ of $\mathcal{W} \times \mathcal{W}$. Therefore

$$\begin{aligned} \Pi_{\mathcal{M}||\mathcal{N}} &\,:\, w_0 \mapsto w_1 \\ \Pi_{\mathcal{N}||\mathcal{M}} &\,:\, w_0 \mapsto w_2. \end{aligned} \tag{5.8}$$

**Definition 5.2.1.** *Parallel Projection* [5]

A stable operator $\Pi : \mathcal{L} \to \mathcal{L}$ (with $\Pi 0 = 0$) is called a parallel projection if for any $x_1, x_2 \in \mathcal{L}$

$$\Pi(\Pi x_1 + (I - \Pi)x_2) = \Pi x_1 \tag{5.9}$$

where $I$ denotes the identity on $\mathcal{L}$.

Thus, $\Pi_{\mathcal{M}||\mathcal{N}}$ and $\Pi_{\mathcal{N}||\mathcal{M}}$ are parallel projections considering that for any $w_1, w_2 \in \mathcal{W}$

$$\Pi(\Pi w_1 + (I - \Pi)w_2) = \Pi w_1, \tag{5.10}$$

for $\Pi \in \left\{\Pi_{\mathcal{M}||\mathcal{N}}, \Pi_{\mathcal{N}||\mathcal{M}}\right\}$.

Consider the *summation operator*

$$\Sigma_{\mathcal{M},\mathcal{N}} : \mathcal{M} \times \mathcal{N} \to \mathcal{W} : (m, n) \mapsto m + n. \tag{5.11}$$

The stability of the standard feedback interconnection, Fig. 5.1, is equivalent to $\Sigma_{\mathcal{M},\mathcal{N}}$ having an inverse defined on the whole of $\mathcal{W}$ which is bounded. In fact, if $\Sigma_{\mathcal{M},\mathcal{N}}$ has a bounded inverse, then $\Sigma^{-1}_{\mathcal{M},\mathcal{N}} = H_{P,C}$. It can be shown that a necessary condition for $[P, C]$ to be stable is that $\mathcal{M}$ and $\mathcal{N}$ are closed subsets of $\mathcal{W}$ [5]. Let $\mathcal{W}_1$ and $\mathcal{W}_2$ be closed subsets of a Banach space $\mathcal{W}$. We define

$$\begin{aligned}\vec{\delta}(\mathcal{W}_1, \mathcal{W}_2) &:= \begin{cases} \inf\{\|(\mathcal{T} - I)|_{\mathcal{W}_1}\|\}, & \mathcal{T} \text{ is a causal} \\ & \quad \text{bijective map from } \mathcal{W}_1 \text{ to } \mathcal{W}_2 \\ & \quad \text{with } \mathcal{T}0 = 0, \\ \infty, & \text{if no such operator } \mathcal{T} \text{ exists,} \end{cases} \\ \delta(\mathcal{W}_1, \mathcal{W}_2) &= \max\left\{\vec{\delta}(\mathcal{W}_1, \mathcal{W}_2), \vec{\delta}(\mathcal{W}_2, \mathcal{W}_1)\right\}. \end{aligned} \tag{5.12}$$

**Theorem 5.2.1.** *Consider the feedback system shown in Fig. 5.1. Let $\mathcal{M} := \mathcal{G}_P$ and $\mathcal{N} := \mathcal{G}_C$. Assume that $[P, C]$ is fg-stable. Suppose that $P$ is perturbed to $P_1$ and $\mathcal{M}_1 := \mathcal{G}_{P1}$. If*

$$\vec{\delta}(\mathcal{M}, \mathcal{M}_1) < \left\|\Pi_{\mathcal{M}||\mathcal{N}}\right\|^{-1} \tag{5.13}$$

*then $[P_1, C]$ is fg-stable. Furthermore*

$$\left\|\Pi_{\mathcal{M}_1||\mathcal{N}}\right\| < \left\|\Pi_{\mathcal{M}||\mathcal{N}}\right\| \frac{1 + \vec{\delta}(\mathcal{M}, \mathcal{M}_1)}{1 - \left\|\Pi_{\mathcal{M}||\mathcal{N}}\right\| \vec{\delta}(\mathcal{M}, \mathcal{M}_1)}. \tag{5.14}$$

*Proof.* See [13]. □

## 5.3 Upper bounds on the Gap Metric and the stability margin

In this section, we suggest a method to find an upper bound on the gap metric between two nonlinear systems as well as a method to compute an upper bound on $\Pi_{\mathcal{M}||\mathcal{N}}$.

**Theorem 5.3.1.** *Consider nonlinear dynamical systems given by*

$$\begin{aligned} N &: \ \dot{x} = f(x, u)\,, \ x_0 = 0; \\ \hat{N} &: \ \dot{\hat{x}} = \hat{f}(\hat{x}, u)\,, \ \hat{x}_0 = 0. \end{aligned} \tag{5.15}$$

*Let $\gamma(N)$ and $\gamma(\hat{N})$ denote their gain respectively. Then*

$$\delta(N, \hat{N}) \leq \gamma(N) + \gamma(\hat{N}). \tag{5.16}$$

*Proof.* We have

$$\begin{aligned}\|x-\hat{x}\| &\le \|x\| + \|\hat{x}\| \\ &\le \gamma(N)\,\|u\| + \gamma(\hat{N})\,\|u\| \\ &\le \big(\gamma(N)+\gamma(\hat{N})\big)\,\|u\| \\ &\le \big(\gamma(N)+\gamma(\hat{N})\big)\left\|\begin{bmatrix}u\\x\end{bmatrix}\right\|.\end{aligned} \tag{5.17}$$

Define $\mathcal{T}$ as

$$\mathcal{T}\begin{bmatrix}u\\x\end{bmatrix} := \begin{bmatrix}u\\\hat{x}\end{bmatrix}. \tag{5.18}$$

□

It is trivial that $\mathcal{T}$ is bijective. We have

$$\begin{aligned}\vec{\delta}(N,\hat{N}) &= \|I-\mathcal{T}\| \\ &= \sup \frac{\left\|(I-\mathcal{T})\begin{bmatrix}u\\x\end{bmatrix}\right\|}{\left\|\begin{bmatrix}u\\x\end{bmatrix}\right\|} \\ &= \sup \frac{\left\|\begin{bmatrix}u-u\\x-\hat{x}\end{bmatrix}\right\|}{\left\|\begin{bmatrix}u\\x\end{bmatrix}\right\|} \\ &= \sup \frac{\|x-\hat{x}\|}{\left\|\begin{bmatrix}u\\x\end{bmatrix}\right\|} \\ &\le \gamma(N)+\gamma(\hat{N}) \quad \text{using (5.17)}\end{aligned} \tag{5.19}$$

Similarly

$$\vec{\delta}(\hat{N},N) \le \gamma(N)+\gamma(\hat{N}). \tag{5.20}$$

Consequently,

$$\begin{aligned}\delta(N,\hat{N}) &= \max\{\vec{\gamma}(N,\hat{N}),\vec{\gamma}(\hat{N},N)\} \\ &\le \delta(N)+\delta(\hat{N}).\end{aligned} \tag{5.21}$$

**Theorem 5.3.2.** *Consider the standard feedback configuration depicted in Fig. 5.1. Suppose that $\gamma(P)\gamma(C)<1$. Let $\Pi_{\mathcal{M}||\mathcal{N}}$ be defined as (5.6) and (5.7). Then*

$$\left\|\Pi_{\mathcal{M}||\mathcal{N}}\right\| \le \frac{\big(1+\gamma(P)\big)\big(1+\gamma(C)\big)}{1-\gamma(P)\gamma(C)}. \tag{5.22}$$

*Proof.* From the feedback configuration, we have

$$\begin{aligned} \|u_1\| &\leq \|u_0\| + \gamma(C)\,\|y_0 - y_1\| \\ &\leq \|u_0\| + \gamma(C)\,\|y_0\| + \gamma(C)\gamma(P)\,\|u_1\|\,. \end{aligned} \tag{5.23}$$

Consequently

$$\|u_1\| \leq \frac{1}{1-\gamma(C)\gamma(P)}\,\|u_0\| + \frac{\gamma(C)}{1-\gamma(C)\gamma(P)}\,\|y_0\|\,. \tag{5.24}$$

Therefore

$$\begin{aligned} \left\|\begin{bmatrix} u_1 \\ y_1 \end{bmatrix}\right\| &\leq \|u_1\| + \|y_1\| \\ &\leq \|u_1\| + \gamma(P)\,\|u_1\| \\ &\leq \frac{1+\gamma(P)}{1-\gamma(C)\gamma(P)}\,\|u_0\| + \frac{\gamma(C)\big(1+\gamma(P)\big)}{1-\gamma(C)\gamma(P)}\,\|y_0\|\,. \end{aligned} \tag{5.25}$$

Since $\|a\| \leq \left\|\begin{bmatrix} a \\ b \end{bmatrix}\right\|$,

$$\begin{aligned} \left\|\begin{bmatrix} u_1 \\ y_1 \end{bmatrix}\right\| &\leq \frac{1+\gamma(P)+\gamma(C)\big(1+\gamma(P)\big)}{1-\gamma(C)\gamma(P)} \left\|\begin{bmatrix} u_0 \\ y_0 \end{bmatrix}\right\| \\ &= \frac{\big(1+\gamma(P)\big)\big(1+\gamma(C)\big)}{1-\gamma(C)\gamma(P)} \left\|\begin{bmatrix} u_0 \\ y_0 \end{bmatrix}\right\|. \end{aligned} \tag{5.26}$$

On the other hand, Equation (5.8) implies

$$\Pi_{\mathcal{M}||\mathcal{N}} \begin{bmatrix} u_0 \\ y_0 \end{bmatrix} = \begin{bmatrix} u_1 \\ y_1 \end{bmatrix}. \tag{5.27}$$

Thus

$$\left\|\Pi_{\mathcal{M}||\mathcal{N}}\right\| = \sup_{\left\|\begin{bmatrix} u_0 \\ y_0 \end{bmatrix}\right\| \neq 0} \frac{\left\|\begin{bmatrix} u_1 \\ y_1 \end{bmatrix}\right\|}{\left\|\begin{bmatrix} u_0 \\ y_0 \end{bmatrix}\right\|}. \tag{5.28}$$

Using (5.26)

$$\left\|\Pi_{\mathcal{M}||\mathcal{N}}\right\| \leq \frac{\big(1+\gamma(P)\big)\big(1+\gamma(C)\big)}{1-\gamma(C)\gamma(P)}. \tag{5.29}$$

□

**Example 5.3.1.** Consider the feedback configuration of Fig. 5.1. Assume that the plant is the circuit shown in Fig. 5.2, where the inductance of the SSR is nonlinear and $L(\cdot)$ is defined as Fig. 5.3 and $R = 10$. The state equation of the system is

$$\begin{aligned} \dot{x}(t) &= L^{-1}(u_1(t) - Rx(t)),\ x(0) = 0 \\ y_1(t) &= x(t) \end{aligned} \tag{5.30}$$

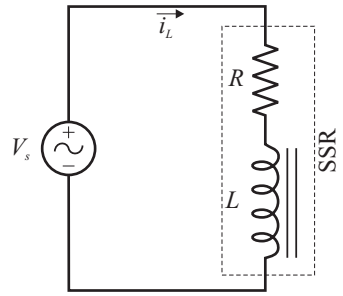


Figure 5.2: $P$ in Example 5.3.1.

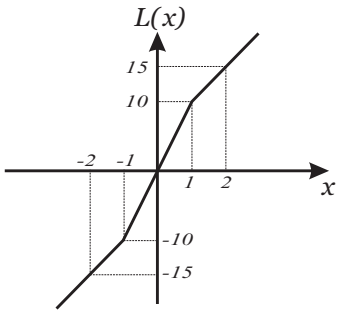


Figure 5.3: Inductance of SSR.

where $x(t) := i_L(t)$ and $u_1(t) := V_s(t)$. Let $C = -c$ where $c$ is a positive non-zero constant. Let $\mathcal{U} = \mathcal{Y} = \mathcal{L}_\infty$. Since the instantaneous gains of $P$ and $C$ are zero and one, respectively, the loop is well-posed. First, we will find the $\left\|\Pi_{\mathcal{M}||\mathcal{N}}\right\|$ by a direct method similar to the solution of Example 1 in [13]. Then, we will compute the upper bound on $\left\|\Pi_{\mathcal{M}||\mathcal{N}}\right\|$ by the suggested method.

*I. Direct computation:*

The feedback equation is

$$\dot{x} = L^{-1}(u_0 + cy_0 - (10 + c)x),\ x(0) = 0. \tag{5.31}$$

We have

$$\Pi_{\mathcal{M}||\mathcal{N}} : \begin{bmatrix} u_0 \\ y_0 \end{bmatrix} \mapsto \begin{bmatrix} u_1 \\ y_1 \end{bmatrix} = \begin{bmatrix} u_0 + cy_0 - cx \\ x \end{bmatrix}. \tag{5.32}$$

Let $v_0 := u_0 + cy_0$. For any $v_0$, $u_0 = y_0$ gives the mapping with the smallest input norm. Therefore, $v_0 = (1 + c)u_0$ and

$$\begin{aligned} \left\|\Pi_{\mathcal{M}||\mathcal{N}}\right\| &= \left\| \begin{bmatrix} u_0 \\ y_0 \end{bmatrix} \mapsto \begin{bmatrix} u_0 + cy_0 - cx \\ x \end{bmatrix} \right\| \\ &= \left\| \begin{bmatrix} u_0 \\ y_0 \end{bmatrix} \mapsto \begin{bmatrix} v_0 - cx \\ x \end{bmatrix} \right\| \\ &= (1 + c) \left\| v_0 \mapsto \begin{bmatrix} v_0 - cx \\ x \end{bmatrix} \right\| \\ &= (1 + c) \times \max\{\left\| v_0 \mapsto \left(v_0 - cx\right) \right\|, \|v_0 \mapsto x\|\}. \end{aligned} \tag{5.33}$$

We now show that $\|v_0 \mapsto x\| = {}^{1}\!/_{10+c}$. Suppose that for any arbitrary chosen interval $[0,T]$, the maximum of $x(t)$, which is positive, occurs at $t_0 \in [0,T]$. Then, for any $\epsilon > 0$, there exists $t_1$ such that $0 < t_1 < t_0$, $x(t_1) > x(t_0) - \epsilon$ and $\dot{x}(t_1) > 0$. Consequently, $L^{-1}\big(v_0(t_1) - (10+c)x(t_1)\big) > 0$. Since $\operatorname{sgn} L^{-1}(x) = \operatorname{sgn} x$, $v_0(t_1) > (10+c)x(t_1)$. Thus, $v_0(t_1) > (10+c)x(t_0) - (1+c)\epsilon$ for any $\epsilon$. Similarly, if the minimum of $x(t)$ in $[0,T]$, which is negative, occurs at $\acute{t}_0$, for any $\acute{\epsilon} > 0$, there exists $\acute{t}_1$ such that $v_0(\acute{t}_1) < (10+c)x(\acute{t}_0) - (1+c)\acute{\epsilon}$. Consequently, $\|v_0\|_T \geq (10+c)\,\|x\|_T$. To show that this upper bound on $\|v_0 \mapsto x\|$ can be approached arbitrary closely, let $v_0 = 1$ for all $t$. It is trivial that $x(t) = \big(1 - e^{-(1+0.1c)t}\big)/(10+c)$. So $\|v_0\| = 1$ and $\|x\| = {}^{1}\!/_{10+c}$. Consequently, $\|v_0 \mapsto x\| = {}^{1}\!/_{10+c}$. Next, we compute $\big\|v_0 \mapsto \big(v_0 - cx\big)\big\|$. Trivially, $\big\|v_0 \mapsto \big(v_0 - cx\big)\big\| \leq 1 + \|v_0 \mapsto (cx)\| = 1 + \frac{c}{10+c}$. This upper bound can be approached arbitrarily closely by the input $v_0 = 1$ for $0 \leq t < T$ and $v_0 = -1$ for $t \geq T$. We have $x(t) = \big(1 - e^{-(1+0.1c)t}\big)/(10+c)$ for $0 \leq t < T$. Thus, $\big(v_0 - cx\big)(T) = -(1 + \frac{c}{10+c}) + e^{-(1+0.1c)T}$. Therefore, $\|v_0\| = 1$ and $\|v_0 - cx\| = 1 + \frac{c}{10+c}$ which implies that $\big\|v_0 \mapsto \big(v_0 - cx\big)\big\| = 1 + \frac{c}{10+c}$. Consequently, $\big\|\Pi_{\mathcal{M}||\mathcal{N}}\big\| = 1 + \frac{c}{10+c}$.

*II. The suggested method:*

To find $\gamma(P)$, let $\Phi(x,u) = L^{-1}(u - 10x) + 3x/2$ and $\Gamma := \left[\begin{array}{c|c} -3/2 & 1 \\ \hline 1 & 0 \end{array}\right]$. We use the computational methods introduced in Section 2.3.1. Fig. 5.4 shows the plot of $\dfrac{\|\Phi(x,u)\|}{\left\|\begin{bmatrix} x \\ u \end{bmatrix}\right\|}$ versus $\left\|\begin{bmatrix} x \\ u \end{bmatrix}\right\|$ for $2 \times 10^6$ randomly chosen input vector. Therefore, $\gamma(\Phi) = 0.7$. Using the method introduced in Section 2.3.2, we have $\gamma(\Gamma) = 2/3$. Theorem 4.1.1 implies that

$$\gamma(P) \leq 0.639. \tag{5.34}$$

Since $C = -c$ is a constant, $\gamma(C) = c$. Theorem 5.3.2 implies that $\big\|\Pi_{\mathcal{M}||\mathcal{N}}\big\| \leq \frac{1.639(1+c)}{1-0.639\,c}$ if $c < 1.56$. Apparently, the obtained upper bound is closer to the actual value when $c$ approaches zero.

**Example 5.3.2.** Consider the plant introduced in the previous example. Suppose that the system is perturbed by time delay $h$. That is

$$P_1 : \begin{cases} \dot{x}(t) = L^{-1}(u_1(t) - Rx(t)),\ x(0) = 0 \\ y_1(t) = x(t-h). \end{cases} \tag{5.35}$$

First, we will compute an upper bound on the gap between the plant $P$ and the perturbation $P_1$ by a direct method similar to the solution of Example 1 in [13]. Then, we will compute the upper bound on the gap by the suggested method.

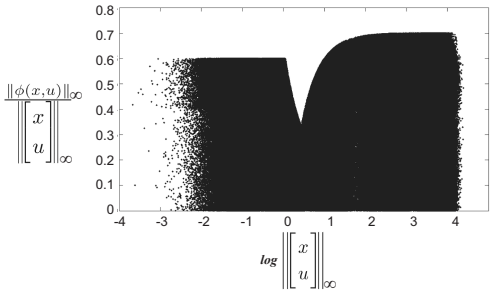


Figure 5.4: Gain of $\|\Phi(x,u)\|$ versus $\log \left\| \begin{bmatrix} x \\ u \end{bmatrix} \right\|$.

*I. Direct computation:*

Let $\mathcal{M}_1 := \mathcal{G}_{P1}$ and define a mapping $\mathcal{T} : \mathcal{M} \to \mathcal{M}_1$ as

$$\mathcal{T}\begin{bmatrix} u_1(t) \\ x(t) \end{bmatrix} = \begin{bmatrix} u_1(t) \\ x(t-h) \end{bmatrix}. \tag{5.36}$$

Thus

$$\begin{aligned} |x(t) - x(t-h)| &\leq \sup_{\hat{t}\in[t-h,t]} |\dot{x}(\hat{t})| \cdot h \\ &\leq \sup_{\hat{t}\in[t-h,t]} |L^{-1}\big(u(\hat{t}) - 10x(\hat{t})\big)| \cdot h. \end{aligned} \tag{5.37}$$

Since $L^{-1}(\cdot)$ is an strictly increasing function,

$$\begin{aligned} &|x(t) - x(t-h)| \\ &\quad \leq L^{-1}\big( \sup_{\hat{t}\in[t-h,t]} |u(\hat{t}) - 10x(\hat{t})|\big) \cdot h \\ &\quad \leq L^{-1}\big( \sup_{\hat{t}\in[t-h,t]} |u(\hat{t})| + \sup_{\hat{t}\in[t-h,t]} |10x(\hat{t})|\big) \cdot h \\ &\quad \leq L^{-1}\big( \sup_{\hat{t}\in[0,t]} |u(\hat{t})| + \sup_{\hat{t}\in[0,t]} |10x(\hat{t})|\big) \cdot h. \end{aligned} \tag{5.38}$$

Therefore

$$\begin{aligned} &\|x(t) - x(t-h)\|_\tau \\ &\quad \leq \left\| L^{-1}\big( \sup_{\hat{t}\in[0,t]} |u(\hat{t})| + \sup_{\hat{t}\in[0,t]} |10x(\hat{t})|\big) \right\|_\tau \cdot h \\ &\quad \leq L^{-1}\big(11 \max\{\|u\|_\tau, \|x\|_\tau\}\big) \cdot h \\ &\quad \leq 2.2 \max\{\|u\|_\tau, \|x\|_\tau\} \cdot h. \end{aligned} \tag{5.39}$$

Hence

$$\|I - \mathcal{T}\| = \sup_{\tau, \|u_1\|_\tau \neq 0} \frac{\|x(t) - x(t-h)\|_\tau}{\max\{\|u_1\|_\tau, \|x\|_\tau\}} \leq 2.2\, h. \tag{5.40}$$

Consequently, $\vec{\delta}(\mathcal{M}, \mathcal{M}_1) \leq 2.2\,h$. On the other hand, let $u(t) = 1$ on $[0, h]$. It is Trivial that $(Pu)(t) = 0.1(1 - e^{-10t})$. For any $w \in \mathcal{M}_1$, we have $w_h = \begin{bmatrix} * \\ 0 \end{bmatrix}$ which is implied by the time delay in $P_1$. Therefore

$$\begin{aligned}
\vec{\delta}(\mathcal{M}, \mathcal{M}_1) &= \sup_{u_1, y_1 \neq 0} \frac{\left\| (\mathcal{T} - I) \begin{bmatrix} u_1 \\ y_1 \end{bmatrix} \right\|}{\left\| \begin{bmatrix} u_1 \\ y_1 \end{bmatrix} \right\|} \\
&\geq \sup_{u_1, y_1 \neq 0} \frac{\left\| \begin{bmatrix} * \\ 0 \end{bmatrix} - \begin{bmatrix} u_1 \\ Pu_1 \end{bmatrix} \right\|_h}{\max\{\|u_1\|_h, \|Pu_1\|_h\}} \\
&= \frac{\max\{\|* - u_1\|_h, \|Pu_1\|_h\}}{\max\{\|u_1\|_h, \|Pu_1\|_h\}} \\
&\geq \frac{\|Pu_1\|_h}{\max\{\|u_1\|_h, \|Pu_1\|_h\}} \\
&= 0.1(1 - e^{-10h}).
\end{aligned} \tag{5.41}$$

Consequently

$$0.1(1 - e^{-10h}) \leq \vec{\delta}(P, P_1) \leq 2.2\,h. \tag{5.42}$$

*II. The suggested method:*

Since $P$ is autonomous, $\gamma(P) = \gamma(P_1)$. Using Theorem 5.3.1, $\vec{\delta}(P, P_1) = 2\gamma(P)$. Using (5.34), $\vec{\delta}(P, P_1) \leq 1.278$. It is clear that for $h > 0.58$ the suggested method provides smaller upper bound than the direct method.

## 5.4 Chapter Summary

In this chapter, we have considered the computation of the gap metric and the corresponding robust stability margin. Our results are applicable to a class of a nonlinear systems which satisfy a given inequality. The suggested methods have computational advantage compared to previous work in the sense that they are applicable to wider range of nonlinear systems. Our methods are based on two inequalities derived for the gap metric and the stability margin with respect to the gain of the relevant systems. An example is provided to illustrate the results.

# Chapter 6

# The Large Gain Theorem

## 6.1 Introduction

One of the well-accepted and widely-used methods to study stability of systems is the input-output approach. It was initiated by Popov, Zames, and Sandberg, in the 1960s [42] [56] [32]. So far, it has been a fruitful area which has resulted in many of the recent developments in control theory, such as robust control and small-gain based nonlinear stabilization techniques. The input-output stability theory considers systems as mappings from an input space of functions into an output space. In this theory, the well-behaved input and output signals are considered as members of input and output spaces. Therefore, if the "well-behaved" inputs produce well-behaved outputs, the system is called stable.

The main contribution of the input-output stability theory in control theory is through the well-known small-gain theorem. In this context, the most notable contributions have also been made by Zames and Sandberg, e.g. [56] [32]. The small gain theorem says that the feedback loop will be stable if the loop gain is less than one. This simple rule has been a basis for numerous stabilization techniques such as nonlinear $\mathcal{H}_\infty$ control [15].

Stability of systems, in its various forms, continues to inspire researchers. Motivated by the classical small gain theorem, "nonlinear gain" small gain theorems are discussed in such references as [21] [39] [18]. The notion of non-uniform in time robust global asymptotic output stability was introduced in [22] for a wide class of systems. A small-gain theorem for a wide class of feedback systems was proposed in [23]. In [14], it was shown that for an open loop unstable system which is closed loop stable the gain must exceed one.

In this chapter, the minimum gain of a system is studied. Although it has been showed that the minimum gain is not a norm on space of operators, a new stability condition has been derived for feedback systems based on the minimum gain of the open-loop systems.

The chapter is organized as follows. In Section 6.2, the minimum gain of an operator

is defined and some of its properties are derived. In Section 6.3, the large gain theorem is stated. An example is also provided to illustrate the usage of the theorem.

## 6.2 Minimum Gain of an Operator

Let $H : \mathcal{U} \to \mathcal{Y}$ denote an operator. We define the minimum gain of $H$ as follows:

$$\nu(H) = \inf_{0 \neq u \in \mathcal{U}} \frac{\|(Hu)_T\|}{\|u_T\|} \tag{6.1}$$

where the infimum is taken over all $u \in \mathcal{U}$ and all $T$ in $\mathbb{R}^+$ for which $u_T \neq 0$. It is trivial that the minimum gain of an operator is less or equal to its induced norm. It is also obvious that if a minimum gain of a system is infinite, then it is unstable. In other words, the minimum gain of a stable system is always finite. The converse is, however, not true.

**Lemma 6.2.1.** *Let $M \in \mathbb{R}^{n\times n}$. Define $H : \mathcal{X}_2 \to \mathcal{X}_2$ as $Hx := Mx$, then*

$$\nu(H) = \underline{\sigma}(M). \tag{6.2}$$

*Proof.* The proofs for the continuous-time and discrete-time cases are the same and only the first one is given here. We use the following property of the smallest singular value of matrices (e.g. [57] pp. 21):

$$\underline{\sigma}(M) = \min_{\|x\|=1} \|Mx\| = \min_{x\neq 0} \frac{\|Mx\|}{\|x\|}. \tag{6.3}$$

Let $M = U\Sigma V^T$ be the Singular Value Decomposition (SVD) of $M$, where $V = [v_1, v_2, \cdots, v_n] \in \mathbb{R}^{n\times n}$ and $U, \Sigma \in \mathbb{R}^{n\times n}$ [57]. It is well-known that $v_n$ is the minimizer of (6.3), e.g. [57]. Let $x \in \mathcal{L}_2$, we have

$$\begin{aligned} \|Mx\|^2 &= \int_0^\infty \|Mx(t)\|_2^2 \, dt \\ &\geq \int_0^\infty \underline{\sigma}(M)^2 \|x(t)\|_2^2 \, dt \\ &= \underline{\sigma}(M)^2 \int_0^\infty \|x(t)\|_2^2 \, dt = \underline{\sigma}(M)^2 \|x\|^2 \end{aligned} \tag{6.4}$$

which shows that $\underline{\sigma}(M)$ is a lower bound for $\nu(H)$. To show that it is the greatest lower bound, let $x(t) = \frac{v_n}{\|v_n\|} e^{-t}$. We have

$$\|x\|^2 = \int_0^\infty \left\| \frac{v_n}{\|v_n\|} e^{-t} \right\|^2 dt = \int_0^\infty \left\| e^{-t} \right\|^2 dt = {}^1\!/_2 \tag{6.5}$$

and

$$\begin{aligned}\|Mx\|^2 &= \int_0^\infty \left\| M \frac{v_n}{\|v_n\|} e^{-t} \right\|^2 dt \\ &= \int_0^\infty \|Mv_n\|^2 \frac{e^{-2t}}{\|v_n\|^2}\, dt \\ &= \int_0^\infty \|\underline{\sigma}(M) v_n\|^2 \frac{e^{-2t}}{\|v_n\|^2}\, dt \\ &= \|\underline{\sigma}(M)\|^2 \int_0^\infty e^{-2t}\, dt = {}^1\!/_2 \, \|\underline{\sigma}(M)\|^2 .\end{aligned} \tag{6.6}$$

Equations (6.5) and (6.6) imply that $\nu(H)$ is equal to $\underline{\sigma}(M)$ for some input. This completes the proof.

□

**Lemma 6.2.2.** *Let $\Phi(\cdot,\cdot) : \mathbb{R}^+ \times \mathbb{R}^n \to \mathbb{R}^n$ ($\Phi(\cdot,\cdot) : \mathbb{Z}^+ \times \mathbb{R}^n \to \mathbb{R}^n$ in discrete time) and $H$ be the operator defined as*

$$H : \mathcal{X}_p \to \mathcal{X}_p \,; \quad Hx(t) := \Phi(t, x(t)). \tag{6.7}$$

*Suppose there exists a constant $\mu_p$ such that*

$$\mu_p \|x\|_p \leq \|\Phi(t,x)\|_p, \ \forall x \in \mathbb{R}^n, \ \forall t \geq 0 \tag{6.8}$$

*then $\mu_p \leq \nu_p(H)$.*

*Proof.* Let $x \in \mathcal{L}_p$, for $p \neq \infty$,

$$\begin{aligned}\|Hx\|_{\mathcal{L}_p}^p &= \int_0^\infty \|\Phi(t,x(t))\|^p \ dt \geq \int_0^\infty \mu_p^p \, \|x(t)\|_p \ dt \\ &= \mu_p^p \int_0^\infty \|x(t)\|^p \ dt = \mu_p^p \, \|x\|_{\mathcal{L}_p}^p .\end{aligned} \tag{6.9}$$

For $p = \infty$,

$$\begin{aligned}\|Hx\|_{\mathcal{L}_\infty} &= \sup_t \|\Phi(t,x(t))\| \geq \sup_t \mu_p \, \|x(t)\| \\ &= \mu_p \sup_t \|x(t)\| = \mu_p \, \|x\|_{\mathcal{L}_\infty}^p .\end{aligned} \tag{6.10}$$

Equations (6.9) and (6.10) imply that $\mu_p$ is a lower bound for $\nu(H)$. This completes the proof.

□

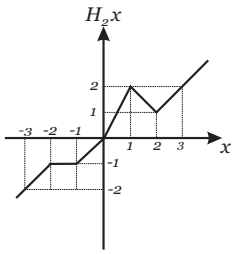


Figure 6.1: $H_2$ in Example 6.2.1.

**Example 6.2.1.** *Memory less Nonlinearities:* Let $X = \mathcal{L}_\infty$, and consider nonlinear operators $H_1(u) = u^2$ and $H_2(.)$ defined by the graph in the plane shown in Fig. 6.1. We have

$$\nu(H_1) = \inf_{0 \neq u \in \mathcal{L}_\infty} \frac{\|(H_1 u)_T\|_{\mathcal{L}_\infty}}{\|u_T\|_{\mathcal{L}_\infty}} = \inf_{0 \neq u \in \mathcal{L}_\infty} |u| = 0. \tag{6.11}$$

The minimum gain $\nu(H_2)$ is easily determined from the slope of the graph of $H_2$.

$$\nu(H_2) = \inf_{0 \neq u \in \mathcal{L}_\infty} \frac{\|(H_2 u)_T\|_{\mathcal{L}_\infty}}{\|u_T\|_{\mathcal{L}_\infty}} = 0.5. \tag{6.12}$$

**Lemma 6.2.3.** *Let $g(t)$ be the impulse response of a continuous-time, stable, LTI system. Let $G(s)$ denote the Laplace transform of $g(t)$. Furthermore, assume that there exists a row in $G(s)$ where all elements are strictly proper, namely there is $i$ such that for all $j$, $\lim_{s\to\infty} G_{ij}(s) = 0$. Let $H$ stand for the convolution operator defined by*

$$H(z(t)) = \int_0^t g(t-\tau) z(\tau) d\tau. \tag{6.13}$$

*We have*

$$\nu(H) = 0. \tag{6.14}$$

*Proof.* Let $\hat{x}(t) = [\hat{x}_1(t)\ \hat{x}_2(t)\ \cdots\ \hat{x}_n(t)]^T$,

$$\hat{x}_k(t) = \begin{cases} \sin(\omega t) & k = i, \\ 0 & \text{otherwise.} \end{cases}$$

where $i$ corresponds to the strictly proper row in $G(s)$ and $\omega \geq \pi$. Let

$$x(t) := \hat{x}(t) - \hat{x}\left(t - \left\lfloor \frac{\omega}{\pi} \right\rfloor \frac{\pi}{\omega}\right) \tag{6.15}$$

where $\lfloor r \rfloor$ denotes the floor function of a real number r, which is the largest integer less

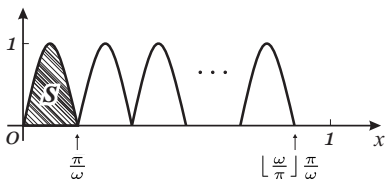


Figure 6.2: $|\hat{x}(t)|$.

than or equal to $r$, namely $\forall r \in \mathbb{R}\ ; \lfloor r \rfloor := \sup\{n \in \mathbb{Z} | n \leq r\}$. It is trivial that

$$x(t) = \begin{cases} \begin{bmatrix} 0 \\ 0 \\ \vdots \\ \sin(\omega t) \\ \vdots \\ 0 \end{bmatrix} & \text{ith row} \qquad 0 \leq t \leq \left\lfloor \frac{\omega}{\pi} \right\rfloor, \\ 0 & t > \left\lfloor \frac{\omega}{\pi} \right\rfloor. \end{cases}$$

and

$$\|x(t)\| = \left| \hat{x}_i(t) - \hat{x}_i \left( t - \left\lfloor \frac{\omega}{\pi} \right\rfloor \frac{\pi}{\omega} \right) \right|$$

Thus,

$$\|x\|_{\mathcal{L}_\infty} = \sup_t |\sin(\omega t)| = 1 \tag{6.16}$$

$$\begin{aligned} \|x\|_{\mathcal{L}_2}^2 &= \int_0^{\lfloor \frac{\omega}{\pi} \rfloor \frac{\pi}{\omega}} |\sin(\omega t)|^2 \, dt \\ &= {}^1\!/_2 \left( t - \frac{\sin(2\omega t)}{2\omega} \right) \Bigg|_0^{\lfloor \frac{\omega}{\pi} \rfloor \frac{\pi}{\omega}} \\ &= \left\lfloor \frac{\omega}{\pi} \right\rfloor \frac{\pi}{2\omega} - \frac{\sin\left(2\pi \lfloor \frac{\omega}{\pi} \rfloor\right)}{4\omega} \end{aligned} \tag{6.17}$$

$$\|x\|_{\mathcal{L}_1} = \int_0^{\lfloor \frac{\omega}{\pi} \rfloor \frac{\pi}{\omega}} |\sin(\omega t)| \, dt. \tag{6.18}$$

To calculate (6.18), consider the graph of $|\hat{x}(t)|$ depicted in Fig. 6.2. The number of peaks is $\left\lfloor \frac{\omega}{\pi} \right\rfloor$. Moreover,

$$S = \int_0^{\frac{\pi}{\omega}} \sin(\omega t) \, dt = \frac{2}{\omega}. \tag{6.19}$$

Consequently,

$$\|x\|_{\mathcal{L}_1} = \left\lfloor \frac{\omega}{\pi} \right\rfloor S = \left\lfloor \frac{\omega}{\pi} \right\rfloor \frac{2}{\omega}. \tag{6.20}$$

To calculate the norm of the output $\|y\|$, we can first find the response of the system to input $\hat{x}(t)$, namely $\hat{y}(t)$, and then obtain the output using $y(t) = \hat{y}(t) - \hat{y}\left(t - \left\lfloor \frac{\omega}{\pi} \right\rfloor \frac{\pi}{\omega}\right)$ implied

by the linearity property of the system and (6.15). If we let $\omega \to \infty$, the response of the system to $\hat{x}(t)$ approaches to zero. The reason is that the amplitude of all elements of the $i$-th row of $G(s)$ approaches to zero at high frequencies. Therefore, $\lim_{w\to\infty} \|\hat{y}(t)\| = 0$ and consequently

$$\lim_{w\to\infty} \|y\| = 0. \tag{6.21}$$

On the other hand, (6.17) and (6.20) imply

$$\lim_{w\to\infty} \|x\|_{\mathcal{L}_2} = {}^1\!/_2, \lim_{w\to\infty} \|x\|_{\mathcal{L}_1} = \frac{2}{\pi}. \tag{6.22}$$

Equations (6.16), (6.21) and (6.22) imply

$$\nu_1(H) = 0,\ \nu_2(H) = 0,\ \nu_\infty(H) = 0. \tag{6.23}$$

□

**Corollary 6.2.1.** *The minimum gain of a system with a strictly proper stable transfer function is zero.*

**Lemma 6.2.4.** *Let $g(t)$ be the impulse response of a continuous-time (discrete-time) LTI system. Let $G(s)$ $(G(z))$ denote the Laplace transform (z-transform) of $g(t)$. Furthermore, assume that $G(s)$ $(G(z))$ has at least one zero in the RHP (outside of the unit circle). Let $H$ stand for the convolution operator defined by*

$$H(z(t)) = \int_0^t g(t-\tau)z(\tau)d\tau \tag{6.24}$$

*for continuous-time case and*

$$H(z(t)) = \sum_{l=0}^{t} g(t-l)z(l) \tag{6.25}$$

*for discrete-time one. We have*

$$\nu(H) = 0. \tag{6.26}$$

*Proof.* The proofs for the continuous-time and discrete-time cases are the same and only the first one is given here.

Let $s_0$ be the RHP zero of $G(s)$, namely there exists $w$ such that $G(s_0)w = 0$. If $\sigma_0 + i\omega_0 = s_0 \in \mathbb{C}$, trivially $s_0^*$ is also a RHP zero of $G(s)$. Let

$$u(t) = \begin{cases} w\, e^{s_0 t} & \text{if } s_0 \in \mathbb{R}, \\ w\, e^{\sigma_0 t} \sin(\omega_0 t) & \text{if } s_0 \in \mathbb{C}. \end{cases} \tag{6.27}$$

Consequently,

$$U(s) = \begin{cases} w \cdot \frac{1}{s-s_0} & \text{if } s_0 \in \mathbb{R}. \\ w \cdot \frac{\omega_0}{(s-\sigma_0)^2+\omega_0^2} & \text{if } s_0 \in \mathbb{C}. \end{cases} \tag{6.28}$$

We have

$$Y(s) = \begin{cases} G(s) \cdot w \cdot \frac{1}{s-s_0} & \text{if } s_0 \in \mathbb{R}. \\ G(s) \cdot w \cdot \frac{\omega_0}{(s-\sigma_0)^2+\omega_0^2} & \text{if } s_0 \in \mathbb{C}. \end{cases} \tag{6.29}$$

Since $G(s)$ is assumed to be stable, $Y(s)$ is a stable signal. It is important to note that $Y(s)$ does not have a pole at $s_0$. The reason is that the pole at $s_0$ is canceled by the zero of $G(s)$ at $s_0$. Since all poles of $Y(s)$ are in LHP, $y(t)$ is a decaying signal. On the other hand, $u(t)$ is an unstable signal, rising by time. If we truncate both $u(t)$ and $y(t)$ at $T$, which is chosen sufficiently large, the corresponding gain of the system will be small. By increasing $T$, the gain can be decreased as much as desired. Therefore, $\nu(H) = 0$.

□

**Lemma 6.2.5.** *Let $H : \mathcal{D}_h \subseteq \mathcal{U} \to \mathcal{Y}$ be a possibly unstable operator. Let $\mathcal{R}_h$ denote the range of $H$, namely $\mathcal{R}_h = \{y \in \mathcal{Y} : y = Hu \text{ for some } u \in \mathcal{D}_h\}$. Assume that $H$ has a stable right inverse, i.e., there exists $H^{-1} : \mathcal{R}_h \to \mathcal{D}_h$ such that*

$$H \cdot H^{-1} = I \tag{6.30}$$

*and $H^{-1}$ is stable. Moreover, assume that $\gamma(H^{-1}) < \infty$ Then*

$$\nu(H) = \frac{1}{\gamma(H^{-1})}. \tag{6.31}$$

*Proof.* Let $y(t) := Hu(t)$, which implies that $u(t) = H^{-1}y(t)$. Therefore

$$\begin{aligned} \nu(H) &= \inf_{u \in \mathcal{U}} \frac{\|y_T\|}{\|u_T\|} = \inf_{u \in \mathcal{D}_h} \frac{\|y_T\|}{\|u_T\|} = \inf_{u \in \mathcal{D}_h} \frac{1}{\frac{\|u_T\|}{\|y_T\|}} \\ &= \frac{1}{\sup\limits_{u \in \mathcal{D}_h} \frac{\|u_T\|}{\|y_T\|}} = \frac{1}{\sup\limits_{u \in \mathcal{D}_h} \frac{\|H^{-1}y_T\|}{\|y_T\|}} \\ &= \frac{1}{\sup\limits_{y \in \mathcal{R}_h} \frac{\|H^{-1}y_T\|}{\|y_T\|}} = \frac{1}{\gamma(H^{-1})}. \end{aligned} \tag{6.32}$$

□

**Corollary 6.2.2.** Unstable, bi-proper, LTI systems

1. *Let $g(t)$ be the impulse response of a continues-time, unstable, bi-proper, LTI system. Let $H$ stand for the convolution operator defined by*

$$H(z(t)) = \int_0^t g(t-\tau)z(\tau)d\tau. \tag{6.33}$$

*Let $G(s)$ be the Laplace transform of $g(t)$. We have*

$$\nu(H) = \left\|G^{-1}(s)\right\|_{\mathcal{H}_\infty}^{-1}. \tag{6.34}$$

2. *Let $g(t)$ be the impulse response of a discrete-time, unstable, strictly proper, LTI system. Let $H$ denote the convolution operator defined by*

$$H(z(t)) = \sum_{l=0}^{t} g(t-l)z(l). \tag{6.35}$$

*Let $G(z)$ be the $z$-transform of $g(t)$. We have*

$$\nu(H) = \left\|G^{-1}(z)\right\|_{\mathcal{H}_\infty}^{-1}. \tag{6.36}$$

*Proof.* The proofs for continuous-time and discrete-time are the same and only the first one comes here.

For bi-proper systems, the inverse system exists. Let $y(t) := Hu(t)$, we have

$$\begin{aligned}
\nu(H) &= \inf_{u\in\mathcal{X}_e} \frac{\|y_T\|}{\|u_T\|} \\
&= \inf_{u\in\mathcal{X}_e} \frac{1}{\frac{\|u_T\|}{\|y_T\|}} \\
&= \frac{1}{\sup\limits_{u\in\mathcal{X}_e} \frac{\|u_T\|}{\|y_T\|}} \\
&= \frac{1}{\sup\limits_{y\in\mathcal{X}_e} \frac{\|u_T\|}{\|y_T\|}} \\
&= \frac{1}{\sup\limits_{u\in\mathcal{X}_e} \frac{\|G^{-1}u_T\|}{\|y_T\|}}.
\end{aligned} \tag{6.37}$$

□

**Example 6.2.2.** Let

$$G(s) = \frac{s+1}{s-1} \tag{6.38}$$

and $H : \mathcal{D}_h \subset \mathcal{L}_2 \to \mathcal{L}_2$ be an operator defined as (6.33). Equation (6.36) implies that

$$\nu(H) = \left\|G^{-1}(s)\right\|_{\mathcal{H}_\infty}^{-1} = 1. \tag{6.39}$$

For instance, let $u(t) := (1-2t)\,e^{-t}\,u_{-1}(t)$, where $u_{-1}(t)$ denotes the step function. We have $U(s) = \frac{s-1}{(s+1)^2}$ and consequently $Y(S) = \frac{1}{s+1}$ which shows that $y(t) = e^{-t}\,u_{-1}(t)$. This reveals that $\nu(H) \leq \frac{\|y\|_{\mathcal{L}_2}}{\|u\|_{\mathcal{L}_2}} = 1$. It is important to note that there is no input that satisfies $\frac{\|y\|_{\mathcal{L}_2}}{\|u\|_{\mathcal{L}_2}} < 1$. This can be shown by contradiction. Assume there exists some input $\hat{u} \in \mathcal{L}_2^e$ such that $\frac{\|\hat{y}\|_{\mathcal{L}_2}}{\|\hat{u}\|_{\mathcal{L}_2}} < 1$ where $\hat{y}$ is the corresponding output. We have $\|\hat{y}\| < \|\hat{u}\| < \infty$. On the other hand, $\hat{u} = G^{-1}\,\hat{y}$. Since $\left\|G^{-1}\right\|_{\mathcal{H}_\infty} = 1\ \|\hat{u}\| \leq \|\hat{y}\|$ which is a contradiction.

The minimum gain of operators satisfies the *positivity* and the *positive homogeneity* properties. To see this, we have

$$\nu(\cdot) \geq 0 \tag{6.40}$$

and

$$\begin{aligned} \nu(\lambda H) &= \inf_{0 \neq u \in \mathcal{X}_e} \frac{\|\lambda H u\|}{\|u\|} \\ &= |\lambda| \inf_{0 \neq u \in \mathcal{X}_e} \frac{\|Hu\|}{\|u\|} = |\lambda|\ \nu(H) \end{aligned} \tag{6.41}$$

However, it can be shown that it fails to satisfy the triangle inequality. For instance, suppose that $H_1$ and $H_2$ are memoryless nonlinearities depicted in Fig. 6.3. It is trivial that $\nu(H_1) = 0$, $\nu(H_2) = 0$ and $\nu(H_1 + H_2) = 1$. This shows that $\nu(H_1 + H_2) > \nu(H_1) + \nu(H_2)$. Consequently, the minimum gain of an operator is not a norm or even a semi-norm on the space of operators.

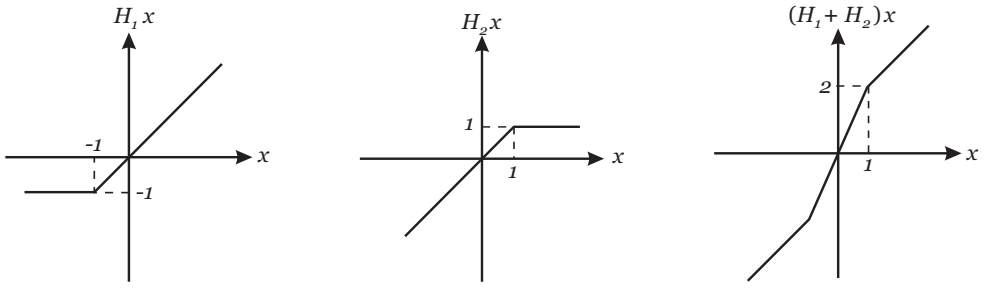


(a) $H_1$ (b) $H_2$ (c) $H_1 + H_2$

Figure 6.3: The triangle inequality is not satisfied by $\nu(\cdot)$.

**Lemma 6.2.6.** *Let $H : \mathcal{U} \to \mathcal{Y}$ denote an operator. Suppose that there exists a nonzero stable operator $K : \mathcal{R} \to \mathcal{U}$ such that $HK : \mathcal{R} \to \mathcal{Y}$ is stable, then $\nu(H) < \infty$.*

*Proof.* Let $0 \neq r(t) \in \mathcal{R}$ such that $r \notin \mathrm{Ker}(K)$, then $u(t) = K\,r(t) \in \mathcal{U}$, $u \neq 0$ and $y(t) = HK\,r(t) \in \mathcal{Y}$, implied by the stability of $K$ and $HK$, respectively. Therefore $\|u\|_{\mathcal{U}} \neq 0$ and $\|u\|_{\mathcal{U}}, \|y\|_{\mathcal{Y}} < \infty$. Consequently, $\nu(H) \leq \frac{\|y\|_{\mathcal{Y}}}{\|u\|_{\mathcal{U}}} < \infty$. □

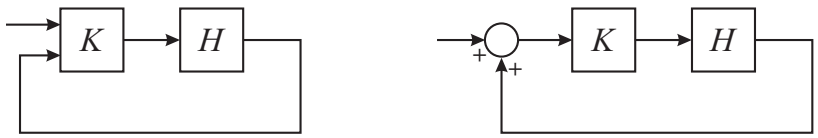


(a) (b)

Figure 6.4: Stabilizable system.

**Corollary 6.2.3.** *Any system that can be stabilized by a stable system with the mentioned properties in Lemma 6.2.6 and a structure as shown in either Fig. 6.4(a) or Fig. 6.4(b), has a finite minimum gain.*

*Proof.* The corollary is based on Lemma 6.2.6 and the proof follows a similar routine as the proof of the lemma with defining a new $\mathcal{R}$ equals $\mathcal{R} \oplus \mathcal{Y}$ in 6.4(a) or $\mathcal{R} + \mathcal{Y}$ in 6.4(b). □

**Theorem 6.2.1.** Sub-multiplicative property
*Let $H_1, H_2 : \mathcal{X} \to \mathcal{X}$ be causal operators. Then*

$$\nu(H_1 H_2) \leq \nu(H_1)\nu(H_2). \tag{6.42}$$

*Proof.* Let $u \in \mathcal{X}$, we have

$$\|H_1 H_2 u\| \geq \nu(H_1) \|H_2 u\| \geq \nu(H_1)\nu(H_2) \|u\| . \tag{6.43}$$

Considering the fact that $\nu(H_1 H_2)$ is the infimum gain of the $H_1 H_2$, Inequality (6.43) implies (6.42). □

## 6.3 Large Gain Theorem

In this section, we concentrate on the feedback system shown in Fig. 6.5. Under mild conditions on $H_1$ and $H_2$ (e.g., the product of the instantaneous gains is less than one [1]), the feedback configuration is guaranteed to be well-posed. The equations describing this feedback system, to be known as the *Feedback Equations*, are:

$$\begin{aligned} e_1 &= u_1 - y_2 \\ e_2 &= u_2 + y_1 \\ y_1 &= H_1 e_1 \\ y_2 &= H_2 e_2. \end{aligned} \tag{6.44}$$

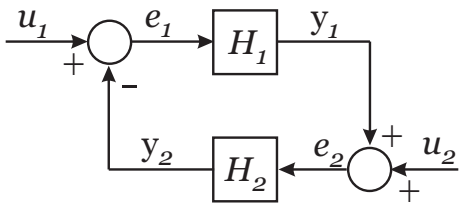


Figure 6.5: The feedback system.

**Theorem 6.3.1.** *Consider the feedback interconnection described by (6.44) and shown in Fig. 6.5. If* $1 < \nu(H_1)\nu(H_2) < \infty$*, the feedback system is input-output-stable.*

*Proof.* To show stability of the feedback interconnection, we must show that $u_1, u_2 \in \mathcal{X}$ imply that $e_1$, $e_2$, $y_1$ and $y_2$ are also in $\mathcal{X}$. According to the definition of $\nu$, we have

$$\nu(H_1)\,\|e_{1T}\| \le \|y_{1T}\| \tag{6.45}$$

$$\nu(H_2)\,\|e_{2T}\| \le \|y_{2T}\| \tag{6.46}$$

On the other hand,

$$y_{1T} = e_{2T} - u_{2T} \tag{6.47}$$

$$y_{2T} = u_{1T} - e_{1T} \tag{6.48}$$

Thus,

$$\|y_{1T}\| \le \|e_{2T}\| + \|u_{2T}\| \tag{6.49}$$

$$\|y_{2T}\| \le \|e_{1T}\| + \|u_{1T}\| \tag{6.50}$$

Substituting (6.45) and (6.46) in (6.49) and (6.50), respectively,

$$\nu(H_1)\,\|e_{1T}\| \le \|e_{2T}\| + \|u_{2T}\| \tag{6.51}$$

$$\nu(H_2)\,\|e_{2T}\| \le \|e_{1T}\| + \|u_{1T}\| \tag{6.52}$$

Using (6.46) and (6.50), Equation (6.51) implies that

$$\begin{aligned} \nu(H_2)\nu(H_1)\,\|e_{1T}\| &\le \nu(H_2)\,\|e_{2T}\| + \nu(H_2)\,\|u_{2T}\| \\ &\le \|y_{2T}\| + \nu(H_2)\,\|u_{2T}\| \\ &\le \|e_{1T}\| + \|u_{1T}\| + \nu(H_2)\,\|u_{2T}\|\,. \end{aligned} \tag{6.53}$$

Since $\nu(H_1)\nu(H_2) > 1$,

$$\|e_{1T}\| \le \frac{1}{\nu(H_1)\nu(H_2) - 1}\left(\|u_{1T}\| + \nu(H_2)\,\|u_{2T}\|\right). \tag{6.54}$$

Similarly,

$$\|e_{2T}\| \leq \frac{1}{\nu(H_1)\nu(H_2)-1}\left(\nu(H_1)\|u_{1T}\| + \|u_{2T}\|\right). \tag{6.55}$$

Moreover, substituting (6.55) and (6.54) in (6.49) and (6.50), respectively,

$$\|y_{1T}\| \leq \frac{\nu(H_1)}{\nu(H_1)\nu(H_2)-1}\left(\|u_{1T}\| + \nu(H_2)\|u_{2T}\|\right) \tag{6.56}$$

and

$$\|y_{2T}\| \leq \frac{\nu(H_2)}{\nu(H_1)\nu(H_2)-1}\left(\nu(H_1)\|u_{1T}\| + \|u_{2T}\|\right). \tag{6.57}$$

Hence, the norms of $\|e_{1T}\|$, $\|1_{2T}\|$, $\|y_{1T}\|$ and $\|y_{2T}\|$ are bounded. If, in addition, $u_1,\ u_2 \in \mathcal{X}$, then (6.54-6.57) must also be satisfied if $T$ approaches $\infty$. Therefore,

$$\|e_1\| \leq \frac{1}{\nu(H_1)\nu(H_2)-1}\left(\|u_1\| + \nu(H_2)\|u_2\|\right) \tag{6.58}$$

$$\|e_2\| \leq \frac{1}{\nu(H_1)\nu(H_2)-1}\left(\nu(H_1)\|u_1\| + \|u_2\|\right) \tag{6.59}$$

$$\|y_1\| \leq \frac{\nu(H_1)}{\nu(H_1)\nu(H_2)-1}\left(\|u_1\| + \nu(H_2)\|u_2\|\right) \tag{6.60}$$

$$\|y_2\| \leq \frac{\nu(H_2)}{\nu(H_1)\nu(H_2)-1}\left(\nu(H_1)\|u_1\| + \|u_2\|\right). \tag{6.61}$$

Consequently, $e_1$, $e_2$, $y_1$ and $y_2$ are also in $\mathcal{X}$. □

**Example 6.3.1.** Let $H_1$ be the convolution operator defined by (6.13) where $g(t)$ is the impulse response of

$$G(s) = k\frac{s+1}{s-1}$$

where $k \in \mathbb{R}$. Let $H_2$ be a memoryless nonlinearity depicted in Fig. 6.1. As shown in Example 6.2.2, $\nu(H_1/k) = 1$ which implies that $\nu(H_1) = |k|$. On the other hand, we have $\nu(H_2) = 0.5$. Consequently $\nu(H_1)\nu(H_2) = 0.5|k|$. The large gain theorem, namely Theorem 6.3.1, guarantees that the feedback system is stable if $|k| > 2$.

## 6.4 Chapter Summary

The minimum gain of an operator as well as some of its properties are introduced. These properties are useful in the computation of the minimum gain of a system. For instance, it is shown that the minimum gain of strictly proper, stable, LTI systems are zero. When it comes to the metric properties, the minimum gain of an operator fails to satisfy the triangular

inequality which implies that it is not a metric or a norm in the space of operators. Finally, the so-called large gain theorem is stated and proved. This theorem implies a new stability condition for feedback interconnection of nonlinear systems. An example is provided to illustrate the derived stability condition.

# Chapter 7

# Disturbance Attenuation: A Case Study

## 7.1 Introduction

There is no doubt that disturbance attenuation is one of the most important objectives in any closed-loop system. Therefore, it is important to quantify the influence of various inputs on various signals inside the feedback loop and develop tools to calculate such quantities. This chapter is based on our earlier work presented in Chapter 4. The plant of interest is a multitank system consistent of three interconnected tanks. First, the mathematical model of the plant is derived using physical relations. Then, the gray box method is used to identify the parameters of the model. Finally, it is assumed that the plant is controlled by a proportional controller and the disturbance attenuation of the closed-loop plant is investigated.

## 7.2 The Multitank System

Liquid level control problems related to multitank systems are commonly encountered in industrial storage tanks. For instance, steel producing companies around the world have repeatedly confirmed that substantial benefits are gained from accurate mould level control in continuous bloom casting. Mould level oscillations tend to stir foreign particles and flux powder into molten metal, resulting in surface defects in the final product [19].

The multitank system consists of three tanks placed one above another. The top tank has a constant cross section while the other two have variable cross sections as shown in Fig. 7.1. A pump is used to circulate liquid from the supply tank into the upper tank. The liquid flows through the tanks due to gravity. The output orifices can be controlled by electrical valves to act as constant or time-varying flow resistors. Generally speaking, the system has four inputs and three outputs. The inputs are three valve controls and one pump

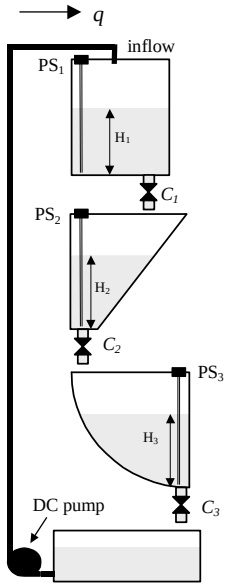


Figure 7.1: Configuration of the multitank system

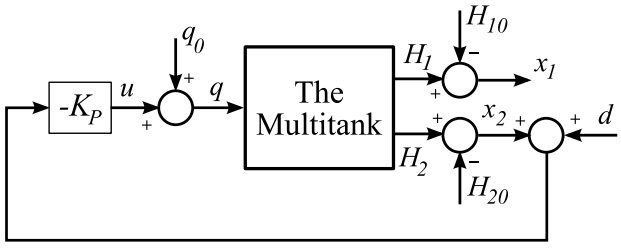


Figure 7.2: Closed loop multitank system

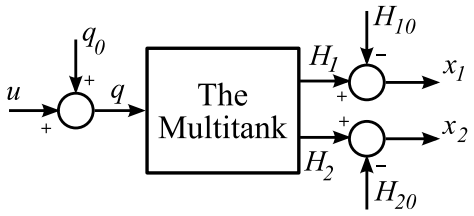


Figure 7.3: Block diagram of the identified system

control signal. The three valve controls are driven by appropriate Pulse-Width Modulation (PWM [16]) signals transmitted from the I/O board to the power interface, and from the power interface to the DC motors connected to the valves. The pump control signal, which acts by controlling the speed of the pump motor, is a sequence of PWM pulses configured and generated by the logic of XILINX chip of the I/O board. The output signals are the levels of the liquid measured by pressure transducers. All signals are connected to the analog inputs/outputs of a multipurpose PC I/O board.

The system states are the liquid levels $H_1$, $H_2$ and $H_3$. The general objective of the pilot is to control the liquid levels by four input signals: liquid inflow $q$ and valve settings $C_1$, $C_2$ and $C_3$. Among various system configurations, our purpose is to control level of the middle tank, i.e. $H_2$, by the liquid inflow $q$ using a proportional controller. We assume that $d$ is the disturbance (or noise) signal and study the disturbance attenuation of the closed-loop system. The block diagram of the closed-loop system is depicted in Fig. 7.2.

## 7.3 Identification

The block diagram of the plant is depicted in Fig. 7.3. First, a mathematical model of the plant is developed based on the physics of the process. Next, we set an experiment to acquire the step response of the system in order to obtain an approximate model of the system or more precisely, an approximate time constants of the system. Using the approximate time constants, a Random Binary Sequence (RBS) signal is built and applied to the plant [26]. Finally, the RBS response is divided to two sections; one section is used to identify the model and another one to validate the model.

### 7.3.1 The Mathematical Model

The Bernoulli's law can be applied to find the laminar outflow rate of an ideal fluid [30]. By applying mass balance and assuming a laminar outflow, the model describing the dynamics

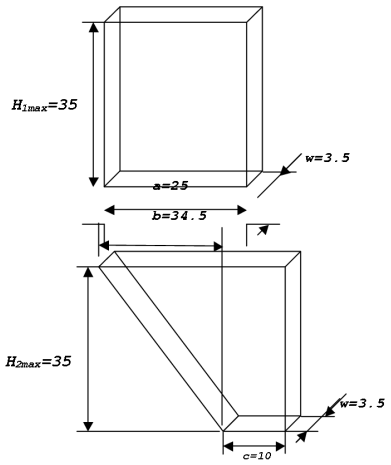


Figure 7.4: Geometrical parameters of the tanks

of the process can be obtained.

$$\begin{cases} \dfrac{dV_1}{dt} = q - C_1\sqrt{H_1} \\ \dfrac{dV_2}{dt} = C_1\sqrt{H_1} - C_2\sqrt{H_2} \end{cases} \tag{7.1}$$

where $V_1$ and $V_2$ are the fluid volumes in Tank 1 and Tank 2, respectively and $C_1$ and $C_2$ are the resistances of the output orifices. Hence,

$$\begin{cases} \dfrac{dV_1}{dH_1}\dfrac{dH_1}{dt} = q - C_1{H_1}^{\alpha_1} \\ \dfrac{dV_2}{dH_2}\dfrac{dH_2}{dt} = C_1{H_1}^{\alpha_1} - C_2{H_2}^{\alpha_2} \end{cases} \tag{7.2}$$

where $\alpha_1 = 0.5$ and $\alpha_2 = 0.5$ for laminar flows. For the real system where turbulence and acceleration of the liquid are not negligible, the outflow rate does not follow the Bernoulli law and more general coefficients $\alpha_1$ and $\alpha_2$ should be considered [19] [30]. The values of $\frac{dV_1}{dH_1}$ and $\frac{dV_2}{dH_2}$ depend on the shape of the tanks shown in Fig. 7.4. Since the cross-sectional area of Tank 1 is constant, $\frac{dV_1}{dH_1} = aw$. For Tank 2, we have $\frac{dV_1}{dH_1} = cw + \frac{H_2}{H_{2max}}bw$. Therefore,

$$\begin{cases} \frac{dH_1}{dt} = \frac{1}{aw}\left(q - C_1 H_1^{\alpha_1}\right) \\ \frac{dH_2}{dt} = \frac{1}{cw + \frac{H_2}{H_{2max}}bw}\left(C_1 H_1^{\alpha_1} - C_2 H_2^{\alpha_2}\right) \end{cases} \tag{7.3}$$

Let $x_1 := H_1 - H_{10}$, $x_2 := H_2 - H_{20}$ and $q = u + q_0$ where $H_{10}$ and $H_{20}$ are operating points and $q_0$ is the corresponding input. It is trivial that $q_0 = C_1 H_{10}^{\alpha_1} = C_2 H_{20}^{\alpha_2}$. The numerical values for the coefficients are $a = 0.25$, $w = 0.035$, $H_{2max} = 0.35$, $b = 0.345$, $c = 0.1$ [19]. Hence, the state equation of the open-loop system is

$$\begin{cases} \frac{dx_1}{dt} = 114.2857\left(u + (0.15C_1)^{\alpha_1} - C_1(x_1 + 0.15)^{\alpha_1}\right) \\ \frac{dx_2}{dt} = \frac{1}{0.0035 + 0.0345(x_2 + 0.1)}\left(C_1(x_1 + 0.15)^{\alpha_1} - C_2(x_2 + 0.1)^{\alpha_2}\right) \end{cases} \tag{7.4}$$

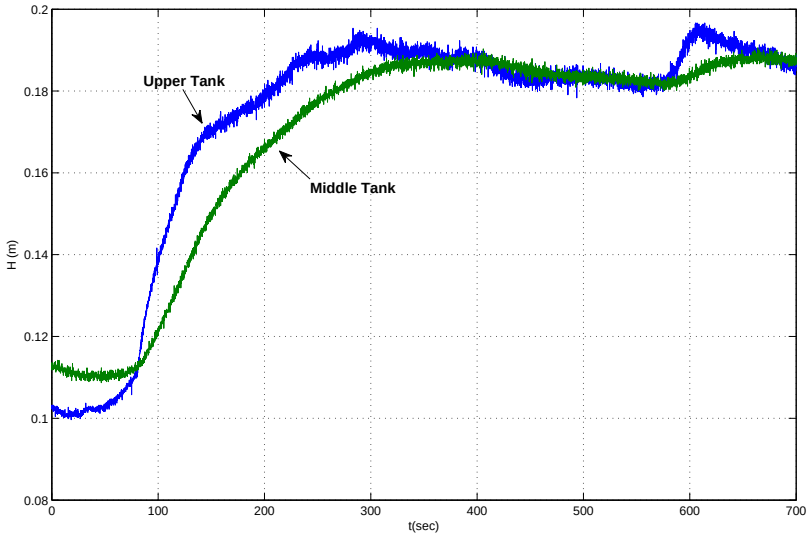


Figure 7.5: The step response

### 7.3.2 Data Acquisition

To build an appropriate RBS signal, we need to acquire approximate time constants of the system. Therefore, we set an experiment to obtain step responses. The step responses are depicted in Fig. 7.5. Hence, the approximate time constant of the system are $\tau_1 \approx 80s$ and $\tau_2 \approx 150s$. We will use the time constants to determine frequency of the RBS signal. We choose $T_s = 10\,\mathrm{sec}$. To perform the RBS test we need to determine the pass band which can be calculated from the following formula [26]:

$$f = \frac{kT_s}{\tau\pi} \tag{7.5}$$

where $k = 2 \sim 3$. We select $f = 0.0612$. The produced RBS signal and response of the system are illustrated in Fig. 7.6.

### 7.3.3 Data Pre-Processing and Identification

We do the identification and validation for each of the outputs separately. After down sampling the data, the mean value of the data should be removed and to reduce computational errors, we increase the values of the levels by using centimeter unit. Then, we filter the data by a low pass filter to attenuate noise. The bandwidth of the system is approximately equal to inverse of the time constant. We choose one decade upper than the bandwidth as cut-off

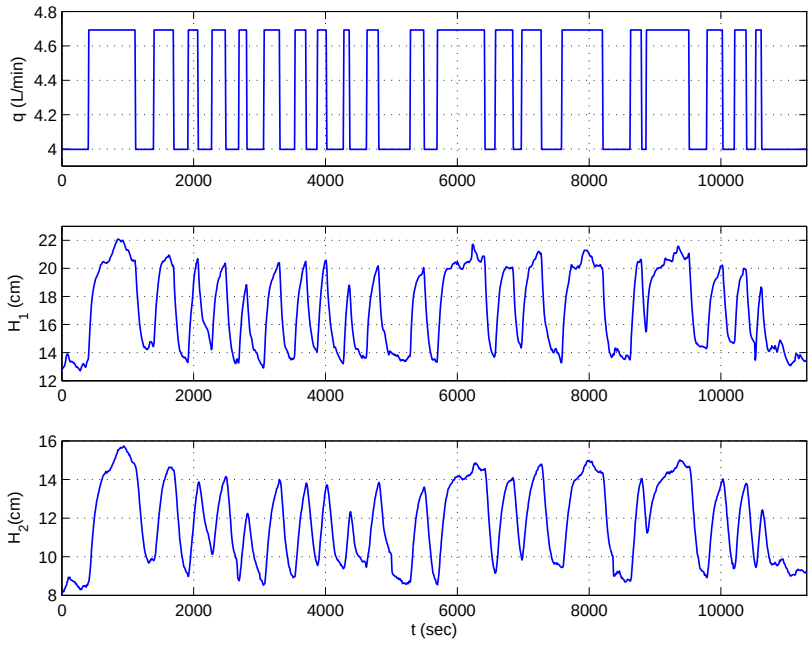


Figure 7.6: The RBS response

Table 7.1: The identified parameters.

| Parameter | $C_1$ | $C_2$ | $\alpha_1$ | $\alpha_2$ |
|---|---|---|---|---|
| Value | $1.432 \times 10^{-4}$ | $1.488 \times 10^{-4}$ | 0.3833 | 0.3341 |

frequency of the low-pass filter. Therefore,

$$f_{1,cut-off} = \frac{10T_s}{\tau_1 \pi} = 0.3979$$
$$f_{2,cut-off} = \frac{10T_s}{\tau_2 \pi} = 0.2122 \tag{7.6}$$

Next, From 1130 data points of the pair of input-output, we choose the first 750 points for identification and the remaining 380 points for validation and remove the mean values of two set of data. We use the Identification Toolbox of MATLAB to identify $C_1$, $C_2$, $\alpha_1$ and $\alpha_2$ by the gray box method. The identification and validation curves are depicted in Fig. 7.7 and 7.8, respectively.

The identified values for the mentioned parameters are given in Table 7.1.

### 7.3.4 Disturbance Attenuation

The problem of our interest is to study the disturbance attenuation of the closed loop system depicted in Fig.7.2. In order to calculate the disturbance rejection amplitude, we need to find

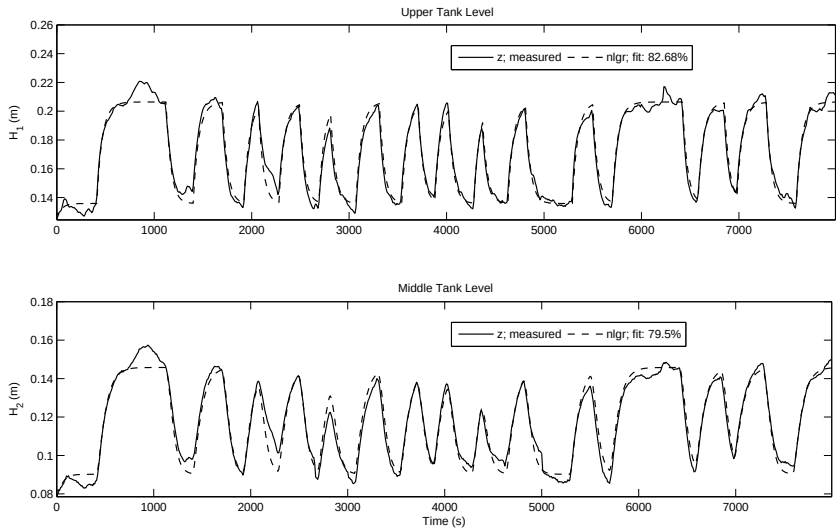


Figure 7.7: Identification

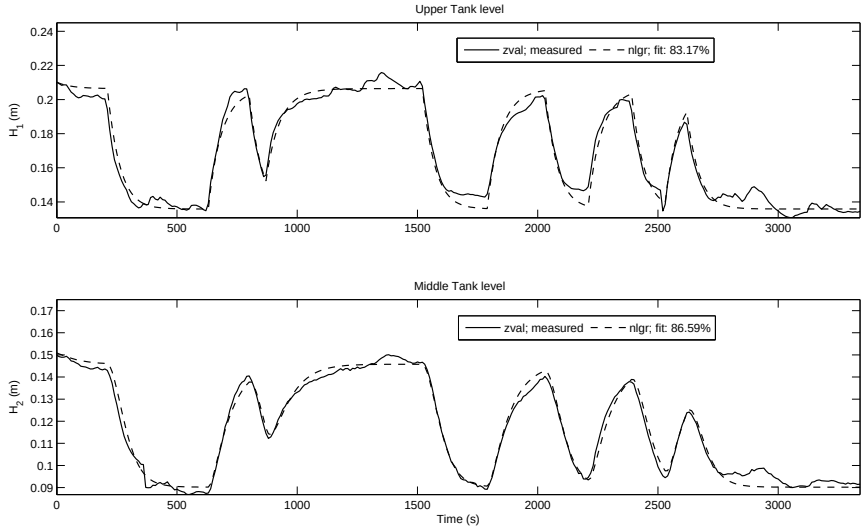


Figure 7.8: Validation

the gain of the system from the disturbance signal to the output by the methods mentioned in Section 5.3. The state equations of the closed-loop system are

$$\begin{cases} \dot{x}_1 = \frac{1}{aw}\left(q_0 - K_P(x_2+d) - C_1(x_1+H_{10})^{\alpha_1}\right) \\ \dot{x}_2 = \frac{1}{cw+\frac{x_2+H_{20}}{H_{2max}}bw}\left(C_1(x_1+H_{10})^{\alpha_1} - C_2(x_2+H_{20})^{\alpha_2}\right) \end{cases} \tag{7.7}$$

and $\dot{x} = \begin{pmatrix} \dot{x}_1 \\ \dot{x}_2 \end{pmatrix} = f(x,d)$. To find appropriate $A$ and $B$ matrices, we define a function which calculates $\gamma_\infty(\Gamma)\cdot\gamma_\infty(\Phi)$ in a local region $\left\|\begin{bmatrix} x \\ d \end{bmatrix}\right\|_\infty \leq \hat{r}$ for given $A$ and $B$ in MATLAB. Then using *fminsearch* function of MATLAB, we minimize the function with respect to $A$ and $B$. Choosing $\hat{r} = 0.06$, we obtain $A = \begin{pmatrix} -0.0360 & -0.0149 \\ 0.0215 & -0.0425 \end{pmatrix}$ and $B = \begin{pmatrix} 0.0141 \\ 0.0066 \end{pmatrix}$. Therefore, $\Phi(x,d) = \begin{bmatrix} \Phi_1(x,d) \\ \Phi_2(x,d) \end{bmatrix}$ where

$$\begin{cases} \Phi_1(x,d) = 0.00791 - 0.00266\,d + 0.00346\,x_2 - 0.0164\,(x_1+0.150)^{0.3833} \\ \qquad\qquad + 0.0360\,x_1 \\ \Phi_2(x,d) = \left(0.000143\,(x_1+0.15)^{0.3833} - 0.00015\,(x_2+0.1)^{0.3341}\right)\times \\ \qquad\qquad (0.007 + 0.0345\,x_2)^{-1} - 0.0215\,x_1 + 0.0425\,x_2 - 0.00657\,d. \end{cases} \tag{7.8}$$

Computation with the methods proposed in [50] provides $\gamma_\infty(\Gamma) < 32.9194$, $\gamma_\infty(\Theta) < 0.2975$, and $\gamma_\infty(\Omega) = 1$. Let $\eta = 1$ which gives $\gamma_\infty(\Omega) + \eta\gamma_\infty(\Theta) = 1.2975$. By choosing different values for $M_p$ and $\eta$, different bounds can be obtained. For now, we choose $M_p = 20$. Therefore, $\gamma_\infty^{\mathcal{D}}(\Phi)$ should satisfy

$$\gamma_\infty^{\mathcal{D}}(\Phi) < \frac{M_p - \gamma_\infty(\Omega) - \eta\gamma_\infty(\theta)}{(M_p+\eta)\gamma_\infty(\Gamma)} = 0.0271. \tag{7.9}$$

$\frac{\|\Phi(x,d)\|_\infty}{\left\|\begin{bmatrix} x \\ d \end{bmatrix}\right\|_\infty}$ versus $\left\|\begin{bmatrix} x \\ d \end{bmatrix}\right\|_\infty$ is depicted in Fig. 7.9. Let us take $\mathcal{D}$ as the region where $\frac{\|\Phi(x,d)\|_\infty}{\left\|\begin{bmatrix} x \\ d \end{bmatrix}\right\|_\infty} < 0.049$, i.e. $\gamma_\infty^{\mathcal{D}}(\Phi) = 0.027$. Consequently $r_x = 0.049$ and $r_d = 0.049$. Let $\epsilon = 0.048$ and $\delta = 0.0023 \leq \frac{1-\gamma_\infty^{\mathcal{D}}(\Phi)\gamma_\infty(\Gamma)}{\gamma_\infty(\Omega)+\eta(\gamma_\infty(\Theta)+\gamma_\infty^{\mathcal{D}}(\Phi)\gamma_\infty(\Gamma))}\epsilon = 0.0024$. According to Theorem 3.3.2, for any input $d$ which satisfies $\|d\|_{\mathcal{L}_\infty} < \min(\eta\delta, r_d) = 0.0023$ and any initial state satisfying $\|x_0\|_\infty < \delta = 0.0023$, $x$ is bounded as $\|x\|_{\mathcal{L}_\infty} < \epsilon = 0.048$. In other words, if $-2.3\text{mm} \leq d \leq 2.3\text{mm}$, $14.77\text{cm} \leq H_{10} \leq 15.23\text{cm}$ and $8.77\text{cm} \leq H_{20} \leq 10.23\text{cm}$ then $10.2\text{cm} \leq H_1 \leq 19.8\text{cm}$ and $5.2\text{cm} \leq H_2 \leq 14.8\text{cm}$.

Now, Let $\eta = 4$. Therefore, $\gamma_\infty(\Omega) + \eta\gamma_\infty(\Theta) = 2.19$. By choosing $M_p = 22$, $\gamma_\infty^{\mathcal{D}}(\Phi)$ should satisfy

$$\gamma_\infty^{\mathcal{D}}(\Phi) < \frac{M_p - \gamma_\infty(\Omega) - \eta\gamma_\infty(\theta)}{(M_p+\eta)\gamma_\infty(\Gamma)} = 0.0231. \tag{7.10}$$

Table 7.2: Bounds obtained by various $\eta$ and $M_p$.

| $\hat{r}$ | $\eta$ | $M_p$ | $\|x_0\|_\infty <$ (in mm) | $\|d\|_{\mathcal{L}_\infty} <$ (in mm) | $\|x\|_{\mathcal{L}_\infty} <$ (in mm) |
|---|---|---|---|---|---|
| 0.06 | 0.1 | 8 | 5.8 | 0.58 | 45 |
| | 0.1 | 20 | 5 | 0.5 | 50 |
| | 1 | 20 | 2.3 | 2.3 | 48 |
| | 3 | 19 | 1.7 | 5 | 30 |
| | 4 | 22 | 1.4 | 5.6 | 30 |
| | 5 | 24 | 0.51 | 2.6 | 12 |
| | 8 | 38 | 0.72 | 5.7 | 28 |
| | 10 | 120 | 0.4 | 4.1 | 48 |
| 0.03 | 0.1 | 2 | 12.5 | 1.25 | 21.5 |
| | 1 | 9 | 4.58 | 4.58 | 38.2 |
| | 10 | 15 | 1.13 | 11.3 | 16.5 |
| | 100 | 130 | 0.11 | 11 | 15 |

Let $\mathcal{D}$ be the region where $\gamma_\infty^{\mathcal{D}}(\Phi) = 0.023$. Hence, $\frac{\|\Phi(x,d)\|_\infty}{\left\|\begin{bmatrix} x \\ d \end{bmatrix}\right\|_\infty} < 0.0302$ in $\mathcal{D}$. Thus, $r_x = 0.0302$ and $r_d = 0.0302$. Let $\epsilon = 0.03$ and

$$\delta = 0.0013 \leq \frac{1 - \gamma_\infty^{\mathcal{D}}(\Phi)\gamma_\infty(\Gamma)}{\gamma_\infty(\Omega) + \eta(\gamma_\infty(\Theta) + \gamma_\infty^{\mathcal{D}}(\Phi)\gamma_\infty(\Gamma))}\,\epsilon = 0.0014. \tag{7.11}$$

According to Theorem 3.3.2, for any input $d$ which satisfies $\|d\|_{\mathcal{L}_\infty} < \min(\eta\delta, r_d) = 0.0056$ and any initial state satisfying $\|x_0\|_\infty < \delta = 0.0013$, $x$ is bounded as $\|x\|_{\mathcal{L}_\infty} < \epsilon = 0.03$. In other words, if $-5.6\text{mm} \leq d \leq 5.6\text{mm}$, $14.86\text{cm} \leq H_{10} \leq 15.14\text{cm}$ and $9.86\text{cm} \leq H_{20} \leq 10.14\text{cm}$ then $12\text{cm} \leq H_1 \leq 18\text{cm}$ and $7\text{cm} \leq H_2 \leq 13\text{cm}$.

By choosing other values for $\eta$ and $M_p$, other bounds can be obtained. Moreover, $\hat{r}$ can also be changed to acquire required bounds. For example, let $\hat{r} = 0.03$. By minimizing $\gamma_\infty(\Gamma) \cdot \gamma_\infty(\Phi)$ in a local region $\left\|\begin{bmatrix} x \\ d \end{bmatrix}\right\|_\infty \leq \hat{r} = 0.03$, we obtain

$$A = \begin{pmatrix} -0.0204 & -0.0171 \\ 0.0262 & -0.0347 \end{pmatrix}, \quad B = \begin{pmatrix} 0.0124 \\ 0.0001 \end{pmatrix}. \tag{7.12}$$

For this case, $\frac{\|\Phi(x,d)\|_\infty}{\left\|\begin{bmatrix} x \\ d \end{bmatrix}\right\|_\infty}$ versus $\left\|\begin{bmatrix} x \\ d \end{bmatrix}\right\|_\infty$ is depicted in Fig. 7.10. For both $\hat{r} = 0.03$ and $\hat{r} = 0.06$ cases, some of the results are summarized in Table 7.2.

## 7.4 Chapter Summary

Based on Theorem 3.3.2 in Chapter 4, a method proposed to study disturbance attenuation of closed-loop nonlinear systems. The physical plant under examination is a multitank

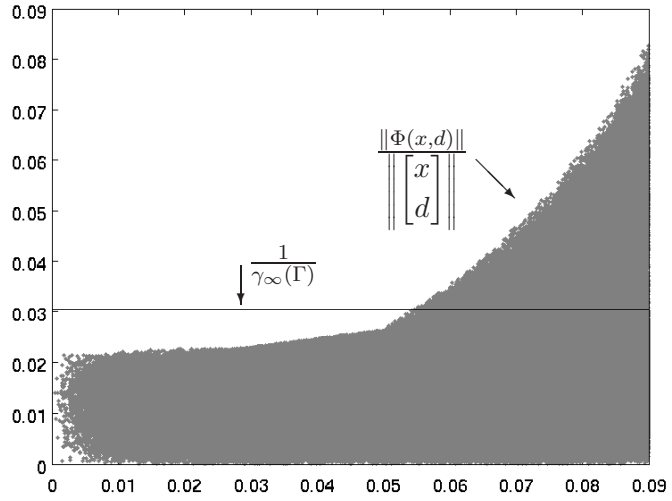


Figure 7.9: Gain of $\|\Phi(x,d)\|$ and $\frac{1}{\gamma_\infty(\Gamma)}$ for $\hat{r} = 0.06$

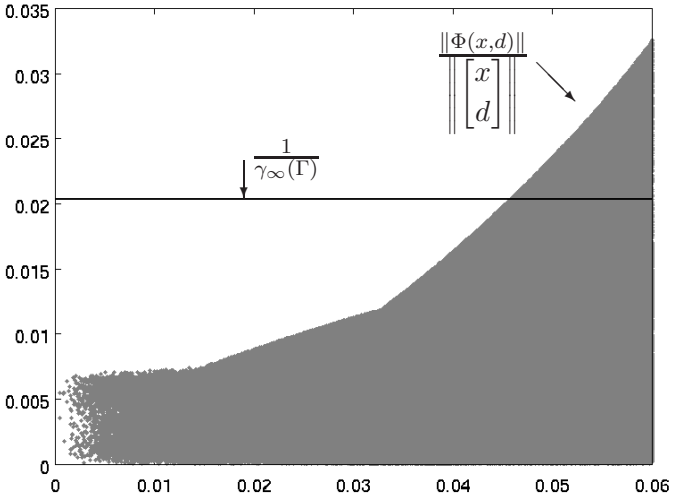


Figure 7.10: Gain of $\|\Phi(x,d)\|$ and $\frac{1}{\gamma_\infty(\Gamma)}$ for $\hat{r} = 0.03$

system. First, the mathematical model of the plant is derived using physical concepts. Then, the parameters of the model are identified by the gray box method. Finally, the disturbance attenuation of the closed-loop plant controlled by a proportional controller is investigated.

# Chapter 8

# Conclusions and Recommendations

## 8.1 Conclusions

In this thesis, different algorithms are developed to provide necessary tools for designing multi-model control systems for nonlinear systems. The major contributions are:

1. New representations for nonlinear systems, called $\zeta_A$ and $\zeta_{AB}$ representations, are proposed. In the $\zeta_A$ representation and its extended version for forced systems, $\zeta_{AB}$ representation, a nonlinear system is arranged as a feedback interconnection of a memoryless nonlinearity and a linear system with initial state as an input signal. Although interconnection of a memoryless nonlinearity with a linear system has been widely used in literature, the way the initial state is dealt with is the main difference between our decomposition and traditional ones. In $\zeta_A$ and $\zeta_{AB}$ representations, the initial state contributes to the feedback interconnection as an exogenous input while in traditional methods, any change in the initial state is handled by defining a new operator. The $\zeta_A$ and $\zeta_{AB}$ representations can be used to develop new tools for non-zero state nonlinear systems from the input-output theory methods, as presented in this thesis. In other words, the fact that the $\zeta_A$ and $\zeta_{AB}$ representations convert a nonlinear system with non-zero initial state to a combination of a memoryless nonlinearity and a linear system with some input signals and the way initial state is handled by these representations provide a novel viewpoint on all aspects of investigating nonlinear systems.

2. A new framework is developed for the analysis of stability of systems by the $\zeta_A$ and $\zeta_{AB}$ representations. The effectiveness of this usage is originated in the fact that using these representations, stability of nonlinear systems with non-zero initial states can be investigated by the input-output stability methods and stability is interpreted as

input-output stability of the resulting feedback systems. Precisely, new methods are proposed to check stability in the sense of Lyapunov for an unforced nonlinear system by norm of some relevant operators, without finding any Lyapunov-like function. For local stability, a method developed to find some local areas, $\Delta$ and $\Upsilon$, where the initial state $x_0$ belonging to $\Delta$ implies the state staying inside $\Upsilon$ area. The methods are also extended to forced systems.

3. A new method is proposed to compute an upper bound on the $\mathcal{L}_1$, $\mathcal{L}_2$ and $\mathcal{L}_\infty$ norms of a class of nonlinear systems. The method is based on the $\zeta_A$ and $\zeta_{AB}$ representations of nonlinear systems. A method is also proposed to find an upper bound on induced $\mathcal{L}_p$ norms. The second method, Theorem 4.1.2, provides tighter bound for the case $p = 2$. Both proposed methods suffer from a restrictive condition. Another tool is developed to overcome this restriction with the cost of providing only local conditions, namely, an upper bound on system output for bounded input and initial state, and being restricted to $\mathcal{L}_\infty$ induced norm.

4. Based on $\zeta_A$ and $\zeta_{AB}$ representations, methods are proposed to compute an upper bounds on the gap metric and the corresponding stability margin for a class of nonlinear systems.

5. The minimum gain of operators is defined, some of its properties are derived and some computational methods are developed to calculate the minimum gain. For example, it is shown that the minimum gain satisfies the positivity and the positive homogeneity properties but fails to satisfy the triangle inequality.

6. Based on the minimum gain of operators, the large gain theorem is stated. The large gain theorem asserts that the feedback loop will be stable if the minimum loop gain is greater than one.

7. One of the algorithms, which is developed to compute on upper bounds on $\mathcal{L}_\infty$ norm of nonlinear systems, is deployed to study disturbance attenuation of a closed loop system. The system of interest is a multitank system consisting of three tanks placed one above another. It is assumed that a proportional controller is used to control the level of the liquid in one of the tanks. The mathematical model of the open loop system is derived using physics of the plant. The gray box identification method is used to identify the model parameters and the disturbance attenuation of the system is investigated by the proposed method.

## 8.2 Future Work

Some future directions for extending and improving the results of this thesis are as follows:

1. Some of the results are already extended to discrete systems. It is useful to check the applicability of all results on discrete and multirate systems.

2. Almost all of the results are developed based on general classes of nonlinear systems, i.e.

$$N_1 : \dot{x}(t) = f_1(t, x(t)) \tag{8.1}$$

$$N_2 : \ \dot{x}(t) = f_2(t, x(t), u(t)). \tag{8.2}$$

   It may be useful to restrict systems to a narrower class. For example, one may obtain tighter bounds on the $\mathcal{L}_\infty$ norm of systems by restricting the system of interest to

$$N_3 : \ \dot{x}(t) = f_1(t, x(t)) \cdot f_2(t, u(t)). \tag{8.3}$$

3. The $\zeta_A$ and $\zeta_{AB}$ representations convert a nonlinear system with non-zero initial state to a combination of a memoryless nonlinearity and a linear system with some input signals. The way the initial state is handled by these representations provides a novel viewpoint on all aspects in investigating nonlinear systems. We have used $\zeta_A$ and $\zeta_{AB}$ representations in developing all the results presented in this thesis. One interesting work is to use the $\zeta_A$ and $\zeta_{AB}$ representations to study other aspects of nonlinear systems, such as observability, and develop new tools based on these representations.

4. The tools that are developed in this thesis can be used to design multi-model control systems. It would be interesting to design a multi-model control system based on the proposed tools.

# Bibliography


[1] J. A. Ball and J. W. Helton. Interconnection of Nonlinear Causal Systems. *IEEE Trans. on Automatic Control*, 34: 1132 – 1140, 1989.

[2] V. Chellaboina, W. M. Haddad, D. S. Bernstein, and D. A. Wilson. Induced Convolution Operator Norms of Linear Dynamical Systems. *Mathematics of Control, Signals, and Systems*, 13(3): 216 – 239, 2000.

[3] C. T. Chen. *Linear Systems Theory and Design.* 3rd edn., Oxford University Press: New York, 1998.

[4] T. W. S. Chow, H. Z. Tan, and Y. Fang. *Nonlinear System Representation*. Encyclopedia of Electrical and Electronic Engineering, J. G. Webster (Ed.), John Wiley & Sons, 2001.

[5] J. C. Doyle, T. T. Georgiou, and M. C. Smith. The Parallell Projection Operators of A Nonlinear Feedback System. *Systems & Control Letters*, 20(2):79 – 85, 1993.

[6] I. J. Fialho and T. T. Georgiou. A Variational Approach to $\mathcal{L}_\infty$-gain Analysis of Nonlinear Systems. *Proc. 1995 Conf. Decision & Control*, pp. 823 – 828.

[7] B. A. Foss, T. A. Johasen and A. V. Sorensen. Nonlinear Predictive Control Using Local Models - Applied to A Batch Fermentation Process, *Control Engineering Practice,* 3:389 – 396, 1995.

[8] G. F. Franklin, M. L. Workman, and D. Powell. *Digital Control of Dynamic Systems,* 3rd ed., Addison-Wesley Longman: Boston, 1997.

[9] O. Galan, J. A. Romagnoli, A. Palazoglu, and Y. Arkun. Gap Metric Concept and Implications for Multilinear Model-based Controller Design. *Industrial Engineering Chemical Research,* 42: 2189 – 2197, 2003.

[10] T. T. Georgiou, A. Pascoal, and P. P. Khargonekar. On the Robust Stabilizability of Uncertain Linear Time-invariant Plants Using Nonlinear Time-varying Controllers. *Automatica*, 35(5): 617 – 624, 1987.

[11] T. T. Georgiou. Differential Stability and Robust Control of Nonlinear Systems. *Math. Control Signals Syst.*, 6(4):289 – 306, 1993.

[12] T. T. Georgiou. On the Computation of the Gap Metric. *Systems and Control Letters,* 11(4): 253 – 257, 1988.

[13] T. T. Georgiou and M. C. Smith. Robustness Analysis of Nonlinear Feedback Systems: An Inputoutput Approach. *IEEE Trans. on Automatic Control*, 42(9): 1200 – 1221, 1997.

[14] T.T. Georgiou, M. Khammash, and A. Megretski. On a Large-gain Theorem. *Systems and Control Letters*, 32(4): 231 – 234, 1997.

[15] J. W. Hilton and M. R. James. *Extending $\mathcal{H}_\infty$ Control to Nonlinear Systems.* SIAM, 1999.

[16] D. G. Holmes and T. A. Lipo. *Pulse Width Modulation for Power Converters: Principles and Practice.* Wiley-IEEE Press, 2003.

[17] G. D. Howitt and R. Luss. Control of a Collection of Linear Systems by Linear State Feedback Control. *International Journal of Control*, 58(1):79 – 96, 1993.

[18] B. Ingalls and E. D. Sontag. A Small-gain Theorem with Applications to Input/Output Systems, Incremental Stability, Detectability and Interconnection. *Journal of the Franklin Institute*, 339(2): 211 – 229, 2002.

[19] *Multi-tank System User's Manual*, INTECO Ltd., www.inteco.com.pl.

[20] M. R. James and S. Yuliar. Numerical Approximation of the $\mathcal{H}_\infty$ Norm for Nonlinear Systems. *Automatica*, 31(8): 1075 – 1086, 1995.

[21] Z. P. Jiang, A. Teel, and L. Praly. Small-gain Theorem for ISS Systems and Applications. *Mathematics of Control, Signals, and Systems*, 7(2):95 – 120, 1994.

[22] I. Karafyllis. The Non-uniform in Time Small-gain Theorem for a Wide Class of Control Systems with Outputs. *European Journal of Control*, 10(4): 307 – 323, 2004.

[23] I. Karafyllis and Z. P. Jiang. A Small-gain Theorem for a Wide Class of Feedback Systems with Control Applications. *SIAM J. Control and Optimization*, 46(4): 1483 – 1517, 2007.

[24] H. K. Khalil. *Nonlinear Systems*, 3rd edn., Prentice Hall: Upper Saddle River, N.J., 2002.

[25] M. Krstič, I. Kanellakopoulos, and P. Kokotovič. *Nonlinear and Adaptive Control Design*. Wiley-Interscience: New York, 1995.

[26] L. Ljung. *System Identification: Theory for the User*. 2nd ed., Prentice Hall PTR, 1999.

[27] H. J. Marquez. *Nonlinear Control Systems, Analysis and Design*. John Wiley & Sons: New Jersey, 2003.

[28] R. Murray-Smith and T. A. Johansen. *Multiple Model Approaches to Modeling and Control*. Taylor & Francis, London, 1997.

[29] P. Pepe. The Liapunov's Second Method for Continuous Time Difference Equations. *Int. J. Robust and Nonlinear Control*, 13(15):1389 – 1405, 2003.

[30] R. H. Perry and D. W. Green. *Perry's Chemical Engineers' Handbook.* McGraw-Hill, 7th ed, 1997.

[31] B. G. Romanchuk. On the Computation of the Induced $\mathcal{L}_2$ Norm of Single-input Linear Systems with Saturation. *IEEE Trans. on Automatic Control*, 43(2): 262 – 268, 1998.

[32] I. W. Sandberg. On the $\mathcal{L}_2$-boundedness of Solutions of Nonlinear Functional Equations. *Bell System Tech. Journal*, 43(11): 1581 – 1599, 1964.

[33] E.D. Sontag. Input to State Stability: Basic Concepts and Results. In P. Nistri and G. Stefani (Ed.). *Nonlinear and Optimal Control Theory*. 1 st edn., Springer-Verlag: Berlin, 163 – 220, 2006.

[34] E. D. Sontag and Y. Wang. Notions of Input to Output Stability. *Systems and Control Letters*, 38(4-5):235 – 248: 1999.

[35] E. D. Sontag. Smooth Stabilization Implies Coprime Factorization. *IEEE Transactions on Automatic Control*, 34(4):435 – 443, 1989.

[36] E. D. Sontag and Y. Wang. On Characterizations of the Input-to-state Stability Property. *Systems and Control Letters*, 24(5):351 – 359, 1995.

[37] T. E. Stern. *Theory of Nonlinear Networks and Systems, An Introduction.* Addison-Wesley: Massachusetts, 1965.

[38] W. Tan. H. J. Marquez. T. Chen and J. Liu. Multimodel Analysis and Controller Design for Nonlinear Processes. *Computers and Chemical Engineering*, 28:2667 – 2675, 2004.

[39] A. R. Teel. A Nonlinear Small Gain Theorem for the Analysis of Control Systems with Saturation. *IEEE Transactions on Automatic Control*, 41(9): 1256 – 1270, 1996.

[40] M. Vidyasagar. *Nonlinear Systems Analysis.* Society of Industrial and Applied Mathematics: Philadelphia, 2nd edn., 2002.

[41] M. Vidyasagar. *Input-output Analysis of Large-scale Interconnected Systems*. Springer-Verlag: New York, 1981.

[42] V. M. Popov. Absolute Stability of Nonlinear Systems of Automatic Control. *Automation Remote Control*, 22: 857 – 875, 1962.

[43] W. Rugh. Analytical Framework for Gain Scheduling. *IEEE control systems Magazine*, 11(1): 79 – 84, 1991.

[44] J. S. Shamma and M. Athans. Gain Scheduling: Potential Hazards and Possible Remedies. *IEEE control systems Magazine*, 12(3): 101 – 107, 1992.

[45] J. S. Shamma. *Analysis and Design of Gain Scheduled Control Systems.* PhD Thesis, Dept. of Mech. Eng., Massachusetts Ins. of Tech, 1988.

[46] F. G. Shinskey. *Process Control Systems: Application, Design, and Tuning.* 4th ed., McGraw-Hill, New York, 1996.

[47] A. Uppal, W. H. Ray, and A. B. Poore. The Classification of the Dynamic Behavior of Continuous Stirred Tank Reactorss Influence of Reactor Residence Time. *Chemical Engineering Science*, 31:205, 1976.

[48] A. J. van der Schaft. *$\mathcal{L}_2$-gain and Passivity Techniques in Nonlinear Control.* 2nd ed., Springer, London, 2000.

[49] V. Zahedzadeh, H. J. Marquez and T. Chen. On the Robust Stability of Unforced Nonlinear Systems. *Proc. of 45th IEEE Conf. on Decision and Control*, 343 – 348, 2006.

[50] V. Zahedzadeh, H. J. Marquez and T. Chen. On the Stability of a Class of Unforced Nonlinear Systems, An Operator Norm Approach. *IET Control Theory & Applications*, 3(2): 200 – 210, 2008.

[51] V. Zahedzadeh, H. J. Marquez and T. Chen. Upper Bounds for Induced Operator Norms of Nonlinear Systems. *IEEE Trans. on Automatic Control*, 2008.

[52] V. Zahedzadeh, H. J. Marquez and T. Chen. On the Computation of an Upper Bound on the Gap Metric for a Class of Nonlinear Systems. *Proc. of American Control Conf.*, 1917 – 1922, 2008.

[53] V. Zahedzadeh, H. J. Marquez and T. Chen. On the Input-output Stability of Nonlinear Systems: Large Gain Theorem. *Proc. of American Control Conf.*, 3440 – 3445, 2008.

[54] V. Zahedzadeh, H. J. Marquez and T. Chen. Upper Bounds for Induced Operator Norms of Nonlinear Systems. *Proc. of 26th American Control Conf.*, 4727 – 4732, 2007.

[55] G. Zames and A. K. El-Sakkary. Unstable Systems and Feedback: the Gap Metric. *Proc. Allerton Conf.*, 380 – 385, 1980.

[56] G. Zames. On the Input-output Stability for Time-varying Nonlinear Feedback Systems, Part I, Conditions Using Concepts of Loop Gain, Concity and Positivity. *IEEE Transactions on Automatic Control*, 11(2):228 – 238, 1966.

[57] K. Zhou and J. C. Doyle. *Essentials of Robust Control*, Prentice Hall, New Jersey, 1997.

## Examining Committee

Dr. Horacio J. Marquez, Electrical and Computer Engineering

Dr. Tongwen Chen, Electrical and Computer Engineering

Dr. Alan Francis Lynch, Electrical and Computer Engineering

Dr. Mahdi Tavakoli, Electrical and Computer Engineering

Dr. Amos Ben-Zvi, Chemical and Materials Engineering

Dr. Khashayar Khorasani, Electrical and Computer Engineering, Concordia University

# University of Alberta

Gain Analysis and Stability of Nonlinear Control Systems

by

Vahid Zahedzadeh

A thesis submitted to the Faculty of Graduate Studies and Research
in partial fulfillment of the requirements for the degree of

Doctor of Philosophy
in
Control Systems

Department of Electrical and Computer Engineering


Fall 2009
Edmonton, Alberta

*To My Mom and Dad*
*To All South Azerbaijanis Who Are Struggling To Preserve Their Identity...*

# Abstract

The complexity of large industrial engineering systems such as chemical plants has continued to increase over the years. As a result, flexible control systems are required to handle variation in the operating conditions. Some of the challenging elements in the design of control systems are nonlinearity, disturbances and uncertainty in the process model. In the classical approach, first the plant model should be linearized at the nominal operating point and then, a robust controller should be designed for the resulting linear system. However, the performance of a controller designed by this method deteriorates when operation deviates from the nominal point. When the distance between the operating region and the nominal operating point increases, this performance degradation may lead to instability.

In the context of traditional linear control, one method to solve this problem is to consider the impact of nonlinearity as "uncertainty" around the nominal model and design a controller such that the desired performance is satisfied for all possible systems in the uncertainty set. As the size of uncertainty increases, conservatism occurs and at some point, it becomes impossible to design a controller that can provide satisfactory performance.

One of the methods proposed to overcome the aforementioned shortcomings is the so-called Multiple Model approach. Using Multi Models, local designs are performed for various operating regions and membership functions or a supervisory switching scheme is used to interpolate or switch among the controllers as the operating point moves among local regions. Since the Multiple Model method is a natural extension of the linear control method, it inherits some benefits of linear control such as simplicity of analysis and implementation. However, all these benefits are valid locally. For example, the multiple model method may be vulnerable when global stability is taken into account.

The core objective of this thesis is to develop new tools to study stability of closed-loop

nonlinear systems controlled by local controllers in order to improve design of multiple model control systems. For example, one of the aims of this work is to investigate how to determine the region where closed loop system is stable. A secondary objective is to study the effects of the exogenous signals on stability of such systems.

To achieve these goals, first, new representations for nonlinear systems, called $\zeta_A$ and $\zeta_{AB}$ representations, are proposed. In $\zeta_A$ and $\zeta_{AB}$ representations, initial state contributes to the feedback interconnection as an exogenous input. These representations can be used to develop new tools for non-zero state nonlinear systems based on the input-output theory. The $\zeta_A$ and $\zeta_{AB}$ representations convert a nonlinear system with non-zero initial state into a combination of a memoryless nonlinearity and a linear system with some input signals. The way initial state is handled by these representations provides a novel viewpoint on all aspects of investigating nonlinear systems.

Using these representations, stability of nonlinear systems with non-zero initial states can be investigated by the input-output stability methods. Based on this usage, a new framework is developed for the analysis of stability of systems by the $\zeta_A$ and $\zeta_{AB}$ representations. For local stability, a method developed to find a pair of local areas, namely $\Delta$ and $\Upsilon$, where belonging the initial state to $\Delta$ implies staying the state inside $\Upsilon$. The methods are also extended to forced systems.

To compute an upper bound on the $\mathcal{L}_1$, $\mathcal{L}_2$ and $\mathcal{L}_\infty$ norms of a class of nonlinear systems, a new method is proposed based on the $\zeta_A$ and $\zeta_{AB}$ representations. Another Method, which provides tighter bounds, is proposed to find an upper bound on the induced $\mathcal{L}_2$ norm. Both methods are only applicable to globally Lipschitz systems. To overcome this restriction, another tool is developed for local conditions, namely, an upper bound on system output is derived for bounded input and initial state. This method is restricted to the $\mathcal{L}_\infty$ induced norm.

To measure the distance between local systems in multiple model method, some researchers have suggested to use the gap metric. However, since there are no straight-forward method to compute the nonlinear gap metric and using linear gap metric can not guarantee global stability of the system, the mentioned problem is still unsolved. In this thesis based on $\zeta_A$ and $\zeta_{AB}$ representations, a method is proposed to compute an upper bounds on the

gap metric and the corresponding stability margin for a class of nonlinear systems.

The minimum gain of an operator is defined, some of its properties are derived and some computational methods are developed to calculate the minimum gain. Based on the minimum gain of operators, the large gain theorem is stated. The large gain theorem asserts that the feedback loop will be stable if the minimum loop gain is greater than one.

To study disturbance attenuation of a closed loop multitank system, the proposed methods are utilized. It is assumed that a proportional controller is used to control the level of the liquid in one of the tanks. The mathematical model of the open loop system is derived using physics of the plant. The gray box identification method is used to identify the model parameters and the disturbance attenuation of the system is investigated by the proposed method.

# Acknowledgements

The present work has been assisted by many people who had directly or indirectly helped and supported me over the years of my research study. First of all, I would like to express my deepest gratitude towards my supervisors Dr. Horacio J. Marquez and Dr. Tongwen Chen for their guidance, enormous patience, cautiously reviewing manuscripts, discussions and consistent encouragements during the period of research. Without their insight, suggestions, and excitement, this work would have never taken place.

It has been a great honor to work with Dr. Marquez because of his invaluable experience, novel ideas and immense knowledge in nonlinear systems. I appreciate his friendly supervision, generous encouragement and patient guidance. I am thankful to Dr. Chen for his immense knowledge and ability in mathematics and control systems as well as his useful comments on my work.

I am privileged to be part of the friendly environment of the Advanced Control Laboratory. I would like to thank all the members of the group, both past and present, for making it a great place to work. Many thanks to Adarsha Swarnakar, Betty (Batool) Labibi, Reza Banaei, Iman Izadi. I also would like to thank Amr, Masood, Danlei and Jingbo.

I would like to thank the administrative support staff of the department for their efforts especially Pinder Bains and Kathleen Forbes.

Finally, I want to thank my family, especially my parents, for their love, encouragement, and help, which kept me going during the more difficult times.

# Table of Contents

# List of Tables

# List of Figures

# Nomenclature

| | |
|---|---|
| $\mathbf{B}^p(c, \xi)$ | The open ball with center $c$ and radius $\xi$ with norm $p$ |
| $\gamma(\cdot)$ | $\gamma_p(\cdot)$ for all $0 < p \leq \infty$ |
| $\gamma_p(\cdot)$ | The induced norm (gain) of the operator |
| $\mathbf{T}_T$ | The Truncation operator |
| $\mathcal{L}_p$ | $\mathcal{L}_p^r$ where $r$ is a finite integer which can be understood from the text |
| $\mathcal{L}_p^r$ | The Lebesgue $p$-space of $r$-vector valued functions |
| $\mathbb{C}$ | The field of complex numbers |
| $\mathbb{R}$ | The field of real numbers |
| $\mathbb{R}^n$ | The space of $n \times 1$ real vectors |
| $\nu(\cdot)$ | The minimum gain |
| Im$(\cdot)$ | Imaginary part |
| Re$(\cdot)$ | Real part |
| sat$(\cdot)$ | The saturation function |
| $f_T(t)$ | The truncation of $f(t)$ |
| $I_{n\times n}$ | The $n \times n$ identity matrix |
| LHP | The left half plan of the complex plane |
| LTI | Linear time invariant |
| MATLAB | Matrix Laboratory |
| RBS | Random binary sequence |

| | |
|---|---|
| RHP | The right half plan of the complex plane |

# Chapter 1

# Introduction

## 1.1 Overview of Multi-Model Control Systems

The development of large industrial engineering systems such as chemical plants has lead to gradual increase in their complexity. In turn, this complexity demands suitable control systems that should have enough flexibility to be able to handle variations in the operating conditions. Nonlinearity, disturbances and uncertainty in the process or its model are three challenging elements in the design of control systems. The classical approach consists of linearizing the plant model at the nominal operating point and designing a robust controller for the resulting linear system. Although excellent results have been reported in literature, it is well known that the performance of a controller designed by this method deteriorates when operation deviates from the nominal point. This performance degradation may lead to instability when the distance between the operation region and the nominal operating point increases.

To solve this problem in the context of the traditional linear control, the impact of nonlinearity has been considered as "uncertainty" around the nominal model and based on the size of nonlinearity, the controller is designed such that the desired performance is satisfied for all possible systems in the uncertainty set. It is clear that the size of the uncertainty increases as the operating point of the system prowls in a large area. In turn, conservatism occurs as the size of uncertainty increases. At some point, it becomes impossible to design a controller that can provide satisfactory performance.

Thanks to the fact that the model derived by linearization describes the process quite accurately in a small region about the linearization point, some methods are introduced in the literature to overcome the aforementioned shortcomings. In the so-called gain scheduling method, local designs are performed for various operation regions and a gain-scheduling scheme is built to interpolate among the controllers as the operating point moves among

local regions [43] [44] [45] [46]. Although satisfactory results have been reported for some applications and gain scheduling is well-accepted among practitioners today, this method suffers from the lack of a theoretical support for global behavior.

Another linearization-based method, conceptually similar to the gain scheduling method, is the so-called Multiple Model or Multi Model method [17] [7] [28]. The only difference with the gain scheduling approach is that the interpolation is substituted by either membership functions or supervisory switching. In both forms, the switching is done based on the current states. While in the form of membership functions the current states of the system determine the weighting among the local controllers; in the supervisory form, a supervisor selects the suitable local controller from a bank of local controllers, based on the current state of the process.

The main advantage of the Multiple Model method is that it is a natural extension of the linear control method and inherits some benefits of linear control such as simplicity of analysis and implementation. However, it should be taken into account that all these benefits are valid locally. When the global behavior of the system is being investigated, most of the advantages are yet to be established. When it comes to global stability, which is one of the most important features of a control system, multiple model method may be vulnerable. Some researchers have suggested to use the gap metric to measure the distance between local systems [9] [38]. However, since there are no straight-forward methods to compute the nonlinear gap metric and using linear gap metric can not guarantee global stability of the system, the mentioned problem is still unsolved.

The core objective of this thesis is to develop new tools to study stability of closed-loop nonlinear systems controlled by local controllers. This is to say that the aim of our work is to investigate how to determine the region where a closed loop system is stable and to study the effect of the exogenous signals on stability of such systems.

## 1.2 Structure and Outline of the Thesis

### 1.2.1 Thesis Overview

In Chapter 2, after introducing the notation and presenting some preliminary results, a new representation for unforced nonlinear systems, called the $\zeta_A$ representation is proposed. Having only an input-output structure, the $\zeta_A$ representation is an equivalent structure of an unforced nonlinear system, where the initial state is also represented by an input. Then, the $\zeta_A$ representation is extended to forced systems.

In the $\zeta_A$ representation and its extended version for forced systems, which is called $\zeta_{AB}$ representation, a nonlinear system is arranged as a feedback interconnection of a memoryless nonlinearity and a linear system with the initial state as an input signal. The main difference between this decomposition and traditional ones is in the way the initial state is dealt with. Here, the initial state contributes to the feedback interconnection as an exogenous input while in traditional methods, any change in the initial state is handled by defining a new operator.

Chapter 3, starts by investigating stability of unforced nonlinear systems by the $\zeta_A$ representation. Based on operator-theoretic methods, a new framework is developed for the analysis of stability of nonlinear systems. In the proposed approach, since the initial state is considered as an input, stability of an unforced nonlinear system can be investigated by the input-output stability methods and stability of the nonlinear system is interpreted as the input-output stability of the resulting feedback system. Using classical tools, sufficient conditions for global and local stability of the system are obtained. For local stability, the notion of *stability regions* is introduced and is shown to be useful in applications. Then, local stability of unforced nonlinear systems is studied with a new definition of region of attraction, which extends into two regions. Sufficient conditions for local stability in term of those regions are derived. Some examples are given to show the effectiveness of the results. It is important to note that our method does not require finding a Lyapunov-type function.

Chapter 3 continues by investigating stability of forced nonlinear systems. Both global stability and local stability of forced nonlinear systems are considered. Using the $\zeta_A$ and $\zeta_{AB}$ representations of nonlinear systems, some sufficient conditions for global and local stability of forced nonlinear systems are derived.

In Chapter 4, the problem of computing the $\mathcal{L}_p$ operator norm of a nonlinear system is considered. Since it is important to quantify the influence of various inputs on various signals inside the system, this measure has several applications. One of them is in control systems, where the attenuation of disturbance signals is required. The proposed method can be optimized based on some selected parameters. The proposed theorems are applicable to a class of nonlinear systems. However, a method is also provided for computing an upper bound on the induced $\mathcal{L}_\infty$ norm for systems which are not in this class. To illustrate the methods, some examples are also given. The weighting method is introduced in the last section of this chapter. The weighting technique can be used to reduce the intrinsic conservativism in the aforementioned method. An example is also provided to show the

usage of the weighting technique.

Chapter 5 deals with the computation of the gap metric and stability margin for nonlinear systems. The gap metric, which was introduced to systems and control theory by Zames and El-Sakkary [55], can be used to measure system uncertainty. For linear time-invariant (LTI) systems, much work has been done to compute the gap metric. The extension of the gap metric to larger classes of systems was initiated in [10], where the metric is extended to time-varying linear plants. Later, the parallel projection operator for nonlinear systems [5] and its relationship to the differential stabilizability of nonlinear feedback systems [11] paved the road to the extension of the gap metric to a pseudo-metric on nonlinear operators [13].

Unfortunately, there is no generally applicable method of computing the gap metric for nonlinear systems. In fact, there are only a few examples in literature for the computation of the gap metric. Moreover, methods used in those examples are highly dependent upon the case of interest. This is also the case for the corresponding stability margin which can be used to determine the ball of uncertainty in the sense of the gap metric.

In Chapter 5, some upper bounds on the gap metric and the stability margin are derived and based on the methods proposed in Chapter 4, these bounds are computed.

In Chapter 6, stability of nonlinear systems is studied by a proposed method. The method fits in the context of input-output approach to study nonlinear systems. This approach, which was initiated by Popov, Zames, and Sandberg, in the 1960s [42] [56] [32], is one of the well-accepted and widely-used methods to study stability of systems. In fact, many of the recent developments in control theory, such as robust control and small-gain based nonlinear stabilization techniques are the results of this approach. Here, systems are considered as mappings from an input space of functions into an output space and the well-behaved input and output signals are considered as members of input and output spaces. Therefore, if the “well-behaved” inputs produce well-behaved outputs, the system is called stable.

The well-known small-gain theorem is the main contribution of the input-output approach in control theory. According to the small gain theorem, the feedback loop will be stable if the loop gain is less than one. According to our proposed theorem in Chapter 6, the large gain theorem, the feedback loop will be stable if the minimum loop gain is greater than one. In Chapter 6, first we introduce the minimum gain of operators. Then, a new stability condition is derived for feedback systems based on the minimum gains of the open-loop systems. An example is also provided to illustrate the usage of the large gain theorem.

The last chapter, Chapter 7, is the usage of the methods introduced in Chapter 4 in investigating disturbance attenuation of closed-loop systems. There is no doubt that disturbance attenuation is one of the most important objectives in any closed-loop system. Therefore, it is important to quantify the influence of various inputs on various signals inside the system and develop a tool to calculate such quantities.

The system of interest is a multitank system, consisting of three tanks placed one above another. Due to gravity, the liquid flows through the tanks. The objective of the control system is to control the level of the liquid in the middle tank by the flow rate of the liquid entering to the top tank. We study the effect of a disturbance signal, which enters through the output of the plant, on the state of the closed-loop system. The chapter starts with the identification of the plant by the gray box method and continues by investigating the disturbance attenuation of the system.

### 1.2.2 The $\zeta_A$ and $\zeta_{AB}$ Representations

The $\zeta_A$ and $\zeta_{AB}$ representations are equivalent structures of nonlinear systems, which involve only an input-output structure. In this setting, the initial states representing initial conditions is represented as an input. In these representations, a nonlinear system is arranged as a feedback interconnection of a memoryless nonlinearity and a linear system with the initial state as an input signal. Although interconnection of a memoryless nonlinearity with a linear system has been widely used in literature, the way the initial state is dealt with is the main difference between our decomposition and traditional ones. In $\zeta_A$ and $\zeta_{AB}$ representations, the initial state contributes to the feedback interconnection as an exogenous input while in traditional methods, any change in the initial state is handled by defining a new operator.

Consider the following systems:

$$N_1 : \dot{x}(t) = f_1(t, x(t)) \tag{1.1}$$

$$N_2 : \ \dot{x}(t) = f_2(t, x(t), u(t)) \tag{1.2}$$

where $f_1$ and $f_2$ are locally Lipschitz. $N_1$ is an unforced system and $N_2$ is a forced one. In Chapter 2, it is shown that $N_1$ is equivalent to the structure depicted in Fig. 1.1(a) and $N_2$ is equivalent to the ones shown in Fig. 1.1(b) and Fig. 1.1(c). Structures in Fig. 1.1(a) and Fig 1.1(b) are called $\zeta_A$ representation and the one in Fig. 1.1(c) is called $\zeta_{AB}$ representation. The operators $\Phi$, $\Gamma$, $\Omega$ and $\Theta$ are introduced in Chapter 2. These representations are widely used in all other chapters of this thesis.

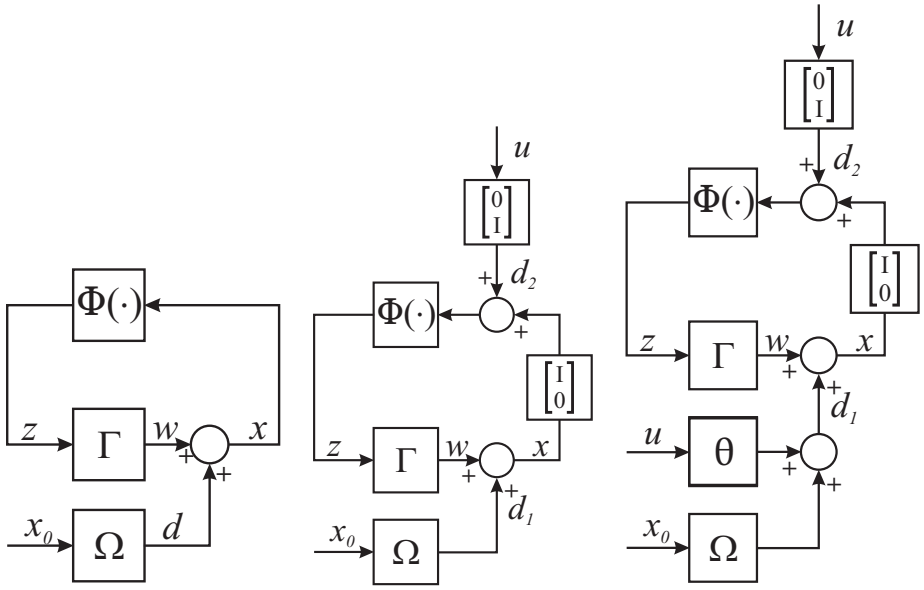


(a) $\zeta_A$ for unforced systems (b) $\zeta_A$ for forced systems (c) $\zeta_{AB}$ for forced systems

Figure 1.1: $\zeta_A$ and $\zeta_{AB}$ representations.

### 1.2.3 Stability of Nonlinear Systems

The fact that the $\zeta_A$ and $\zeta_{AB}$ representations convert a nonlinear system with non-zero initial state to a combination of a memoryless nonlinearity and a linear system with some input signals and the way the initial state is handled by these representations provide a novel viewpoint on all aspects in investigating nonlinear systems. Stability as one of the challenging issues in design and analysis of nonlinear systems can also be studied by these new tools. In Chapter 3, a new framework is developed for the analysis of stability of systems by the $\zeta_A$ and $\zeta_{AB}$ representations. The effectiveness of this usage is originated in the fact that using these representations, stability of nonlinear systems with non-zero initial states can be investigated by the input-output stability methods and stability is interpreted as input-output stability of the resulting feedback systems.

The main contributions of Chapter 3 are Theorems 3.2.1, 3.2.2, 3.2.3, 3.2.4, 3.3.1, 3.3.2 and 3.3.3. Theorems 3.2.1 and 3.2.2 provide new methods to check stability in the sense of Lyapunov for an unforced nonlinear system by norm of some relevant operators; without finding any Lyapunov-like function. For local stability, Theorem 3.2.3 can be used to find some local areas, $\Delta$ and $\Upsilon$, if the initial state $x_0$ is in $\Delta$, then the state will stay in $\Upsilon$. Theorem 3.2.4 is asymptotic version of Theorem 3.2.3. Roughly speaking, Theorem 3.3.1 is an extension of Theorem 3.2.1 to forced systems. Similarly, Theorem 3.3.2 is the extension of Theorem 3.2.3 to forced nonlinear systems. For asymptotic stability of forced nonlinear

systems in a local sense, Theorem 3.3.3 provides the aforementioned $\Delta$ and $\Upsilon$ regions.

### 1.2.4 The Induced Norm of Nonlinear Systems

Most of the computational techniques developed for nonlinear systems are restricted to a narrow class of nonlinear systems for which a particular function, e.g. Lyapunov function or storage function, can be found. Unfortunately, there is not a straight-forward method to find such functions and they can usually be obtained by trial and error [27] [24]. Computing the $\mathcal{L}_p$ operator norm of a nonlinear system is not an exception. In this work, we propose a method to compute an upper bound on the $\mathcal{L}_1$, $\mathcal{L}_2$ and $\mathcal{L}_\infty$ norms of a class of nonlinear systems. The method is based on the $\zeta_A$ and $\zeta_{AB}$ representations of nonlinear systems. The first proposed theorem in this context is Theorem 4.1.1 which provides an upper bound on induced $\mathcal{L}_p$ norms. The next theorem, Theorem 4.1.2 gives tighter bound for the case $p = 2$. Both theorems suffer from a restrictive condition, namely 4.4. Theorem 3.3.2 can be used to overcome the restriction with the cost of providing only local conditions, i.e. an upper bound on the system output is derived for bounded input and initial state. This method is restricted to $\mathcal{L}_\infty$ induced norm.

### 1.2.5 The Gap Metric

Stability and performance of feedback control systems are considerably impacted by model uncertainty. Unlike the linear time-invariant (LTI) systems, where much work has been done to study this effect, the topic for nonlinear systems is quite immature. The gap metric is one of the useful tools to investigate the effect of model uncertainty on control systems. For LTI systems, it has been shown that a perturbed system can be stabilized by any controller which is designed for the nominal system if and only if the distance between the perturbed system and the nominal system is small in the gap metric. The gap metric is also extended to a pseudo-metric on nonlinear operators [13].

The computation of the gap metric for LTI system was developed by Georgiou [12]. Unlike the LTI system case, there is no generally applicable method of computing the gap metric for nonlinear systems. In fact, there are only a few examples in literature for the computation of the gap metric. Moreover, those methods are highly dependent upon the case of interest. This is also the case for the corresponding stability margin which can be used to determine the ball of uncertainty in the sense of the gap metric.

In Chapter 5, we propose a method to compute the gap metric and the corresponding stability margin for a class of nonlinear systems. The method is based on $\zeta_A$ and $\zeta_{AB}$

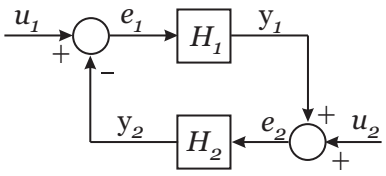


Figure 1.2: The feedback system.

representations. The key results are Theorems 5.3.1 and 5.3.2 which provide upper bounds on the gap metric and the stability margin, respectively. We use the methods proposed in Chapter 4 to calculate the bounds. An example is also provided to illustrate the effectiveness of the results and comparison between the direct computation and the suggested methods.

### 1.2.6 Large Gain Theorem

One of the key results in the input-output stability theory is the small gain theorem, which provides a sufficient condition for stability of interconnected systems. Roughly speaking, the theorem states that the feedback loop will be stable if the loop gain is less than one. For the feedback system depicted in Fig. 1.2, the small gain theorem states that the closed loop system is stable if $\gamma(H_1) \cdot \gamma(H_2) < 1$ where $\gamma(\cdot)$ denotes the gain of operators. This simple rule has been a basis for numerous stabilization techniques such as nonlinear $\mathcal{H}_\infty$ control [15].

In our approach, we first define the minimum gain of an operator $\nu(\cdot)$ as

$$\nu(H) = \inf_{0 \neq u \in \mathcal{U}} \frac{\|(Hu)_T\|}{\|u_T\|} \tag{1.3}$$

where $H : \mathcal{U} \to \mathcal{Y}$ is an operator, $(\cdot)_T$ denotes the Truncation operator, the infimum is taken over all $u \in \mathcal{U}$ and all $T$ in $\mathbb{R}^+$ for which $u_T \neq 0$. Then, some of the properties of the minimum gain are derived and its computation for some cases is discussed. Particularly, it has been showed that the minimum gain satisfies the *positivity* and the *positive homogeneity* properties but fails to satisfy the triangle inequality. Finally, the large gain theorem, Theorem 6.3.1, is stated. Roughly speaking, the large gain theorem asserts that the feedback loop will be stable if the minimum loop gain is greater than one. For the feedback system depicted in Fig. 1.2, the large gain theorem states that the closed loop system is stable if $\nu(H_1) \cdot \nu(H_2) > 1$.

### 1.2.7 The Multitank System

To show applicability and effectiveness of the proposed methods in Chapter 4, we apply Theorem 3.3.2 to study disturbance attenuation of a closed loop system. The system of

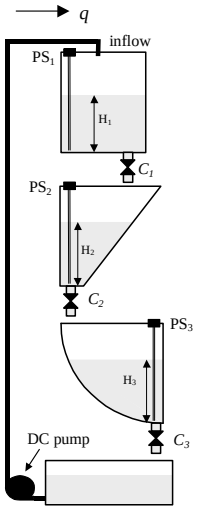


Figure 1.3: Configuration of the multi-tank system.

interest, which is called Multitank system, consists of three tanks placed one above another and due to gravity, the liquid flows through the tanks. The top tank has a constant cross section while the other two have variable cross sections as shown in Fig. 1.3. A pump is used to circulate liquid from the supply tank into the upper tank. We assume that a proportional controller is used to control the level of the liquid in the middle tank by the flow rate of the liquid entering to the top tank.

In chapter 7, which devotes to investigating disturbance attenuation of the controlled Multitank system, first we derive the mathematical model of the open loop system using physics of the plant. The model, which is nonlinear, consists of four parameters that are depend on the configuration of the system. After running some experiments on the plant and collecting data, we use the gray box identification method to identify the parameters. Finally, the disturbance attenuation of the system is investigated by the proposed method in Theorem 3.3.2. A summary of results is presented in Table 7.2.

## 1.3 Contributions

The content of this thesis has been published and presented in the following international journals and conferences:

- Chapter 3: A significant part of this chapter was published in IET Control Theory & Applications [50] and IEEE Conference on Decision and Control, San Diego, 2006 [49].

- Chapter 4: The contents of this chapter were published in American Control Conference, New York, 2007 [54] and accepted for publication in IEEE Transaction on Automatic Control [51].
- Chapter 5: The contents of this chapter were published in American Control Conference, Seattle, 2008 [52].
- Chapter 6: The contents of this chapter were published in American Control Conference, Seattle, 2008 [53].

# Chapter 2

# $\zeta_A$ and $\zeta_{AB}$ Representations

## 2.1 Introduction

Almost all dynamical systems encountered in nature are ruled by nonlinear characteristics and linear models are usually used in order to simplify analysis. Although, for most applications linear models are accurate enough to be used to represent systems in a small region, they fail to provide accurate results when larger operating region is needed to be considered.

In this section, first, we introduce the notation and present some preliminaries results. Next, a new representation for unforced nonlinear systems, called $\zeta_A$ representation, is introduced. The $\zeta_A$ representation is an equivalent structure of an unforced nonlinear system, which involves only an input-output structure. The initial state is also represented by an input in the $\zeta_A$ representation. Finally, an elegant extension of the $\zeta_A$ representation to forced systems, called the $\zeta_{AB}$ representation, is presented.

## 2.2 Background

In general, nonlinear representations can be classified into three types [4]:

- system input-output representation,
- state-space representation, and
- model-free representation.

In the input-output representation, the input-output behavior of a system without any state is considered. In this representation, systems are assumed as mappings from an input space of functions into an output space. Using this approach, one of the well-accepted and widely-used methods to study stability of systems is developed [27] [42] [56] [32]. The state-space representation, on the other hand, highlights states of systems. In this representation,

the dynamic of the system is represented by some states affected by the inputs and the output depends on both the states and inputs [24] [27]. Nonlinear systems, which cannot be modeled by the mentioned methods, might be represented by model-free representations [4].

In the proposed method, a nonlinear system is arranged as a feedback interconnection of a memoryless nonlinearity and a linear system with initial state as an input signal. The main difference between our decomposition and traditional ones is in the way initial state is dealt with. In our method, initial state contributes to the feedback interconnection as an exogenous input while in traditional methods, any change in initial state is handled by defining a new operator. In our approach, since initial state is considered as an input, stability of unforced nonlinear system can be investigated by the input-output stability methods and stability of the nonlinear system is interpreted as the input-output stability of the resulting feedback system.

## 2.3 Notation, Preliminaries, and Computation

### 2.3.1 Notation

Let $\mathbb{R}$ and $\mathbb{C}$ denote the fields of real and complex numbers, respectively. $\mathbb{R}^n$ denotes the space of $n \times 1$ real vectors. The Euclidean norm in $\mathbb{R}^n$ is denoted by $\|\cdot\|$. $I_{n\times n}$ denotes the $n \times n$ identity matrix. LHP and RHP stand for left and right half plan of the complex plane, respectively. Let $\mathbf{B}^p(c, \xi)$ denote the open ball with center $c$ and radius $\xi$ with norm $p$, i.e. $\mathbf{B}^p(c, \xi) := \{x |\ \|x - c\|_p < \xi\}$. $\mathcal{L}_p^r$ denotes Lebesgue $p$-space of $r$-vector valued functions on $[0, \infty]$, with norm $\|\cdot\|$ defined as $\|f\|_p := \left(\int_0^\infty \|f(t)\|^p\, dt\right)^{1/p}$ for $1 \le p \le \infty$ and $\|f\|_\infty := \operatorname{ess\,sup}_{t\in\mathbb{R}} \|f(t)\|$. Usually $r$ is a finite integer; we drop $r$ and write $\mathcal{L}_p$ instead of $\mathcal{L}_p^r$. To distinguish among various norm notations, we indicate the space as a subscript for the norm, such as $\|\cdot\|_{\mathbb{R}^n}$ or $\|\cdot\|_{\mathcal{L}_p}$. Whenever the space is not mentioned, norms with $t$ argument denote Euclidean norm at $t$ and without $t$ denote the $\mathcal{L}_p$ norm where $p$ is as a general number or can clearly be understood from the text. Let $\mathbf{T}_T$ denotes the Truncation operator: for $f(t)\,,\ 0 \le t < \infty,\ \mathbf{T}_T\, f(t) = f(t)$ on $[0, T]$, and zero otherwise. We also denote the truncation of $f(t)$ by $f_T(t) := \mathbf{T}_T\, f(t)$. For an operator $\lambda : \mathcal{L}_p \to \mathcal{L}_p$, let $\gamma_p(\lambda)$ stand for the induced norm (gain) of the operator defined as

$$\gamma_p(\lambda) := \sup_{0 \ne u \in \mathcal{L}_p} \frac{\|(\lambda u)_T\|}{\|u_T\|} \tag{2.1}$$

where the supremum is taken over all $u \in \mathcal{L}_p$ and all $T$ in $\mathbb{R}^+$ for which $u_T \ne 0$. Let $\gamma(\lambda)$ denote $\gamma_p(\lambda)$ for all $0 < p \le \infty$.

**Definition 2.3.1.** *Maximum overshoot* of a signal $x(t)$ is

$$M_P := \frac{\|x\|_{\mathcal{L}_\infty}}{\|x(0)\|_\infty} \tag{2.2}$$

In this thesis, we will frequently use operator gains. In this section, we take a brief look at some of the computational methods for norms.

### 2.3.2 Continuous-time, LTI operators

Let $g(t)$ be the impulse response of a stable linear time invariant (LTI) system. We will denote by $\Gamma$ the convolution operator defined by $\Gamma(z(t)) = \int_0^t g(t-\tau)z(\tau)d\tau$. To compute the gain of $\Gamma$, we use the following lemma that is taken from [2], page 234 (Table 1):

**Lemma 2.3.1.** *Suppose that $\Gamma$ is a linear time-invariant stable operator with impulse response $g(t) : \mathbb{R}^+ \to \mathbb{R}^{n\times n}$. Let $G(s)$ denotes the Laplace transform of $g(t)$. Define*

$$\tilde{g}_{n\times n} := \begin{bmatrix} \|g_{11}\|_{\mathcal{L}_1} & \|g_{12}\|_{\mathcal{L}_1} & \cdots & \|g_{1n}\|_{\mathcal{L}_1} \\ \|g_{21}\|_{\mathcal{L}_1} & \|g_{22}\|_{\mathcal{L}_1} & \cdots & \|g_{2n}\|_{\mathcal{L}_1} \\ \vdots & \vdots & \ddots & \vdots \\ \|g_{n1}\|_{\mathcal{L}_1} & \|g_{n2}\|_{\mathcal{L}_1} & \cdots & \|g_{nn}\|_{\mathcal{L}_1} \end{bmatrix} \tag{2.3}$$

*Then*

$$\gamma_1(\Gamma) = \|\tilde{g}\|_1 \tag{2.4a}$$

$$\gamma_\infty(\Gamma) = \|\tilde{g}\|_\infty \tag{2.4b}$$

$$\gamma_2(\Gamma) = \|G(s)\|_{\mathcal{H}_\infty} \tag{2.4c}$$

where $\|\cdot\|_{\mathcal{H}_\infty}$ denotes $\mathcal{H}_\infty$ norm. Some standard algorithms to compute the $H_\infty$-norm can be found in several references. See for example [57]. To compute $\|g_{ij}\|_{\mathcal{L}_1} = \int_0^\infty |g_{ij}(t)|dt$ for strictly proper systems, any numerical integral approximation method, e.g. rectangular and trapezoidal, can be used.

### 2.3.3 Autonomous and non-autonomous memoryless nonlinearities

In this section, the operator of interest is in the form of $\Phi(t, x(t))$, where $\Phi(\cdot,\cdot) : \mathbb{R}^+ \times \mathbb{R}^n \to \mathbb{R}^n$. It is also assumed that $\Phi(t, 0) = 0$.

**Lemma 2.3.2.** *Suppose that there exists a constant $\mu_p$ such that*

$$\|\Phi(t, x)\|_p \le \mu_p\|x\|_p, \ \forall x \in \mathbb{R}^n, \ \forall t \ge 0 \tag{2.5}$$

*then $\gamma_p(\Phi) \le \mu_p$.*

*Proof.* See reference [41] pp. 40. □

With direct computation, the $\infty$-norm, 2-norm and 1-norm of a memoryless autonomous nonlinear operator can be found approximately with arbitrary accuracy. MATLAB can also be used to find the aforementioned norms.

**Example 2.3.1.** Consider the following memoryless nonlinearity.

$$\Phi(x) = \begin{bmatrix} \Phi_1(x) \\ \Phi_2(x) \\ \Phi_3(x) \end{bmatrix} = \begin{bmatrix} -0.2\,x_2 + \sin(0.5\,x_2) - \sin(0.5\,x_3) \\ -0.2\,x_1 + \sin(0.5\,x_1) - \sin(0.5\,x_3) \\ 1 - \cos(0.5\,x_1) + \sin(0.5\,x_2) \end{bmatrix}$$

where $x = \begin{bmatrix} x_1 & x_2 & x_3 \end{bmatrix}^{\mathrm{T}}$. Let

$$g(x_1, x_2, x_3) := \frac{\|x\|_2}{\|\Phi(x)\|_2} = \frac{\sqrt{x_1^2 + x_2^2 + x_3^2}}{\sqrt{\Phi_1^2(x_1, x_2, x_3) + \Phi_2^2(x_1, x_2, x_3) + \Phi_3^2(x_1, x_2, x_3)}}.$$

Using the "fminsearch" command of MATLAB, the minimum of $g(x_1, x_2, x_3)$ is $1.2678$ and consequently $\gamma_2(\Phi) \approx \frac{1}{1.2678} = 0.7888$.

### 2.3.4 $\Omega$-operator

**Definition 2.3.2.** For continuous-time, we define operator $\Omega$ as

$$\Omega(x(t)) := e^{At} x_0 \tag{2.6}$$

where $A \in \mathbb{R}^{n \times n}$ with all eigenvalues in LHP and $x(0) = x_0$. Similarly, for discrete-time

$$\Omega(x(t)) := A^t x_0 \tag{2.7}$$

where $A \in \mathbb{R}^{n \times n}$ with all eigenvalues in $\mathbb{D}$ and $x(0) = x_0$.

**Lemma 2.3.3.** *If* $x_i(0) < \infty\,, \forall i = 1 \cdots n$ *then* $\Omega(x) \in \mathcal{X}_p$.

*Proof.* The proofs for continuous-time and discrete-time are the same and only the first one comes here. Since $x_i(0) < \infty$, $\|x(0)\|_p < \infty$. On the other hand, because all eigenvalues of $A$ are in LHP, $\|e^{At}\|_p < \infty$, $\forall t \geq 0$. Since $\Omega(x) = e^{At} x_0$, $\|\Omega(x)(t)\|_p < \|e^{At}\|_p \|x_0\|_p < \infty$. This completes the proof for $p = \infty$. For $p = [1, \infty)$, in addition, $e^{At}$ is a continuous time signal and vanishes as $t \to \infty$. Therefore $\|e^{At}\|_{\mathcal{L}_p}^p = \int_0^\infty \|e^{At}\|_p^p dt < \infty$. We have $\|\Omega(x)\|_{\mathcal{L}_p} = \int_0^\infty \|e^{At} x_0\|_p^p dt \leq \int_0^\infty \|e^{At}\|_p^p \|x_0\|_p^p dt = \|x_0\|_p^p \cdot \int_0^\infty \|e^{At}\|_p^p dt = \|x_0\|_p^p \cdot \|e^{At}\|_{\mathcal{L}_p}^p < \infty$, and consequently, $\Omega(x) \in \mathcal{L}_p$. □

We have the following lemma about the gain of $\Omega$.

**Lemma 2.3.4.** *For continuous-time, the $\mathcal{L}_\infty$-gain of $\Omega$, which is defined by (2.6), is*

$$\gamma_\infty(\Omega) = \|e^{At}\|_{\mathcal{L}_\infty} \tag{2.8}$$

*And for discrete-time, where $\Omega$ defined by (2.7),*

$$\gamma_\infty(\Omega) = \|A^t\|_{\ell_\infty} \tag{2.9}$$

*Proof.* The proofs for continuous-time and discrete-time are the same and only the first one comes here. First we show that $\|e^{At}\|_{\mathcal{L}_\infty}$ is an upper bound for $\gamma_\infty(\Omega)$.

$$\|e^{At}x_0\|_{\mathcal{L}_\infty} \leq \|e^{At}\|_{\mathcal{L}_\infty}\|x_0\|_\infty \leq \|e^{At}\|_{\mathcal{L}_\infty}\|x(t)\|_{\mathcal{L}_\infty} \tag{2.10}$$

Next, we show that this upper bound is achievable for an input signal. Let $x(t) = I_{n\times n}\ \forall t \geq 0$, then $\|x(t)\|_{\mathcal{L}_\infty} = 1$ and $\|e^{At}x_0\|_{\mathcal{L}_\infty} = \|e^{At}\|_{\mathcal{L}_\infty}$. This completes the proof. □

**Lemma 2.3.5.** *The following equations are true for $\Omega$:*

*(i)* $\|\Omega(x)\|_{\mathcal{L}_2} = \|e^{At}\|_{\mathcal{L}_2} \cdot \|x_0\|_2$ *for continuous-time*

*(ii)* $\|\Omega(x)\|_{\ell_2} = \|A^t\|_{\ell_2} \cdot \|x_0\|_2$ *for discrete-time*

*(iii)* $\|\Omega(x)\|_{\mathcal{L}_1} \leq \|e^{At}\|_{\mathcal{L}_1} \cdot \|x_0\|_1$ *for continuous-time*

*(iv)* $\|\Omega(x)\|_{\ell_1} \leq \|A^t\|_{\ell_1} \cdot \|x_0\|_1$ *for discrete-time*

*Proof.* Since proofs are similar for continuous-time and discrete-time, we only prove (i) and (iii) here.
(i).

$$\begin{aligned}
\|\Omega(x_0)\|_{\mathcal{L}_2}^2 &= \int_0^\infty (e^{At}x_0)^*\ (e^{At}x_0)\, dt \\
&= \int_0^\infty x_0^*\,(e^{At})^*\ (e^{At})\, x_0\, dt \\
&= x_0^* \int_0^\infty (e^{At})^*\ (e^{At})\, dt\, x_0 \\
&= x_0^*\, \|e^{At}\|_{\mathcal{L}_2}^2\, x_0 \\
&= \|x_0\|_2^2\, \|e^{At}\|_{\mathcal{L}_2}^2
\end{aligned}$$

(iii).

$$\begin{aligned} \|\Omega(x_0)\|_{\mathcal{L}_1} &= \int_0^\infty \|e^{At}x_0\|_1\, dt \\ &\leq \int_0^\infty \|e^{At}\|_1\|x_0\|_1\, dt \\ &= \|x_0\|_1 \int_0^\infty \|e^{At}\|_1\, dt \\ &= \|x_0\|_1\|e^{At}\|_{\mathcal{L}_1} \end{aligned} \tag{2.11}$$

□

Lemma 2.3.5 gives the 2-norm gain of $\Omega$-operators and an upper bound for the 1-norm gain. Denoting the upper bound of $\gamma_1$ by $\hat{\gamma_1}$, we have

$$\gamma_2(\Omega) = \|e^{At}\|_{\mathcal{L}_2} \tag{2.12a}$$

$$\hat{\gamma_1}(\Omega) := \|e^{At}\|_{\mathcal{L}_1} \tag{2.12b}$$

for continuous-time and

$$\gamma_2(\Omega) = \|A^t\|_{\ell_2} \tag{2.12c}$$

$$\hat{\gamma_1}(\Omega) := \|A^t\|_{\ell_1} \tag{2.12d}$$

for discrete-time.

**Example 2.3.2.** Let

$$A = \begin{bmatrix} -0.225 & -0.175 & 0.075 & 0.525 \\ 0.200 & -0.400 & -0.150 & 0.200 \\ 0.200 & -0.400 & -0.400 & 0.200 \\ 0.125 & -0.125 & -0.125 & -0.625 \end{bmatrix}$$

Fig. 2.1 shows $\|e^{At}\|_\infty$ and $\|A^t\|_\infty$ versus $t$. Computation shows that $\gamma_\infty(\Omega) \approx 1.4351$ for continuous-time and $\gamma_\infty(\Omega) = 1.2$ for discrete-time.

**Lemma 2.3.6.** *For any $\Omega$-operator, $\gamma_\infty(\Omega) \geq 1$.*

*Proof.* Since for $t = 0$, $e^{At} = I$ and $A^t = I$. It turns out that $\|e^{At}\|_{\mathcal{L}_\infty} \geq 1$ and $\|A^t\|_{\ell_\infty} \geq 1$. Consequently, $\gamma_\infty(\Omega) \geq 1$. □

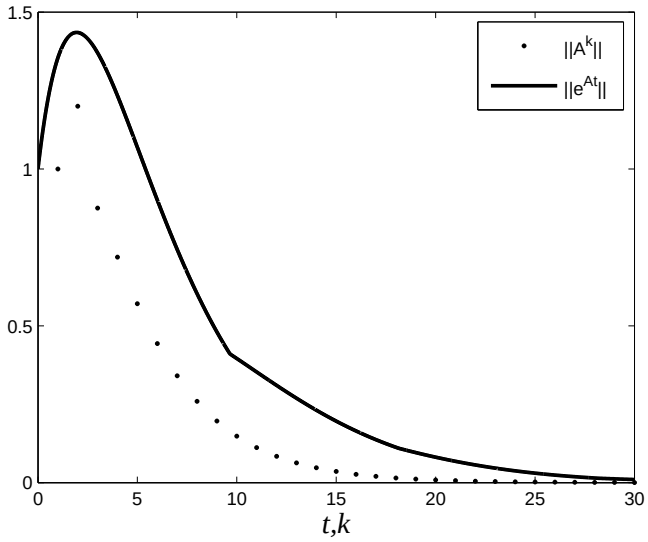


Figure 2.1: $\|e^{At}\|_\infty$ and $\|A^t\|_\infty$ versus $t$ in Example 2.3.2.

## 2.4 $\zeta_A$ Representation

### 2.4.1 Continuous-time systems

Assume that the nonlinear system of interest is

$$\dot{x}(t) = f(t, x(t)) \tag{2.13}$$

where $f : \mathbb{R}^+ \times \mathbb{R}^n \to \mathbb{R}^n$ is locally Lipschitz. It is well-known, [27], that stability for other points or any desired trajectory can be transformed to the study of the stability of the origin. Let $A \in \mathbb{R}^{n\times n}$ whose all eigenvalues are in LHP. Define

$$\begin{aligned} &\Phi(t, x) : \mathbb{R}^+ \times \mathbb{R}^n \to \mathbb{R}^n \\ &\Phi(t, x) := f(t, x) - Ax \end{aligned} \tag{2.14}$$

and consequently

$$\dot{x} = Ax + \Phi(t, x) \tag{2.15}$$

The block diagram of (2.15) is depicted in Fig. 2.2. $\Phi(t, x)$ is a non-autonomous static nonlinearity and $\Lambda$ is a linear system with the following state equation.

$$\Lambda : \dot{x} = Ax + z \tag{2.16}$$

It is well-known, e.g. [3], that the response of $\Lambda$ is

$$x(t) = e^{At}x_0 + \int_0^t e^{A(t-\tau)}z(\tau)\, d\tau \tag{2.17}$$

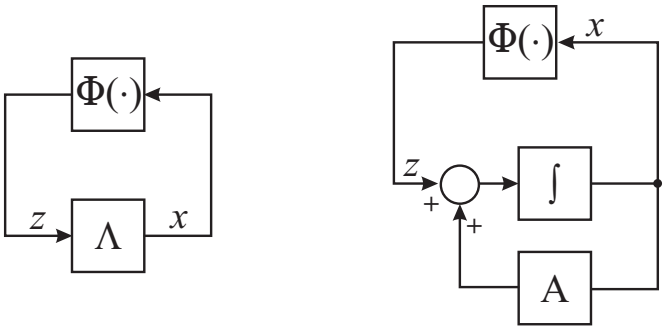


Figure 2.2: Block diagram for (2.15) and (2.24).

which reveals that $\Lambda$ is not a linear operator for $x_0 \neq 0$. Let

$$\Gamma : \mathcal{L}_p \to \mathcal{L}_p, \quad \Gamma(z(t)) := \int_0^t e^{A(t-\tau)} z(\tau)\, d\tau, \tag{2.18a}$$

and

$$\Omega : \mathcal{L}_p \to \mathcal{L}_p, \quad \Omega(x(t)) := e^{At} x(0) \tag{2.18b}$$

Since $A$ is a stable matrix, it is easy to prove that $\Gamma : \mathcal{L}_p \to \mathcal{L}_p$, $\Omega : \mathcal{L}_p \to \mathcal{L}_p$ and also $\Gamma$ are linear autonomous operators and $\Omega$ is a $\Omega$-operator which is defined in Section 2.3.4. The state space representations for $\Gamma$ is

$$\Gamma : \left[\begin{array}{c|c} A & I \\ \hline I & 0 \end{array}\right] \tag{2.19}$$

Let $\Lambda_{x_0}$ denote $\Lambda$ with the initial condition $x_0$. Therefore,

$$\Lambda_{x_0}(z(t)) := e^{At} x_0 + \int_0^t e^{A(t-\tau)} z(\tau)\, d\tau \tag{2.20}$$

substituting (2.18) and (2.20),

$$\Lambda_{x_0}(z(t)) = \Omega(x_0(t)) + \Gamma(z(t)) \tag{2.21}$$

Since $\Phi$ is static, the structure shown in Fig. 2.2 can be represented by its equivalent, which is depicted in Fig. 2.3. This representation of the nonlinear system will be referenced to as the $\zeta_A$ representation with operator ordered set $[\Phi, \Gamma, \Omega]$.

### 2.4.2 Discrete-time systems

In this case, we assume that the nonlinear system of interest is

$$x(t+1) = f(t, x(t+1)) \tag{2.22}$$

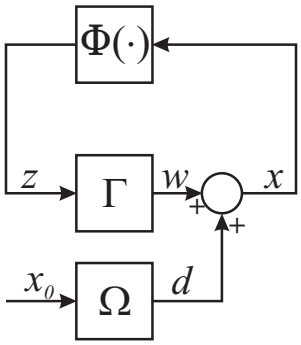


Figure 2.3: Equivalent block diagram using new operators.

where $f : \mathbb{Z}^+ \times \mathbb{R}^n \to \mathbb{R}^n$ is locally Lipschitz. Let $A \in \mathbb{R}^{n\times n}$ have all of its eigenvalues inside the unit circle. Define

$$\begin{aligned} &\Phi(t,x) : \mathbb{Z}^+ \times \mathbb{R}^n \to \mathbb{R}^n \\ &\Phi(t,x) := f(t,x) - Ax \end{aligned} \tag{2.23}$$

and consequently

$$x(t+1) = Ax(t) + \Phi(t, x(t)) \tag{2.24}$$

The block diagram of (2.24) is depicted in Fig. 2.2. $\Phi(t,x)$ is a static nonlinearity and $\Lambda$ is a linear system with the following state equation.

$$\Lambda : x(t+1) = Ax(t) + z(t) \tag{2.25}$$

It is well-known, e.g. [8], that the response of $\Lambda$ is

$$x(t) = A^t\, x_0 + \sum_{l=0}^{t} A^{t-l-1} z(l) \tag{2.26}$$

which reveals that $\Lambda$ is not a linear operator for $x_0 \neq 0$. Let

$$\Gamma : \ell_p \to \ell_p, \quad \Gamma(z(t)) := \sum_{l=0}^{t} A^{t-l-1} z(l), \tag{2.27a}$$

and

$$\Omega : \ell_p \to \ell_p, \quad \Omega(x(t)) := A^t x(0) \tag{2.27b}$$

Since $A$ is a stable matrix, it is not hard to prove that $\Gamma : \ell_p \to \ell_p$, $\Omega : \ell_p \to \ell_p$ and also $\Gamma$ is a linear autonomous operator and $\Omega$ is a $\Omega$-operator defined in Section 2.3.4. The state space representations for $\Gamma$ is $\left[\begin{array}{c|c} A & I \\ \hline I & 0 \end{array}\right]$. Let $\Lambda_{x_0}$ denote $\Lambda$ with the initial condition equals $x_0$. Therefore,

$$\Lambda_{x_0}(z(t)) := A^t\, x_0 + \sum_{l=0}^{t} A^{t-l-1} z(l) \tag{2.28}$$

substituting (2.27) in (2.28),

$$\Lambda_{x_0}(z(t)) = \Omega(x(t)) + \Gamma(z(t)) \tag{2.29}$$

Similar to the continuous-time case, since $\Phi$ is static, the structure shown in Fig. 2.2 can be represented by its equivalent, which is depicted in Fig. 2.3. This representation of the discrete nonlinear system will be referenced to as the $\zeta_A$ representation with operator ordered set of $[\Phi, \Gamma, \Omega]$.

## 2.5 $\zeta_{AB}$ Representation

### 2.5.1 Continuous-time systems

For forced nonlinear systems, suppose that the system of interest is

$$N: \ \dot{x}(t) = f(t, x(t), u(t)) \tag{2.30}$$

where $f : \mathbb{R} \times \mathbb{R}^n \times \mathbb{R}^m \to \mathbb{R}^n$ is locally Lipschitz. Let $A \in \mathbb{R}^{n\times n}$ and $B \in \mathbb{R}^{n\times m}$. Define

$$\Phi(x, u, t) := f(t, x, u) - Ax - Bu. \tag{2.31}$$

Let

$$\Theta : \mathcal{L}_p \to \mathcal{L}_p, \quad \Theta(u(t)) := \int_0^t e^{A(t-\tau)} Bu(\tau)\, d\tau, \tag{2.32}$$

and $\Gamma$ and $\Omega$ be defined in the same formulas as in (2.18). The nonlinear system is equivalent to the structure represented in Fig. 2.4(a). This representation of the nonlinear system is called the $\zeta_{AB}$ representation with ordered operator set $[\Phi, \Gamma, \Theta, \Omega]$.

It is important to note that $\left[\begin{array}{c|c} A & I \\ \hline I & 0 \end{array}\right]$ and $\left[\begin{array}{c|c} A & B \\ \hline I & 0 \end{array}\right]$ are state-space realizations for $\Gamma$ and $\Theta$, respectively. Since $A$ and $B$ are chosen arbitrary, $\zeta_A$ and $\zeta_{AB}$ representations are not unique. A useful choice for the $\zeta_{AB}$ representation is $B = 0$, which implies $\theta = 0$ and simplifies the $\zeta_{AB}$ structure as the structure shown in Fig. 2.4(b). For forced systems, this representation is also called $\zeta_A$ representation.

### 2.5.2 Discrete-time systems

Similarly, for a forced nonlinear system with the following state equation

$$N: \ x(t+1) = f(t, x(t), u(t)) \tag{2.33}$$

where $f : \mathbb{Z}^+ \times \mathbb{R}^n \times \mathbb{R}^m \to \mathbb{R}^n$ is locally Lipschitz, let $A \in \mathbb{R}^{n\times n}$ have all of its eigenvalues inside the unit circle and $B \in \mathbb{R}^{n\times m}$. Define

$$\Phi(x, u, t) := f(t, x, u) - Ax - Bu. \tag{2.34}$$

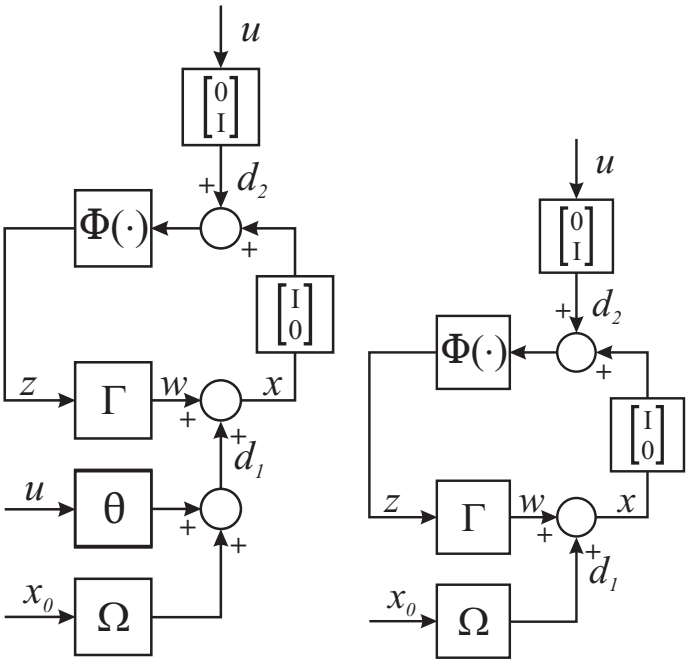


(a) $\zeta_{AB}$ (b) $\zeta_A$

Figure 2.4: $\zeta_A$ and $\zeta_{AB}$ representations for forced systems.

Let

$$\Theta : \ell_p \to \ell_p, \quad \Theta(u(t)) := \sum_{l=0}^{t} A^{t-l-1} B u(l) \tag{2.35}$$

and $\Gamma$ and $\Omega$ be defined in the same formulas as in (2.27). The nonlinear system is equivalent to the structure represented in Fig. 2.4(a). This representation of the nonlinear system is called the $\zeta_{AB}$ representation with ordered operator set $[\Phi, \Gamma, \Theta, \Omega]$.

It is important to note that $\left[\begin{array}{c|c} A & I \\ \hline I & 0 \end{array}\right]$ and $\left[\begin{array}{c|c} A & B \\ \hline I & 0 \end{array}\right]$ are state-space realizations for $\Gamma$ and $\Theta$, respectively. Since $A$ and $B$ are chosen arbitrary, $\zeta_A$ and $\zeta_{AB}$ representations are not unique. A useful choice for the $\zeta_{AB}$ representation is $B = 0$, which implies $\theta = 0$ and simplifies the $\zeta_{AB}$ structure as the structure shown in Fig. 2.4(b). For forced systems, this representation is also called $\zeta_A$ representation.

# Chapter 3

# Stability

## 3.1 Introduction

The traditional approach to study stability involves Lyapunov methods [27] [40] [24]. In these methods, the notion of stability is restricted to unforced systems and stability of *equilibrium points*. The analysis requires finding a so-called Lyapunov function, whose derivatives along the system trajectories must be negative definite, or semi-definite. Finding this function is usually challenging, thus limiting the application of this method.

An alternative way to study the stability of nonlinear systems is the so-called *input-output* stability approach. The input-output theory of systems was initiated in the 1960s by G. Zames and I. Sandberg [56] [32]. Unlike the Lyapunov method, the input-output stability theory considers systems as mappings from an input space of functions into an output space. This method suffers from a problem similar to the Lyapunov method. Indeed, the study of stability in this method involves finding a storage function, which is as difficult to find as a Lyapunov function.

In [35], bridging in some sense the two classical notions of stability, the concept of *input to state stability (ISS)* was introduced. Roughly speaking, in an ISS system, if the inputs are small, then system trajectories converge to a ball in state space, whose radius depends upon the input size, see [33], [34] and the references therein for more details. This notion differs from the input-output theory mainly in that it takes into account the initial states, which are ignored in the input-output stability. It is also different from stability in the sense of Lyapunov because it considers forced systems. Checking for ISS is usually very difficult as it requires finding a so-called ISS Lyapunov function with very stringent conditions.

Along with the aforementioned three major approaches, stability of systems, in its various forms, continues to inspire researchers. Motivated by the classical small gain theorem,“nonlinear” small gain theorems are discussed in [21], [39], and [18]. The notion of

non-uniform in time robust global asymptotic output stability is introduced in [22] for a wide class of systems. An extension of the second method of Lyapunov to study the stability of infinite-dimensional discrete-time systems is presented in [29].

In this chapter, we study stability of nonlinear systems. Using the $\zeta_A$ representation for nonlinear systems, we develop a new framework for the analysis of stability of systems based on operator-theoretic methods. In our approach, since initial state is considered as an input, stability of unforced nonlinear system can be investigated by the input-output stability methods and stability of the nonlinear system is interpreted as the input-output stability of the resulting feedback system. After decomposing the system, sufficient conditions for global and local stability of the system are derived using classical tools. For local stability, the notion of *stability regions* is introduced and is shown to be useful in applications. A method to compute the stability region is also developed. It is important to note that our method does not require finding a Lyapunov-type function.

This chapter has two sections. The first section is devoted to stability of unforced systems. In the first part, the $\zeta_A$ representation is used to provide sufficient conditions for global stability and global asymptotic stability of unforced nonlinear systems in terms of conditions on the gain of certain operators. In the second part of the section, local stability of unforced nonlinear systems is studied with a new definition of region of attraction, which extends into two regions. Sufficient conditions for local stability in term of those regions are derived. Some examples are given to show the effectiveness of the results.

In the second section of this chapter, stability of forced nonlinear system is studied. This section also consists of two parts. In the first part, global stability and in the second part local stability of forced nonlinear systems are considered. Using the $\zeta_A$ and $\zeta_{AB}$ representations of nonlinear systems, some sufficient conditions for global and local stability of forced nonlinear systems are derived.

## 3.2 Unforced Systems

### 3.2.1 Global Stability

The following theorem provides a sufficient condition for stability of unforced nonlinear systems.

**Theorem 3.2.1.** *Given a continuous time system of the form (2.13) with $\zeta_A$ representation of $[\Phi, \Gamma, \Omega]$,*

*(i) if $\gamma_\infty(\Phi) \cdot \gamma_\infty(\Gamma) < 1$ then the system is globally stable in sense of Lyapunov.*

*(ii) if, in addition to (i),* $\gamma_2(\Phi) \cdot \gamma_2(\Gamma) < 1$ *then the system is globally asymptotically stable in sense of Lyapunov.*

The following lemma (e.g [25] pp. 491), which is a corollary of the Barbalat's lemma, will be used in the proof.

**Lemma 3.2.1.** *Consider the function* $\phi : \mathbb{R}^+ \to \mathbb{R}$. *If* $\phi, \dot{\phi} \in \mathcal{L}_\infty$, *and* $\phi \in \mathcal{L}_p$ *for some* $p \in [1, \infty)$, *then* $\lim_{t\to\infty} \phi(t) = 0$.

*Proof.*

(i) In this section of the proof all of the norms are either $\infty$-norm or $\mathcal{L}_\infty$-norm, depending on the case. Because both $\Omega$ and $\Gamma$ map zero into zero, their biases are zero. According to Lemma 2.3.3, $\|x_0\| < \infty$ implies that $d \in \mathcal{L}_\infty$. According to the small gain theorem, e.g. [27], $\gamma_\infty(\Phi).\gamma_\infty(\Gamma) < 1$ implies that all internal signals of the system are in $\mathcal{L}_\infty$. To show that the system is stable in the sense of Lyapunov, it is enough to show that for any given $\epsilon$ there exists $\delta$ such that $\|x_0\|_{\mathbb{R}^n} < \delta \Longrightarrow \|x(t)\|_{\mathbb{R}^n} < \epsilon$ for all $t \geq 0$. Without loss of generality, it can be assumed that the norm in $\mathbb{R}^n$ is $\|.\|_\infty$, e.g. [40]. We claim that for any given $\epsilon$, $\delta$ can be chosen as $\delta < \frac{1-\gamma_\infty(\Phi)\gamma_\infty(\Gamma)}{\gamma_\infty(\Omega)}\epsilon$. To prove this, since $\|x_0\| < \delta < \frac{1-\gamma_\infty(\Phi)\gamma_\infty(\Gamma)}{\gamma_\infty(\Omega)}\,\epsilon$ then $\|d(t)\| \leq \gamma_\infty(\Omega)\|x_0\| < (1 - \gamma_\infty(\Phi)\gamma_\infty(\Gamma))\,\epsilon$. Besides, $\|x\| \leq \|d\| + \|w\|$ and $\|w\| \leq \gamma_\infty(\Phi)\gamma_\infty(\Gamma)\|x\|$. Therefore $\|x\| \leq \frac{1}{(1-\gamma_\infty(\Phi)\gamma_\infty(\Gamma))}\|d\| < \epsilon$. Since for any given $\epsilon$ there exists some $\delta < \frac{1-\gamma_\infty(\Phi)\gamma_\infty(\Gamma)}{\gamma_\infty(\Omega)}\,\epsilon$, stability is global. It is important to note that since $\gamma_\infty(\Omega) \geq 1$, $\gamma_\infty(\Phi) \geq 0$ and $\gamma_\infty(\Gamma) \geq 0$ then $\frac{1-\gamma_\infty(\Phi)\gamma_\infty(\Gamma)}{\gamma_\infty(\Omega)} \leq 1$ and $\delta \leq \epsilon$.

(ii) In this section of proof, all of the norms are either 2-norm or $\mathcal{L}_2$-norm unless it is clarified. According to lemma 2.3.5(i), $\|x_0\| < \infty$ implies that $\|d\| = \gamma_2(\Omega).\|x_0\| < \infty$ and consequently $d \in \mathcal{L}_2$. According to small gain theorem, e.g. [27], $\gamma_2(\Phi).\gamma_2(\Gamma) < 1$ implies that all internal signals of the system are in $\mathcal{L}_2$. Therefore, $x \in \mathcal{L}_\infty \cap \mathcal{L}_2$ and consequently there exists closed set $\mathcal{D}$ such that $x(t) \in \mathcal{D}$ for all $t$. Assuming that $f(x,t)$ is locally Lipschitz in $\mathcal{D}$, there exists $\mu$ such that

$$\forall\, x_1, x_2 \in \mathcal{D} \qquad \|f(x_2,t) - f(x_1,t)\|_\infty \leq \mu\|x_2 - x_1\|_\infty \tag{3.1}$$

Taking $x_1 = 0$ and $x_2 = x(t)$

$$\forall\, x(t) \in \mathcal{D} \qquad \|f(x(t),t)\|_\infty \leq \mu\|x(t)\|_\infty \tag{3.2}$$

Since $x \in \mathcal{L}_\infty$, $\|x(t)\|_\infty \leq \|x\|_{\mathcal{L}_\infty}$ for all $t$. Substituting in (3.2), $\|\dot{x}(t)\|_\infty = \|f(x(t),t)\|_\infty \leq \mu\|x\|_{\mathcal{L}_\infty}$ for all $t$. In turn, this means that $\dot{x} \in \mathcal{L}_\infty$. Now, we use the corollary of the Barbalat's lemma, i.e. 3.2.1. Assuming $\phi(t) := \|x(t)\|_2^2 = x^T(t)x(t)$, it is trivial that $\phi \in \mathcal{L}_\infty$.

Since $\dot{x} \in \mathcal{L}_\infty$, we have

$$\dot{\phi}(t) = \dot{x}^T(t)x(t) + x^T(t)\dot{x}(t) < \infty, \quad \forall\, t \tag{3.3}$$

which means $\dot{\phi} \in \mathcal{L}_\infty$. On the other hand,

$$\int_0^\infty |\phi(t)|dt = \int_0^\infty \|x(t)\|_2^2 dt = \|x\|_{\mathcal{L}_2}^2 < \infty \tag{3.4}$$

that reveals that $\phi \in \mathcal{L}_1$. Corollary 3.2.1 implies that $\lim_{t\to\infty} \phi(t) = 0$ and consequently $\lim_{t\to\infty} x(t) = 0$. □

**Theorem 3.2.2.** *Given a discrete time system of the form (2.22) with $\zeta_A$ representation of $[\Phi, \Gamma, \Omega]$,*

*(i) if $\gamma_\infty(\Phi) \cdot \gamma_\infty(\Gamma) < 1$ then the system is globally stable in sense of Lyapunov.*

*(ii) if, in addition to (i), $\gamma_2(\Phi) \cdot \gamma_2(\Gamma) < 1$ then the system is globally asymptotically stable in sense of Lyapunov.*

*Proof.* The proof follows the same lines as the proof of Theorem 3.2.2 and is omitted. It is important to note that in the discrete-time domain, $x \in \ell_2 \cap \ell_\infty$ implies that $x(t) \to 0$ as $t \to \infty$ and there is no need for the second part of the proof where the corollary of Barbalat's lemma is used. □

Theorems 3.2.1 and 3.2.2 can be used to check the stability of nonlinear systems with the help of the mentioned computation methods. Moreover, $A$ plays the role of a free parameter. It is important to note that both theorems state sufficient conditions for stability. This implies that it is sufficient to find just one $A$ which satisfies the conditions of the theorems. If such a matrix $A$ is found the system is stable even if there exists other $A$ matrices which fail the conditions. If such a matrix $A$ cannot be found or does not exist, the stability or instability of the system can not be proven using these theorems.

To compare the results with LTI systems, consider the following perturbed LTI system

$$\dot{x} = (M + \Delta M)x \tag{3.5}$$

Let $\Phi(x) = (M + \Delta M + \alpha I)x$ where $\alpha > 0$. Consequently, $A = -\alpha I$ and $\Gamma$ defined as (2.18a) or equivalently (2.19). To compute $\gamma_\infty(\Gamma)$, Lemma 2.3.1 can be used. The impulse response of $\Gamma$ is $G(s) = \frac{1}{s-\alpha} I$ and $g_{ii}(t) = e^{-\alpha t}$ and $g_{ij}(t) = 0$ for $i \neq j$. Equation (2.3) implies $\|\tilde{g}_{ii}(t)\| = 1$ and $\|\tilde{g}_{ij}(t)\| = 0$ for $i \neq j$. Consequently, $\gamma_2(\Gamma) = \frac{1}{\alpha}$ and $\gamma_\infty(\Gamma) = 1$.

On the other hand, $\gamma_\infty(\Phi) = \|M+\Delta M+\alpha I\|_\infty$. According to Theorem 3.2.1, the stability condition is $\|M + \Delta M + \alpha I\|_\infty < 1$ or equivalently $\lambda_{\max}(M + \Delta M) < -\alpha < 0$, where $\lambda_{\max}$ denotes the maximum eigenvalue. This is to say that the perturbation $\Delta M$ should not move the eigenvalues of the system to RHP or $j\omega$ axis.

**Example 3.2.1.** Consider the following nonlinear system

$$\dot{x} = f(x) = \begin{cases} 0.25\,x_1 - x_2 - \text{sat}\,(x_1) - \text{sat}\,(x_2) \\ 4\,x_1 - 3\,x_2 - \text{sat}\,(x_1) - \sin(x_2) \end{cases} \tag{3.6}$$

where $\text{sat}\,(x) = \text{sgn}\,(x)\ \min(1, |x|)$ and $\text{sgn}\,(\cdot)$ is the signum function. Let

$$A = \begin{bmatrix} -0.25 & -1.5 \\ 3.5 & -3.5 \end{bmatrix}. \tag{3.7}$$

Therefore,

$$\Phi(x) = f(x) - A\,x = \begin{cases} 0.5\,x_1 + 0.5\,x_2 - \text{sat}\,(x_1) - \text{sat}\,(x_2) \\ 0.5\,x_1 + 0.5\,x_2 - \text{sat}\,(x_1) - \sin(x_2) \end{cases}.$$

Figure 3.1 shows the plot of $\frac{\|\Phi(x)\|}{\|x\|}$ versus $\|x\|$ established at $10^6$ randomly chosen points. Using methods described in Sections 2.3.2 to 2.3.4, we have $\gamma_\infty(\Phi) = 1$, $\gamma_\infty(\Gamma) = 0.9531$, $\gamma_2(\Phi) = 1$, and $\gamma_2(\Gamma) = 0.8217$. Since $\gamma_\infty(\Phi)\,\gamma_\infty(\Gamma) = 0.9531 < 1$, the system is globally stable. More interestingly, $\gamma_2(\Phi)\,\gamma_2(\Gamma) = 0.8217 < 1$ implies that the system is asymptotically globally stable. To illustrate the system response, the phase portrait as well as the vector field diagram are depicted in Fig. 3.2.

*Remark* 3.2.1. It is important to notice that the converse Lyapunov theorem [24] [27] guarantees that there exists a Lyapunov function for any stable system. However, there is not a general method to find it. Indeed, the process of finding or constructing a Lyapunov function can be challenging. For instance, the trivial candidate of Lyapunov function, i.e. $V(x) = \frac{1}{2}(\alpha\,x_1^2 + \beta\,x_2^2)$ where $\alpha, \beta > 0$, cannot pass the conditions of Lyapunov functions in the previous example. To see this,

$$\begin{aligned} \dot{V}(x) &= [\alpha x_1 \quad \beta x_2] \cdot f(x) \\ &= 0.25\,\alpha\,x_1^2 + (4\,\beta - \alpha)\,x_1\,x_2 - 3\,\beta x_2^2 \\ &\quad - \alpha\,x_1(\text{sat}\,(x_1) + \text{sat}\,(x_2)) - \beta\,x_2(\text{sat}\,(x_1) + \sin(x_2)) \end{aligned} \tag{3.8}$$

Apparently, $\dot{V}(x_1, 0) = \alpha\,x_1(0.25\,x_1 - \text{sat}\,(x_1))$. For any $x_1 > \max(1, 4\,\alpha)$, we have $\dot{V} > 0$; thus, $V(x)$ fails the Lyapunov conditions and cannot be used to prove stability of the system.

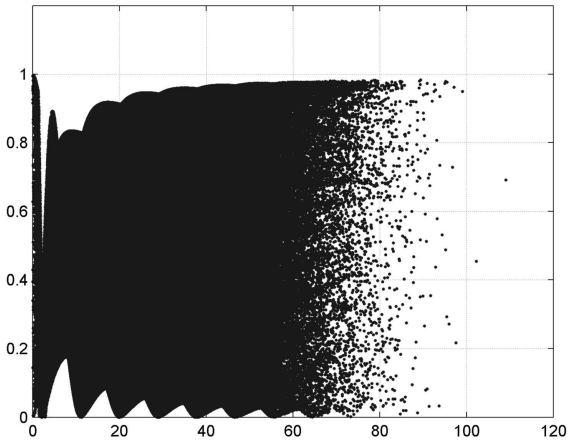


(a) $\frac{\|\Phi(x)\|_2}{\|x\|_2}$ versus $\|x\|_2$

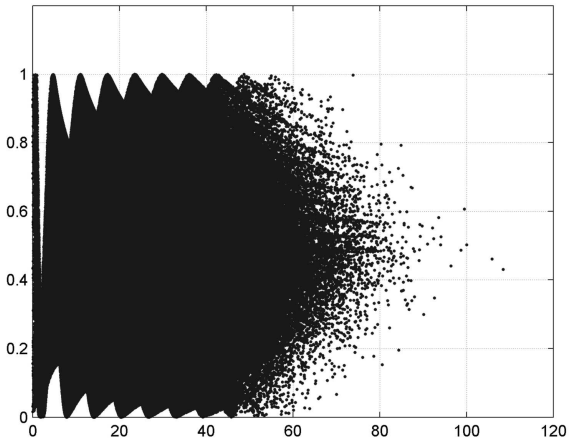


(b) $\frac{\|\Phi(x)\|_\infty}{\|x\|_\infty}$ versus $\|x\|_\infty$

Figure 3.1: $\gamma_2(\Phi)$ and $\gamma_\infty(\Phi)$ in Example 3.2.1.

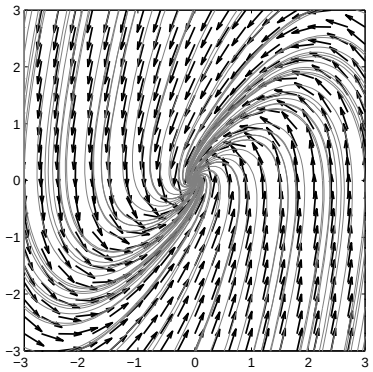


Figure 3.2: Phase portrait for Example 3.2.1.

**Example 3.2.2.** Consider the following nonlinear system

$$\begin{cases} \dot{x_1} &= -2\,x_1 + x_2 + \sin(0.5\,x_2) - \sin(0.5\,x_3) \\ \dot{x_2} &= -x_1 - x_2 + \sin(0.5\,x_1) - \sin(0.5\,x_3) \\ \dot{x_3} &= 1 - x_3 - \cos(0.5\,x_1) + \sin(0.5\,x_2) \end{cases} \tag{3.9}$$

Let $A = \begin{bmatrix} -2.0 & 1.2 & 0 \\ -0.8 & -1.0 & 0 \\ 0 & 0 & -1.0 \end{bmatrix}$ and

$$\Phi(x_1, x_2, x_3) = \begin{bmatrix} -0.2\,x_2 + \sin(0.5\,x_2) - \sin(0.5\,x_3) \\ -0.2\,x_1 + \sin(0.5\,x_1) - \sin(0.5\,x_3) \\ 1 - \cos(0.5\,x_1) + \sin(0.5\,x_2) \end{bmatrix} \tag{3.10}$$

Similar to the previous examples, we use the computational methods introduced in Section 2.3.1. We plot $\frac{\|\Phi(x)\|}{\|x\|}$ versus $\|x\|$ instead of plotting versus $x_1$, $x_2$ and $x_3$. plots are established at $2 \times 10^6$ randomly chosen points. As shown in Fig. 3.3, $\gamma_2(\Phi) \approx 0.8$ and $\gamma_\infty(\Phi) \approx 0.8$. Computation also shows that $\gamma_2(\Gamma) \approx 1.000$ and $\gamma_\infty(\Gamma) \approx 1.0005$. Since $\gamma_\infty(\Phi)\,\gamma_\infty(\Gamma) = 0.7938 < 1$ and $\gamma_2(\Phi)\,\gamma_2(\Gamma) = 0.7846 < 1$, the system is globally asymptotically stable.

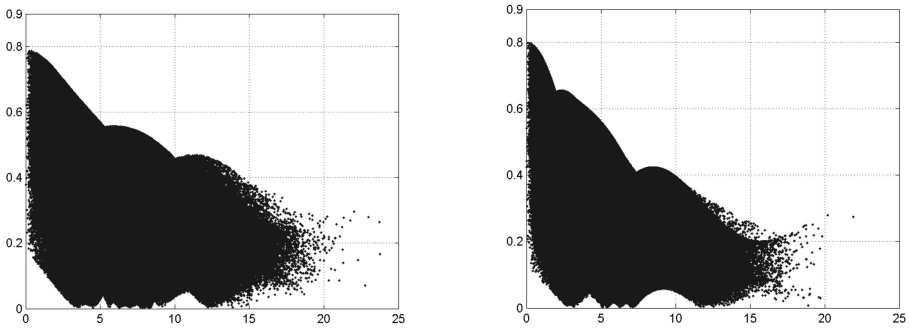


(a) $\frac{\|\Phi(x)\|_2}{\|x\|_2}$ versus $\|x\|_2$ (b) $\frac{\|\Phi(x)\|_\infty}{\|x\|_\infty}$ versus $\|x\|_\infty$

Figure 3.3: Local gains in Example 3.2.2.

### 3.2.2 Local Stability

**Definition 3.2.1.** Given a nonlinear system of the form either (2.13) or (2.22), we define the ordered pair $[\Delta, \Upsilon]$ as follows:

$$[\Delta, \Upsilon] := \{\Delta, \Upsilon \subset \mathbb{R}^n;\ x(0) \in \Delta \Rightarrow x(t) \in \Upsilon, \forall t \geq 0\} \tag{3.11}$$

We will refer to $\Delta$ and $\Upsilon$ as the $\Delta$ and $\Upsilon$ regions and collect all $[\Delta, \Upsilon]$ pairs of a system in a set denoted by $\mathcal{S}_{\Delta\Upsilon}$.

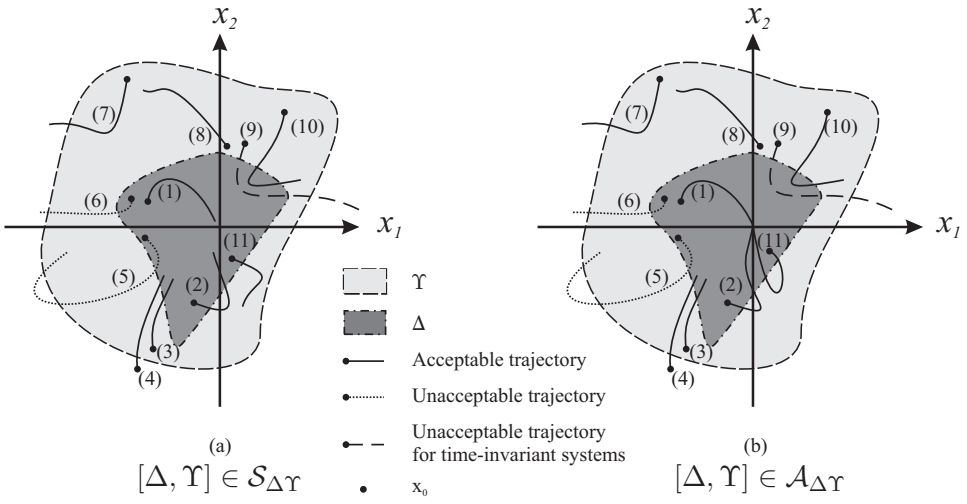


Figure 3.4: Acceptable and unacceptable trajectories.

**Definition 3.2.2.** For a given system, if $[\Delta, \Upsilon] \in \mathcal{S}_{\Delta\Upsilon}$ and for any $x(0) \in \Delta$ we have $x(t) \to 0$ as $t \to \infty$ then $\Delta$ and $\Upsilon$ are called asymptotic regions and we collect all such pairs in $\mathcal{A}_{\Delta\Upsilon}$.

Fig. 3.4 shows acceptable and unacceptable trajectories for both $[\Delta, \Upsilon] \in \mathcal{S}_{\Delta\Upsilon}$ and $[\Delta, \Upsilon] \in \mathcal{A}_{\Delta\Upsilon}$. As shown in this figure, $[\Delta, \Upsilon] \in \mathcal{S}_{\Delta\Upsilon}$ guarantees that the trajectories starting from inside of $\Delta$, such as (1),(2), and (11), will stay inside $\Upsilon$. Therefore, trajectories (5) and (6) can never occur because both trajectories cross the boundary of the $\Upsilon$ region. Notice that there is no guarantee that trajectories starting inside of $\Upsilon$, such as (7), stay inside $\Upsilon$. The definition of $\mathcal{S}_{\Delta\Upsilon}$ assures that trajectories such as (5) and (6) which start from $\Delta$ and go outside of $\Upsilon$ are not possible. An interesting case is (9). This case is possible for non-autonomous systems but impossible for autonomous systems. The reason is that for autonomous systems we can transfer $t = 0$ to any $t = t_0$. Since this trajectory passed through $\Delta$, we can transfer the starting point to any point on the trajectory which is also inside $\Delta$. With the new starting point, $[\Delta, \Upsilon] \in \mathcal{S}_{\Delta\Upsilon}$ guarantees that the trajectory will stay inside $\Upsilon$ which is not observed by (9). Therefore, for autonomous systems, any trajectory, which has intersection with $\Delta$, stays inside $\Upsilon$. Fig. 3.4(b) is very similar to Fig. 3.4(a). The only difference is that all trajectories starting from $\delta$, such as (1) and (2), terminate at the origin. For autonomous systems, any trajectory which has a point inside $\delta$ also end at the origin for the same reason explained earlier. Therefore, for autonomous systems, (3), (4) and (10) (and also (5), (6) and (9)) should also terminate at the origin.

**Corollary 3.2.1.** *If* $[\Delta, \Upsilon] \in \mathcal{S}_{\Delta\Upsilon}$

- $\Delta \subset \Upsilon$,
- $\Delta = \Upsilon$ *implies that* $\Upsilon$ *is an invariant set for the nonlinear system.*

**Proposition 3.2.1.** *Consider a system with* $\zeta_A$ *representation of* $[\Phi, \Gamma, \Omega]$. *Assume that* $\Upsilon$ *is a given bounded subset of* $\mathbb{R}^n$, *i. e.* $\|x\|_p < \epsilon$ *for all* $x \in \Upsilon$ *and* $p \in \{2, \infty\}$. *Let* $0 < \delta \leq \frac{1-\gamma_p(\Phi)\gamma_p(\Gamma)}{\gamma_p(\Omega)}\epsilon$ *and*

$$\Delta := \{x \in \mathbb{R}^n \,,\ \|x\|_p < \delta\} \tag{3.12}$$

*Then* $[\Delta, \Upsilon] \in \mathcal{S}_{\Delta\Upsilon}$.

*Proof.* The proof follows a routine similar to the proof of Theorem 3.2.1 and is omitted. □

Proposition 3.2.1 shows a method to compute $[\Delta, \Upsilon]$ regions.

**Definition 3.2.3.** Local gain $\gamma_p^{\mathcal{D}}(\Phi)$ of a static operator $\Phi$, where $p \in \{2, \infty\}$, is the maximum $p$-norm gain of the operator for all of the members inside the region $\mathcal{D}$, respectively. i.e.

$$\gamma_p^{\mathcal{D}}(\Phi) = \sup_{\substack{x \in \mathcal{D} - \{0\} \\ \forall t \geq 0}} \frac{\|\Phi(t,x)\|_p}{\|x\|_p} \tag{3.13}$$

**Theorem 3.2.3.** *Consider a nonlinear system with state space representation of either (2.13) or (2.22), and let* $[\Phi, \Gamma, \Omega]$ *be a* $\zeta_A$ *representation. Let* $M_p > \gamma_\infty(\Omega)$ *be a fixed number and*

$$\hat{\mathcal{D}} := \left\{ x \in \mathbb{R}^n \mid \gamma_\infty^{\hat{\mathcal{D}}}(\Phi) < \frac{1}{\gamma_\infty(\Gamma)}\left(1 - \frac{\gamma_\infty(\Omega)}{M_P}\right) \quad \forall t \geq 0 \right\} \tag{3.14a}$$

*Assume that* $\mathcal{D}$ *is a simply connected subset of* $\hat{\mathcal{D}}$ *that includes the origin. Let* $\xi = \inf_{x \in \partial\mathcal{D}} \|x\|_\infty$ *where* $\partial\mathcal{D}$ *is the boundary of* $\mathcal{D}$. *Let* $\Upsilon$ *be a ball inside* $\mathcal{D}$ *centered at the origin with radius* $\epsilon < \xi$. *i.e.*

$$\Upsilon = \{x \in \mathcal{D} \mid \|x\|_\infty < \epsilon\} \tag{3.14b}$$

*and let*

$$\Delta := \left\{ x \in \mathbb{R}^n \mid \|x\| < \delta,\ \delta := \frac{1 - \gamma_\infty^{\hat{\mathcal{D}}}(\Phi)\gamma_\infty(\Gamma)}{\gamma_\infty(\Omega)}\,\epsilon \right\} \tag{3.14c}$$

*Then,*

1. $[\Delta, \Upsilon] \in \mathcal{S}_{\Delta\Upsilon}$

2. *if $x_0 \in \Delta$ then $M_P$ is the maximum overshoot of $x(t)$.*

*Proof.* Since $M_p > \gamma_\infty(\Omega)$, (3.14a) reveals that $\gamma_\infty^{\hat{\mathcal{D}}}(\Phi)\gamma_\infty(\Gamma) < 1$. To prove the theorem we reason by contradiction. Since we assumed that systems of our interest are locally Lipschitz, trajectories of the system are continuous. As a consequence, if $x$ were to leave $\Upsilon$, it should cross the boundary of $\Upsilon$. Suppose that $x$ crosses the boundary of $\Upsilon$ at $t = T$; then $\|\mathbf{T}_T x\| = \|x_T\| = \epsilon$. Since the boundary of $\Upsilon$ is in $\mathcal{D}$, $\|x_T\| \leq \|d_T\| + \|w_T\| \leq \gamma_\infty(\Omega)\|x_0\| + \gamma_\infty^{\hat{\mathcal{D}}}(\Phi)\gamma_\infty(\Gamma)\|x_T\|$. Then $\|x_T\| \leq \frac{\gamma_\infty(\Omega)}{1-\gamma_\infty^{\hat{\mathcal{D}}}(\Phi)\gamma_\infty(\Gamma)}\|x_0\| < \frac{\gamma_\infty(\Omega)}{1-\gamma_\infty^{\hat{\mathcal{D}}}(\Phi)\gamma_\infty(\Gamma)}\delta < \epsilon$. Which contradicts the fact that $\|x_T\| = \epsilon$. Therefore, $x(t) \in \Upsilon;\ \forall t \geq 0$. That is $[\Delta, \Upsilon] \in \mathcal{S}_{\Delta\Upsilon}$. To show the second part, from (3.14a), we have $\frac{\gamma_\infty(\Omega)}{1-\gamma_\infty^{\hat{\mathcal{D}}}(\Phi)\gamma_\infty(\Gamma)} < M_p$. On the other hand, $\|x\| \leq \frac{\gamma_\infty(\Omega)}{1-\gamma_\infty^{\hat{\mathcal{D}}}(\Phi)\gamma_\infty(\Gamma)}\|x_0\| < M_p\|x_0\|$ □

**Theorem 3.2.4.** *Let $[\Phi, \Gamma, \Omega]$ be a $\zeta_A$ representation for a nonlinear system in the form of either (2.13) or (2.22). Let $\Upsilon := \{x \in \mathbb{R}^n \mid \|x\| < \epsilon\}$ and $\Delta := \{x \in \mathbb{R}^n \mid \|x\| < \delta, \}$. If $[\Delta, \Upsilon] \in \mathcal{S}_{[\Delta,\Upsilon]}$ and $\gamma_2^\Upsilon(\Phi).\gamma_2(\Gamma) < 1$ then $[\Delta, \Upsilon] \in \mathcal{A}_{[\Delta,\Upsilon]}$.*

*Proof.* Since $[\Delta, \Upsilon] \in \mathcal{S}_{[\Delta,\Upsilon]}$, any trajectory starting from $\Delta$ will stay inside $\Upsilon$. According to the $\zeta_A$ representation, $\|x\|_{\mathcal{L}_2} < \frac{1-\gamma_2^\Upsilon(\Phi)\,\gamma_2(\Gamma)}{\gamma_2(\Omega)}\|x_0\|_2 < \infty$ and consequently $x \in \mathcal{L}_2$.

For discrete-time systems, since $\gamma_2^\Upsilon(\Phi).\gamma_2(\Gamma) < 1$, $\|x\|_{\ell_2} < \infty$ and as a result $x(t) \in \ell_2$. Consequently $x(t) \to 0$ as $t \to \infty$. It turns out that $[\Delta, \Upsilon] \in \mathcal{A}_{[\Delta,\Upsilon]}$.

For continuous-time systems, Corollary 3.2.1 should be used. Since $x(t) \in \Upsilon$ for all $t$, $x \in \mathcal{L}_\infty$ and consequently $x \in \mathcal{L}_2 \cap \mathcal{L}_\infty$. The proof, which is omitted here, follows the same outline as the proof of Theorem 3.2.1(ii) with $\mathcal{D} \equiv \Upsilon$.

□

**Corollary 3.2.2.** *Let $[\Phi, \Gamma, \Omega]$ be a $\zeta_A$ representation for a nonlinear system in the form of either (2.13) or (2.22). If there exists a region around the origin $\hat{\mathcal{D}}$ where $\gamma_\infty^{\hat{\mathcal{D}}}(\Phi)\gamma_\infty(\Gamma) < 1$, then the system is locally stable. If in addition $\gamma_2^{\hat{\mathcal{D}}}(\Phi)\gamma_2(\Gamma) < 1$, then the system is locally asymptotically stable.*

*Proof.* Since $\gamma_\infty^{\hat{\mathcal{D}}}(\Phi)\gamma_\infty(\Gamma) < 1$, there exists $M_p > \gamma_\infty(\Omega)$ such that $\gamma_\infty^{\hat{\mathcal{D}}}(\Phi) < \frac{1}{\gamma_\infty(\Gamma)}\left(1 - \frac{\gamma_\infty(\Omega)}{M_P}\right)$. Let $\mathcal{D}$ be a simply connected subset of $\hat{\mathcal{D}}$ that includes the origin. Let $\xi = \inf_{x\in\partial\mathcal{D}} \|x\|_\infty$ where $\partial\mathcal{D}$ is the boundary of $\mathcal{D}$. For any $\epsilon$ that satisfies $0 < \epsilon < \xi$, $\Delta$ and $\Upsilon$ can be constructed as (3.14) and $\delta > 0$ in (3.14c) can be found. Theorem 3.2.3 guarantees that $[\Delta, \Upsilon] \in \mathcal{S}_{\Delta\Upsilon}$ or equivalently

$$\|x(0)\| < \delta \Longrightarrow \|x(t)\| < \epsilon,\ \forall t \geq 0 \tag{3.15}$$

The second part is trivial consequence of Theorem 3.2.4. □

**Corollary 3.2.3.** Sufficient condition of stability in Lyapunov Linearization Method

*If the linearized system of a nonlinear system is stable, the nonlinear system is locally asymptotically stable.*

*Proof.* Let $A$ be the linearized part, i.e. $A = \frac{\partial f(x)}{\partial x}\Big|_{x=0}$. Since $A$ is stable, $\gamma_\infty(\Gamma) < \infty$ and $\gamma_2(\Gamma) < \infty$. Since $\Phi(x)$ only includes the higher order terms in $x$, the exists a region around the origin $\hat{\mathcal{D}}$ where $\gamma_\infty^{\hat{\mathcal{D}}}(\Phi)$ and $\gamma_2^{\hat{\mathcal{D}}}(\Phi)$ can be made arbitrarily small. Thus, Corollary 3.2.2 implies local asymptotic stability of the nonlinear system. □

**Example 3.2.3.** Consider the following nonlinear system.

$$\begin{cases} \dot{x}_1 = -2x_1 + x_2 - \sqrt{x_1^3}/3 + x_2^2/4 \\ \dot{x}_2 = -2x_1 + 2x_2 + x_1^2/10 - 5\sin(x_2)/2 \end{cases} \tag{3.16}$$

Let choose $A = \begin{bmatrix} -2 & 1 \\ -2 & -3 \end{bmatrix}$ then $\Phi(x) = \begin{cases} -\sqrt{x_1^3}/3 + x_2^2/4 \\ +5x_2 + x_1^2/10 - 5\sin(x_2)/2 \end{cases}$. Using (2.4b) and (2.8) respectively, $\gamma_\infty(\Gamma) = 0.5378$ and $\gamma_\infty(\Omega) = 1$. Direct computation, as discussed in Section 2.3.3, gives $\gamma_\infty(\Phi) = \infty$, which implies that Theorem (3.2.1) can not be applied. Assume that $M_P = 1.5$, then $\gamma_\infty^{\mathcal{D}}(\Phi) < \frac{1}{\gamma_\infty(\Gamma)}\left(1 - \frac{\gamma_\infty(\Omega)}{M_p}\right) = 0.6197$. $\gamma_\infty(\Phi)$ is plotted versus $x$ in Fig. 3.5(a) and its junction with the plan $\gamma_\infty^{\mathcal{D}}(\Phi)$ is marked. The junction determines the boundary of $\mathcal{D}$, as shown in Fig. 3.5(c). $\gamma_2(\Phi)$ and its junction with $\frac{1}{\gamma_2(\Gamma)}$ are shown in Fig. 3.5(b). Since $\mathcal{L}_\infty$-norm is used, the largest ball inside $\mathcal{D}$, i.e. $\Upsilon$, is the square shown in Fig. 3.5(c). Since $M_P = 1.5$, the largest $\Delta$ area is another square inside $\Upsilon$ and smaller than it with factor $M_P$, as shown in Fig. 3.5(c). Theorem 3.2.3 guarantees that any trajectory starting from inside $\Delta$ will stay inside $\Upsilon$. Moreover, since $\Upsilon$ and $\Delta$ are placed inside the region where $\gamma_2(\Phi)\gamma_2(\Gamma) < 1$, Theorem 3.2.4 guarantees that all trajectories starting from $\Delta$ end at the origin. Since the system is autonomous, this is also the case for all trajectories which has intersection with $\Delta$. System trajectories as well as some of its responses to various initial conditions are depicted in Fig. 3.6. In the first graph, since the initial states (or one of them) are not in $\Delta$, stability is not guaranteed and the system is unstable. For the rest, initial states are in $\Delta$ and consequently, the system is stable and states terminate at the origin.

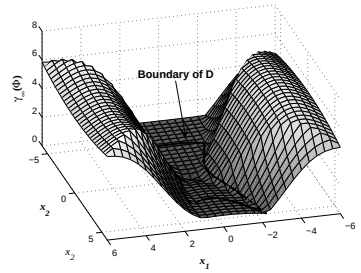


(a) $\gamma_\infty(\Phi)$ crossed by $\frac{1}{\gamma_2(\Gamma)}\left(1-\frac{\gamma_\infty(\Omega)}{M_p}\right)$

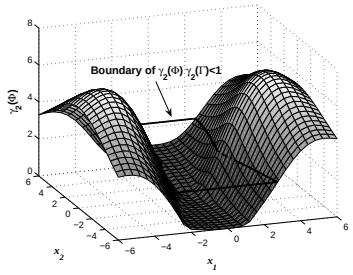


(b) $\gamma_2(\Phi)$ crossed by $\frac{1}{\gamma_2(\Gamma)}$

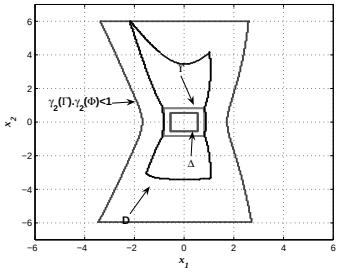


(c) Regions

Figure 3.5: Various regions in Example 3.2.3

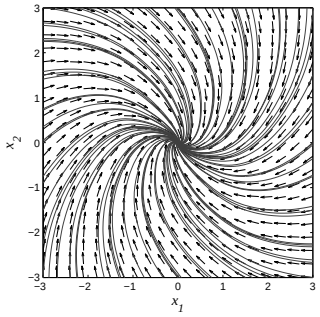

(a) System trajectories for Example 3.2.3

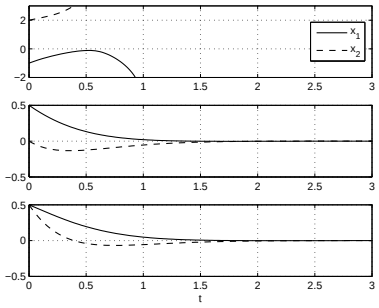


(b) Some responses for the system in Example 3.2.3

Figure 3.6: Simulation results for Example 3.2.3.

## 3.3 Forced Systems

### 3.3.1 Global Stability

**Proposition 3.3.1.** *For a forced nonlinear system with $\zeta_{AB}$ representation of $[\Phi, \Theta, \Gamma, \Omega]$, if $u \in \mathcal{X}_p$ and $\gamma_p(\Phi)\gamma_p(\Gamma) < 1$ then $x \in \mathcal{X}_p$ for any initial state $x_0$.*

*Proof.* The proof for discrete-time systems is very similar to the continuous-time case and is omitted.

Since $A$ is stable, $\|e^{At}\|_{\mathcal{L}_p} < \infty$ and $u \in \mathcal{L}_p$ implies that $\|d_1\| \leq \|e^{At}\|_{\mathcal{L}_p} \cdot \|x_0\|_p + \gamma_\infty(\theta)\|u(t)\|_p < \infty$ and $d_1 \in \mathcal{L}_p$. On the other hand, since $\left\| \begin{bmatrix} 0 \\ I_{m\times m} \end{bmatrix} \right\|_p = 1$, and $u \in \mathcal{L}_p$ then $d_2 \in \mathcal{L}_p$. According to small gain theorem, e.g. [27], since input signals to the loop, i.e. $d_1$,$d_2$, are in $\mathcal{L}_p$ and $\left\| \begin{bmatrix} I_{n\times n} \\ 0 \end{bmatrix} \right\|_p = 1$, $\gamma_p(\Phi) \cdot \gamma_p(\Gamma) < 1$ implies that all internal signals of the system are in $\mathcal{L}_p$. Therefore, $x \in \mathcal{L}_p$ □

**Definition 3.3.1.** A nonlinear system in the form of either (2.30) or (2.33) is called *stable in general* or *generally stable* if

$$\forall \epsilon > 0, t \geq 0 \; \exists \delta, \eta > 0; \quad \left.\begin{matrix} \|x_0\| < \delta \\ \|u(t)\| < \eta\delta \end{matrix}\right\} \Rightarrow \|x(t)\| < \epsilon \tag{3.17}$$

In addition, if for any $x_0$ and input that satisfies $u(t) \to 0$ as $t \to \infty$, the state also satisfies $x(t) \to 0$ as $t \to \infty$, then the system is called *asymptotically generally stable*.

Any Euclidean norm can be used in the definition but once a norm is chosen, it should be used for all norms. Besides, it is trivial to show that if a system is general (asymptotic) stable using an arbitrary Euclidean norm, the property holds for all Euclidean norms.

**Definition 3.3.2.** A system is called $\mathcal{X}_p$*−(asymptotically) generally stable* or $\mathcal{X}_p$*− (asymptotically) stable in general* if it is (asymptotically) generally stable for input $u \in \mathcal{X}_p$.

**Lemma 3.3.1.** *For a generally (asymptotically) stable system, if $u = 0$ then the system is (asymptotically) stable in sense of Lyapunov.*

*Proof.* The proof follows directly from the definition by taking $u = 0$. □

**Lemma 3.3.2.** *ISS systems are generally stable.*

*Proof.* Considering that $\|u\|_{\mathcal{X}_\infty} < \epsilon_1$ implies that there exists $\epsilon_2$ such that $\|u(t)\|_p < \epsilon_2$ for all $t > 0$ and $p \in [1, \infty)$, this lemma is very similar to Lemma 2.7 in [36] and the proof follows same outline as its proof. □

**Lemma 3.3.3.** *A generally stable system is ISS stable if and only if there exists a class $\mathcal{K}$ function $\sigma_1$ and $T > 0$ such that $x(t) \leq \sigma_1(\|u\|_{\mathcal{L}_\infty})$ for all $t > T$.*

*Proof.* This lemma is also similar to Lemma 2.7 in [36] and the proof is the same. □

Lemmas 3.3.2 and 3.3.3 show that the set of ISS systems is a subset of the set of generally stable systems but the inverse is not true in general. Generally speaking, for a generally stable system the condition in Lemma 3.3.3 should be satisfied to guarantee ISS stability.

The following theorem provides a sufficient condition for stability of systems in general.

**Theorem 3.3.1.** *For a forced nonlinear system with $\zeta_{AB}$ representation of $[\Phi, \Theta, \Gamma, \Omega]$,*

*(i) If $\gamma_\infty(\Phi) \cdot \gamma_\infty(\Gamma) < 1$ then the system is $\mathcal{X}_\infty-$ globally generally stable.*

*(ii) In addition to (i), if $\gamma_2(\Phi).\gamma_2(\Gamma) < 1$ then the system is $\mathcal{X}_2 \cap \mathcal{X}_\infty-$ globally asymptotically generally stable.*

*Proof.* The proof for discrete-time systems is very similar and is omitted.
(i) In this section of the proof, all norms are either $\infty$-norm or $\mathcal{L}_\infty$-norm depend on the case. According to Proposition 3.3.1, since $u \in \mathcal{L}_\infty$ then $x \in \mathcal{L}_\infty$. To show that the system is generally stable, it is enough to show that for any given $\epsilon$ there exist $\delta$ and $\eta$ such that $\left.\begin{matrix}\|x_0\|_\infty < \delta \\ \|u(t)\|_\infty < \eta\delta\end{matrix}\right\} \Rightarrow \|x(t)\|_\infty < \epsilon$ for all $t \geq 0$. Choose $\eta > 0$ arbitrary. We claim that for any given $\epsilon$, $\delta$ can be chosen as $\delta < \frac{1-\gamma_\infty(\Phi)\gamma_\infty(\Gamma)}{\eta(\gamma_\infty(\Theta)+\gamma_\infty(\Phi)\gamma_\infty(\Gamma))+\gamma_\infty(\Omega)}\epsilon$. To prove,

$$\begin{aligned}
\|x\| &\leq \|d_1\| + \|w\| \\
&\leq \|d_1\| + \gamma_\infty(\Phi)\gamma_\infty(\Gamma)(\|d_2\| + \|x\|) \\
&\leq \gamma_\infty(\Omega)\|x_0\| + [\gamma_\infty(\Theta) + \gamma_\infty(\Phi)\gamma_\infty(\Gamma)]\|u\| + \gamma_\infty(\Phi)\gamma_\infty(\Gamma)\|x\| \\
&< \gamma_\infty(\Omega)\delta + [\gamma_\infty(\Theta) + \gamma_\infty(\Phi)\gamma_\infty(\Gamma)]\,\eta\delta + \gamma_\infty(\Phi)\gamma_\infty(\Gamma)\|x\| \\
&< (\gamma_\infty(\Omega) + \eta\,[\gamma_\infty(\Theta) + \gamma_\infty(\Phi)\gamma_\infty(\Gamma)])\,\delta + \gamma_\infty(\Phi)\gamma_\infty(\Gamma)\|x\|
\end{aligned}$$

then $\|x\| < \frac{\gamma_\infty(\Omega)+\eta(\gamma_\infty(\Theta)+\gamma_\infty(\Phi)\gamma_\infty(\Gamma))}{1-\gamma_\infty(\Phi)\gamma_\infty(\Gamma)}\delta < \epsilon$. Since for any given $\epsilon$ there exists some $\delta$, stability is global.

(ii) According to Proposition (3.3.1), since $u \in \mathcal{L}_2 \cap \mathcal{L}_\infty$ then $x \in \mathcal{L}_2 \cap \mathcal{L}_\infty$ and consequently there exist closed sets $\mathcal{D}_u$ and $\mathcal{D}_x$ such that $u(t) \in \mathcal{D}_u$ and $x(t) \in \mathcal{D}_x$ for all $t$. Assuming that $f(x, u, t)$ is locally Lipschitz in both $u \in \mathcal{D}_u$ and $x \in \mathcal{D}_x$, there exists $\mu$ such that

$$\forall\, x_1, x_2 \in \mathcal{D}_x,\ \forall\, u \in \mathcal{D}_u, \quad \|f(x_2, u, t) - f(x_1, u, t)\|_\infty \leq \mu\|x_2 - x_1\|_\infty \tag{3.18}$$

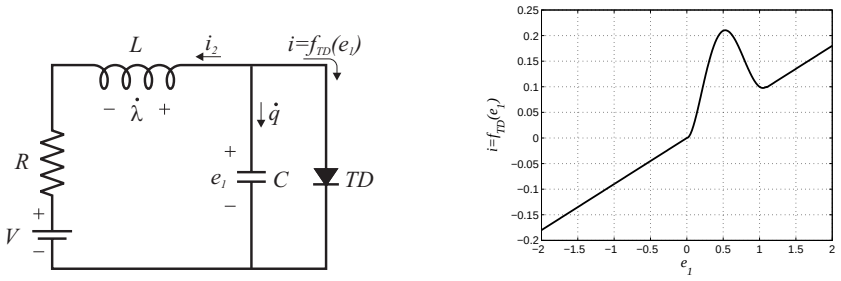


(a) The circuit (b) Tunnel diode characterization

Figure 3.7: Tunnel diode oscillator in Example 3.3.1.

Taking $x_1 = 0$ and $x_2 = x(t)$

$$\forall\, x(t) \in \mathcal{D}_x,\ \forall\, u(t) \in \mathcal{D}_u, \quad \|f(x(t), u(t), t)\|_\infty \leq \mu \|x(t)\|_\infty \tag{3.19}$$

Since $x \in \mathcal{L}_\infty$, $\|x(t)\|_\infty \leq \|x\|_{\mathcal{L}_\infty}$ for all $t$. Substituting in (3.19),

$$\|\dot{x}(t)\|_\infty = \|f(x(t), u(t), t)\|_\infty \leq \mu \|x\|_{\mathcal{L}_\infty} \tag{3.20}$$

for all $t$. In turn, this means that $\dot{x} \in \mathcal{L}_\infty$. Considering $x \in \mathcal{L}_2 \cap \mathcal{L}_\infty$ and $\dot{x} \in \mathcal{L}_\infty$, the rest of the proof follows same lines of the proof of Theorem 3.2.1(ii) and omitted here. □

Similar to Section 3.2.1, $A$ and $B$ play the role of free parameters in Proposition 3.3.1 and Theorem 3.3.1. Likewise, it is sufficient to find just one pair of $A$ and $B$ which satisfies the conditions of the proposition or the theorem. If such a pair is found, the proposition or the theorem can be used even if there exists other pairs of $A$ and $B$ matrices which fail the conditions. If such a pair of $A$ and $B$ cannot be found or does not exist, the proposition or the theorem cannot be used.

**Example 3.3.1.** (*"Hard" tunnel diode oscillator*) ( [37] pp. 446) The network of Fig. 3.7(a) represents a tunnel diode with some associated capacitance and inductance, biased by a combination of voltage source and resistance. The state equations for this network may be written as

$$\begin{aligned} \dot{q} &= -i_2 - f_{TD}(e_1), & e_1 &= \tfrac{q}{C}, \\ \dot{\lambda} &= e_1 - R i_2 - V, & i_2 &= \tfrac{\lambda}{L}, \end{aligned} \tag{3.21}$$

where the function $f_{TD}(e_1)$ represents the tunnel diode branch relation. Let $x_1 := q = e_1$, $x_2 := -\lambda = -i_2$, $R = 1$, $L = 1$, $u = V$ and $f_{TD}(\cdot)$ be

$$i = f_{TD}(e_1) = \begin{cases} -1.7e_1^5 + 6.6e_1^4 - 8.4e_1^3 + 3.6e_1^2 & 0 < e_1 \leq 1.1 \\ 0.09e_1 & \text{otherwise} \end{cases}$$

which is depicted in Fig. 3.7(b). Substituting defined states,

$$\dot{x} = f(x) = \begin{cases} x_2 - f_{TD}(x_1) \\ -x_1 - x_2 + u \end{cases}$$

Choosing $A = \begin{bmatrix} -0.3 & 1 \\ -1 & -1 \end{bmatrix}$, we have $\Phi(x) = \begin{pmatrix} 0.3x_1 - f_{TD}(x_1) \\ 0 \end{pmatrix}$. Computation shows that $\gamma_\infty(\Phi) = \gamma_2(\Phi) < 0.3$, $\gamma_\infty(\Gamma) < 2.17$ and $\gamma_2(\Gamma) = 1.641$. Since $\gamma_2(\Phi).\gamma_2(\Gamma) < 1$ and $\gamma_\infty(\Phi).\gamma_\infty(\Gamma) < 1$, according to Theorem 3.3.1, the system is $\mathcal{L}_2 \cap \mathcal{L}_\infty-$ globally asymptotically generally stable. This means that for any initial state and input $\{u \in \mathcal{L}_2 \cap \mathcal{L}_\infty : \lim_{t\to\infty} u \to 0\}$, state is bounded and approaches 0 as $t \to \infty$.

### 3.3.2 Local Stability

**Theorem 3.3.2.** *Let $[\Phi, \Theta, \Gamma, \Omega]$ be a $\zeta_{AB}$ representation for a nonlinear system. Let $\eta > 0$ and $M_p > \gamma_\infty(\Omega) + \eta\gamma_\infty(\theta)$ and*

$$\hat{\mathcal{D}} := \left\{ \begin{bmatrix} x \\ u \end{bmatrix} \in \mathbb{R}^{n+m} \;\middle|\; \gamma_\infty^{\hat{\mathcal{D}}}(\Phi) < \frac{M_p - \gamma_\infty(\Omega) - \eta\gamma_\infty(\theta)}{(M_p + \eta)\gamma_\infty(\Gamma)} \right\} \tag{3.22}$$

*Let $\mathcal{D} := \mathbf{B}^\infty(o, \xi_D)$ be an open ball inside $\hat{\mathcal{D}}$. Let $\mathcal{D}_x$ and $\mathcal{D}_u$ be the images of $\mathcal{D}$ under $\begin{bmatrix} I_{n\times n} & 0_{n\times m} \\ 0_{m\times n} & 0_{m\times m} \end{bmatrix}$ and $\begin{bmatrix} 0_{n\times n} & 0_{n\times m} \\ 0_{m\times n} & I_{m\times m} \end{bmatrix}$, respectively. Consequently, $\mathcal{D}_x$ and $\mathcal{D}_u$ are also open balls in $\mathbb{R}^n$ and $\mathbb{R}^m$ respectively. Let $\xi_x$ and $\xi_u$ denote respectively their radius, i.e. $\mathcal{D}_x = \mathbf{B}^\infty(0, \xi_x)$ and $\mathcal{D}_u = \mathbf{B}^\infty(0, \xi_u)$. Choose $\epsilon$ and $\delta$ such that $0 < \epsilon < \xi_x$ and*

$$0 < \delta \leq \frac{1 - \gamma_\infty^{\mathcal{D}}(\Phi)\gamma_\infty(\Gamma)}{\gamma_\infty(\Omega) + \eta(\gamma_\infty(\Theta) + \gamma_\infty^{\mathcal{D}}(\Phi)\gamma_\infty(\Gamma))}\,\epsilon$$

*If $\|u\|_{\mathcal{X}_\infty} < \min(\eta\,\delta, \xi_u)$ and $\|x_0\|_\infty \leq \delta$, then*

$$\|x\|_{\mathcal{X}_\infty} < \epsilon \tag{3.23}$$

*Proof.* The proof for discrete-time systems is very similar and is omitted. In this proof, vector norms are Euclidean $\infty$-norm for constant vectors and $\mathcal{X}_\infty$-norm for time-varying ones.

It is trivial that $M_p - \gamma_\infty(\Omega) - \eta\gamma_\infty(\theta) < M_p + \eta$; therefore $\gamma_\infty^{\mathcal{D}}(\Phi)\gamma_\infty(\Gamma) < 1$. We use contradiction to prove the theorem. Since we assumed that systems of interest are locally Lipschitz, system trajectories are continuous. Consequently, if $x$ were to leave the ball with radius $\epsilon$, it should cross the boundary of the ball. Suppose that $x$ crosses the boundary at $t = T$. As a result, $\|\mathbf{T}_T x\| = \|x_T\| = \epsilon$. Since $\epsilon < \xi_x$ and $\|u\| < \min(\eta\,\delta, \xi_u)$ guarantees

that $u \in \mathcal{D}_u$, we have $\begin{bmatrix} x_T \\ u_T \end{bmatrix} \in \mathcal{D}$ and consequently

$$\begin{aligned}
\|x_T\| &\leq \|d_{1T}\| + \|w_T\| \\
&\leq \|d_{1T}\| + \gamma_\infty^{\mathcal{D}}(\Phi)\gamma_\infty(\Gamma)(\|d_{2T}\| + \|x_T\|) \\
&\leq \gamma_\infty(\Theta)\|u_T\| + \gamma_\infty(\Omega)\|x_0\| + \gamma_\infty^{\mathcal{D}}(\Phi)\gamma_\infty(\Gamma)\|x_T\| + \gamma_\infty^{\mathcal{D}}(\Phi)\gamma_\infty(\Gamma)\|u_T\| \\
&\leq \gamma_\infty(\Omega)\|x_0\| + [\gamma_\infty(\Theta) + \gamma_\infty^{\mathcal{D}}(\Phi)\gamma_\infty(\Gamma)]\|u_T\| + \gamma_\infty^{\mathcal{D}}(\Phi)\gamma_\infty(\Gamma)\|x_T\| \\
&< \gamma_\infty(\Omega)\delta + \left[\gamma_\infty(\Theta) + \gamma_\infty^{\mathcal{D}}(\Phi)\gamma_\infty(\Gamma)\right]\eta\delta + \gamma_\infty(\Phi)^{\mathcal{D}}\gamma_\infty(\Gamma)\|x_T\| \\
&= \left(\gamma_\infty(\Omega) + \eta\left[\gamma_\infty(\Theta) + \gamma_\infty^{\mathcal{D}}(\Phi)\gamma_\infty(\Gamma)\right]\right)\delta + \gamma_\infty^{\mathcal{D}}(\Phi)\gamma_\infty(\Gamma)\|x_T\| \qquad (3.24)
\end{aligned}$$

Then

$$\begin{aligned}
\epsilon &= \|x_T\| < \frac{\gamma_\infty(\Omega) + \eta\left[\gamma_\infty(\Theta) + \gamma_\infty^{\mathcal{D}}(\Phi)\gamma_\infty(\Gamma)\right]}{1 - \gamma_\infty^{\mathcal{D}}(\Phi)\gamma_\infty(\Gamma)}\|x_0\| \\
&\leq \frac{\gamma_\infty(\Omega) + \eta\left[\gamma_\infty(\Theta) + \gamma_\infty^{\mathcal{D}}(\Phi)\gamma_\infty(\Gamma)\right]}{1 - \gamma_\infty^{\mathcal{D}}(\Phi)\gamma_\infty(\Gamma)}\,\delta \\
&\leq \epsilon \qquad (3.25)
\end{aligned}$$

Which is a contradiction. Therefore, $x(t) \in \Upsilon;\ \forall t \geq 0$. That is $[\Delta, \Upsilon] \in \mathcal{S}_{\Delta\Upsilon}$. To show the second part, from (3.22), with some mathematical manipulation, we have $\frac{\gamma_\infty(\Omega)+\eta\left[\gamma_\infty(\Theta)+\gamma_\infty^{\mathcal{D}}(\Phi)\gamma_\infty(\Gamma)\right]}{1-\gamma_\infty^{\mathcal{D}}(\Phi)\gamma_\infty(\Gamma)} \leq M_p$. On the other hand, with a very similar procedure to (3.25),

$$\|x\| < \frac{\gamma_\infty(\Omega) + \eta\left[\gamma_\infty(\Theta) + \gamma_\infty^{\mathcal{D}}(\Phi)\gamma_\infty(\Gamma)\right]}{1 - \gamma_\infty^{\mathcal{D}}(\Phi)\gamma_\infty(\Gamma)}\|x_0\| \leq M_p\|x_0\|.$$

□

**Theorem 3.3.3.** *In Theorem 3.3.2, if in addition $\mathcal{D}$ satisfies $\gamma_2(\Gamma)\gamma_2^{\mathcal{D}}(\Phi) < 1$ Then $[\Delta, \Upsilon] \in \mathcal{A}_{[\Delta,\Upsilon]}$ for $\{u \in \mathcal{X}_2 \cap \mathcal{X}_\infty : \|u\|_{\mathcal{X}_\infty} < \min(\eta\,\delta, \xi_u)\}$.*

*Proof.* The proof for discrete-time systems is very similar and is omitted.

Theorem 3.3.2 guarantees that $[\Delta, \Upsilon] \in \mathcal{S}_{[\Delta,\Upsilon]}$ for all $u$ that satisfies

$$\{u \in \mathcal{L}_2 \cap \mathcal{L}_\infty : \|u\|_{\mathcal{L}_\infty} < \min(\eta\,\delta, \xi_u)\}$$

which means that $x$ stays in $\Upsilon \subset \mathcal{D}_x$. Since $\|u\|_{\mathcal{L}_\infty} < \xi_u$, $u \in \mathcal{D}_u$ then $\begin{bmatrix} x \\ u \end{bmatrix} \in \mathcal{D}$. According to Small Gain Theorem, $\gamma_2(\Gamma).\gamma_2^{\mathcal{D}}(\Phi) < 1$ guarantees that the loop is $\mathcal{L}_2$ internally stable and $x \in \mathcal{L}_2$ if $d_1$ and $d_2$ are in $\mathcal{L}_2$. Since $x_0 < \infty$ and $u \in \mathcal{L}_2$, $d_1$ and $d_2$ are in $\mathcal{L}_2$. Consequently, $x \in \mathcal{L}_2$. By the argument used in the proof of Theorem 3.3.1, it is easy to show that $\dot{x} \in \mathcal{L}_\infty$. Having $x \in \mathcal{L}_2 \cap \mathcal{L}_\infty$ and $\dot{x} \in \mathcal{L}_\infty$, Corollary 3.2.1 can be used as the proof of 3.2.1(ii) to show that $x \to 0$ as $t \to \infty$. This shows that $[\Delta, \Upsilon] \in \mathcal{A}_{[\Delta,\Upsilon]}$.

□

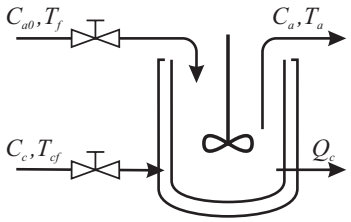


Figure 3.8: A simplified schematic of CSTR system.

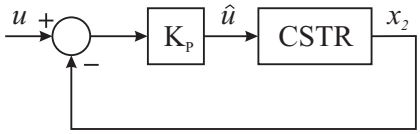


Figure 3.9: The CSTR system controlled by a proportional controller.

**Example 3.3.2.** Consider an example of continuous-stirred tank reactor (CSTR) system shown in Fig. 3.8, where an irreversible, first-order reaction takes place. CSTR is used to convert reactants to products. The reactant is fed constantly into a vessel where a chemical reaction takes place and yields the desired product. The heat generated by the chemical reaction is removed by the coolant medium that is circulated through a jacket. The following mathematical model is taken from [47],

$$\begin{cases} \dot{\hat{x}}_1 = -\hat{x}_1 + D_a(1-\hat{x}_1)e^{\frac{\hat{x}_2}{1+\frac{\hat{x}_2}{\varphi}}} \\ \dot{\hat{x}}_2 = -\hat{x}_2 + B_h D_a(1-\hat{x}_1)e^{\frac{\hat{x}_2}{1+\frac{\hat{x}_2}{\varphi}}} + \beta_h(\hat{u}-\hat{x}_2) \end{cases} \tag{3.26}$$

where $\hat{x}_1$, $\hat{x}_2$, and $\hat{u}_1$ are the dimensionless reagent conversion, the temperature (output), and the coolant temperature (input), respectively. The numerical values for the coefficients are $D_a = 0.072$, $\varphi = 20$, $B_h = 8$, and $\beta_h = 0.3$

Three operating points are considered in [9]. One of them is an unstable point, $\hat{u}_{10} = 0, \hat{x}_{10} = 0.4472$, and $\hat{x}_{20} = 2.7517$. Let transfer the origin of the state plane into this unstable point, which is investigated here. Therefore, we define $x_1 := \hat{x}_1 - \hat{x}_{10}$ and $x_2 = \hat{x}_2 - \hat{x}_{20}$. We study the closed-loop system which is depicted in Fig. 3.9 where $K_P = 100$ is a proportional controller and $u$ is an exogenous input which can be interpreted as sensor noise or disturbance. This controller can stabilize the closed-loop system locally. In this example, we want to determine the corresponding local region.

The state equations for closed-loop system are

$$\begin{cases} \dot{x_1} = -x_1 - 0.4472 + 0.072(0.5528 - x_1)e^{\frac{20x_2+55.034}{22.7517+x_2}} \\ \dot{x_2} = -31.3x_2 - 3.5772 + 0.576(0.5528 - x_1)e^{\frac{20x_2+55.034}{22.7517+x_2}} + 30u \end{cases} \tag{3.27}$$

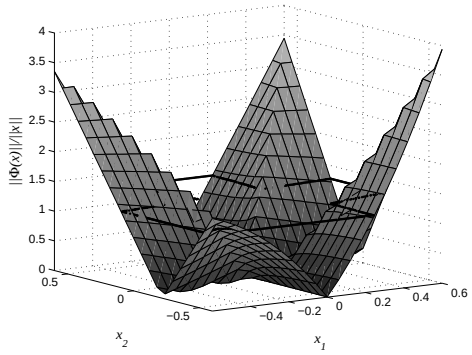


Figure 3.10: $\frac{\|\Phi(x)\|_\infty}{\|x\|_\infty}$ and the boundary of $\mathcal{D}$.

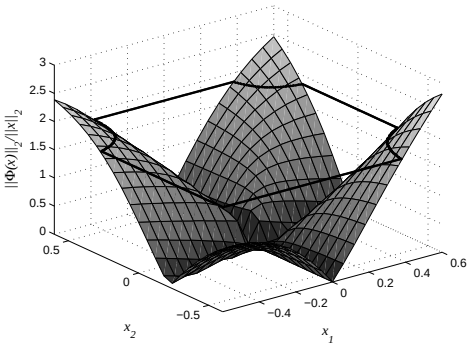


Figure 3.11: $\frac{\|\Phi(x)\|_2}{\|x\|_2}$ and the boundary of $\gamma_2(\Gamma)\gamma_2(\Phi) < 1$.

Let $A = \begin{bmatrix} -1.81 & 0.357 \\ -6.474 & -28.143 \end{bmatrix}$ and $B = \begin{bmatrix} 0 \\ 30 \end{bmatrix}$ then $\Phi(x) = \begin{bmatrix} \Phi_1(x) \\ \Phi_2(x) \end{bmatrix}$ where $\Phi_1(x) = -0.81x_1 - 0.357x_2 - 0.4472 + 0.072(0.5528 - x_1)e^{\frac{20x_2+55.034}{22.7517+x_2}}$ and $\Phi_2(x) = -3.157x_2 + 6.474x_1 - 3.5772 + 0.576(0.5528 - x_1)e^{\frac{20x_2+55.034}{22.7517+x_2}}$. Computation shows that upper bound can not be found for $\gamma_\infty(\Phi)$ and $\gamma_2(\Phi)$. Therefore, global stability can not be proved. For the linear systems, computation with the given methods gives $\gamma_\infty(\Gamma) < 0.5354, \gamma_2(\Gamma) = 0.5423, \gamma_\infty(\Theta) < 1.221$, and $\gamma_\infty(\Omega) = 1$. Let $\eta = 0.1$ and $M_P = 3 > \gamma_\infty(\Omega) + \eta\gamma_\infty(\Theta)$. Since $\Phi$ is independent from $u$, $\hat{\mathcal{D}} \subset \mathbb{R}^2$. For this example, since $\hat{\mathcal{D}}$ is simply connected set, $\hat{\mathcal{D}} = \mathcal{D}$. The surface of $\frac{\|\Phi(x)\|_\infty}{\|x\|_\infty}$ as well as the boundary of $\mathcal{D}$ is depicted in Fig. 3.10. Fig. 3.11 shows $\frac{\|\Phi(x)\|_2}{\|x\|_2}$ and the boundary of $\gamma_2(\Gamma)\gamma_2(\Phi) < 1$. The various subsets of $\mathbb{R}^2$ are depicted in Fig. 3.12. The maximum value for $\epsilon$ is $0.1519$ and consequently the maximum value for $\Delta$ is $0.0402$. According to Theorem 3.3.2, for any input $u$ which satisfies $\|u\|_{\mathcal{L}_\infty} < \eta\delta = 0.004$ and any initial state satisfying $\|x_0\|_\infty < \delta = 0.0402$, $x$ is bounded as $\|x\|_{\mathcal{L}_\infty} < \epsilon = 0.1519$. Besides, in addition to the mentioned condition, if $u \in \mathcal{L}_2$ and $u \to 0$ as $t \to \infty$ then $x \to 0$ as $t \to \infty$, according to Theorem 3.3.3.

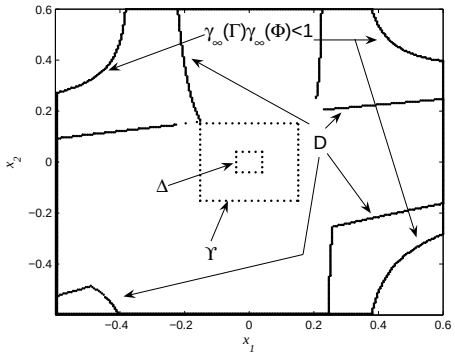


Figure 3.12: Various sets in Example 3.3.2.

## 3.4 Chapter Summary

In this chapter, we have considered stability of nonlinear systems. Our results are applicable to a variety of nonlinear systems. The suggested method of checking stability of nonlinear systems has significant computational advantage compared to previous work, in the sense that there is no need to find any Lyapunov-like function. Initial insight for our formulation was provided by a new representation for nonlinear systems, which transforms a nonlinear system, with non-zero initial state, into a feedback interconnection of two operators. Then, some well-known concepts from input-output theory were used to derive sufficient conditions for stability of the original nonlinear system. Finally, local stability of nonlinear systems was studied with a new definition of region of attraction. Since the new representation is not unique for a nonlinear system, all suggested methods can be optimized based on the selected parameters in the representation. This optimization will be the subject of future work.

# Chapter 4

# Upper bounds

## 4.1 Introduction

The complex structure of nonlinear systems is the major obstacle in the development of simple and efficient computational methods to test stability, compute system norms, etc. As a consequence, a majority of the computational techniques available in the literature are restricted to a narrow class of nonlinear systems for which a particular function, e.g. Lyapunov function or storage function, can be found by trial and error [27], [24].

In this chapter, we consider the problem of computing the $\mathcal{L}_p$ operator norm of a nonlinear system, a problem which has remained a challenge in the systems literature. The importance of this problem originates from the fact that the influence of various inputs on various signals inside the system can be quantified by such a measure. One of the applications of this measure is in control systems, where the attenuation of disturbance signals is required. The subject has attracted considerable attention for both linear and nonlinear systems. For linear systems, computing the $\mathcal{L}_p$ norm(s) has a well established solution; see, for example, reference [2]. For nonlinear systems, however, computation of the $\mathcal{L}_p$ operator norm continues to be a challenge. In [6], the $\mathcal{L}_\infty$-gain of nonlinear systems is characterized by means of the value function of an associated variational problem. The $\mathcal{L}_2$ gain, also referred to as the $\mathcal{H}_\infty$ gain of a nonlinear system, can be approximated using storage functions and the theory of dissipative systems [48]. This approach is, however, conservative and finding storage functions is difficult; see also [20] for a numerical approximation of the $\mathcal{H}_\infty$ norm. In [31], a computational method is proposed to compute the $\mathcal{L}_2$ induced norm for single-input linear systems with saturation.

In this chapter, we propose a method to compute an upper bound on the $\mathcal{L}_1$, $\mathcal{L}_2$ and $\mathcal{L}_\infty$ norms of a class of continuous-time nonlinear systems. Our method can be optimized based on some selected parameters. For systems not included in this class, a method is also

provided for computing an upper bound of the $\mathcal{L}_\infty$ norm.

This chapter is organized as follows: In section 4.1.1, we propose a method to compute upper bounds on the induced norm of nonlinear systems and provide two illustrative examples. In section 4.2, we introduce the weighting method, which can be used to reduce the intrinsic conservativism in the aforementioned method. An example is provided to illustrate the usage of the weighting technique.

### 4.1.1 The proposed method

In this section, we obtain a computable upper bound for induced operator norms. We will use the structure shown in Fig. 2.4(b); namely, the $\zeta_A$ representation for forced system. In this structure, it is trivial to show that

$$\begin{aligned}\|x\|_{\mathcal{L}_p} &\leq \|w\|_{\mathcal{L}_p} + \|d\|_{\mathcal{L}_p} \\ &\leq \gamma_p(\Gamma)\gamma_p(\Phi)\left\|\begin{bmatrix} x \\ u \end{bmatrix}\right\|_{\mathcal{L}_p} + \|d\|_{\mathcal{L}_p} \\ &\leq \gamma_p(\Gamma)\gamma_p(\Phi)\left\|\begin{bmatrix} x \\ u \end{bmatrix}\right\|_{\mathcal{L}_p} + \gamma_p(\Omega)\|x_0\|_p\end{aligned} \tag{4.1}$$

The computation of $\gamma_p(\Gamma)$, $\gamma_p(\Omega)$ and $\gamma_p(\Phi)$ was discussed in Reference [49].

**Lemma 4.1.1.** *The following equation is true for $x, u \in \mathcal{L}_p$:*

$$\left\|\begin{bmatrix} x \\ u \end{bmatrix}\right\|_{\mathcal{L}_p} \leq \|x\|_{\mathcal{L}_p} + \|u\|_{\mathcal{L}_p} \tag{4.2}$$

*Moreover, if $x, u \in \mathcal{L}_2$*

$$\left\|\begin{bmatrix} x \\ u \end{bmatrix}\right\|^2_{\mathcal{L}_2} = \|x\|^2_{\mathcal{L}_2} + \|u\|^2_{\mathcal{L}_2} \quad . \tag{4.3}$$

*Proof.* The proof is trivial and is omitted. □

The first part of this lemma, (4.2), is true for all Banach spaces; however, the second part is true when the temporal norm is $\mathcal{L}_2$ with the Euclidean 2-norm chosen as the corresponding spatial norm.

**Theorem 4.1.1.** *Let $[\Phi, \Gamma, \Omega]$ be a $\zeta_A$ representation for a forced system, $N$. If*

$$\gamma_p(\Gamma)\gamma_p(\Phi) < 1 \tag{4.4}$$

*then*

$$\gamma_p(N) \leq \frac{\gamma_p(\Gamma)\gamma_p(\Phi)}{1 - \gamma_p(\Gamma)\gamma_p(\Phi)}. \tag{4.5}$$

*Proof.* Substituting (4.2) in (4.1) implies that

$$\|x\| \leq \gamma_p(\Gamma)\gamma_p(\Phi)\left(\|x\| + \|u\|\right) + \gamma_p(\Omega)\|x_0\|. \tag{4.6}$$

Thus

$$(1 - \gamma_p(\Gamma)\gamma_p(\Phi))\|x\| \leq \gamma_p(\Gamma)\gamma_p(\Phi)\|u\| + \gamma_p(\Omega)\|x_0\|. \tag{4.7}$$

Since $\gamma_p(\Gamma)\gamma_p(\Phi) < 1$,

$$\|x\| \leq \frac{\gamma_p(\Gamma)\gamma_p(\Phi)}{1 - \gamma_p(\Gamma)\gamma_p(\Phi)}\|u\| + \frac{\gamma_p(\Omega)}{1 - \gamma_p(\Gamma)\gamma_p(\Phi)}\|x_0\| \tag{4.8}$$

which implies (4.5). □

Inequality (4.5) can be used as an upper bound for the $\mathcal{L}_p$ induced norm. It is important to note that since the $\zeta_A$ representation is not unique, the solution of the following minimization problem is the lowest upper bound that can be obtained by our method:

$$\gamma_p(N) \leq \min_A \frac{\gamma_p(\Gamma)\gamma_p(\Phi)}{1 - \gamma_p(\Gamma)\gamma_p(\Phi)} \tag{4.9}$$

where $\Gamma(s) = \left[\begin{array}{c|c} A & I \\ \hline I & 0 \end{array}\right]$ and $\Phi(x,u) = f(x,u) - Ax$. Unfortunately, there is no existing method to find $A$ which provides the lowest upper bound. A good strategy is to define a function in MATLAB with input $A$ and output $\frac{\gamma_p(\Gamma)\gamma_p(\Phi)}{1-\gamma_p(\Gamma)\gamma_p(\Phi)}$ and use *fminsearch* to minimize it.

The method provided by Theorem 4.1.1 is general in the sense of the induced norm, $\gamma_p$. An interesting case occurs when the temporal norm is $\mathcal{L}_2$ with the Euclidean 2-norm chosen as the corresponding spatial norm. The reason is that a quite mature theory, namely; $\mathcal{H}_\infty$ optimization, has been developed for linear systems in this case. Suppose $\Gamma$ is a continuous-time linear time-invariant stable operator with impulse response $g(t) : \mathbb{R}^+ \to \mathbb{R}^{n\times n}$ $(g(t) : \mathbb{Z}^+ \to \mathbb{R}^{n\times n})$. Let $G(s)$ denote the Laplace transform of $g(t)$. We have

$$\gamma_2(\Gamma) := \|G(s)\|_{\mathcal{H}_\infty} \tag{4.10}$$

In this case, the following theorem provides lower upper bounds for the induced norm $\gamma_2$ than Theorem 4.1.1.

**Theorem 4.1.2.** *Let $[\Phi, \Gamma, \Omega]$ be a $\zeta_A$ representation for a forced system, $N$. If $\gamma_2(\Gamma)\gamma_2(\Phi) < 1$ then*

$$\gamma_2(N) \leq \frac{\gamma_2(\Gamma)\gamma_2(\Phi)}{\sqrt{1 - \gamma_2(\Gamma)^2\gamma_2(\Phi)^2}}. \tag{4.11}$$

*Proof.* Inequality (4.1) implies that

$$(\|x\| - \gamma_2(\Omega)\|x_0\|)^2 \leq \left(\gamma_2(\Gamma)\gamma_2(\Phi)\left\|\begin{bmatrix} x \\ u \end{bmatrix}\right\|\right)^2 \tag{4.12a}$$

Using (4.3),

$$\|x\|^2 - 2\gamma_2(\Omega)\|x_0\|\|x\| + \gamma_2(\Omega)^2\|x_0\|^2 \leq \gamma_2(\Gamma)^2\gamma_2(\Phi)^2\left(\|x\|^2 + \|u\|^2\right) \tag{4.12b}$$

For simplicity, let $\alpha := \gamma_2(\Gamma)\gamma_2(\Phi)$

$$\|x\|^2 - \frac{2\gamma_2(\Omega)}{1-\alpha^2}\|x_0\|\|x\| + \frac{\gamma_2(\Omega)^2}{1-\alpha^2}\|x_0\|^2 \leq \frac{\alpha^2}{1-\alpha^2}\|u\|^2. \tag{4.12c}$$

Hence

$$\left(\|x\| - \frac{\gamma_2(\Omega)}{1-\alpha^2}\|x_0\|\right)^2 \leq \frac{\alpha^2\gamma_2(\Omega)^2}{(1-\alpha^2)^2}\|x_0\|^2 + \frac{\alpha^2}{1-\alpha^2}\|u\|^2. \tag{4.12d}$$

Since $a^2 + b^2 \leq (a+b)^2$ for all $a, b \geq 0$, we have

$$\|x\| - \frac{\gamma_2(\Omega)}{1-\alpha^2}\|x_0\| \leq \frac{\alpha\gamma_2(\Omega)}{(1-\alpha^2)}\|x_0\| + \frac{\alpha}{\sqrt{1-\alpha^2}}\|u\| \tag{4.12e}$$

Consequently

$$\|x\| \leq \frac{\gamma_2(\Gamma)\gamma_2(\Phi)}{\sqrt{1-\gamma_2(\Gamma)^2\gamma_2(\Phi)^2}}\|u\| + \frac{\gamma_2(\Omega)}{1-\gamma_2(\Gamma)\gamma_2(\Phi)}\|x_0\| \tag{4.12f}$$

which implies (4.11). □

Similarly, the solution of the following minimization problem is the lowest upper bound that can be obtained by our method:

$$\gamma_2(N) \leq \min_A \frac{\gamma_2(\Gamma)\gamma_2(\Phi)}{\sqrt{1-\gamma_2(\Gamma)^2\gamma_2(\Phi)^2}} \tag{4.13}$$

where $\Gamma(s) = \left[\begin{array}{c|c} A & I \\ \hline I & 0 \end{array}\right]$ and $\Phi(x,u) = f(x,u) - Ax$. Equivalently,

$$\gamma_2(N) \leq \min_A \frac{1}{\sqrt{\left\|(sI-A)^{-1}\right\|_{\mathcal{H}_\infty}^{-2} \gamma_2^{-2}(f(x,u)-Ax) - 1}}. \tag{4.14}$$

**Example 4.1.1.** (*RLC circuit with non-ideal inductor*) The network of Fig. 4.1 represents a RLC circuit with a non-ideal inductor. The inductor has nonzero resistance and saturation characteristic as shown in Fig. 4.2(a), where $\lambda$ is the flux linkage. The relationship of the magnetic flux linkage to terminal voltage of an inductor is given by Faraday's law; namely $v_L(t) = d\lambda(t)/dt$. The state equations for this network may be written as

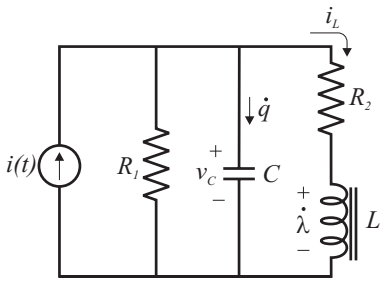


Figure 4.1: RLC circuit in Example 4.1.1.

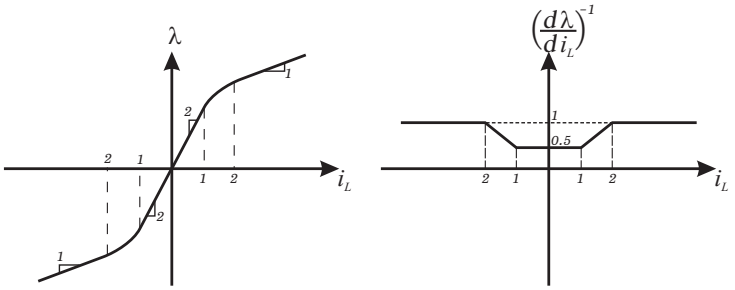


Figure 4.2: The characteristic of the inductance in Example 4.1.1.

$$v_L = \dot{\lambda} = \frac{d\lambda}{di_L}\frac{di_L}{dt} \tag{4.15a}$$

$$\frac{di_L}{dt} = \left(\frac{d\lambda}{di_L}\right)^{-1}(v_C - R_2 i_L) \tag{4.15b}$$

where $\left(\frac{d\lambda}{di_L}\right)^{-1}$ is depicted in Fig. 4.2(b) versus $i_L$, and

$$C\frac{dV_C}{dt} = i - \frac{V_C}{R_1} - i_L. \tag{4.15c}$$

Defining $x_1 := i_L$, $x_2 := v_C$ and $u := i$,

$$\begin{cases} \dot{x}_1 &= (x_2 - R_2 x_1)\left(\frac{d\lambda}{dx_1}\right)^{-1} \\ \dot{x}_2 &= \frac{u}{C} - \frac{x_2}{R_1 C} - \frac{x_1}{C} \end{cases}. \tag{4.15d}$$

Let $R_1 = \frac{1}{2}$, $R_2 = 1$ and $C = 2$. Assuming $A = \begin{bmatrix} -1 & 0.5 \\ -0.5 & -1 \end{bmatrix}$, we have

$$\Phi(x_1, x_2, u) = \begin{bmatrix} x_1 - 0.5\, x_2 + (x_2 - x_1)\left(\frac{d\lambda}{dx_1}\right)^{-1} \\ \frac{u}{C} \end{bmatrix}. \tag{4.15e}$$

We use the computational methods that has been introduced in [49]. Since there are three independent variables in $\gamma_p(\Phi)$, i.e. $x_1$, $x_2$ and $u$, we plot $\frac{\|\Phi(x,u)\|}{\left\|\begin{bmatrix} x \\ u \end{bmatrix}\right\|}$ versus $\left\|\begin{bmatrix} x \\ u \end{bmatrix}\right\|$ instead of

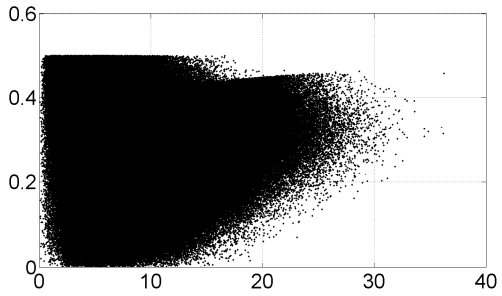


(a) $p = 1$

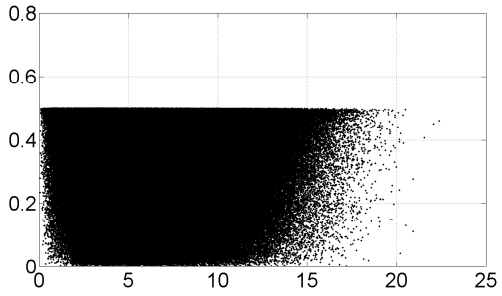


(b) $p = 2$

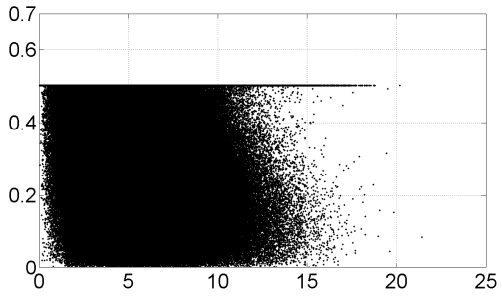


(c) $p = \infty$

Figure 4.3: Gain of $\|\Phi(x,u)\|_p$ versus $\left\|\begin{bmatrix} x \\ u \end{bmatrix}\right\|_p$ in Example 4.1.1.

plotting versus $x_1$, $x_2$ and $u$, as shown in Fig. 4.3. Therefore, $\gamma_1(\Phi) \approx 0.50$, $\gamma_2(\Phi) \approx 0.50$ and $\gamma_\infty(\Phi) \approx 0.50$. Computation also shows that $\gamma_1(\Gamma) \approx 1.237$, $\gamma_2(\Gamma) \approx 1.00$ and $\gamma_\infty(\Gamma) \approx 1.237$. Theorems 4.1.1 and 4.1.2 imply that $\gamma_1(N) \leq 1.62$, $\gamma_2(N) \leq 0.577$ and $\gamma_\infty(N) \leq 1.62$, respectively.

There is no doubt that the condition $\gamma_p(\Gamma)\gamma_p(\Phi) < 1$ in Theorems 4.1.1 and 4.1.2 is restrictive. For example, polynomial systems are excluded by the aforementioned condition. The following theorem might be used to overcome this shortcoming. The result provides an upper bound on system output for bounded input and initial state.

**Theorem 4.1.3.** *Let $[\Phi, \Theta, \Gamma, \Omega]$ be a $\zeta_{AB}$ representation for a nonlinear system. Let $\eta > 0$ and $M_p > \gamma_\infty(\Omega) + \eta\gamma_\infty(\theta)$ and*

$$\hat{\mathcal{D}} := \left\{ \begin{bmatrix} x \\ u \end{bmatrix} \in \mathbb{R}^{n+m} \;\middle|\; \gamma_\infty^{\hat{\mathcal{D}}}(\Phi) < \frac{M_p - \gamma_\infty(\Omega) - \eta\gamma_\infty(\theta)}{(M_p + \eta)\gamma_\infty(\Gamma)} \right\}. \tag{4.16}$$

*Let $\mathcal{D} := \mathbf{B}^\infty(0, r_D)$ be an open ball inside $\hat{\mathcal{D}}$. Assume that $\mathcal{D}_x$ and $\mathcal{D}_u$ are the images of $\mathcal{D}$ under $\left[\begin{array}{c|c} I_{n\times n} & 0_{n\times m} \\ \hline 0_{m\times n} & 0_{m\times m} \end{array}\right]$ and $\left[\begin{array}{c|c} 0_{n\times n} & 0_{n\times m} \\ \hline 0_{m\times n} & I_{m\times m} \end{array}\right]$, respectively. Therefore, $\mathcal{D}_x$ and $\mathcal{D}_u$ are also open balls in $\mathbb{R}^n$ and $\mathbb{R}^m$ respectively. Let $r_x$ and $r_u$ denote respectively their radius, i.e. $\mathcal{D}_x = \mathbf{B}^\infty(0, r_x)$ and $\mathcal{D}_u = \mathbf{B}^\infty(0, r_u)$. Choose $\epsilon$ and $\delta$ such that $0 < \epsilon < r_x$ and*

$$0 < \delta \leq \frac{1 - \gamma_\infty^{\mathcal{D}}(\Phi)\gamma_\infty(\Gamma)}{\gamma_\infty(\Omega) + \eta(\gamma_\infty(\Theta) + \gamma_\infty^{\mathcal{D}}(\Phi)\gamma_\infty(\Gamma))}\,\epsilon$$

*If $\|u\|_{\mathcal{L}_\infty} < \min(\eta\,\delta, r_u)$ and $\|x_0\|_\infty \leq \delta$, then*

$$\|x\|_{\mathcal{L}_\infty} < \epsilon. \tag{4.17}$$

*Proof.* It is trivial that $M_p - \gamma_\infty(\Omega) - \eta\gamma_\infty(\theta) < M_p + \eta$; therefore $\gamma_\infty^{\mathcal{D}}(\Phi)\gamma_\infty(\Gamma) < 1$. We use contradiction to prove the theorem. Since we have assumed that systems of interest are locally Lipschitz, system trajectories are continuous. Consequently, if $x$ were to leave the ball with radius $\epsilon$, it should cross the boundary of the ball. Suppose that $x$ crosses the boundary at $t = \tau$. As a result, $\|\mathbf{T}_\tau x\| = \|x\|_\tau = \epsilon$. Since $\epsilon < r_x$ and $\|u\| < \min(\eta\,\delta, r_u)$ guarantees that $u \in \mathcal{D}_u$, we have $\begin{bmatrix} x_\tau \\ u_\tau \end{bmatrix} \in \mathcal{D}$ and consequently

$$\begin{aligned}
\|x_\tau\| &\leq \|d_{1\tau}\| + \|w_\tau\| \\
&\leq \|d_{1\tau}\| + \gamma_\infty^{\mathcal{D}}(\Phi)\gamma_\infty(\Gamma)(\|d_{2\tau}\| + \|x_\tau\|) \\
&\leq \gamma_\infty(\Theta)\|u_\tau\| + \gamma_\infty(\Omega)\|x_0\| \\
&\quad + \gamma_\infty^{\mathcal{D}}(\Phi)\gamma_\infty(\Gamma)\|x_\tau\| + \gamma_\infty^{\mathcal{D}}(\Phi)\gamma_\infty(\Gamma)\|u_\tau\| \\
&\leq \gamma_\infty(\Omega)\|x_0\| + [\gamma_\infty(\Theta) + \gamma_\infty^{\mathcal{D}}(\Phi)\gamma_\infty(\Gamma)]\|u_\tau\| \\
&\quad + \gamma_\infty^{\mathcal{D}}(\Phi)\gamma_\infty(\Gamma)\|x_\tau\| \\
&< \gamma_\infty(\Omega)\delta + \left[\gamma_\infty(\Theta) + \gamma_\infty^{\mathcal{D}}(\Phi)\gamma_\infty(\Gamma)\right]\eta\delta \\
&\quad + \gamma_\infty^{\mathcal{D}}(\Phi)\gamma_\infty(\Gamma)\|x_\tau\| \\
&= \left(\gamma_\infty(\Omega) + \eta\left[\gamma_\infty(\Theta) + \gamma_\infty^{\mathcal{D}}(\Phi)\gamma_\infty(\Gamma)\right]\right)\delta \\
&\quad + \gamma_\infty^{\mathcal{D}}(\Phi)\gamma_\infty(\Gamma)\|x_\tau\|
\end{aligned} \tag{4.18}$$

Then

$$\begin{aligned}\epsilon &= \|x_\tau\| \\ &< \frac{\gamma_\infty(\Omega)+\eta\left[\gamma_\infty(\Theta)+\gamma_\infty^{\mathcal{D}}(\Phi)\gamma_\infty(\Gamma)\right]}{1-\gamma_\infty^{\mathcal{D}}(\Phi)\gamma_\infty(\Gamma)}\|x_0\| \\ &\leq \frac{\gamma_\infty(\Omega)+\eta\left[\gamma_\infty(\Theta)+\gamma_\infty^{\mathcal{D}}(\Phi)\gamma_\infty(\Gamma)\right]}{1-\gamma_\infty^{\mathcal{D}}(\Phi)\gamma_\infty(\Gamma)}\,\delta \\ &\leq \epsilon \end{aligned} \tag{4.19}$$

Which is a contradiction. Therefore, $x(t) < \epsilon;\ \forall t \geq 0$, i.e. $\|x\| < r_x$. □

**Example 4.1.2.** Consider a multi-tank system depicted in Fig. 4.4. Suppose that a proportional controller is utilized to adjust the fluid level in the second tank $H_2$ by input flow $q$. The problem of interest is to find an upper bound on the gain of the closed loop system shown in Fig. 4.5. The following mathematical model is taken from [19]:

$$\begin{cases} \frac{dH_1}{dt} = \frac{1}{aw}\left(q - C_1 H_1^{\alpha_1}\right) \\ \frac{dH_2}{dt} = \frac{1}{cw+\frac{H_2}{H_{2max}}bw}\left(C_1 H_1^{\alpha_1} - C_2 H_2^{\alpha_2}\right) \end{cases} \tag{4.20}$$

The transfer function of the controller is $K(s) = K_P$. Let $x_1 := H_1 - H_{10}$, $x_2 := H_2 - H_{20}$ and $q = q_0 - K_P(x_2 + u)$ where $H_{10}$ and $H_{20}$ are operating points and $q_0$ is the corresponding input. It is trivial that $q_0 = C_1 H_{10}^{\alpha_1} = C_2 H_{20}^{\alpha_2}$. The numerical values for the coefficients are $a = 0.25$, $w = 0.035$, $H_{2max} = 0.35$, $b = 0.345$, $c = 0.1$, $C_1 = 5.66 \times 10^{-5}$, $C_2 = 5.58 \times 10^{-5}$, $\alpha_1 = 0.29$ and $\alpha_2 = 0.226$ [19]. Suppose $K_P = 10^{-5}$. The state equations for the closed-loop system are

$$\begin{cases} \dot{x}_1 = \frac{1}{aw}\left(q_0 - K_P(x_2+u) - C_1(x_1+H_{10})^{\alpha_1}\right) \\ \dot{x}_2 = \frac{1}{cw+\frac{x_2+H_{20}}{H_{2max}}bw}\left(C_1(x_1+H_{10})^{\alpha_1} - C_2(x_2+H_{20})^{\alpha_2}\right) \end{cases} \tag{4.21}$$

and $\dot{x} = \begin{pmatrix} \dot{x}_1 \\ \dot{x}_2 \end{pmatrix} = f(x,u)$. Let

$$A = \begin{pmatrix} -0.0072 & -0.0114 \\ 0.0094 & -0.0118 \end{pmatrix}, \quad B = \begin{pmatrix} -0.0114 \\ 0 \end{pmatrix}, \tag{4.22}$$

which are linearized parts of $f(x,u)$ at $x = 0$ and $u = 0$, i.e. $A = \left.\frac{\partial f(x,u)}{\partial x}\right|_{x,u=0}$ and $B = \left.\frac{\partial f(x,u)}{\partial u}\right|_{x,u=0}$. Therefore,

$$\Phi(x,u) = \begin{bmatrix} 0.00373 + 0.0072x_1 - 0.00647(x_1+0.15)^{0.29} \\ \frac{5.66\times10^{-5}(x_1+0.15)^{0.29} - 5.58\times10^{-5}(x_2+0.0934)^{0.226}}{0.0067+0.0345x_2} - 0.0094x_1 + 0.01176x_2 \end{bmatrix}. \tag{4.23}$$

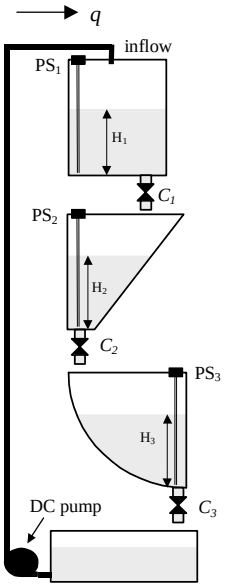


Figure 4.4: Configuration of the multitank system [19].

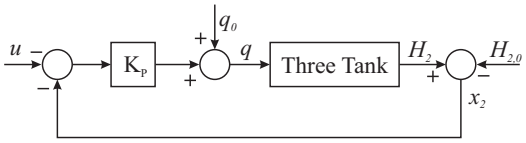


Figure 4.5: Closed loop multitank system.

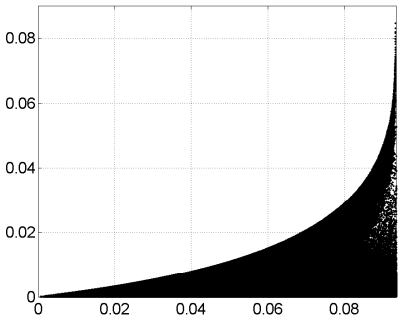


Figure 4.6: $\frac{\|\Phi(x)\|_\infty}{\|x\|_\infty}$ versus $\|x\|_\infty$.

Computation with the methods proposed in [50] provides $\gamma_\infty(\Gamma) < 151.3$, $\gamma_\infty(\Theta) < 0.9756$, and $\gamma_\infty(\Omega) = 1.036$. Let $\eta = 3.0382$ which gives $M_P = 4 > \gamma_\infty(\Omega) + \eta\gamma_\infty(\Theta)$. Since $\Phi$ is independent from $u$, $\hat{\mathcal{D}} \subset \mathbb{R}^2$. $\frac{\|\Phi(x)\|_\infty}{\|x\|_\infty}$ versus $\|x\|_\infty$ is depicted in Fig. 4.6. Since $\hat{\mathcal{D}}$ is independent of $u$, $r_u = \infty$. Let us take $\hat{\mathcal{D}}$ as the region where $\frac{\|\Phi(x)\|_\infty}{\|x\|_\infty} < 0.0023$, i.e. $\gamma_\infty^{\mathcal{D}}(\Phi) = 0.0023$. Consequently $r_x = 0.0155$. Let $\epsilon = 0.015$ and $\delta = 0.0019 \leq \frac{1-\gamma_\infty^{\mathcal{D}}(\Phi)\gamma_\infty(\Gamma)}{\gamma_\infty(\Omega)+\eta(\gamma_\infty(\Theta)+\gamma_\infty^{\mathcal{D}}(\Phi)\gamma_\infty(\Gamma))}\epsilon$. According to Theorem 4.1.3, for any input $u$ which satisfies $\|u\|_{\mathcal{L}_\infty} < \min(\eta\delta, r_u) = 0.00587$ and any initial state satisfying $\|x_0\|_\infty < \delta = 0.0019$, $x$ is bounded as $\|x\|_{\mathcal{L}_\infty} < \epsilon = 0.015$.

## 4.2 Weighting Technique

As shown in the previous section, the proposed methods are based on the $\zeta_A$ representation. Adding some weighting on state or input vectors may tighten the calculated bounds. However, there is no general rule which provides useful weighting matrices; therefore, they should be chosen by trial and error. In this section, we study the effect of the weighting and we show the effectiveness by an example.

In the $\zeta_A$ representation for continuous-time systems shown in Fig. 2.3, let $\hat{x} := W_x x$ where $W_x$ is nonsingular. Consequently,

$$\dot{\hat{x}} = W_x A W_x^{-1}\hat{x} + W_x\Phi(W_x^{-1}\hat{x}) \tag{4.24}$$

Denoting $\hat{A} := W_x A W_x^{-1}$, $\hat{\Phi}(x) := W_x\Phi(W_x^{-1}x)$, $\hat{\Gamma} := \left[\begin{array}{c|c} \hat{A} & I \\ \hline I & 0 \end{array}\right]$ and $\Omega(x(t)) := e^{\hat{A}t}x_0$, it is easy to show that ordered operator set $[\hat{\Phi}, \hat{\Gamma}, \hat{\Omega}]$ is a $\zeta_A$ representation for the weighted system, i.e. the system with initial state $\hat{x}_0 := W_x x_0$ and state $\hat{x}$.

Similarly, in the $\zeta_{AB}$ representation shown in Fig. 2.4(a) for continuous-time systems,

let $\hat{x} := W_x x$ and $\hat{u} := W_u u$ where $W_x$ and $W_u$ are nonsingular. Consequently,

$$\dot{\hat{x}} = W_x A W_x^{-1}\hat{x} + W_x B W_u^{-1}\hat{u} + W_x \Phi(W_x^{-1}\hat{x}, W_u^{-1}\hat{u}) \tag{4.25}$$

Denoting $\hat{A} := W_x A W_x^{-1}$, $\hat{B} := W_x B W_u^{-1}$, $\hat{\Phi}(x,u) := W_x \Phi(W_x^{-1}x, W_u^{-1}u)$, $\hat{\Gamma} := \left[\begin{array}{c|c} \hat{A} & I \\ \hline I & 0 \end{array}\right]$, $\hat{\Theta} := \left[\begin{array}{c|c} \hat{A} & \hat{B} \\ \hline I & 0 \end{array}\right]$ and $\Omega(x(t)) := e^{\hat{A}t}x_0$, it is trivial to show that ordered operator set $[\hat{\Phi}, \hat{\Gamma}, \hat{\Theta}, \hat{\Omega}]$ is a $\zeta_{AB}$ representation for the weighted system, i.e. the system with input $\hat{u}$, state $\hat{x}$ and initial state $\hat{x}_0$. A very similar argument can be made for forced system with $\zeta_A$ representation.

It is important to note that the mapping $\hat{u} \to \hat{x}$ is different than $u \to x$. However, Theorems 4.1.1, 4.1.2 and 4.1.3 can be used to find corresponding upper bounds for the weighted system. Then, using the definitions of $\hat{x}$, $\hat{u}$ and $\hat{x}_0$, the corresponding bounds can be found for the main system. Suppose that the inequality found for the weighted system is $\|\hat{x}\|_p \leq \gamma_{p,u} \|\hat{u}\|_p + \gamma_{p,x_0} \|\hat{x}_0\|_p$ where $\gamma_{p,u}$ and $\gamma_{p,x_0}$ are derived by either (4.8) or (4.12f). Therefore,

$$\begin{aligned} \|x\| &\leq \left\|W_x^{-1}\right\| \|\hat{x}\| \\ &\leq \left\|W_x^{-1}\right\| \gamma_u \|\hat{u}\| + \left\|W_x^{-1}\right\| \gamma_{x_0} \|\hat{x}_0\| \\ &\leq \left\|W_x^{-1}\right\| \gamma_u \|W_u\| \|u\| + \left\|W_x^{-1}\right\| \gamma_{x_0} \|W_x\| \|x_0\| . \end{aligned} \tag{4.26}$$

It is important to note that norms used for $\left\|W_x^{-1}\right\|$ and $\|W_u\|$ are the corresponding induced norms. Similarly, if an upper bound obtained for the weighted system is $\gamma(\hat{N})$ then

$$\gamma(N) \leq \left\|W_x^{-1}\right\| \gamma(\hat{N}) \|W_u\| . \tag{4.27}$$

There is no method to compute $\left\|W_x^{-1}\right\|$ and $\|W_u\|$ in general. However, in some special cases, such as the case where 2-norm is used for the spatial norm or the case where weighting matrices are multiplication of a scalar by the identity matrix, $\left\|W_x^{-1}\right\|$ and $\|W_u\|$ can be calculated. The following example illustrates the usage and effectiveness of the weighting technique.

**Example 4.2.1.** Consider the following nonlinear system

$$N : \begin{cases} \dot{x}_1 = -x_1 + x_2 + 0.5\text{sat}\,(x_2) - 0.25\sin(x_1) + 0.25\text{sat}\,(u) \\ \dot{x}_2 = -x_1 - x_2 + 0.5\text{sat}\,(x_1) - 0.25\sin(x_2) - 0.25u \end{cases} \tag{4.28}$$

where sat $(\cdot)$ is depicted in Fig. 4.7. Let $A = \begin{bmatrix} -0.9 & 0.9 \\ -0.9 & -1.1 \end{bmatrix}$. Hence,

$$\Phi(x_1, x_2, u) = \begin{bmatrix} -0.1x_1 + 0.1x_2 + 0.5\,\text{sat}\,(x_2) - 0.25\,\sin(x_1) + 0.25\,\text{sat}\,(u) \\ -0.1x_1 + 0.1x_2 + 0.5\text{sat}\,(x_1) - 0.25\sin(x_2) - 0.25u \end{bmatrix}. \tag{4.29}$$

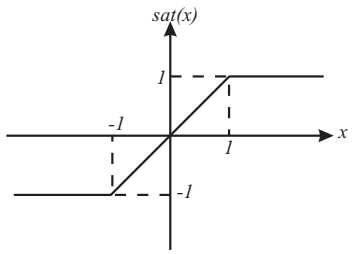


Figure 4.7: The saturation function sat $(\cdot)$.

Table 4.1: Derived bounds with various $W_u$ (Example 4.2.1).

| $W_u$ | $\gamma_1(\hat{N})$ | $\gamma_2(\hat{N})$ | $\gamma_\infty(\hat{N})$ | $\gamma_1(N)$ | $\gamma_2(N)$ | $\gamma_\infty(N)$ |
|---|---|---|---|---|---|---|
| 1.75 | 1.361 | 0.580 | 3.029 | 2.382 | 1.015 | 5.301 |
| 1 | 1.66 | 0.71 | 5.95 | 1.66 | 0.71 | 5.95 |
| 2 | 1.290 | 0.575 | 2.30 | 2.58 | 1.15 | 4.6 |
| minimum | | | | 1.66 | 0.71 | 4.6 |

Let $W_u = 1.75$ and $W_x = I_{2\times 2}$. Therefore, $\left\|W_x^{-1}\right\| = 1$ and $\|W_u\| = 1.75$. As shown in Fig. 4.8, we plot $\frac{\left\|\hat{\Phi}(\hat{x},\hat{u})\right\|}{\left\|\begin{bmatrix}\hat{x}\\ \hat{u}\end{bmatrix}\right\|}$ versus $\left\|\begin{bmatrix}\hat{x}\\ \hat{u}\end{bmatrix}\right\|$ instead of plotting versus $\hat{x}_1$, $\hat{x}_2$ and $\hat{u}$. Therefore, $\gamma_1(\hat{\Phi}) \approx 0.46$, $\gamma_2(\hat{\Phi}) \approx 0.5$ and $\gamma_\infty(\hat{\Phi}) \approx 0.6$. Computation also shows that $\gamma_1(\hat{\Gamma}) \approx 1.253$, $\gamma_2(\hat{\Gamma}) \approx 1.003$ and $\gamma_\infty(\hat{\Gamma}) \approx 1.253$. Therefore, $\gamma_1(\hat{N}) \leq 1.361$, $\gamma_2(\hat{N}) \leq 0.58$ and $\gamma_\infty(\hat{N}) \leq 3.029$. Using (4.27), $\gamma_1(N) \leq 2.382$, $\gamma_2(N) \leq 1.015$ and $\gamma_\infty(N) \leq 5.301$. The results obtained for various values of $W_u$ are summarized in Table 4.1. As can be seen, tighter bounds can be found by trying different values for the weighting matrices.

## 4.3 Chapter Summary

This chapter offers a contribution to the calculation of upper bounds on the $\mathcal{L}_1$, $\mathcal{L}_2$ and $\mathcal{L}_\infty$ induced operator norms of continuous-time nonlinear systems. Based on the $\zeta_A$ representation of nonlinear systems, methods are presented to compute the aforementioned bounds.

The main limitation of the proposed methods is inequality (4.4) that restricts the usage of the method for a class of the nonlinear systems and the freedom on choosing the parameter $A$. To lessen the restrictions encountered in the computation of the $\mathcal{L}_\infty$ norm of a system, a method is given to compute an upper bound on the $\mathcal{L}_\infty$ norm of the system output with respect to $\mathcal{L}_\infty$ norm of the input. This method does not suffer from the previous limitations. In the last section, our methods are improved by the use of a weighting technique on the $\zeta_A$ representation. An example is provided to show the effectiveness of the weighting technique.

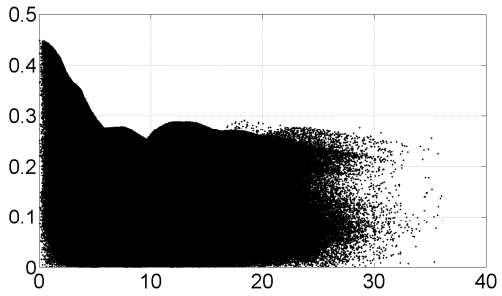


(a) $p = 1$

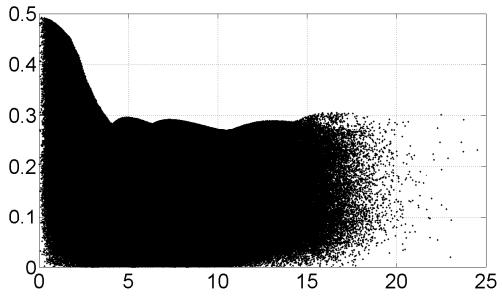


(b) $p = 2$

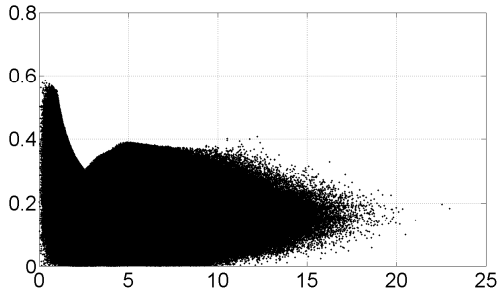


(c) $p = \infty$

Figure 4.8: Gain of $\left\|\hat{\Phi}(\hat{x},\hat{u})\right\|_p$ versus $\left\|\begin{bmatrix}\hat{x}\\ \hat{u}\end{bmatrix}\right\|_p$ in Example 4.2.1 for $W_u = 1.75$.

# Chapter 5

# The Gap Metric

## 5.1 Introduction

Model uncertainty often has a significant effect on stability and performance of feedback control systems. For linear time-invariant (LTI) systems, much work has been done to study this effect. One important concept used to measure system uncertainty is the gap metric which was introduced to systems and control theory by Zames and El-Sakkary [55]. For LTI systems, it has been shown that a perturbed system can be stabilized by any controller which is designed for the nominal system if and only if the distance between the perturbed system and the nominal system is small in the gap metric. The computation of the gap metric for LTI systems was developed by Georgiou [12].

The extension of the gap metric to larger classes of systems was initiated in [10], where the metric was extended to time-varying linear plants. Later, the parallel projection operator for nonlinear systems [5] and its relationship to the differential stabilizability of nonlinear feedback systems [11] paved the road to the extension of the gap metric to a pseudo-metric on nonlinear operators [13].

Unlike the LTI system case, there is no generally applicable method of computing the gap metric for nonlinear systems. In fact, there are only a few examples in literature for the computation of the gap metric. Moreover, those methods are highly dependent upon the case of interest. This is also the case for the corresponding stability margin which can be used to determine the ball of uncertainty in the sense of the gap metric.

This chapter deals with the computation of the gap metric and stability margin for nonlinear systems. We will consider the extension of the gap metric to nonlinear systems given in [13]. We derive upper bounds on the gap metric and the stability margin with respect to the operator norm (gain) of the plant, perturbed system and controller and based on the results of Chapter 4 on the upper bound of the gain of nonlinear systems. The suggested

methods are only applicable to a class of nonlinear systems which satisfy an inequality.

The chapter is organized as follows: In Section 5.2, first, we introduce the notation. Then, the gap metric for the nonlinear systems is introduced. The main contribution of this paper is contained in Section 5.3 where Theorems 5.3.1 and 5.3.2 are stated and proved. These theorems provide upper bounds on the gap metric and the stability margin, respectively. In Section 5.3, an example is also solved to illustrate the effectiveness of the results and comparison between the direct computation and the suggested methods. Since the literature suffers from the lack of widely-applicable computation methods and there are just a few examples which are highly dependent to the studied systems, it is indeed hard to construct example which both satisfies our required condition and is compatible by the previously suggested methods such as the method used in [13].

## 5.2 Background

### 5.2.1 Notation

Let $\mathcal{U} := \mathcal{L}$ and $\mathcal{Y} := \mathcal{L}$ denote input and output signal spaces, respectively. A nonlinear time-varying system can be thought of as a possibly unbounded operator $H : \mathcal{D}_h \rightarrow \mathcal{Y}$ where $\mathcal{D}_h \subseteq \mathcal{U}$. The action of $H$ on any $u \in \mathcal{D}_h$ is denoted by $Hu$. A system $H$ is called *stable* if $\mathcal{D}_h = \mathcal{U}$. For an operator $H : \mathcal{U} \rightarrow \mathcal{Y}$ , let $\gamma(H)$ stand for the induced norm (gain) of the operator defined as

$$\gamma(H) := \sup_{\substack{u \in \mathcal{U} \\ u \neq 0}} \frac{\|Hu\|_T}{\|u\|_T} \tag{5.1}$$

where the supremum is taken over all $u \in \mathcal{U}$ and all $T$ in $\mathbb{R}^+$ for which $u_T \neq 0$. Let $\gamma_p(H)$ stand for $\gamma(H)$ in $\mathcal{L}_p$. A system $H$ is called *finite gain stable (fg-stable)* if $H0 = 0$ and $\gamma(H) < \infty$.

### 5.2.2 The Gap Metric

Let $[P, C]$ denote the feedback configuration shown in Figure 5.1. This configuration is standard in literature, e.g. [13] and can be described by the following equations.

$$\begin{aligned} y_1 &= Pu_1 \\ u_2 &= Cy_2 \\ u_0 &= u_1 + u_2 \\ y_0 &= y_1 + y_2 \end{aligned} \tag{5.2}$$

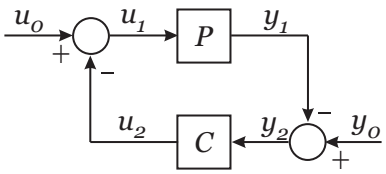


Figure 5.1: The standard feedback configuration, $[P, C]$.

where $P$ and $C$ denote the nominal plant and the controller and $u_0$ and $y_0$ are the input and measurement disturbances, respectively. Let $u_i \in \mathcal{U}$, $y_i \in \mathcal{Y}$ and $w_i := \begin{bmatrix} u_i \\ y_i \end{bmatrix}$ for $i \in \{0, 1, 2\}$ and $\mathcal{W} := \mathcal{U} \times \mathcal{Y}$. We assume that the product of the instantaneous gains of $P$ and $C$ is less than one. This assumption guarantees the well-posedness of the feedback configuration, e.g. [13] [1]. Similar to [13], we assume that the feedback configuration is always well-posed. The closed-loop operator is defined as

$$H_{P,C} : \mathcal{W} \to \mathcal{W} \times \mathcal{W}\,,\ H_{P,C} : w_0 \mapsto (w_1, w_2). \tag{5.3}$$

The graph of the plant is

$$\mathcal{G}_P = \left\{ \begin{pmatrix} u \\ Pu \end{pmatrix} \,:\, u \in \mathcal{U},\, Pu \in \mathcal{Y} \right\} \subset \mathcal{W}. \tag{5.4}$$

If the domain of $P$ is $U$, the condition $Pu \in \mathcal{Y}$ is unnecessary. To have compatible notation with [13], we define the graph of $C$ as follows

$$\mathcal{G}_C = \left\{ \begin{pmatrix} Cy \\ y \end{pmatrix} \,:\, Cy \in \mathcal{U},\, y \in \mathcal{Y} \right\} \subset \mathcal{W}. \tag{5.5}$$

In some literature, e.g [5], this graph is also called inverse graph. Let

$$\mathcal{M} := \mathcal{G}_P\,,\ \mathcal{N} := \mathcal{G}_C. \tag{5.6}$$

The following operators are useful in the study of the closed-loop system stability.

$$\Pi_{\mathcal{M}||\mathcal{N}} := \Pi_1 H_{P,C}\,,\ \Pi_{\mathcal{N}||\mathcal{M}} := \Pi_2 H_{P,C} \tag{5.7}$$

where $\Pi_i : \mathcal{W} \times \mathcal{W} \to \mathcal{W}$ denote the natural projection onto the $i$th component $(i \in \{1, 2\})$ of $\mathcal{W} \times \mathcal{W}$. Therefore

$$\begin{aligned} \Pi_{\mathcal{M}||\mathcal{N}} &\,:\, w_0 \mapsto w_1 \\ \Pi_{\mathcal{N}||\mathcal{M}} &\,:\, w_0 \mapsto w_2. \end{aligned} \tag{5.8}$$

**Definition 5.2.1.** *Parallel Projection* [5]

A stable operator $\Pi : \mathcal{L} \to \mathcal{L}$ (with $\Pi 0 = 0$) is called a parallel projection if for any $x_1, x_2 \in \mathcal{L}$

$$\Pi(\Pi x_1 + (I - \Pi)x_2) = \Pi x_1 \tag{5.9}$$

where $I$ denotes the identity on $\mathcal{L}$.

Thus, $\Pi_{\mathcal{M}||\mathcal{N}}$ and $\Pi_{\mathcal{N}||\mathcal{M}}$ are parallel projections considering that for any $w_1, w_2 \in \mathcal{W}$

$$\Pi(\Pi w_1 + (I - \Pi)w_2) = \Pi w_1, \tag{5.10}$$

for $\Pi \in \left\{\Pi_{\mathcal{M}||\mathcal{N}}, \Pi_{\mathcal{N}||\mathcal{M}}\right\}$.

Consider the *summation operator*

$$\Sigma_{\mathcal{M},\mathcal{N}} : \mathcal{M} \times \mathcal{N} \to \mathcal{W} : (m, n) \mapsto m + n. \tag{5.11}$$

The stability of the standard feedback interconnection, Fig. 5.1, is equivalent to $\Sigma_{\mathcal{M},\mathcal{N}}$ having an inverse defined on the whole of $\mathcal{W}$ which is bounded. In fact, if $\Sigma_{\mathcal{M},\mathcal{N}}$ has a bounded inverse, then $\Sigma^{-1}_{\mathcal{M},\mathcal{N}} = H_{P,C}$. It can be shown that a necessary condition for $[P, C]$ to be stable is that $\mathcal{M}$ and $\mathcal{N}$ are closed subsets of $\mathcal{W}$ [5]. Let $\mathcal{W}_1$ and $\mathcal{W}_2$ be closed subsets of a Banach space $\mathcal{W}$. We define

$$\begin{aligned}\vec{\delta}(\mathcal{W}_1, \mathcal{W}_2) &:= \begin{cases} \inf\{\|(\mathcal{T} - I)|_{\mathcal{W}_1}\|\}, & \mathcal{T} \text{ is a causal} \\ & \quad \text{bijective map from } \mathcal{W}_1 \text{ to } \mathcal{W}_2 \\ & \quad \text{with } \mathcal{T}0 = 0, \\ \infty, & \text{if no such operator } \mathcal{T} \text{ exists,} \end{cases} \\ \delta(\mathcal{W}_1, \mathcal{W}_2) &= \max\left\{\vec{\delta}(\mathcal{W}_1, \mathcal{W}_2), \vec{\delta}(\mathcal{W}_2, \mathcal{W}_1)\right\}. \end{aligned} \tag{5.12}$$

**Theorem 5.2.1.** *Consider the feedback system shown in Fig. 5.1. Let $\mathcal{M} := \mathcal{G}_P$ and $\mathcal{N} := \mathcal{G}_C$. Assume that $[P, C]$ is fg-stable. Suppose that $P$ is perturbed to $P_1$ and $\mathcal{M}_1 := \mathcal{G}_{P1}$. If*

$$\vec{\delta}(\mathcal{M}, \mathcal{M}_1) < \left\|\Pi_{\mathcal{M}||\mathcal{N}}\right\|^{-1} \tag{5.13}$$

*then $[P_1, C]$ is fg-stable. Furthermore*

$$\left\|\Pi_{\mathcal{M}_1||\mathcal{N}}\right\| < \left\|\Pi_{\mathcal{M}||\mathcal{N}}\right\| \frac{1 + \vec{\delta}(\mathcal{M}, \mathcal{M}_1)}{1 - \left\|\Pi_{\mathcal{M}||\mathcal{N}}\right\| \vec{\delta}(\mathcal{M}, \mathcal{M}_1)}. \tag{5.14}$$

*Proof.* See [13]. □

## 5.3 Upper bounds on the Gap Metric and the stability margin

In this section, we suggest a method to find an upper bound on the gap metric between two nonlinear systems as well as a method to compute an upper bound on $\Pi_{\mathcal{M}||\mathcal{N}}$.

**Theorem 5.3.1.** *Consider nonlinear dynamical systems given by*

$$\begin{aligned} N &: \ \dot{x} = f(x, u)\,, \ x_0 = 0; \\ \hat{N} &: \ \dot{\hat{x}} = \hat{f}(\hat{x}, u)\,, \ \hat{x}_0 = 0. \end{aligned} \tag{5.15}$$

*Let $\gamma(N)$ and $\gamma(\hat{N})$ denote their gain respectively. Then*

$$\delta(N, \hat{N}) \leq \gamma(N) + \gamma(\hat{N}). \tag{5.16}$$

*Proof.* We have

$$\begin{aligned}\|x-\hat{x}\| &\le \|x\| + \|\hat{x}\| \\ &\le \gamma(N)\,\|u\| + \gamma(\hat{N})\,\|u\| \\ &\le \big(\gamma(N)+\gamma(\hat{N})\big)\,\|u\| \\ &\le \big(\gamma(N)+\gamma(\hat{N})\big)\left\|\begin{bmatrix}u\\x\end{bmatrix}\right\|.\end{aligned} \tag{5.17}$$

Define $\mathcal{T}$ as

$$\mathcal{T}\begin{bmatrix}u\\x\end{bmatrix} := \begin{bmatrix}u\\\hat{x}\end{bmatrix}. \tag{5.18}$$

□

It is trivial that $\mathcal{T}$ is bijective. We have

$$\begin{aligned}\vec{\delta}(N,\hat{N}) &= \|I-\mathcal{T}\| \\ &= \sup \frac{\left\|(I-\mathcal{T})\begin{bmatrix}u\\x\end{bmatrix}\right\|}{\left\|\begin{bmatrix}u\\x\end{bmatrix}\right\|} \\ &= \sup \frac{\left\|\begin{bmatrix}u-u\\x-\hat{x}\end{bmatrix}\right\|}{\left\|\begin{bmatrix}u\\x\end{bmatrix}\right\|} \\ &= \sup \frac{\|x-\hat{x}\|}{\left\|\begin{bmatrix}u\\x\end{bmatrix}\right\|} \\ &\le \gamma(N)+\gamma(\hat{N}) \quad \text{using (5.17)}\end{aligned} \tag{5.19}$$

Similarly

$$\vec{\delta}(\hat{N},N) \le \gamma(N)+\gamma(\hat{N}). \tag{5.20}$$

Consequently,

$$\begin{aligned}\delta(N,\hat{N}) &= \max\{\vec{\gamma}(N,\hat{N}),\vec{\gamma}(\hat{N},N)\} \\ &\le \delta(N)+\delta(\hat{N}).\end{aligned} \tag{5.21}$$

**Theorem 5.3.2.** *Consider the standard feedback configuration depicted in Fig. 5.1. Suppose that $\gamma(P)\gamma(C)<1$. Let $\Pi_{\mathcal{M}||\mathcal{N}}$ be defined as (5.6) and (5.7). Then*

$$\left\|\Pi_{\mathcal{M}||\mathcal{N}}\right\| \le \frac{\big(1+\gamma(P)\big)\big(1+\gamma(C)\big)}{1-\gamma(P)\gamma(C)}. \tag{5.22}$$

*Proof.* From the feedback configuration, we have

$$\begin{aligned} \|u_1\| &\leq \|u_0\| + \gamma(C)\,\|y_0 - y_1\| \\ &\leq \|u_0\| + \gamma(C)\,\|y_0\| + \gamma(C)\gamma(P)\,\|u_1\|\,. \end{aligned} \tag{5.23}$$

Consequently

$$\|u_1\| \leq \frac{1}{1-\gamma(C)\gamma(P)}\,\|u_0\| + \frac{\gamma(C)}{1-\gamma(C)\gamma(P)}\,\|y_0\|\,. \tag{5.24}$$

Therefore

$$\begin{aligned} \left\|\begin{bmatrix} u_1 \\ y_1 \end{bmatrix}\right\| &\leq \|u_1\| + \|y_1\| \\ &\leq \|u_1\| + \gamma(P)\,\|u_1\| \\ &\leq \frac{1+\gamma(P)}{1-\gamma(C)\gamma(P)}\,\|u_0\| + \frac{\gamma(C)\big(1+\gamma(P)\big)}{1-\gamma(C)\gamma(P)}\,\|y_0\|\,. \end{aligned} \tag{5.25}$$

Since $\|a\| \leq \left\|\begin{bmatrix} a \\ b \end{bmatrix}\right\|$,

$$\begin{aligned} \left\|\begin{bmatrix} u_1 \\ y_1 \end{bmatrix}\right\| &\leq \frac{1+\gamma(P)+\gamma(C)\big(1+\gamma(P)\big)}{1-\gamma(C)\gamma(P)} \left\|\begin{bmatrix} u_0 \\ y_0 \end{bmatrix}\right\| \\ &= \frac{\big(1+\gamma(P)\big)\big(1+\gamma(C)\big)}{1-\gamma(C)\gamma(P)} \left\|\begin{bmatrix} u_0 \\ y_0 \end{bmatrix}\right\|. \end{aligned} \tag{5.26}$$

On the other hand, Equation (5.8) implies

$$\Pi_{\mathcal{M}||\mathcal{N}} \begin{bmatrix} u_0 \\ y_0 \end{bmatrix} = \begin{bmatrix} u_1 \\ y_1 \end{bmatrix}. \tag{5.27}$$

Thus

$$\left\|\Pi_{\mathcal{M}||\mathcal{N}}\right\| = \sup_{\left\|\begin{bmatrix} u_0 \\ y_0 \end{bmatrix}\right\| \neq 0} \frac{\left\|\begin{bmatrix} u_1 \\ y_1 \end{bmatrix}\right\|}{\left\|\begin{bmatrix} u_0 \\ y_0 \end{bmatrix}\right\|}. \tag{5.28}$$

Using (5.26)

$$\left\|\Pi_{\mathcal{M}||\mathcal{N}}\right\| \leq \frac{\big(1+\gamma(P)\big)\big(1+\gamma(C)\big)}{1-\gamma(C)\gamma(P)}. \tag{5.29}$$

□

**Example 5.3.1.** Consider the feedback configuration of Fig. 5.1. Assume that the plant is the circuit shown in Fig. 5.2, where the inductance of the SSR is nonlinear and $L(\cdot)$ is defined as Fig. 5.3 and $R = 10$. The state equation of the system is

$$\begin{aligned} \dot{x}(t) &= L^{-1}(u_1(t) - Rx(t)),\ x(0) = 0 \\ y_1(t) &= x(t) \end{aligned} \tag{5.30}$$

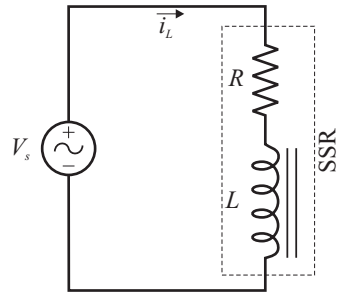


Figure 5.2: $P$ in Example 5.3.1.

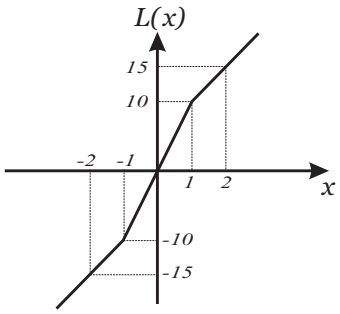


Figure 5.3: Inductance of SSR.

where $x(t) := i_L(t)$ and $u_1(t) := V_s(t)$. Let $C = -c$ where $c$ is a positive non-zero constant. Let $\mathcal{U} = \mathcal{Y} = \mathcal{L}_\infty$. Since the instantaneous gains of $P$ and $C$ are zero and one, respectively, the loop is well-posed. First, we will find the $\left\|\Pi_{\mathcal{M}||\mathcal{N}}\right\|$ by a direct method similar to the solution of Example 1 in [13]. Then, we will compute the upper bound on $\left\|\Pi_{\mathcal{M}||\mathcal{N}}\right\|$ by the suggested method.

*I. Direct computation:*

The feedback equation is

$$\dot{x} = L^{-1}(u_0 + cy_0 - (10 + c)x),\ x(0) = 0. \tag{5.31}$$

We have

$$\Pi_{\mathcal{M}||\mathcal{N}} : \begin{bmatrix} u_0 \\ y_0 \end{bmatrix} \mapsto \begin{bmatrix} u_1 \\ y_1 \end{bmatrix} = \begin{bmatrix} u_0 + cy_0 - cx \\ x \end{bmatrix}. \tag{5.32}$$

Let $v_0 := u_0 + cy_0$. For any $v_0$, $u_0 = y_0$ gives the mapping with the smallest input norm. Therefore, $v_0 = (1 + c)u_0$ and

$$\begin{aligned} \left\|\Pi_{\mathcal{M}||\mathcal{N}}\right\| &= \left\| \begin{bmatrix} u_0 \\ y_0 \end{bmatrix} \mapsto \begin{bmatrix} u_0 + cy_0 - cx \\ x \end{bmatrix} \right\| \\ &= \left\| \begin{bmatrix} u_0 \\ y_0 \end{bmatrix} \mapsto \begin{bmatrix} v_0 - cx \\ x \end{bmatrix} \right\| \\ &= (1 + c) \left\| v_0 \mapsto \begin{bmatrix} v_0 - cx \\ x \end{bmatrix} \right\| \\ &= (1 + c) \times \max\{\left\| v_0 \mapsto \left(v_0 - cx\right) \right\|, \|v_0 \mapsto x\|\}. \end{aligned} \tag{5.33}$$

We now show that $\|v_0 \mapsto x\| = {}^{1}\!/_{10+c}$. Suppose that for any arbitrary chosen interval $[0,T]$, the maximum of $x(t)$, which is positive, occurs at $t_0 \in [0,T]$. Then, for any $\epsilon > 0$, there exists $t_1$ such that $0 < t_1 < t_0$, $x(t_1) > x(t_0) - \epsilon$ and $\dot{x}(t_1) > 0$. Consequently, $L^{-1}\big(v_0(t_1) - (10+c)x(t_1)\big) > 0$. Since $\operatorname{sgn} L^{-1}(x) = \operatorname{sgn} x$, $v_0(t_1) > (10+c)x(t_1)$. Thus, $v_0(t_1) > (10+c)x(t_0) - (1+c)\epsilon$ for any $\epsilon$. Similarly, if the minimum of $x(t)$ in $[0,T]$, which is negative, occurs at $\acute{t}_0$, for any $\acute{\epsilon} > 0$, there exists $\acute{t}_1$ such that $v_0(\acute{t}_1) < (10+c)x(\acute{t}_0) - (1+c)\acute{\epsilon}$. Consequently, $\|v_0\|_T \geq (10+c)\,\|x\|_T$. To show that this upper bound on $\|v_0 \mapsto x\|$ can be approached arbitrary closely, let $v_0 = 1$ for all $t$. It is trivial that $x(t) = \big(1 - e^{-(1+0.1c)t}\big)/(10+c)$. So $\|v_0\| = 1$ and $\|x\| = {}^{1}\!/_{10+c}$. Consequently, $\|v_0 \mapsto x\| = {}^{1}\!/_{10+c}$. Next, we compute $\big\|v_0 \mapsto \big(v_0 - cx\big)\big\|$. Trivially, $\big\|v_0 \mapsto \big(v_0 - cx\big)\big\| \leq 1 + \|v_0 \mapsto (cx)\| = 1 + \frac{c}{10+c}$. This upper bound can be approached arbitrarily closely by the input $v_0 = 1$ for $0 \leq t < T$ and $v_0 = -1$ for $t \geq T$. We have $x(t) = \big(1 - e^{-(1+0.1c)t}\big)/(10+c)$ for $0 \leq t < T$. Thus, $\big(v_0 - cx\big)(T) = -(1 + \frac{c}{10+c}) + e^{-(1+0.1c)T}$. Therefore, $\|v_0\| = 1$ and $\|v_0 - cx\| = 1 + \frac{c}{10+c}$ which implies that $\big\|v_0 \mapsto \big(v_0 - cx\big)\big\| = 1 + \frac{c}{10+c}$. Consequently, $\big\|\Pi_{\mathcal{M}||\mathcal{N}}\big\| = 1 + \frac{c}{10+c}$.

*II. The suggested method:*

To find $\gamma(P)$, let $\Phi(x,u) = L^{-1}(u - 10x) + 3x/2$ and $\Gamma := \left[\begin{array}{c|c} -3/2 & 1 \\ \hline 1 & 0 \end{array}\right]$. We use the computational methods introduced in Section 2.3.1. Fig. 5.4 shows the plot of $\dfrac{\|\Phi(x,u)\|}{\left\|\begin{bmatrix} x \\ u \end{bmatrix}\right\|}$ versus $\left\|\begin{bmatrix} x \\ u \end{bmatrix}\right\|$ for $2 \times 10^6$ randomly chosen input vector. Therefore, $\gamma(\Phi) = 0.7$. Using the method introduced in Section 2.3.2, we have $\gamma(\Gamma) = 2/3$. Theorem 4.1.1 implies that

$$\gamma(P) \leq 0.639. \tag{5.34}$$

Since $C = -c$ is a constant, $\gamma(C) = c$. Theorem 5.3.2 implies that $\big\|\Pi_{\mathcal{M}||\mathcal{N}}\big\| \leq \frac{1.639(1+c)}{1-0.639\,c}$ if $c < 1.56$. Apparently, the obtained upper bound is closer to the actual value when $c$ approaches zero.

**Example 5.3.2.** Consider the plant introduced in the previous example. Suppose that the system is perturbed by time delay $h$. That is

$$P_1 : \begin{cases} \dot{x}(t) = L^{-1}(u_1(t) - Rx(t)),\ x(0) = 0 \\ y_1(t) = x(t-h). \end{cases} \tag{5.35}$$

First, we will compute an upper bound on the gap between the plant $P$ and the perturbation $P_1$ by a direct method similar to the solution of Example 1 in [13]. Then, we will compute the upper bound on the gap by the suggested method.

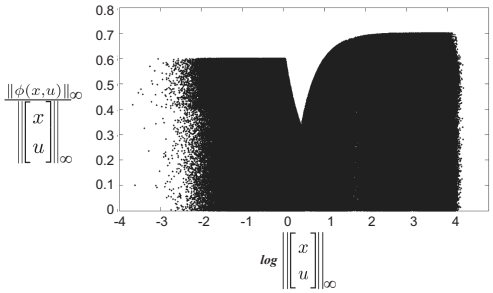


Figure 5.4: Gain of $\|\Phi(x,u)\|$ versus $\log \left\| \begin{bmatrix} x \\ u \end{bmatrix} \right\|$.

*I. Direct computation:*

Let $\mathcal{M}_1 := \mathcal{G}_{P1}$ and define a mapping $\mathcal{T} : \mathcal{M} \to \mathcal{M}_1$ as

$$\mathcal{T}\begin{bmatrix} u_1(t) \\ x(t) \end{bmatrix} = \begin{bmatrix} u_1(t) \\ x(t-h) \end{bmatrix}. \tag{5.36}$$

Thus

$$\begin{aligned} |x(t) - x(t-h)| &\leq \sup_{\hat{t}\in[t-h,t]} |\dot{x}(\hat{t})| \cdot h \\ &\leq \sup_{\hat{t}\in[t-h,t]} |L^{-1}\big(u(\hat{t}) - 10x(\hat{t})\big)| \cdot h. \end{aligned} \tag{5.37}$$

Since $L^{-1}(\cdot)$ is an strictly increasing function,

$$\begin{aligned} &|x(t) - x(t-h)| \\ &\quad \leq L^{-1}\big( \sup_{\hat{t}\in[t-h,t]} |u(\hat{t}) - 10x(\hat{t})|\big) \cdot h \\ &\quad \leq L^{-1}\big( \sup_{\hat{t}\in[t-h,t]} |u(\hat{t})| + \sup_{\hat{t}\in[t-h,t]} |10x(\hat{t})|\big) \cdot h \\ &\quad \leq L^{-1}\big( \sup_{\hat{t}\in[0,t]} |u(\hat{t})| + \sup_{\hat{t}\in[0,t]} |10x(\hat{t})|\big) \cdot h. \end{aligned} \tag{5.38}$$

Therefore

$$\begin{aligned} &\|x(t) - x(t-h)\|_\tau \\ &\quad \leq \left\| L^{-1}\big( \sup_{\hat{t}\in[0,t]} |u(\hat{t})| + \sup_{\hat{t}\in[0,t]} |10x(\hat{t})|\big) \right\|_\tau \cdot h \\ &\quad \leq L^{-1}\big(11 \max\{\|u\|_\tau, \|x\|_\tau\}\big) \cdot h \\ &\quad \leq 2.2 \max\{\|u\|_\tau, \|x\|_\tau\} \cdot h. \end{aligned} \tag{5.39}$$

Hence

$$\|I - \mathcal{T}\| = \sup_{\tau, \|u_1\|_\tau \neq 0} \frac{\|x(t) - x(t-h)\|_\tau}{\max\{\|u_1\|_\tau, \|x\|_\tau\}} \leq 2.2\, h. \tag{5.40}$$

Consequently, $\vec{\delta}(\mathcal{M}, \mathcal{M}_1) \leq 2.2\,h$. On the other hand, let $u(t) = 1$ on $[0, h]$. It is Trivial that $(Pu)(t) = 0.1(1 - e^{-10t})$. For any $w \in \mathcal{M}_1$, we have $w_h = \begin{bmatrix} * \\ 0 \end{bmatrix}$ which is implied by the time delay in $P_1$. Therefore

$$\begin{aligned}
\vec{\delta}(\mathcal{M}, \mathcal{M}_1) &= \sup_{u_1, y_1 \neq 0} \frac{\left\| (\mathcal{T} - I) \begin{bmatrix} u_1 \\ y_1 \end{bmatrix} \right\|}{\left\| \begin{bmatrix} u_1 \\ y_1 \end{bmatrix} \right\|} \\
&\geq \sup_{u_1, y_1 \neq 0} \frac{\left\| \begin{bmatrix} * \\ 0 \end{bmatrix} - \begin{bmatrix} u_1 \\ Pu_1 \end{bmatrix} \right\|_h}{\max\{\|u_1\|_h, \|Pu_1\|_h\}} \\
&= \frac{\max\{\|* - u_1\|_h, \|Pu_1\|_h\}}{\max\{\|u_1\|_h, \|Pu_1\|_h\}} \\
&\geq \frac{\|Pu_1\|_h}{\max\{\|u_1\|_h, \|Pu_1\|_h\}} \\
&= 0.1(1 - e^{-10h}).
\end{aligned} \tag{5.41}$$

Consequently

$$0.1(1 - e^{-10h}) \leq \vec{\delta}(P, P_1) \leq 2.2\,h. \tag{5.42}$$

*II. The suggested method:*

Since $P$ is autonomous, $\gamma(P) = \gamma(P_1)$. Using Theorem 5.3.1, $\vec{\delta}(P, P_1) = 2\gamma(P)$. Using (5.34), $\vec{\delta}(P, P_1) \leq 1.278$. It is clear that for $h > 0.58$ the suggested method provides smaller upper bound than the direct method.

## 5.4 Chapter Summary

In this chapter, we have considered the computation of the gap metric and the corresponding robust stability margin. Our results are applicable to a class of a nonlinear systems which satisfy a given inequality. The suggested methods have computational advantage compared to previous work in the sense that they are applicable to wider range of nonlinear systems. Our methods are based on two inequalities derived for the gap metric and the stability margin with respect to the gain of the relevant systems. An example is provided to illustrate the results.

# Chapter 6

# The Large Gain Theorem

## 6.1 Introduction

One of the well-accepted and widely-used methods to study stability of systems is the input-output approach. It was initiated by Popov, Zames, and Sandberg, in the 1960s [42] [56] [32]. So far, it has been a fruitful area which has resulted in many of the recent developments in control theory, such as robust control and small-gain based nonlinear stabilization techniques. The input-output stability theory considers systems as mappings from an input space of functions into an output space. In this theory, the well-behaved input and output signals are considered as members of input and output spaces. Therefore, if the "well-behaved" inputs produce well-behaved outputs, the system is called stable.

The main contribution of the input-output stability theory in control theory is through the well-known small-gain theorem. In this context, the most notable contributions have also been made by Zames and Sandberg, e.g. [56] [32]. The small gain theorem says that the feedback loop will be stable if the loop gain is less than one. This simple rule has been a basis for numerous stabilization techniques such as nonlinear $\mathcal{H}_\infty$ control [15].

Stability of systems, in its various forms, continues to inspire researchers. Motivated by the classical small gain theorem, "nonlinear gain" small gain theorems are discussed in such references as [21] [39] [18]. The notion of non-uniform in time robust global asymptotic output stability was introduced in [22] for a wide class of systems. A small-gain theorem for a wide class of feedback systems was proposed in [23]. In [14], it was shown that for an open loop unstable system which is closed loop stable the gain must exceed one.

In this chapter, the minimum gain of a system is studied. Although it has been showed that the minimum gain is not a norm on space of operators, a new stability condition has been derived for feedback systems based on the minimum gain of the open-loop systems.

The chapter is organized as follows. In Section 6.2, the minimum gain of an operator

is defined and some of its properties are derived. In Section 6.3, the large gain theorem is stated. An example is also provided to illustrate the usage of the theorem.

## 6.2 Minimum Gain of an Operator

Let $H : \mathcal{U} \to \mathcal{Y}$ denote an operator. We define the minimum gain of $H$ as follows:

$$\nu(H) = \inf_{0 \neq u \in \mathcal{U}} \frac{\|(Hu)_T\|}{\|u_T\|} \tag{6.1}$$

where the infimum is taken over all $u \in \mathcal{U}$ and all $T$ in $\mathbb{R}^+$ for which $u_T \neq 0$. It is trivial that the minimum gain of an operator is less or equal to its induced norm. It is also obvious that if a minimum gain of a system is infinite, then it is unstable. In other words, the minimum gain of a stable system is always finite. The converse is, however, not true.

**Lemma 6.2.1.** *Let $M \in \mathbb{R}^{n\times n}$. Define $H : \mathcal{X}_2 \to \mathcal{X}_2$ as $Hx := Mx$, then*

$$\nu(H) = \underline{\sigma}(M). \tag{6.2}$$

*Proof.* The proofs for the continuous-time and discrete-time cases are the same and only the first one is given here. We use the following property of the smallest singular value of matrices (e.g. [57] pp. 21):

$$\underline{\sigma}(M) = \min_{\|x\|=1} \|Mx\| = \min_{x\neq 0} \frac{\|Mx\|}{\|x\|}. \tag{6.3}$$

Let $M = U\Sigma V^T$ be the Singular Value Decomposition (SVD) of $M$, where $V = [v_1, v_2, \cdots, v_n] \in \mathbb{R}^{n\times n}$ and $U, \Sigma \in \mathbb{R}^{n\times n}$ [57]. It is well-known that $v_n$ is the minimizer of (6.3), e.g. [57]. Let $x \in \mathcal{L}_2$, we have

$$\begin{aligned} \|Mx\|^2 &= \int_0^\infty \|Mx(t)\|_2^2 \, dt \\ &\geq \int_0^\infty \underline{\sigma}(M)^2 \|x(t)\|_2^2 \, dt \\ &= \underline{\sigma}(M)^2 \int_0^\infty \|x(t)\|_2^2 \, dt = \underline{\sigma}(M)^2 \|x\|^2 \end{aligned} \tag{6.4}$$

which shows that $\underline{\sigma}(M)$ is a lower bound for $\nu(H)$. To show that it is the greatest lower bound, let $x(t) = \frac{v_n}{\|v_n\|} e^{-t}$. We have

$$\|x\|^2 = \int_0^\infty \left\| \frac{v_n}{\|v_n\|} e^{-t} \right\|^2 dt = \int_0^\infty \left\| e^{-t} \right\|^2 dt = {}^1\!/_2 \tag{6.5}$$

and

$$\begin{aligned}\|Mx\|^2 &= \int_0^\infty \left\| M \frac{v_n}{\|v_n\|} e^{-t} \right\|^2 dt \\ &= \int_0^\infty \|Mv_n\|^2 \frac{e^{-2t}}{\|v_n\|^2}\, dt \\ &= \int_0^\infty \|\underline{\sigma}(M) v_n\|^2 \frac{e^{-2t}}{\|v_n\|^2}\, dt \\ &= \|\underline{\sigma}(M)\|^2 \int_0^\infty e^{-2t}\, dt = {}^1\!/_2 \, \|\underline{\sigma}(M)\|^2 .\end{aligned} \tag{6.6}$$

Equations (6.5) and (6.6) imply that $\nu(H)$ is equal to $\underline{\sigma}(M)$ for some input. This completes the proof.

□

**Lemma 6.2.2.** *Let $\Phi(\cdot,\cdot) : \mathbb{R}^+ \times \mathbb{R}^n \to \mathbb{R}^n$ ($\Phi(\cdot,\cdot) : \mathbb{Z}^+ \times \mathbb{R}^n \to \mathbb{R}^n$ in discrete time) and $H$ be the operator defined as*

$$H : \mathcal{X}_p \to \mathcal{X}_p \,; \quad Hx(t) := \Phi(t, x(t)). \tag{6.7}$$

*Suppose there exists a constant $\mu_p$ such that*

$$\mu_p \|x\|_p \leq \|\Phi(t,x)\|_p, \ \forall x \in \mathbb{R}^n, \ \forall t \geq 0 \tag{6.8}$$

*then $\mu_p \leq \nu_p(H)$.*

*Proof.* Let $x \in \mathcal{L}_p$, for $p \neq \infty$,

$$\begin{aligned}\|Hx\|_{\mathcal{L}_p}^p &= \int_0^\infty \|\Phi(t,x(t))\|^p \ dt \geq \int_0^\infty \mu_p^p \, \|x(t)\|_p \ dt \\ &= \mu_p^p \int_0^\infty \|x(t)\|^p \ dt = \mu_p^p \, \|x\|_{\mathcal{L}_p}^p .\end{aligned} \tag{6.9}$$

For $p = \infty$,

$$\begin{aligned}\|Hx\|_{\mathcal{L}_\infty} &= \sup_t \|\Phi(t,x(t))\| \geq \sup_t \mu_p \, \|x(t)\| \\ &= \mu_p \sup_t \|x(t)\| = \mu_p \, \|x\|_{\mathcal{L}_\infty}^p .\end{aligned} \tag{6.10}$$

Equations (6.9) and (6.10) imply that $\mu_p$ is a lower bound for $\nu(H)$. This completes the proof.

□

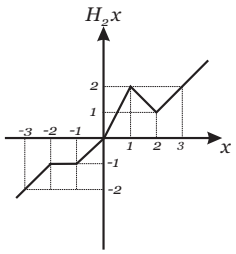


Figure 6.1: $H_2$ in Example 6.2.1.

**Example 6.2.1.** *Memory less Nonlinearities:* Let $X = \mathcal{L}_\infty$, and consider nonlinear operators $H_1(u) = u^2$ and $H_2(.)$ defined by the graph in the plane shown in Fig. 6.1. We have

$$\nu(H_1) = \inf_{0 \neq u \in \mathcal{L}_\infty} \frac{\|(H_1 u)_T\|_{\mathcal{L}_\infty}}{\|u_T\|_{\mathcal{L}_\infty}} = \inf_{0 \neq u \in \mathcal{L}_\infty} |u| = 0. \tag{6.11}$$

The minimum gain $\nu(H_2)$ is easily determined from the slope of the graph of $H_2$.

$$\nu(H_2) = \inf_{0 \neq u \in \mathcal{L}_\infty} \frac{\|(H_2 u)_T\|_{\mathcal{L}_\infty}}{\|u_T\|_{\mathcal{L}_\infty}} = 0.5. \tag{6.12}$$

**Lemma 6.2.3.** *Let $g(t)$ be the impulse response of a continuous-time, stable, LTI system. Let $G(s)$ denote the Laplace transform of $g(t)$. Furthermore, assume that there exists a row in $G(s)$ where all elements are strictly proper, namely there is $i$ such that for all $j$, $\lim_{s\to\infty} G_{ij}(s) = 0$. Let $H$ stand for the convolution operator defined by*

$$H(z(t)) = \int_0^t g(t-\tau) z(\tau) d\tau. \tag{6.13}$$

*We have*

$$\nu(H) = 0. \tag{6.14}$$

*Proof.* Let $\hat{x}(t) = [\hat{x}_1(t)\ \hat{x}_2(t)\ \cdots\ \hat{x}_n(t)]^T$,

$$\hat{x}_k(t) = \begin{cases} \sin(\omega t) & k = i, \\ 0 & \text{otherwise.} \end{cases}$$

where $i$ corresponds to the strictly proper row in $G(s)$ and $\omega \geq \pi$. Let

$$x(t) := \hat{x}(t) - \hat{x}\left(t - \left\lfloor \frac{\omega}{\pi} \right\rfloor \frac{\pi}{\omega}\right) \tag{6.15}$$

where $\lfloor r \rfloor$ denotes the floor function of a real number r, which is the largest integer less

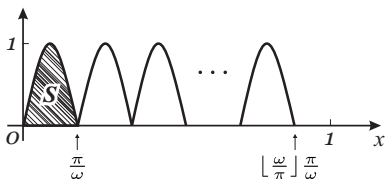


Figure 6.2: $|\hat{x}(t)|$.

than or equal to $r$, namely $\forall r \in \mathbb{R}\ ; \lfloor r \rfloor := \sup\{n \in \mathbb{Z} | n \leq r\}$. It is trivial that

$$x(t) = \begin{cases} \begin{bmatrix} 0 \\ 0 \\ \vdots \\ \sin(\omega t) \\ \vdots \\ 0 \end{bmatrix} & \text{ith row} \qquad 0 \leq t \leq \left\lfloor \frac{\omega}{\pi} \right\rfloor, \\ 0 & t > \left\lfloor \frac{\omega}{\pi} \right\rfloor. \end{cases}$$

and

$$\|x(t)\| = \left| \hat{x}_i(t) - \hat{x}_i \left( t - \left\lfloor \frac{\omega}{\pi} \right\rfloor \frac{\pi}{\omega} \right) \right|$$

Thus,

$$\|x\|_{\mathcal{L}_\infty} = \sup_t |\sin(\omega t)| = 1 \tag{6.16}$$

$$\begin{aligned} \|x\|_{\mathcal{L}_2}^2 &= \int_0^{\lfloor \frac{\omega}{\pi} \rfloor \frac{\pi}{\omega}} |\sin(\omega t)|^2 \, dt \\ &= {}^1\!/_2 \left( t - \frac{\sin(2\omega t)}{2\omega} \right) \Bigg|_0^{\lfloor \frac{\omega}{\pi} \rfloor \frac{\pi}{\omega}} \\ &= \left\lfloor \frac{\omega}{\pi} \right\rfloor \frac{\pi}{2\omega} - \frac{\sin\left(2\pi \lfloor \frac{\omega}{\pi} \rfloor\right)}{4\omega} \end{aligned} \tag{6.17}$$

$$\|x\|_{\mathcal{L}_1} = \int_0^{\lfloor \frac{\omega}{\pi} \rfloor \frac{\pi}{\omega}} |\sin(\omega t)| \, dt. \tag{6.18}$$

To calculate (6.18), consider the graph of $|\hat{x}(t)|$ depicted in Fig. 6.2. The number of peaks is $\left\lfloor \frac{\omega}{\pi} \right\rfloor$. Moreover,

$$S = \int_0^{\frac{\pi}{\omega}} \sin(\omega t) \, dt = \frac{2}{\omega}. \tag{6.19}$$

Consequently,

$$\|x\|_{\mathcal{L}_1} = \left\lfloor \frac{\omega}{\pi} \right\rfloor S = \left\lfloor \frac{\omega}{\pi} \right\rfloor \frac{2}{\omega}. \tag{6.20}$$

To calculate the norm of the output $\|y\|$, we can first find the response of the system to input $\hat{x}(t)$, namely $\hat{y}(t)$, and then obtain the output using $y(t) = \hat{y}(t) - \hat{y}\left(t - \left\lfloor \frac{\omega}{\pi} \right\rfloor \frac{\pi}{\omega}\right)$ implied

by the linearity property of the system and (6.15). If we let $\omega \to \infty$, the response of the system to $\hat{x}(t)$ approaches to zero. The reason is that the amplitude of all elements of the $i$-th row of $G(s)$ approaches to zero at high frequencies. Therefore, $\lim_{w\to\infty} \|\hat{y}(t)\| = 0$ and consequently

$$\lim_{w\to\infty} \|y\| = 0. \tag{6.21}$$

On the other hand, (6.17) and (6.20) imply

$$\lim_{w\to\infty} \|x\|_{\mathcal{L}_2} = {}^1\!/_2, \lim_{w\to\infty} \|x\|_{\mathcal{L}_1} = \frac{2}{\pi}. \tag{6.22}$$

Equations (6.16), (6.21) and (6.22) imply

$$\nu_1(H) = 0,\ \nu_2(H) = 0,\ \nu_\infty(H) = 0. \tag{6.23}$$

□

**Corollary 6.2.1.** *The minimum gain of a system with a strictly proper stable transfer function is zero.*

**Lemma 6.2.4.** *Let $g(t)$ be the impulse response of a continuous-time (discrete-time) LTI system. Let $G(s)$ $(G(z))$ denote the Laplace transform (z-transform) of $g(t)$. Furthermore, assume that $G(s)$ $(G(z))$ has at least one zero in the RHP (outside of the unit circle). Let $H$ stand for the convolution operator defined by*

$$H(z(t)) = \int_0^t g(t-\tau)z(\tau)d\tau \tag{6.24}$$

*for continuous-time case and*

$$H(z(t)) = \sum_{l=0}^{t} g(t-l)z(l) \tag{6.25}$$

*for discrete-time one. We have*

$$\nu(H) = 0. \tag{6.26}$$

*Proof.* The proofs for the continuous-time and discrete-time cases are the same and only the first one is given here.

Let $s_0$ be the RHP zero of $G(s)$, namely there exists $w$ such that $G(s_0)w = 0$. If $\sigma_0 + i\omega_0 = s_0 \in \mathbb{C}$, trivially $s_0^*$ is also a RHP zero of $G(s)$. Let

$$u(t) = \begin{cases} w\, e^{s_0 t} & \text{if } s_0 \in \mathbb{R}, \\ w\, e^{\sigma_0 t} \sin(\omega_0 t) & \text{if } s_0 \in \mathbb{C}. \end{cases} \tag{6.27}$$

Consequently,

$$U(s) = \begin{cases} w \cdot \frac{1}{s-s_0} & \text{if } s_0 \in \mathbb{R}. \\ w \cdot \frac{\omega_0}{(s-\sigma_0)^2+\omega_0^2} & \text{if } s_0 \in \mathbb{C}. \end{cases} \tag{6.28}$$

We have

$$Y(s) = \begin{cases} G(s) \cdot w \cdot \frac{1}{s-s_0} & \text{if } s_0 \in \mathbb{R}. \\ G(s) \cdot w \cdot \frac{\omega_0}{(s-\sigma_0)^2+\omega_0^2} & \text{if } s_0 \in \mathbb{C}. \end{cases} \tag{6.29}$$

Since $G(s)$ is assumed to be stable, $Y(s)$ is a stable signal. It is important to note that $Y(s)$ does not have a pole at $s_0$. The reason is that the pole at $s_0$ is canceled by the zero of $G(s)$ at $s_0$. Since all poles of $Y(s)$ are in LHP, $y(t)$ is a decaying signal. On the other hand, $u(t)$ is an unstable signal, rising by time. If we truncate both $u(t)$ and $y(t)$ at $T$, which is chosen sufficiently large, the corresponding gain of the system will be small. By increasing $T$, the gain can be decreased as much as desired. Therefore, $\nu(H) = 0$.

□

**Lemma 6.2.5.** *Let $H : \mathcal{D}_h \subseteq \mathcal{U} \to \mathcal{Y}$ be a possibly unstable operator. Let $\mathcal{R}_h$ denote the range of $H$, namely $\mathcal{R}_h = \{y \in \mathcal{Y} : y = Hu \text{ for some } u \in \mathcal{D}_h\}$. Assume that $H$ has a stable right inverse, i.e., there exists $H^{-1} : \mathcal{R}_h \to \mathcal{D}_h$ such that*

$$H \cdot H^{-1} = I \tag{6.30}$$

*and $H^{-1}$ is stable. Moreover, assume that $\gamma(H^{-1}) < \infty$ Then*

$$\nu(H) = \frac{1}{\gamma(H^{-1})}. \tag{6.31}$$

*Proof.* Let $y(t) := Hu(t)$, which implies that $u(t) = H^{-1}y(t)$. Therefore

$$\begin{aligned} \nu(H) &= \inf_{u \in \mathcal{U}} \frac{\|y_T\|}{\|u_T\|} = \inf_{u \in \mathcal{D}_h} \frac{\|y_T\|}{\|u_T\|} = \inf_{u \in \mathcal{D}_h} \frac{1}{\frac{\|u_T\|}{\|y_T\|}} \\ &= \frac{1}{\sup\limits_{u \in \mathcal{D}_h} \frac{\|u_T\|}{\|y_T\|}} = \frac{1}{\sup\limits_{u \in \mathcal{D}_h} \frac{\|H^{-1}y_T\|}{\|y_T\|}} \\ &= \frac{1}{\sup\limits_{y \in \mathcal{R}_h} \frac{\|H^{-1}y_T\|}{\|y_T\|}} = \frac{1}{\gamma(H^{-1})}. \end{aligned} \tag{6.32}$$

□

**Corollary 6.2.2.** Unstable, bi-proper, LTI systems

1. *Let $g(t)$ be the impulse response of a continues-time, unstable, bi-proper, LTI system. Let $H$ stand for the convolution operator defined by*

$$H(z(t)) = \int_0^t g(t-\tau)z(\tau)d\tau. \tag{6.33}$$

*Let $G(s)$ be the Laplace transform of $g(t)$. We have*

$$\nu(H) = \left\|G^{-1}(s)\right\|_{\mathcal{H}_\infty}^{-1}. \tag{6.34}$$

2. *Let $g(t)$ be the impulse response of a discrete-time, unstable, strictly proper, LTI system. Let $H$ denote the convolution operator defined by*

$$H(z(t)) = \sum_{l=0}^{t} g(t-l)z(l). \tag{6.35}$$

*Let $G(z)$ be the $z$-transform of $g(t)$. We have*

$$\nu(H) = \left\|G^{-1}(z)\right\|_{\mathcal{H}_\infty}^{-1}. \tag{6.36}$$

*Proof.* The proofs for continuous-time and discrete-time are the same and only the first one comes here.

For bi-proper systems, the inverse system exists. Let $y(t) := Hu(t)$, we have

$$\begin{aligned}
\nu(H) &= \inf_{u\in\mathcal{X}_e} \frac{\|y_T\|}{\|u_T\|} \\
&= \inf_{u\in\mathcal{X}_e} \frac{1}{\frac{\|u_T\|}{\|y_T\|}} \\
&= \frac{1}{\sup\limits_{u\in\mathcal{X}_e} \frac{\|u_T\|}{\|y_T\|}} \\
&= \frac{1}{\sup\limits_{y\in\mathcal{X}_e} \frac{\|u_T\|}{\|y_T\|}} \\
&= \frac{1}{\sup\limits_{u\in\mathcal{X}_e} \frac{\|G^{-1}u_T\|}{\|y_T\|}}.
\end{aligned} \tag{6.37}$$

□

**Example 6.2.2.** Let

$$G(s) = \frac{s+1}{s-1} \tag{6.38}$$

and $H : \mathcal{D}_h \subset \mathcal{L}_2 \to \mathcal{L}_2$ be an operator defined as (6.33). Equation (6.36) implies that

$$\nu(H) = \left\|G^{-1}(s)\right\|_{\mathcal{H}_\infty}^{-1} = 1. \tag{6.39}$$

For instance, let $u(t) := (1-2t)\,e^{-t}\,u_{-1}(t)$, where $u_{-1}(t)$ denotes the step function. We have $U(s) = \frac{s-1}{(s+1)^2}$ and consequently $Y(S) = \frac{1}{s+1}$ which shows that $y(t) = e^{-t}\,u_{-1}(t)$. This reveals that $\nu(H) \leq \frac{\|y\|_{\mathcal{L}_2}}{\|u\|_{\mathcal{L}_2}} = 1$. It is important to note that there is no input that satisfies $\frac{\|y\|_{\mathcal{L}_2}}{\|u\|_{\mathcal{L}_2}} < 1$. This can be shown by contradiction. Assume there exists some input $\hat{u} \in \mathcal{L}_2^e$ such that $\frac{\|\hat{y}\|_{\mathcal{L}_2}}{\|\hat{u}\|_{\mathcal{L}_2}} < 1$ where $\hat{y}$ is the corresponding output. We have $\|\hat{y}\| < \|\hat{u}\| < \infty$. On the other hand, $\hat{u} = G^{-1}\,\hat{y}$. Since $\left\|G^{-1}\right\|_{\mathcal{H}_\infty} = 1\ \|\hat{u}\| \leq \|\hat{y}\|$ which is a contradiction.

The minimum gain of operators satisfies the *positivity* and the *positive homogeneity* properties. To see this, we have

$$\nu(\cdot) \geq 0 \tag{6.40}$$

and

$$\begin{aligned} \nu(\lambda H) &= \inf_{0 \neq u \in \mathcal{X}_e} \frac{\|\lambda H u\|}{\|u\|} \\ &= |\lambda| \inf_{0 \neq u \in \mathcal{X}_e} \frac{\|Hu\|}{\|u\|} = |\lambda|\ \nu(H) \end{aligned} \tag{6.41}$$

However, it can be shown that it fails to satisfy the triangle inequality. For instance, suppose that $H_1$ and $H_2$ are memoryless nonlinearities depicted in Fig. 6.3. It is trivial that $\nu(H_1) = 0$, $\nu(H_2) = 0$ and $\nu(H_1 + H_2) = 1$. This shows that $\nu(H_1 + H_2) > \nu(H_1) + \nu(H_2)$. Consequently, the minimum gain of an operator is not a norm or even a semi-norm on the space of operators.

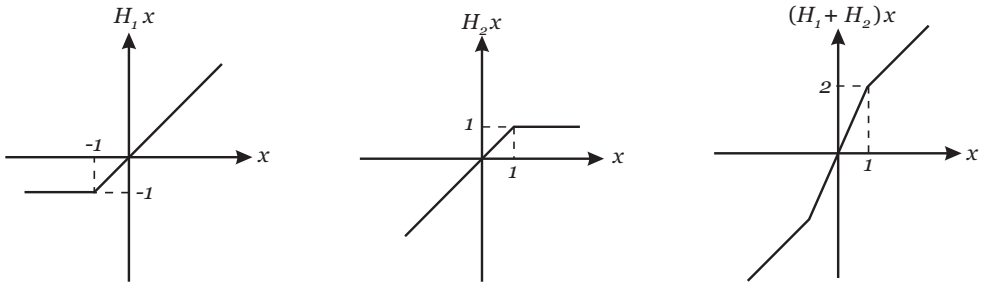


(a) $H_1$ (b) $H_2$ (c) $H_1 + H_2$

Figure 6.3: The triangle inequality is not satisfied by $\nu(\cdot)$.

**Lemma 6.2.6.** *Let $H : \mathcal{U} \to \mathcal{Y}$ denote an operator. Suppose that there exists a nonzero stable operator $K : \mathcal{R} \to \mathcal{U}$ such that $HK : \mathcal{R} \to \mathcal{Y}$ is stable, then $\nu(H) < \infty$.*

*Proof.* Let $0 \neq r(t) \in \mathcal{R}$ such that $r \notin \mathrm{Ker}(K)$, then $u(t) = K\,r(t) \in \mathcal{U}$, $u \neq 0$ and $y(t) = HK\,r(t) \in \mathcal{Y}$, implied by the stability of $K$ and $HK$, respectively. Therefore $\|u\|_{\mathcal{U}} \neq 0$ and $\|u\|_{\mathcal{U}}, \|y\|_{\mathcal{Y}} < \infty$. Consequently, $\nu(H) \leq \frac{\|y\|_{\mathcal{Y}}}{\|u\|_{\mathcal{U}}} < \infty$. □

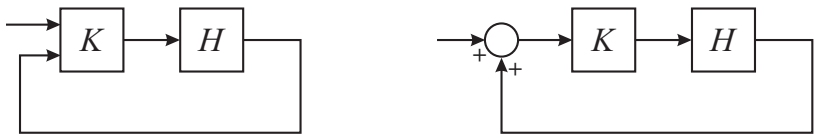


(a) (b)

Figure 6.4: Stabilizable system.

**Corollary 6.2.3.** *Any system that can be stabilized by a stable system with the mentioned properties in Lemma 6.2.6 and a structure as shown in either Fig. 6.4(a) or Fig. 6.4(b), has a finite minimum gain.*

*Proof.* The corollary is based on Lemma 6.2.6 and the proof follows a similar routine as the proof of the lemma with defining a new $\mathcal{R}$ equals $\mathcal{R} \oplus \mathcal{Y}$ in 6.4(a) or $\mathcal{R} + \mathcal{Y}$ in 6.4(b). □

**Theorem 6.2.1.** Sub-multiplicative property
*Let $H_1, H_2 : \mathcal{X} \to \mathcal{X}$ be causal operators. Then*

$$\nu(H_1 H_2) \leq \nu(H_1)\nu(H_2). \tag{6.42}$$

*Proof.* Let $u \in \mathcal{X}$, we have

$$\|H_1 H_2 u\| \geq \nu(H_1) \|H_2 u\| \geq \nu(H_1)\nu(H_2) \|u\| . \tag{6.43}$$

Considering the fact that $\nu(H_1 H_2)$ is the infimum gain of the $H_1 H_2$, Inequality (6.43) implies (6.42). □

## 6.3 Large Gain Theorem

In this section, we concentrate on the feedback system shown in Fig. 6.5. Under mild conditions on $H_1$ and $H_2$ (e.g., the product of the instantaneous gains is less than one [1]), the feedback configuration is guaranteed to be well-posed. The equations describing this feedback system, to be known as the *Feedback Equations*, are:

$$\begin{aligned} e_1 &= u_1 - y_2 \\ e_2 &= u_2 + y_1 \\ y_1 &= H_1 e_1 \\ y_2 &= H_2 e_2. \end{aligned} \tag{6.44}$$

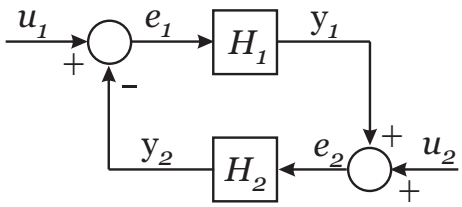


Figure 6.5: The feedback system.

**Theorem 6.3.1.** *Consider the feedback interconnection described by (6.44) and shown in Fig. 6.5. If* $1 < \nu(H_1)\nu(H_2) < \infty$*, the feedback system is input-output-stable.*

*Proof.* To show stability of the feedback interconnection, we must show that $u_1, u_2 \in \mathcal{X}$ imply that $e_1$, $e_2$, $y_1$ and $y_2$ are also in $\mathcal{X}$. According to the definition of $\nu$, we have

$$\nu(H_1)\,\|e_{1T}\| \le \|y_{1T}\| \tag{6.45}$$

$$\nu(H_2)\,\|e_{2T}\| \le \|y_{2T}\| \tag{6.46}$$

On the other hand,

$$y_{1T} = e_{2T} - u_{2T} \tag{6.47}$$

$$y_{2T} = u_{1T} - e_{1T} \tag{6.48}$$

Thus,

$$\|y_{1T}\| \le \|e_{2T}\| + \|u_{2T}\| \tag{6.49}$$

$$\|y_{2T}\| \le \|e_{1T}\| + \|u_{1T}\| \tag{6.50}$$

Substituting (6.45) and (6.46) in (6.49) and (6.50), respectively,

$$\nu(H_1)\,\|e_{1T}\| \le \|e_{2T}\| + \|u_{2T}\| \tag{6.51}$$

$$\nu(H_2)\,\|e_{2T}\| \le \|e_{1T}\| + \|u_{1T}\| \tag{6.52}$$

Using (6.46) and (6.50), Equation (6.51) implies that

$$\begin{aligned} \nu(H_2)\nu(H_1)\,\|e_{1T}\| &\le \nu(H_2)\,\|e_{2T}\| + \nu(H_2)\,\|u_{2T}\| \\ &\le \|y_{2T}\| + \nu(H_2)\,\|u_{2T}\| \\ &\le \|e_{1T}\| + \|u_{1T}\| + \nu(H_2)\,\|u_{2T}\|\,. \end{aligned} \tag{6.53}$$

Since $\nu(H_1)\nu(H_2) > 1$,

$$\|e_{1T}\| \le \frac{1}{\nu(H_1)\nu(H_2) - 1}\left(\|u_{1T}\| + \nu(H_2)\,\|u_{2T}\|\right). \tag{6.54}$$

Similarly,

$$\|e_{2T}\| \leq \frac{1}{\nu(H_1)\nu(H_2)-1}\left(\nu(H_1)\|u_{1T}\| + \|u_{2T}\|\right). \tag{6.55}$$

Moreover, substituting (6.55) and (6.54) in (6.49) and (6.50), respectively,

$$\|y_{1T}\| \leq \frac{\nu(H_1)}{\nu(H_1)\nu(H_2)-1}\left(\|u_{1T}\| + \nu(H_2)\|u_{2T}\|\right) \tag{6.56}$$

and

$$\|y_{2T}\| \leq \frac{\nu(H_2)}{\nu(H_1)\nu(H_2)-1}\left(\nu(H_1)\|u_{1T}\| + \|u_{2T}\|\right). \tag{6.57}$$

Hence, the norms of $\|e_{1T}\|$, $\|1_{2T}\|$, $\|y_{1T}\|$ and $\|y_{2T}\|$ are bounded. If, in addition, $u_1,\ u_2 \in \mathcal{X}$, then (6.54-6.57) must also be satisfied if $T$ approaches $\infty$. Therefore,

$$\|e_1\| \leq \frac{1}{\nu(H_1)\nu(H_2)-1}\left(\|u_1\| + \nu(H_2)\|u_2\|\right) \tag{6.58}$$

$$\|e_2\| \leq \frac{1}{\nu(H_1)\nu(H_2)-1}\left(\nu(H_1)\|u_1\| + \|u_2\|\right) \tag{6.59}$$

$$\|y_1\| \leq \frac{\nu(H_1)}{\nu(H_1)\nu(H_2)-1}\left(\|u_1\| + \nu(H_2)\|u_2\|\right) \tag{6.60}$$

$$\|y_2\| \leq \frac{\nu(H_2)}{\nu(H_1)\nu(H_2)-1}\left(\nu(H_1)\|u_1\| + \|u_2\|\right). \tag{6.61}$$

Consequently, $e_1$, $e_2$, $y_1$ and $y_2$ are also in $\mathcal{X}$. □

**Example 6.3.1.** Let $H_1$ be the convolution operator defined by (6.13) where $g(t)$ is the impulse response of

$$G(s) = k\frac{s+1}{s-1}$$

where $k \in \mathbb{R}$. Let $H_2$ be a memoryless nonlinearity depicted in Fig. 6.1. As shown in Example 6.2.2, $\nu(H_1/k) = 1$ which implies that $\nu(H_1) = |k|$. On the other hand, we have $\nu(H_2) = 0.5$. Consequently $\nu(H_1)\nu(H_2) = 0.5|k|$. The large gain theorem, namely Theorem 6.3.1, guarantees that the feedback system is stable if $|k| > 2$.

## 6.4 Chapter Summary

The minimum gain of an operator as well as some of its properties are introduced. These properties are useful in the computation of the minimum gain of a system. For instance, it is shown that the minimum gain of strictly proper, stable, LTI systems are zero. When it comes to the metric properties, the minimum gain of an operator fails to satisfy the triangular

inequality which implies that it is not a metric or a norm in the space of operators. Finally, the so-called large gain theorem is stated and proved. This theorem implies a new stability condition for feedback interconnection of nonlinear systems. An example is provided to illustrate the derived stability condition.

# Chapter 7

# Disturbance Attenuation: A Case Study

## 7.1 Introduction

There is no doubt that disturbance attenuation is one of the most important objectives in any closed-loop system. Therefore, it is important to quantify the influence of various inputs on various signals inside the feedback loop and develop tools to calculate such quantities. This chapter is based on our earlier work presented in Chapter 4. The plant of interest is a multitank system consistent of three interconnected tanks. First, the mathematical model of the plant is derived using physical relations. Then, the gray box method is used to identify the parameters of the model. Finally, it is assumed that the plant is controlled by a proportional controller and the disturbance attenuation of the closed-loop plant is investigated.

## 7.2 The Multitank System

Liquid level control problems related to multitank systems are commonly encountered in industrial storage tanks. For instance, steel producing companies around the world have repeatedly confirmed that substantial benefits are gained from accurate mould level control in continuous bloom casting. Mould level oscillations tend to stir foreign particles and flux powder into molten metal, resulting in surface defects in the final product [19].

The multitank system consists of three tanks placed one above another. The top tank has a constant cross section while the other two have variable cross sections as shown in Fig. 7.1. A pump is used to circulate liquid from the supply tank into the upper tank. The liquid flows through the tanks due to gravity. The output orifices can be controlled by electrical valves to act as constant or time-varying flow resistors. Generally speaking, the system has four inputs and three outputs. The inputs are three valve controls and one pump

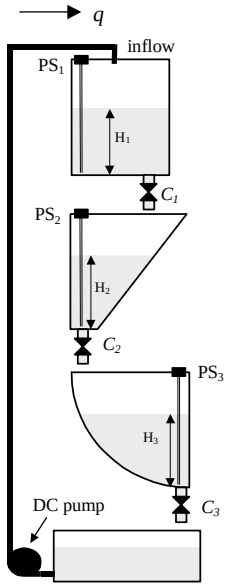


Figure 7.1: Configuration of the multitank system

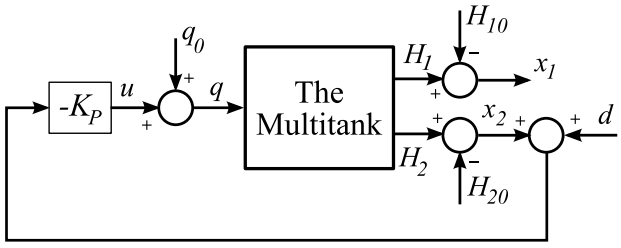


Figure 7.2: Closed loop multitank system

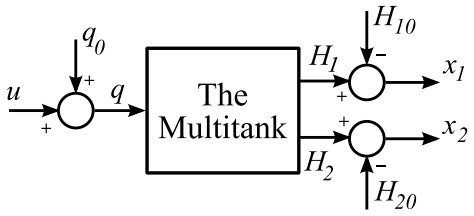


Figure 7.3: Block diagram of the identified system

control signal. The three valve controls are driven by appropriate Pulse-Width Modulation (PWM [16]) signals transmitted from the I/O board to the power interface, and from the power interface to the DC motors connected to the valves. The pump control signal, which acts by controlling the speed of the pump motor, is a sequence of PWM pulses configured and generated by the logic of XILINX chip of the I/O board. The output signals are the levels of the liquid measured by pressure transducers. All signals are connected to the analog inputs/outputs of a multipurpose PC I/O board.

The system states are the liquid levels $H_1$, $H_2$ and $H_3$. The general objective of the pilot is to control the liquid levels by four input signals: liquid inflow $q$ and valve settings $C_1$, $C_2$ and $C_3$. Among various system configurations, our purpose is to control level of the middle tank, i.e. $H_2$, by the liquid inflow $q$ using a proportional controller. We assume that $d$ is the disturbance (or noise) signal and study the disturbance attenuation of the closed-loop system. The block diagram of the closed-loop system is depicted in Fig. 7.2.

## 7.3 Identification

The block diagram of the plant is depicted in Fig. 7.3. First, a mathematical model of the plant is developed based on the physics of the process. Next, we set an experiment to acquire the step response of the system in order to obtain an approximate model of the system or more precisely, an approximate time constants of the system. Using the approximate time constants, a Random Binary Sequence (RBS) signal is built and applied to the plant [26]. Finally, the RBS response is divided to two sections; one section is used to identify the model and another one to validate the model.

### 7.3.1 The Mathematical Model

The Bernoulli's law can be applied to find the laminar outflow rate of an ideal fluid [30]. By applying mass balance and assuming a laminar outflow, the model describing the dynamics

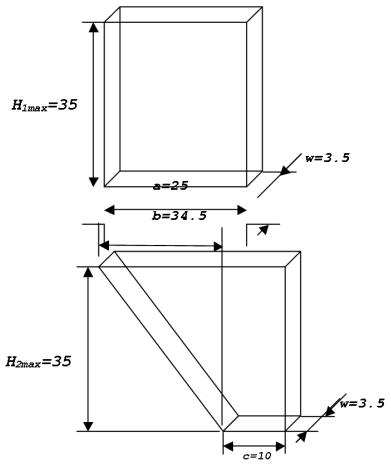


Figure 7.4: Geometrical parameters of the tanks

of the process can be obtained.

$$\begin{cases} \dfrac{dV_1}{dt} = q - C_1\sqrt{H_1} \\ \dfrac{dV_2}{dt} = C_1\sqrt{H_1} - C_2\sqrt{H_2} \end{cases} \tag{7.1}$$

where $V_1$ and $V_2$ are the fluid volumes in Tank 1 and Tank 2, respectively and $C_1$ and $C_2$ are the resistances of the output orifices. Hence,

$$\begin{cases} \dfrac{dV_1}{dH_1}\dfrac{dH_1}{dt} = q - C_1{H_1}^{\alpha_1} \\ \dfrac{dV_2}{dH_2}\dfrac{dH_2}{dt} = C_1{H_1}^{\alpha_1} - C_2{H_2}^{\alpha_2} \end{cases} \tag{7.2}$$

where $\alpha_1 = 0.5$ and $\alpha_2 = 0.5$ for laminar flows. For the real system where turbulence and acceleration of the liquid are not negligible, the outflow rate does not follow the Bernoulli law and more general coefficients $\alpha_1$ and $\alpha_2$ should be considered [19] [30]. The values of $\frac{dV_1}{dH_1}$ and $\frac{dV_2}{dH_2}$ depend on the shape of the tanks shown in Fig. 7.4. Since the cross-sectional area of Tank 1 is constant, $\frac{dV_1}{dH_1} = aw$. For Tank 2, we have $\frac{dV_1}{dH_1} = cw + \frac{H_2}{H_{2max}}bw$. Therefore,

$$\begin{cases} \frac{dH_1}{dt} = \frac{1}{aw}\left(q - C_1 H_1^{\alpha_1}\right) \\ \frac{dH_2}{dt} = \frac{1}{cw + \frac{H_2}{H_{2max}}bw}\left(C_1 H_1^{\alpha_1} - C_2 H_2^{\alpha_2}\right) \end{cases} \tag{7.3}$$

Let $x_1 := H_1 - H_{10}$, $x_2 := H_2 - H_{20}$ and $q = u + q_0$ where $H_{10}$ and $H_{20}$ are operating points and $q_0$ is the corresponding input. It is trivial that $q_0 = C_1 H_{10}^{\alpha_1} = C_2 H_{20}^{\alpha_2}$. The numerical values for the coefficients are $a = 0.25$, $w = 0.035$, $H_{2max} = 0.35$, $b = 0.345$, $c = 0.1$ [19]. Hence, the state equation of the open-loop system is

$$\begin{cases} \frac{dx_1}{dt} = 114.2857\left(u + (0.15C_1)^{\alpha_1} - C_1(x_1 + 0.15)^{\alpha_1}\right) \\ \frac{dx_2}{dt} = \frac{1}{0.0035 + 0.0345(x_2 + 0.1)}\left(C_1(x_1 + 0.15)^{\alpha_1} - C_2(x_2 + 0.1)^{\alpha_2}\right) \end{cases} \tag{7.4}$$

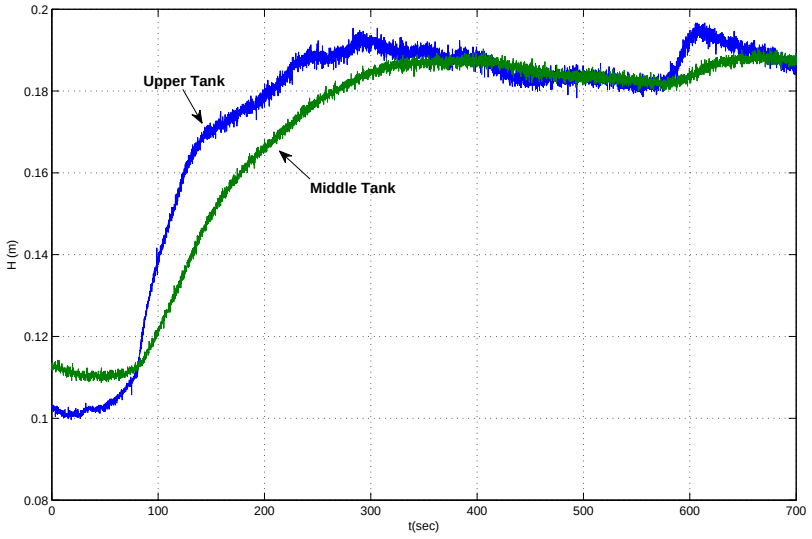


Figure 7.5: The step response

### 7.3.2 Data Acquisition

To build an appropriate RBS signal, we need to acquire approximate time constants of the system. Therefore, we set an experiment to obtain step responses. The step responses are depicted in Fig. 7.5. Hence, the approximate time constant of the system are $\tau_1 \approx 80s$ and $\tau_2 \approx 150s$. We will use the time constants to determine frequency of the RBS signal. We choose $T_s = 10\,\mathrm{sec}$. To perform the RBS test we need to determine the pass band which can be calculated from the following formula [26]:

$$f = \frac{kT_s}{\tau\pi} \tag{7.5}$$

where $k = 2 \sim 3$. We select $f = 0.0612$. The produced RBS signal and response of the system are illustrated in Fig. 7.6.

### 7.3.3 Data Pre-Processing and Identification

We do the identification and validation for each of the outputs separately. After down sampling the data, the mean value of the data should be removed and to reduce computational errors, we increase the values of the levels by using centimeter unit. Then, we filter the data by a low pass filter to attenuate noise. The bandwidth of the system is approximately equal to inverse of the time constant. We choose one decade upper than the bandwidth as cut-off

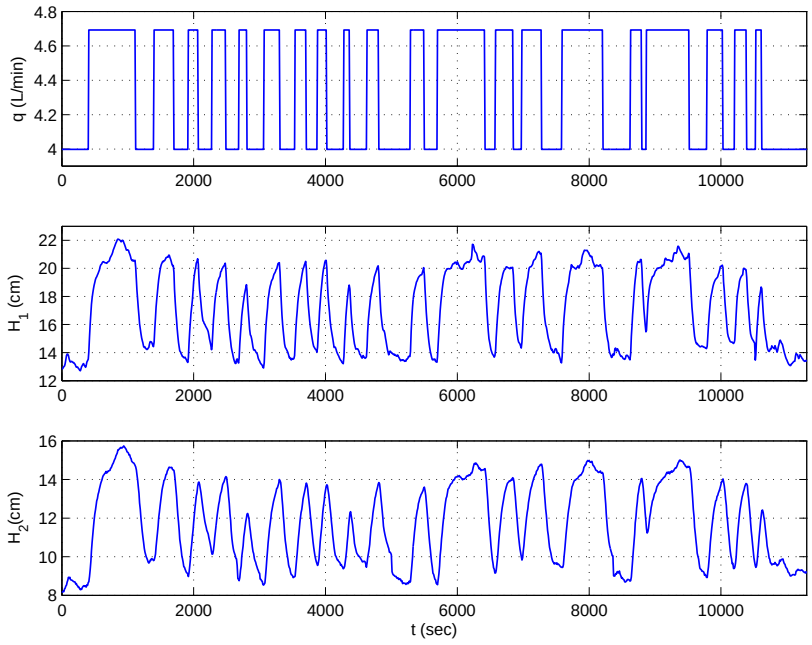


Figure 7.6: The RBS response

Table 7.1: The identified parameters.

| Parameter | $C_1$ | $C_2$ | $\alpha_1$ | $\alpha_2$ |
|---|---|---|---|---|
| Value | $1.432 \times 10^{-4}$ | $1.488 \times 10^{-4}$ | 0.3833 | 0.3341 |

frequency of the low-pass filter. Therefore,

$$f_{1,cut-off} = \frac{10T_s}{\tau_1 \pi} = 0.3979$$
$$f_{2,cut-off} = \frac{10T_s}{\tau_2 \pi} = 0.2122 \tag{7.6}$$

Next, From 1130 data points of the pair of input-output, we choose the first 750 points for identification and the remaining 380 points for validation and remove the mean values of two set of data. We use the Identification Toolbox of MATLAB to identify $C_1$, $C_2$, $\alpha_1$ and $\alpha_2$ by the gray box method. The identification and validation curves are depicted in Fig. 7.7 and 7.8, respectively.

The identified values for the mentioned parameters are given in Table 7.1.

### 7.3.4 Disturbance Attenuation

The problem of our interest is to study the disturbance attenuation of the closed loop system depicted in Fig.7.2. In order to calculate the disturbance rejection amplitude, we need to find

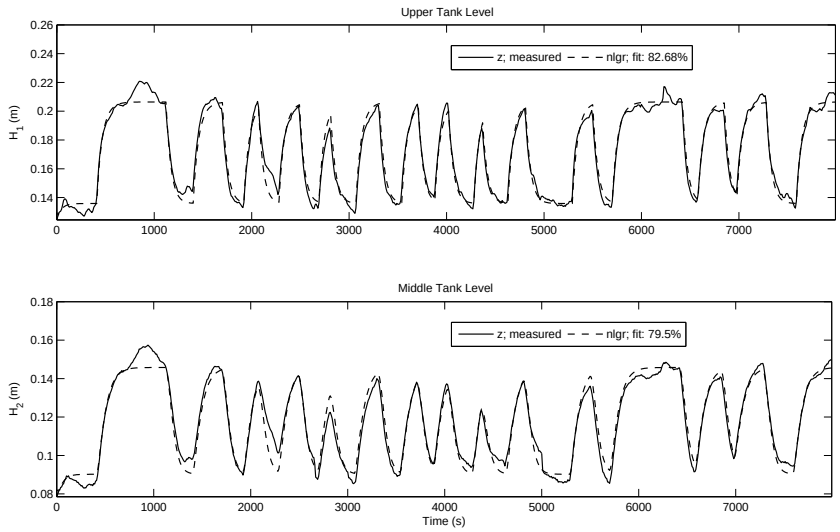


Figure 7.7: Identification

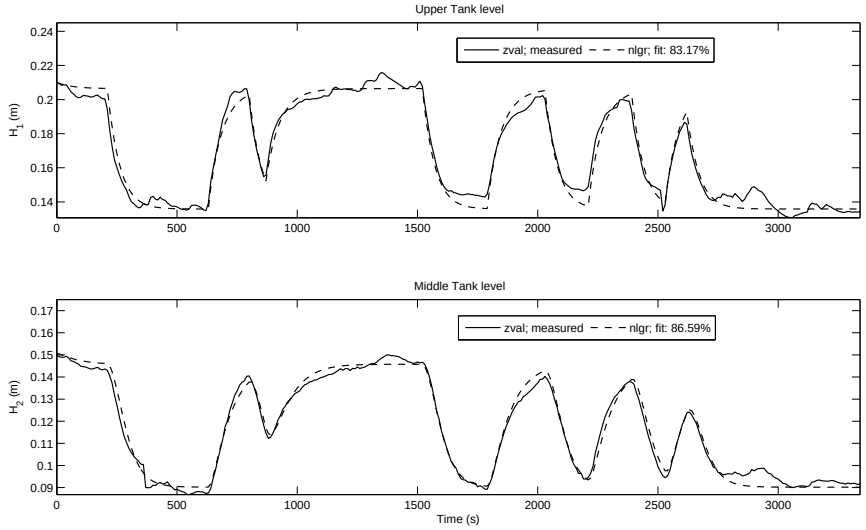


Figure 7.8: Validation

the gain of the system from the disturbance signal to the output by the methods mentioned in Section 5.3. The state equations of the closed-loop system are

$$\begin{cases} \dot{x}_1 = \frac{1}{aw}\left(q_0 - K_P(x_2+d) - C_1(x_1+H_{10})^{\alpha_1}\right) \\ \dot{x}_2 = \frac{1}{cw+\frac{x_2+H_{20}}{H_{2max}}bw}\left(C_1(x_1+H_{10})^{\alpha_1} - C_2(x_2+H_{20})^{\alpha_2}\right) \end{cases} \tag{7.7}$$

and $\dot{x} = \begin{pmatrix} \dot{x}_1 \\ \dot{x}_2 \end{pmatrix} = f(x,d)$. To find appropriate $A$ and $B$ matrices, we define a function which calculates $\gamma_\infty(\Gamma)\cdot\gamma_\infty(\Phi)$ in a local region $\left\|\begin{bmatrix} x \\ d \end{bmatrix}\right\|_\infty \leq \hat{r}$ for given $A$ and $B$ in MATLAB. Then using *fminsearch* function of MATLAB, we minimize the function with respect to $A$ and $B$. Choosing $\hat{r} = 0.06$, we obtain $A = \begin{pmatrix} -0.0360 & -0.0149 \\ 0.0215 & -0.0425 \end{pmatrix}$ and $B = \begin{pmatrix} 0.0141 \\ 0.0066 \end{pmatrix}$. Therefore, $\Phi(x,d) = \begin{bmatrix} \Phi_1(x,d) \\ \Phi_2(x,d) \end{bmatrix}$ where

$$\begin{cases} \Phi_1(x,d) = 0.00791 - 0.00266\,d + 0.00346\,x_2 - 0.0164\,(x_1+0.150)^{0.3833} \\ \qquad\qquad + 0.0360\,x_1 \\ \Phi_2(x,d) = \left(0.000143\,(x_1+0.15)^{0.3833} - 0.00015\,(x_2+0.1)^{0.3341}\right)\times \\ \qquad\qquad (0.007 + 0.0345\,x_2)^{-1} - 0.0215\,x_1 + 0.0425\,x_2 - 0.00657\,d. \end{cases} \tag{7.8}$$

Computation with the methods proposed in [50] provides $\gamma_\infty(\Gamma) < 32.9194$, $\gamma_\infty(\Theta) < 0.2975$, and $\gamma_\infty(\Omega) = 1$. Let $\eta = 1$ which gives $\gamma_\infty(\Omega) + \eta\gamma_\infty(\Theta) = 1.2975$. By choosing different values for $M_p$ and $\eta$, different bounds can be obtained. For now, we choose $M_p = 20$. Therefore, $\gamma_\infty^{\mathcal{D}}(\Phi)$ should satisfy

$$\gamma_\infty^{\mathcal{D}}(\Phi) < \frac{M_p - \gamma_\infty(\Omega) - \eta\gamma_\infty(\theta)}{(M_p+\eta)\gamma_\infty(\Gamma)} = 0.0271. \tag{7.9}$$

$\frac{\|\Phi(x,d)\|_\infty}{\left\|\begin{bmatrix} x \\ d \end{bmatrix}\right\|_\infty}$ versus $\left\|\begin{bmatrix} x \\ d \end{bmatrix}\right\|_\infty$ is depicted in Fig. 7.9. Let us take $\mathcal{D}$ as the region where $\frac{\|\Phi(x,d)\|_\infty}{\left\|\begin{bmatrix} x \\ d \end{bmatrix}\right\|_\infty} < 0.049$, i.e. $\gamma_\infty^{\mathcal{D}}(\Phi) = 0.027$. Consequently $r_x = 0.049$ and $r_d = 0.049$. Let $\epsilon = 0.048$ and $\delta = 0.0023 \leq \frac{1-\gamma_\infty^{\mathcal{D}}(\Phi)\gamma_\infty(\Gamma)}{\gamma_\infty(\Omega)+\eta(\gamma_\infty(\Theta)+\gamma_\infty^{\mathcal{D}}(\Phi)\gamma_\infty(\Gamma))}\epsilon = 0.0024$. According to Theorem 3.3.2, for any input $d$ which satisfies $\|d\|_{\mathcal{L}_\infty} < \min(\eta\delta, r_d) = 0.0023$ and any initial state satisfying $\|x_0\|_\infty < \delta = 0.0023$, $x$ is bounded as $\|x\|_{\mathcal{L}_\infty} < \epsilon = 0.048$. In other words, if $-2.3\text{mm} \leq d \leq 2.3\text{mm}$, $14.77\text{cm} \leq H_{10} \leq 15.23\text{cm}$ and $8.77\text{cm} \leq H_{20} \leq 10.23\text{cm}$ then $10.2\text{cm} \leq H_1 \leq 19.8\text{cm}$ and $5.2\text{cm} \leq H_2 \leq 14.8\text{cm}$.

Now, Let $\eta = 4$. Therefore, $\gamma_\infty(\Omega) + \eta\gamma_\infty(\Theta) = 2.19$. By choosing $M_p = 22$, $\gamma_\infty^{\mathcal{D}}(\Phi)$ should satisfy

$$\gamma_\infty^{\mathcal{D}}(\Phi) < \frac{M_p - \gamma_\infty(\Omega) - \eta\gamma_\infty(\theta)}{(M_p+\eta)\gamma_\infty(\Gamma)} = 0.0231. \tag{7.10}$$

Table 7.2: Bounds obtained by various $\eta$ and $M_p$.

| $\hat{r}$ | $\eta$ | $M_p$ | $\|x_0\|_\infty <$ (in mm) | $\|d\|_{\mathcal{L}_\infty} <$ (in mm) | $\|x\|_{\mathcal{L}_\infty} <$ (in mm) |
|---|---|---|---|---|---|
| 0.06 | 0.1 | 8 | 5.8 | 0.58 | 45 |
| | 0.1 | 20 | 5 | 0.5 | 50 |
| | 1 | 20 | 2.3 | 2.3 | 48 |
| | 3 | 19 | 1.7 | 5 | 30 |
| | 4 | 22 | 1.4 | 5.6 | 30 |
| | 5 | 24 | 0.51 | 2.6 | 12 |
| | 8 | 38 | 0.72 | 5.7 | 28 |
| | 10 | 120 | 0.4 | 4.1 | 48 |
| 0.03 | 0.1 | 2 | 12.5 | 1.25 | 21.5 |
| | 1 | 9 | 4.58 | 4.58 | 38.2 |
| | 10 | 15 | 1.13 | 11.3 | 16.5 |
| | 100 | 130 | 0.11 | 11 | 15 |

Let $\mathcal{D}$ be the region where $\gamma_\infty^{\mathcal{D}}(\Phi) = 0.023$. Hence, $\frac{\|\Phi(x,d)\|_\infty}{\left\|\begin{bmatrix} x \\ d \end{bmatrix}\right\|_\infty} < 0.0302$ in $\mathcal{D}$. Thus, $r_x = 0.0302$ and $r_d = 0.0302$. Let $\epsilon = 0.03$ and

$$\delta = 0.0013 \leq \frac{1 - \gamma_\infty^{\mathcal{D}}(\Phi)\gamma_\infty(\Gamma)}{\gamma_\infty(\Omega) + \eta(\gamma_\infty(\Theta) + \gamma_\infty^{\mathcal{D}}(\Phi)\gamma_\infty(\Gamma))}\,\epsilon = 0.0014. \tag{7.11}$$

According to Theorem 3.3.2, for any input $d$ which satisfies $\|d\|_{\mathcal{L}_\infty} < \min(\eta\delta, r_d) = 0.0056$ and any initial state satisfying $\|x_0\|_\infty < \delta = 0.0013$, $x$ is bounded as $\|x\|_{\mathcal{L}_\infty} < \epsilon = 0.03$. In other words, if $-5.6\text{mm} \leq d \leq 5.6\text{mm}$, $14.86\text{cm} \leq H_{10} \leq 15.14\text{cm}$ and $9.86\text{cm} \leq H_{20} \leq 10.14\text{cm}$ then $12\text{cm} \leq H_1 \leq 18\text{cm}$ and $7\text{cm} \leq H_2 \leq 13\text{cm}$.

By choosing other values for $\eta$ and $M_p$, other bounds can be obtained. Moreover, $\hat{r}$ can also be changed to acquire required bounds. For example, let $\hat{r} = 0.03$. By minimizing $\gamma_\infty(\Gamma) \cdot \gamma_\infty(\Phi)$ in a local region $\left\|\begin{bmatrix} x \\ d \end{bmatrix}\right\|_\infty \leq \hat{r} = 0.03$, we obtain

$$A = \begin{pmatrix} -0.0204 & -0.0171 \\ 0.0262 & -0.0347 \end{pmatrix}, \quad B = \begin{pmatrix} 0.0124 \\ 0.0001 \end{pmatrix}. \tag{7.12}$$

For this case, $\frac{\|\Phi(x,d)\|_\infty}{\left\|\begin{bmatrix} x \\ d \end{bmatrix}\right\|_\infty}$ versus $\left\|\begin{bmatrix} x \\ d \end{bmatrix}\right\|_\infty$ is depicted in Fig. 7.10. For both $\hat{r} = 0.03$ and $\hat{r} = 0.06$ cases, some of the results are summarized in Table 7.2.

## 7.4 Chapter Summary

Based on Theorem 3.3.2 in Chapter 4, a method proposed to study disturbance attenuation of closed-loop nonlinear systems. The physical plant under examination is a multitank

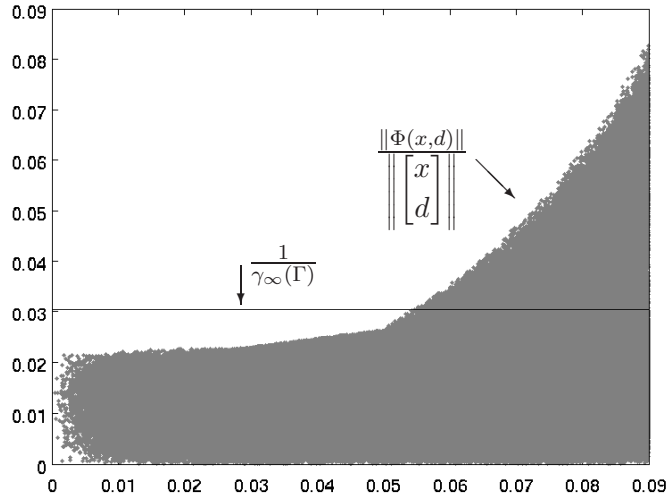


Figure 7.9: Gain of $\|\Phi(x,d)\|$ and $\frac{1}{\gamma_\infty(\Gamma)}$ for $\hat{r} = 0.06$

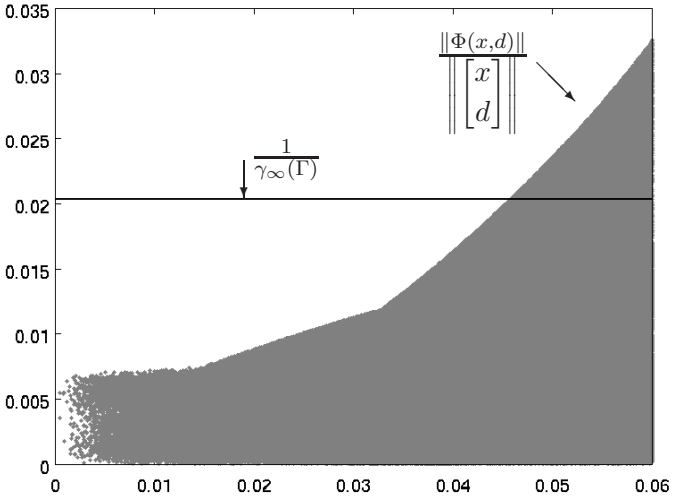


Figure 7.10: Gain of $\|\Phi(x,d)\|$ and $\frac{1}{\gamma_\infty(\Gamma)}$ for $\hat{r} = 0.03$

system. First, the mathematical model of the plant is derived using physical concepts. Then, the parameters of the model are identified by the gray box method. Finally, the disturbance attenuation of the closed-loop plant controlled by a proportional controller is investigated.

# Chapter 8

# Conclusions and Recommendations

## 8.1 Conclusions

In this thesis, different algorithms are developed to provide necessary tools for designing multi-model control systems for nonlinear systems. The major contributions are:

1. New representations for nonlinear systems, called $\zeta_A$ and $\zeta_{AB}$ representations, are proposed. In the $\zeta_A$ representation and its extended version for forced systems, $\zeta_{AB}$ representation, a nonlinear system is arranged as a feedback interconnection of a memoryless nonlinearity and a linear system with initial state as an input signal. Although interconnection of a memoryless nonlinearity with a linear system has been widely used in literature, the way the initial state is dealt with is the main difference between our decomposition and traditional ones. In $\zeta_A$ and $\zeta_{AB}$ representations, the initial state contributes to the feedback interconnection as an exogenous input while in traditional methods, any change in the initial state is handled by defining a new operator. The $\zeta_A$ and $\zeta_{AB}$ representations can be used to develop new tools for non-zero state nonlinear systems from the input-output theory methods, as presented in this thesis. In other words, the fact that the $\zeta_A$ and $\zeta_{AB}$ representations convert a nonlinear system with non-zero initial state to a combination of a memoryless nonlinearity and a linear system with some input signals and the way initial state is handled by these representations provide a novel viewpoint on all aspects of investigating nonlinear systems.

2. A new framework is developed for the analysis of stability of systems by the $\zeta_A$ and $\zeta_{AB}$ representations. The effectiveness of this usage is originated in the fact that using these representations, stability of nonlinear systems with non-zero initial states can be investigated by the input-output stability methods and stability is interpreted as

input-output stability of the resulting feedback systems. Precisely, new methods are proposed to check stability in the sense of Lyapunov for an unforced nonlinear system by norm of some relevant operators, without finding any Lyapunov-like function. For local stability, a method developed to find some local areas, $\Delta$ and $\Upsilon$, where the initial state $x_0$ belonging to $\Delta$ implies the state staying inside $\Upsilon$ area. The methods are also extended to forced systems.

3. A new method is proposed to compute an upper bound on the $\mathcal{L}_1$, $\mathcal{L}_2$ and $\mathcal{L}_\infty$ norms of a class of nonlinear systems. The method is based on the $\zeta_A$ and $\zeta_{AB}$ representations of nonlinear systems. A method is also proposed to find an upper bound on induced $\mathcal{L}_p$ norms. The second method, Theorem 4.1.2, provides tighter bound for the case $p = 2$. Both proposed methods suffer from a restrictive condition. Another tool is developed to overcome this restriction with the cost of providing only local conditions, namely, an upper bound on system output for bounded input and initial state, and being restricted to $\mathcal{L}_\infty$ induced norm.

4. Based on $\zeta_A$ and $\zeta_{AB}$ representations, methods are proposed to compute an upper bounds on the gap metric and the corresponding stability margin for a class of nonlinear systems.

5. The minimum gain of operators is defined, some of its properties are derived and some computational methods are developed to calculate the minimum gain. For example, it is shown that the minimum gain satisfies the positivity and the positive homogeneity properties but fails to satisfy the triangle inequality.

6. Based on the minimum gain of operators, the large gain theorem is stated. The large gain theorem asserts that the feedback loop will be stable if the minimum loop gain is greater than one.

7. One of the algorithms, which is developed to compute on upper bounds on $\mathcal{L}_\infty$ norm of nonlinear systems, is deployed to study disturbance attenuation of a closed loop system. The system of interest is a multitank system consisting of three tanks placed one above another. It is assumed that a proportional controller is used to control the level of the liquid in one of the tanks. The mathematical model of the open loop system is derived using physics of the plant. The gray box identification method is used to identify the model parameters and the disturbance attenuation of the system is investigated by the proposed method.

## 8.2 Future Work

Some future directions for extending and improving the results of this thesis are as follows:

1. Some of the results are already extended to discrete systems. It is useful to check the applicability of all results on discrete and multirate systems.

2. Almost all of the results are developed based on general classes of nonlinear systems, i.e.

$$N_1 : \dot{x}(t) = f_1(t, x(t)) \tag{8.1}$$

$$N_2 : \ \dot{x}(t) = f_2(t, x(t), u(t)). \tag{8.2}$$

   It may be useful to restrict systems to a narrower class. For example, one may obtain tighter bounds on the $\mathcal{L}_\infty$ norm of systems by restricting the system of interest to

$$N_3 : \ \dot{x}(t) = f_1(t, x(t)) \cdot f_2(t, u(t)). \tag{8.3}$$

3. The $\zeta_A$ and $\zeta_{AB}$ representations convert a nonlinear system with non-zero initial state to a combination of a memoryless nonlinearity and a linear system with some input signals. The way the initial state is handled by these representations provides a novel viewpoint on all aspects in investigating nonlinear systems. We have used $\zeta_A$ and $\zeta_{AB}$ representations in developing all the results presented in this thesis. One interesting work is to use the $\zeta_A$ and $\zeta_{AB}$ representations to study other aspects of nonlinear systems, such as observability, and develop new tools based on these representations.

4. The tools that are developed in this thesis can be used to design multi-model control systems. It would be interesting to design a multi-model control system based on the proposed tools.

# Bibliography


[1] J. A. Ball and J. W. Helton. Interconnection of Nonlinear Causal Systems. *IEEE Trans. on Automatic Control*, 34: 1132 – 1140, 1989.

[2] V. Chellaboina, W. M. Haddad, D. S. Bernstein, and D. A. Wilson. Induced Convolution Operator Norms of Linear Dynamical Systems. *Mathematics of Control, Signals, and Systems*, 13(3): 216 – 239, 2000.

[3] C. T. Chen. *Linear Systems Theory and Design.* 3rd edn., Oxford University Press: New York, 1998.

[4] T. W. S. Chow, H. Z. Tan, and Y. Fang. *Nonlinear System Representation*. Encyclopedia of Electrical and Electronic Engineering, J. G. Webster (Ed.), John Wiley & Sons, 2001.

[5] J. C. Doyle, T. T. Georgiou, and M. C. Smith. The Parallell Projection Operators of A Nonlinear Feedback System. *Systems & Control Letters*, 20(2):79 – 85, 1993.

[6] I. J. Fialho and T. T. Georgiou. A Variational Approach to $\mathcal{L}_\infty$-gain Analysis of Nonlinear Systems. *Proc. 1995 Conf. Decision & Control*, pp. 823 – 828.

[7] B. A. Foss, T. A. Johasen and A. V. Sorensen. Nonlinear Predictive Control Using Local Models - Applied to A Batch Fermentation Process, *Control Engineering Practice,* 3:389 – 396, 1995.

[8] G. F. Franklin, M. L. Workman, and D. Powell. *Digital Control of Dynamic Systems,* 3rd ed., Addison-Wesley Longman: Boston, 1997.

[9] O. Galan, J. A. Romagnoli, A. Palazoglu, and Y. Arkun. Gap Metric Concept and Implications for Multilinear Model-based Controller Design. *Industrial Engineering Chemical Research,* 42: 2189 – 2197, 2003.

[10] T. T. Georgiou, A. Pascoal, and P. P. Khargonekar. On the Robust Stabilizability of Uncertain Linear Time-invariant Plants Using Nonlinear Time-varying Controllers. *Automatica*, 35(5): 617 – 624, 1987.

[11] T. T. Georgiou. Differential Stability and Robust Control of Nonlinear Systems. *Math. Control Signals Syst.*, 6(4):289 – 306, 1993.

[12] T. T. Georgiou. On the Computation of the Gap Metric. *Systems and Control Letters,* 11(4): 253 – 257, 1988.

[13] T. T. Georgiou and M. C. Smith. Robustness Analysis of Nonlinear Feedback Systems: An Inputoutput Approach. *IEEE Trans. on Automatic Control*, 42(9): 1200 – 1221, 1997.

[14] T.T. Georgiou, M. Khammash, and A. Megretski. On a Large-gain Theorem. *Systems and Control Letters*, 32(4): 231 – 234, 1997.

[15] J. W. Hilton and M. R. James. *Extending $\mathcal{H}_\infty$ Control to Nonlinear Systems.* SIAM, 1999.

[16] D. G. Holmes and T. A. Lipo. *Pulse Width Modulation for Power Converters: Principles and Practice.* Wiley-IEEE Press, 2003.

[17] G. D. Howitt and R. Luss. Control of a Collection of Linear Systems by Linear State Feedback Control. *International Journal of Control*, 58(1):79 – 96, 1993.

[18] B. Ingalls and E. D. Sontag. A Small-gain Theorem with Applications to Input/Output Systems, Incremental Stability, Detectability and Interconnection. *Journal of the Franklin Institute*, 339(2): 211 – 229, 2002.

[19] *Multi-tank System User's Manual*, INTECO Ltd., www.inteco.com.pl.

[20] M. R. James and S. Yuliar. Numerical Approximation of the $\mathcal{H}_\infty$ Norm for Nonlinear Systems. *Automatica*, 31(8): 1075 – 1086, 1995.

[21] Z. P. Jiang, A. Teel, and L. Praly. Small-gain Theorem for ISS Systems and Applications. *Mathematics of Control, Signals, and Systems*, 7(2):95 – 120, 1994.

[22] I. Karafyllis. The Non-uniform in Time Small-gain Theorem for a Wide Class of Control Systems with Outputs. *European Journal of Control*, 10(4): 307 – 323, 2004.

[23] I. Karafyllis and Z. P. Jiang. A Small-gain Theorem for a Wide Class of Feedback Systems with Control Applications. *SIAM J. Control and Optimization*, 46(4): 1483 – 1517, 2007.

[24] H. K. Khalil. *Nonlinear Systems*, 3rd edn., Prentice Hall: Upper Saddle River, N.J., 2002.

[25] M. Krstič, I. Kanellakopoulos, and P. Kokotovič. *Nonlinear and Adaptive Control Design*. Wiley-Interscience: New York, 1995.

[26] L. Ljung. *System Identification: Theory for the User*. 2nd ed., Prentice Hall PTR, 1999.

[27] H. J. Marquez. *Nonlinear Control Systems, Analysis and Design*. John Wiley & Sons: New Jersey, 2003.

[28] R. Murray-Smith and T. A. Johansen. *Multiple Model Approaches to Modeling and Control*. Taylor & Francis, London, 1997.

[29] P. Pepe. The Liapunov's Second Method for Continuous Time Difference Equations. *Int. J. Robust and Nonlinear Control*, 13(15):1389 – 1405, 2003.

[30] R. H. Perry and D. W. Green. *Perry's Chemical Engineers' Handbook.* McGraw-Hill, 7th ed, 1997.

[31] B. G. Romanchuk. On the Computation of the Induced $\mathcal{L}_2$ Norm of Single-input Linear Systems with Saturation. *IEEE Trans. on Automatic Control*, 43(2): 262 – 268, 1998.

[32] I. W. Sandberg. On the $\mathcal{L}_2$-boundedness of Solutions of Nonlinear Functional Equations. *Bell System Tech. Journal*, 43(11): 1581 – 1599, 1964.

[33] E.D. Sontag. Input to State Stability: Basic Concepts and Results. In P. Nistri and G. Stefani (Ed.). *Nonlinear and Optimal Control Theory*. 1 st edn., Springer-Verlag: Berlin, 163 – 220, 2006.

[34] E. D. Sontag and Y. Wang. Notions of Input to Output Stability. *Systems and Control Letters*, 38(4-5):235 – 248: 1999.

[35] E. D. Sontag. Smooth Stabilization Implies Coprime Factorization. *IEEE Transactions on Automatic Control*, 34(4):435 – 443, 1989.

[36] E. D. Sontag and Y. Wang. On Characterizations of the Input-to-state Stability Property. *Systems and Control Letters*, 24(5):351 – 359, 1995.

[37] T. E. Stern. *Theory of Nonlinear Networks and Systems, An Introduction.* Addison-Wesley: Massachusetts, 1965.

[38] W. Tan. H. J. Marquez. T. Chen and J. Liu. Multimodel Analysis and Controller Design for Nonlinear Processes. *Computers and Chemical Engineering*, 28:2667 – 2675, 2004.

[39] A. R. Teel. A Nonlinear Small Gain Theorem for the Analysis of Control Systems with Saturation. *IEEE Transactions on Automatic Control*, 41(9): 1256 – 1270, 1996.

[40] M. Vidyasagar. *Nonlinear Systems Analysis.* Society of Industrial and Applied Mathematics: Philadelphia, 2nd edn., 2002.

[41] M. Vidyasagar. *Input-output Analysis of Large-scale Interconnected Systems*. Springer-Verlag: New York, 1981.

[42] V. M. Popov. Absolute Stability of Nonlinear Systems of Automatic Control. *Automation Remote Control*, 22: 857 – 875, 1962.

[43] W. Rugh. Analytical Framework for Gain Scheduling. *IEEE control systems Magazine*, 11(1): 79 – 84, 1991.

[44] J. S. Shamma and M. Athans. Gain Scheduling: Potential Hazards and Possible Remedies. *IEEE control systems Magazine*, 12(3): 101 – 107, 1992.

[45] J. S. Shamma. *Analysis and Design of Gain Scheduled Control Systems.* PhD Thesis, Dept. of Mech. Eng., Massachusetts Ins. of Tech, 1988.

[46] F. G. Shinskey. *Process Control Systems: Application, Design, and Tuning.* 4th ed., McGraw-Hill, New York, 1996.

[47] A. Uppal, W. H. Ray, and A. B. Poore. The Classification of the Dynamic Behavior of Continuous Stirred Tank Reactorss Influence of Reactor Residence Time. *Chemical Engineering Science*, 31:205, 1976.

[48] A. J. van der Schaft. *$\mathcal{L}_2$-gain and Passivity Techniques in Nonlinear Control.* 2nd ed., Springer, London, 2000.

[49] V. Zahedzadeh, H. J. Marquez and T. Chen. On the Robust Stability of Unforced Nonlinear Systems. *Proc. of 45th IEEE Conf. on Decision and Control*, 343 – 348, 2006.

[50] V. Zahedzadeh, H. J. Marquez and T. Chen. On the Stability of a Class of Unforced Nonlinear Systems, An Operator Norm Approach. *IET Control Theory & Applications*, 3(2): 200 – 210, 2008.

[51] V. Zahedzadeh, H. J. Marquez and T. Chen. Upper Bounds for Induced Operator Norms of Nonlinear Systems. *IEEE Trans. on Automatic Control*, 2008.

[52] V. Zahedzadeh, H. J. Marquez and T. Chen. On the Computation of an Upper Bound on the Gap Metric for a Class of Nonlinear Systems. *Proc. of American Control Conf.*, 1917 – 1922, 2008.

[53] V. Zahedzadeh, H. J. Marquez and T. Chen. On the Input-output Stability of Nonlinear Systems: Large Gain Theorem. *Proc. of American Control Conf.*, 3440 – 3445, 2008.

[54] V. Zahedzadeh, H. J. Marquez and T. Chen. Upper Bounds for Induced Operator Norms of Nonlinear Systems. *Proc. of 26th American Control Conf.*, 4727 – 4732, 2007.

[55] G. Zames and A. K. El-Sakkary. Unstable Systems and Feedback: the Gap Metric. *Proc. Allerton Conf.*, 380 – 385, 1980.

[56] G. Zames. On the Input-output Stability for Time-varying Nonlinear Feedback Systems, Part I, Conditions Using Concepts of Loop Gain, Concity and Positivity. *IEEE Transactions on Automatic Control*, 11(2):228 – 238, 1966.

[57] K. Zhou and J. C. Doyle. *Essentials of Robust Control*, Prentice Hall, New Jersey, 1997.